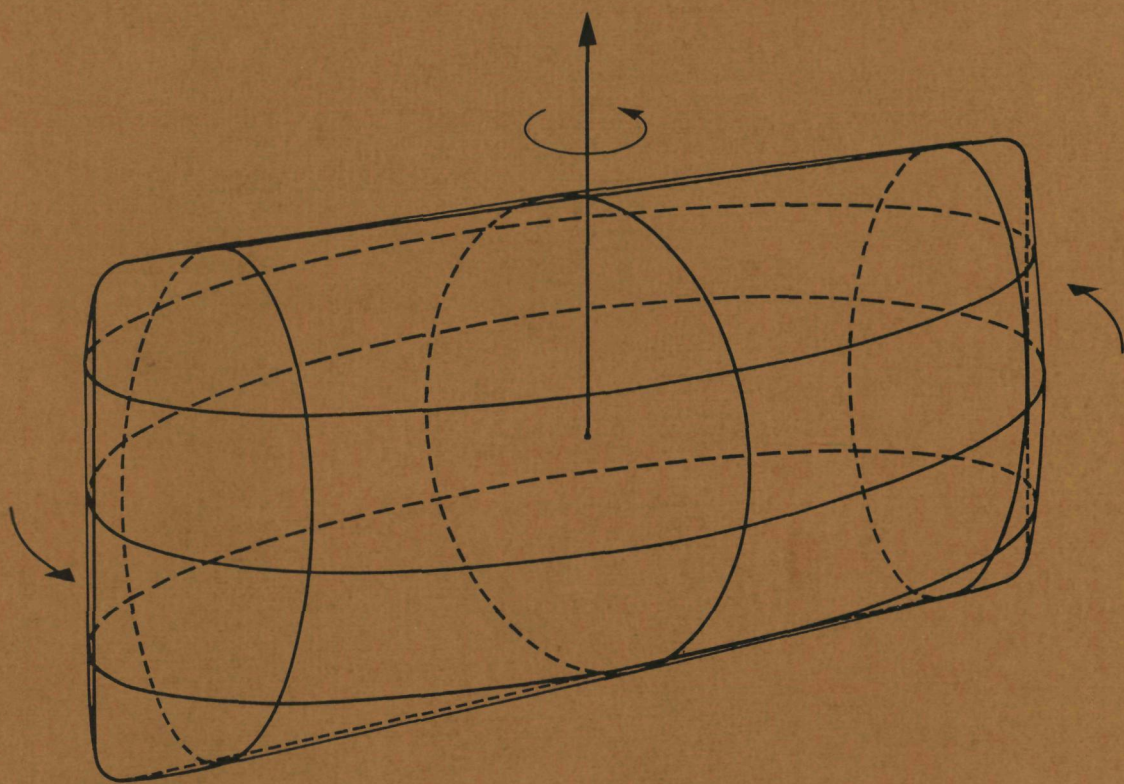
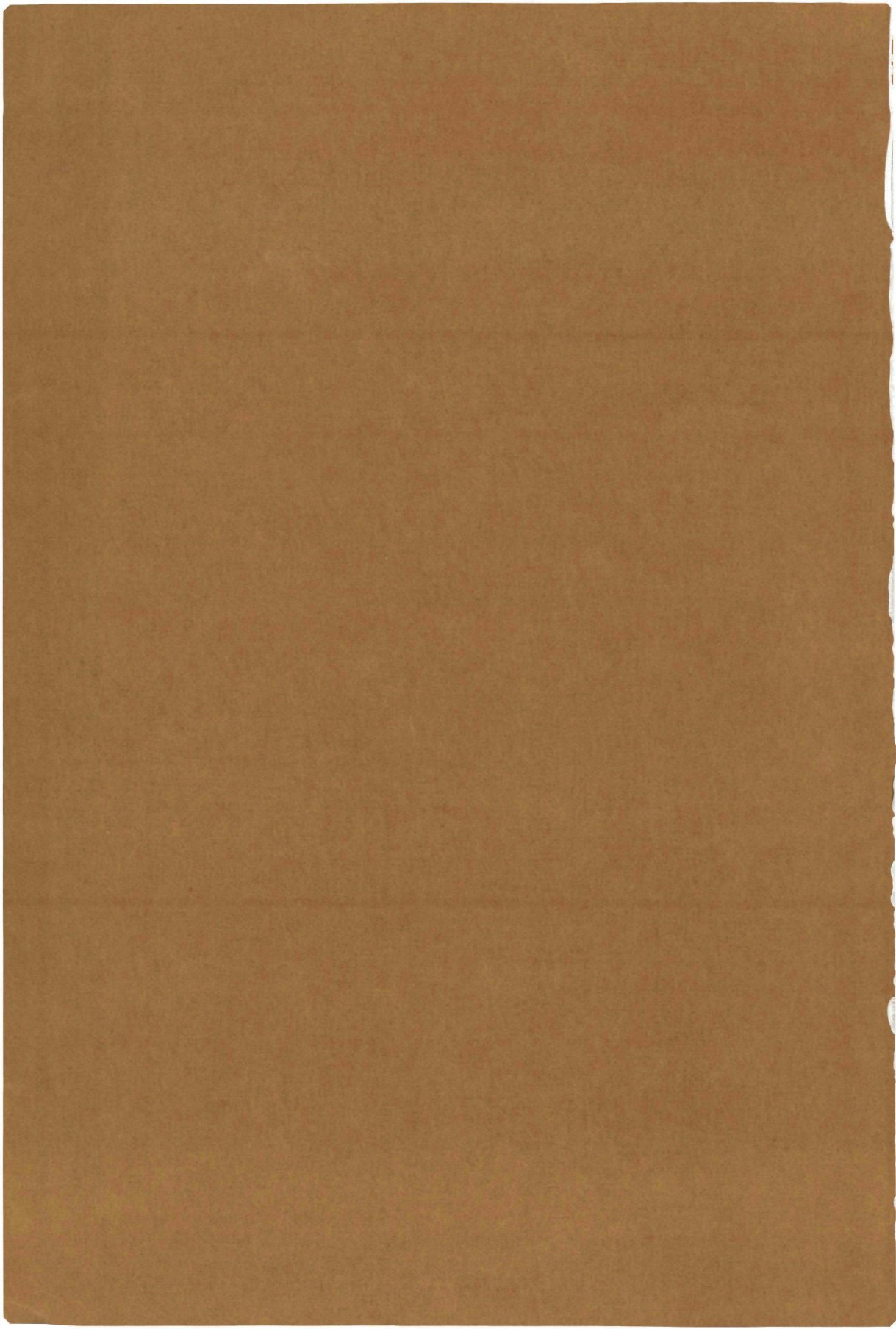


THE MIT BAGMODEL
AND SOME SPECTROSCOPIC APPLICATIONS



A. T. M. AERTS



**THE MIT BAGMODEL
AND SOME SPECTROSCOPIC APPLICATIONS**

Promotor:

Prof.dr.ir. J.J. de Swart

**THE MIT BAGMODEL
AND SOME SPECTROSCOPIC APPLICATIONS**

PROEFSCHRIFT

**TER VERKRIJGING VAN DE GRAAD VAN DOCTOR IN DE
WISKUNDE EN NATUURWETENSCHAPPEN
AAN DE KATHOLIEKE UNIVERSITEIT TE NIJMEGEN, OP GEZAG VAN
DE RECTOR MAGNIFICUS, PROF. DR. P. G. A. B. WIJDEVELD,
VOLGENS BESLUIT VAN HET COLLEGE VAN DECANEN
IN HET OPENBAAR TE VERDEDIGEN
OP WOENSDAG 20 JUNI 1979
DES NAMIDDAGS TE 4 UUR**

DOOR

ADRIANUS THEODORUS MARIA AERTS

GEBOREN TE ETTEN-LEUR

druk: Krips Repro, Meppel

Het doet me plezier iedereen, die op enigerlei wijze heeft bijgedragen aan het tot standkomen van dit proefschrift, hier te kunnen bedanken.

Met name Drs. P.J.G. Mulders ben ik heel erkentelijk voor de zeer prettige samenwerking in de afgelopen drie jaar, tijdens welke hij via talloze discussies in sterke mate de samenstelling van dit werkje beïnvloed heeft. Hij heeft mij nog meer aan zich verplicht door het manuscript nauwkeurig door te lezen en te verbeteren.

Ook wil ik hier de huidige en vroegere medewerkers van het Instituut voor Theoretische Fysika bedanken, met name Dr. M.J. Holwerda, Dr. W.L. G.A.M. van Neerven, Drs. G.J.M. Austen, Drs. E. van Beveren en Drs. A.N. Schellekens, voor de vele en leerzame gedachten wisselingen, waarvoor zij te allen tijde te vinden waren.

Bovendien wil ik hier de medewerkers van het Universitair Reken Centrum en de afdelingen Illustratie en Fotografie van de Fakulteit der Wiskunde en Natuurwetenschappen noemen.

Mijn dank gaat ook uit naar Wilma Lemmers-Vink, voor de snelle en zorgvuldige manier, waarop zij een berucht handschrift heeft omgevormd tot een heel wat prettiger leesbaar en druk-klaar manuscript.

Dit werk is een gedeelte van het onderzoekprogramma van de "Stichting voor Fundamenteel Onderzoek der Materie" (F.O.M.), welke financieel gesteund wordt door de Nederlandse Organisatie voor Zuiver Wetenschappelijk Onderzoek (Z.W.O.).

CHAPTER 1: Introduction and Survey	1
Table of quark flavors	21
CHAPTER 2: The MIT Bagmodel	22
I: The equations of motion and constraint	22
II: Spherical cavity approximation 1: Gross features	30
1: Valence quarks	33
2: Valence gluons	40
III: Spherical cavity approximation 2: Further refinements	51
1: Zeropoint energy	51
2: One gluon exchange	54
IV: The spherical cavity and SU(6,FJ)	68
1: Magnetic moment	72
2: Mean square charge radius	75
3: The axial vector coupling constant	76
CHAPTER 3: Q^6 Dibaryon States	82
I: Introduction	82
II: Classification of the N quark states	84
III: An approximation to the phenomenological bag hamiltonian	88
IV: Evaluation of the color magnetic and color electric terms	92
V: The mass operator and SU(6,FJ) tensor operators	96
VI: Numerical analysis and discussion	100
CHAPTER 4: The $Q^2\bar{Q}^2$ System	114
I: S-wave $Q^2\bar{Q}^2$ states	117
1: Basis states	117
2: The hamiltonian	123
II: Mesons and angular momentum	137

	Page
III: $Q^2\bar{Q}^2$ mesons and orbital excitations	147
1: Asymptotia (Large orbital angular momentum region)	150
2: Small orbital angular momentum ($0 < \ell < 3$)	160
IV: Results and discussion	170
1: Broad states	175
2: The QPC or 3P_0 model	180
3: Narrow states	189
Appendix A	201
Appendix B	202
References	203
Samenvatting	215
Curriculum Vitae	217

CHAPTER 1: INTRODUCTION AND SURVEY

High Energy Physics is a lively field of research in which in the past ten and odd years several major developments have taken place. Some of these were rather sudden, triggered by an unexpected experimental result. They decided on the direction of progress in a certain area of research and made whole new fields accessible for the majority of the physicists. Others were rather slow. They involved ideas which were at first only clearly successful in one particular case, but gradually gained a wider acceptance as a general principle through their ability to connect various phenomena to a common source.

Examples of important experiments, which opened up large new areas of research are the deep inelastic scattering experiments, performed by the SLAC-MIT group [Bl 74, Ga 77], those at Brookhaven and Stanford, which produced the first particles with (hidden) charm [Au 74], while the Stanford experiment also produced a new heavy lepton [Pe 75], and the neutrino-experiment at CERN, which revealed the presence of neutral weak currents [Ha 74, Bl 76]. Of the theoretical ideas one should mention the introduction of charm to account for the absence of strangeness changing neutral currents [Bj 64, Gl 70], the unification of weak and electromagnetic interactions, using the framework of spontaneously broken nonabelian gauge theories [Gl 61, We 67, Sa 68] and the introduction of color as source for the strong interactions [Na 66], involving the use of an unbroken nonabelian gauge theory [Fr 72].

It is with strong interactions that we shall deal primarily in this thesis. In this field no unambiguously established theory exists. There is however a large collection of ideas, known as quantum chromodynamics (QCD) [Fr 78, Ma 78], which are all related to the concept of color. The relation of the various ideas is often rather vague, as they range from abstract to phenomono-

logical, and in need of clarification but the whole of it presents a framework of increasing coherence, which is quite useful as reference.

One can be active in research e.g. by engaging in the field theoretic attempts to derive the spectral properties of the theory. This approach has proven particularly useful in situations, where perturbation theory is applicable. However, strong interaction data seem to indicate a lot of quite interesting nonperturbative aspects of the theory, an important one of which we will be dealing with extensively: confinement [Dr 77]. In trying to account for such a feature one has, due to lack of a fundamental solution, around which one can perturb weakly, to work at a more phenomenological level, to be able to work out the consequences. The usefulness of such an approach, when it is able to account for the available data, consists in its direct interaction with experiment. One can extrapolate the data into areas not yet covered, and thus provide guidelines for planning future experimental set ups, and at the same time tests for the consistency of the chosen formulation of the basic ideas. This way one obtains information about the validity of the initial assumptions and their importance for describing the phenomena. This information can then be used for improving the model by eliminating some of the arbitrariness, or for trying to find a more fundamental solution. In this thesis we will take the second approach and use the bagmodel of the hadron, the strongly interacting, "elementary" particle, as formulated by the MIT group [Ch 74, DeG 75]. We will show, how it is able to account for the static properties of most of the light hadrons, and describe some attempts to go beyond the familiar (from the standard point of view [Ko 69]) to more exotic ones, which are receiving quite some experimental attention nowadays [HI 78].

Let us mention the concepts and their support from the data, which provide the basic features of the MIT bagmodel. We stress again, the fact that the

final theory is still lacking, and that the present choice is, of course, somewhat biased, but, taking all the diverse pieces of evidence, circumstantial and unrelated though they may seem sometimes, together, the resulting picture is quite impressive in its ability to relate the various approaches. However, beyond bias, several distinct traits of the hadron are standing out quite clearly and should be accounted for properly by any model.

Flavor $SU(n,F)$. The hadrons, that are observed in the laboratories, can be labeled by a set of internal or flavor quantum numbers, reflecting strong interaction selection rules. Some flavors are harder to produce than others. To account for hadrons with mass less than 1.8 GeV [Hem 77, La 77], one needs three flavors: isospin (I, I_z) and strangeness (S) or equivalently hypercharge (Y). To account for all states below approximately 4.5 GeV one needs a fourth flavor [Aub 74, Aug 74]: charm (C) and the recently discovered narrow resonances [Hom 76, He 77] around 10 GeV seem to point at a fifth flavor: beauty (B). From the point of view of unification of weak and electromagnetic interactions also a sixth flavor would be welcome [Ha 78]. Flavor symmetry is only approximate ($n \leq 3$) and even badly broken for $n \geq 4$, as can be seen from the above quoted mass regions. Using the fact that specific interactions are only invariant under subgroups of $SU(n,F)$, one is able to derive relations within $SU(n,F)$ multiplets, that are rather well satisfied. U-spin invariance of the electromagnetic interactions relates the mass difference in isospin multiplets, as well as the magnetic moments. Isospin invariance yields mass relations between different isospin multiplets. Assuming $SU(3,F)$ invariance for the strong interactions one can derive the relative coupling strength within the multiplets for the meson-baryon vertices.

Quarks. [Da 76] Hadrons, as far as definite assignments can be made, display a conspicuous preference of some flavor multiplets above others [G1 77]. This

can be rephrased by assuming that baryons (half odd integer spin) are three quark- and mesons (integer spin) are quark-antiquark bound states [Ge 64, Zw 64]. The quarks then are spin 1/2 particles, that belong to the basic n -dimensional multiplet of $SU(n,F)$. Taking also other degrees of freedom (statistics) into account (see below) the lowest baryons can occur in an octet (8), $J^P = 1/2^+$, and a decuplet (10), $J^P = 3/2^+$ and the mesons in nonets (8+1) with $J^P = 0^-$ and 1^- . These states have a mass $M \approx 1$ GeV and therefore can be classified using exclusively $SU(3,F)$. For the higher mass hadrons more general quark configurations $Q^n \bar{Q}^m$ seem to exist, but always with $(n-m)$ a multiple of three or zero triality. We will discuss some examples of these extensively.

SU(6,FS). [Gu 64] Stimulated by the successful combination of spin and isospin in nuclear physics, one has also considered the merger of $SU(3,F)$ and the $SU(2,S)$ of spin into the larger approximate symmetry group $SU(6,FS)$ of flavorspin. (Only $2n = 6$ has been considered extensively until now.) In the 'naive quark model (QM)' scheme this amounts to the combination of an internal symmetry with a property, mechanical spin, which is only defined well for a quark at rest. Explicit dynamical assumptions are needed, such as the nonrelativistic motion of the quarks within the hadron and negligible residual interactions: the quark contributions are simply added to give the hadron contributions. In the naive QM these assumptions had to be interpreted as rules of the game, for they are hard to reconcile with the notion of heavy (because physical thus at some time producible, but not yet seen: $M \geq 3$ GeV) quarks, bound strongly in a light hadron (≈ 0.5 GeV). Equally strange is then also the invariance of spin S alone, witness the considerable coupling with the orbital momentum L and the tight interplay between L and S in the conservation of total spin J . Notwithstanding these dynamical difficulties, hadrons can indeed be accommodated in representations of

$SU(6,FS) \otimes O(3)$ [Gr 67], where $O(3)$ provides the representations for the spatial part of the quark and antiquark wave function labeling the orbital and radial excitations [Ho 73]. In this scheme most hadrons find their place: mesons occurring in 35- and 1- and baryons in 56- and 70-dimensional multiplets of $SU(6,FS)$ [Hem 77]. In the absence of spatial excitations, only the baryon 56-plet is realized, implying that the baryon wave function is completely symmetric under the permutation of the quarks. This means that the quarks have either additional quantum numbers or have other than Fermi Dirac statistics (see below).

Also at the level of $SU(6,FS)$ symmetry breaking one is rather successful [Gi 77]. All the magnetic moments of the lightest 56-plet can be calculated (assuming the additivity of quark properties), up to one common constant with good agreement. One can obtain mass relations within the $SU(6,FS)$ multiplets: one can relate members of different $SU(3,F)$ multiplets to one another [Be 64]. Applying $SU(6,FS)$ invariance to the meson-baryon couplings one can determine the relative strength with which entire $SU(3,F)$ multiplets contribute.

Using a frame in which the quarks have infinite momentum [Gi 74, He 75] in one direction, one can formulate a relativistic type of flavor spin symmetry: $SU(6)_W$ which describes the properties of the quarks that participate in interactions, so-called current quarks, to be distinguished from the above mentioned constituent quarks. Both descriptions are related by a unitary transformation: the 'Melosh transform' [Me 74]. This constituent-current quark connection is particularly useful to study the transition amplitudes for photo-induced reactions ($\gamma N \rightarrow N^*$). Expressing a few matrix elements in terms of known amplitudes, one can obtain the correct magnitudes and signs of quite some other transitions. Making further assumptions (PCAC) one can do the same thing with as much success for the axial current matrix elements in the case of pion induced reactions ($\pi N \rightarrow N^*$).

Color. [Gr 77] The statistics problem for the baryons can be solved at the cost of attributing three extra degrees of freedom: color [Gr 64] to the quarks. The quarks transform as a triplet under color $SU(3,C)$. The three being dictated by the fact that the smallest all-quark state observed in nature is a threequark state. It is the simplest possibility of providing the baryon wave function ($\sim QQQ$) with a part that is completely antisymmetric under quark permutation. The baryons behave as color singlets and also the $Q\bar{Q}$ configuration can occur as a singlet. Combining this with the absence from the spectrum of states like Q , Q^2 and Q^4 , one can generalize this feature and postulate that all observable objects in nature must be color-singlets. This allows only $Q^m\bar{Q}^n$ configurations [Fr 72] with $(m-n)$ an integer multiple of three. In this formulation color is an exact symmetry. The color degree of freedom is hidden or confined. This implies e.g. that the quarks have fractional electric charge. Consider a state like $\Delta^{++} \sim uuu$, build from three up-quarks (Table), up to color identical, which then must have charge $e_u = 2/3 e$. Similarly $\Delta^- \sim ddd$ and $\Omega^- \sim sss$. Quarks with this quantum number assignment are called Gell-Mann-Zweig quarks. One alternative is provided by the Han-Nambu [Ha 65] model, in which the quarks have integral charges. Since the color average over the charge of a particular flavor must be the same as in the GMZ model, this yields an electromagnetically broken variant of color. In the HN theory at some stage colored configurations like Q and Q^2 must be observed. It does not obey the confinement-postulate for all energies and implies a different kind of dynamics [Na 66].

Three other examples, in favor of color, are the two photon decay rate of the pion, the ratio R for production of hadronic final states to that for $\mu^+\mu^-$ in e^+e^- annihilation and the branching ratio for the decay of the heavy lepton τ into leptons and hadrons. The matrix element \mathcal{M} for the process $\pi^0 \rightarrow \gamma\gamma$ can be calculated using PCAC and depends on the flavor-color content

of the pion through the square of the electromagnetic charge

$\mathcal{M} \sim \langle \sum_1 Q_1^2 \rangle \simeq \frac{1}{2}$, where 1 runs over all flavors and colors. This relation is, due to the particular flavor wave function of π^0 , satisfied by both HN and colored GMZ quarks, but not by colorless quarks. It can only be satisfied if the number of colors is exactly three. In principle the two photon decay of pseudoscalar and tensor mesons, in fact any process, which is quadratic in the electromagnetic current, is fit to discriminate between the various color models through their charge assignment. However, one lacks both data, and a reliable way of calculating the matrix elements for other states than π^0 [Ch 77]. Recently, the photon-photon interaction has been observed at DESY in Hamburg [Be 79] in the process $e^+e^- \rightarrow e^+e^-e^+e^-$. One was able to extract from the data a new upper limit on the two-photon decay width of the $\eta'(958)$, which, because of the large flavor singlet content of the η' , is rather sensitive to the charge assignments of the quarks. In the context of phenomenological analyses the new bound $\Gamma_{\eta' \rightarrow \gamma\gamma} < 11.5$ keV favors GMZ quarks.

In e^+e^- annihilation the experimental value of R again favors colored GMZ quarks to the not-colored variety, and is compatible with HN quarks, provided the states around 4.0 GeV are interpreted as colored hadrons, as an alternative to the introduction of charm. Since the photon can carry away color, a spectroscopy ensues, which is rather different from what is observed.

An elegant generalization of HN is provided by the Pati-Salam gauge model [Pa 76], which includes charm and considers the lepton numbers as a fourth color. Baryon and lepton number nonconservation allows the free quarks to decay rapidly into leptons, thus escaping detection. Below the color threshold this model has properties rather similar to the fractional charge one, except for the above mentioned multiphoton features. However, there are strong indications that at least one more flavor (the fifth) and a new heavy

lepton exist, in which case the PS model needs extension, which will delete some of the nice symmetries.

Finally, the heavy lepton τ^- decays to its own neutrino ν_τ and a negatively charged weak boson W^- , which subsequently decays to an $e^- \bar{\nu}_e$, $\mu^- \bar{\nu}_\mu$ or $d' \bar{u}$ pair. The weak current couples equally strong to the electron-, the muon- and the quark-current [We 67, Sa 68]. However, since this result only depends on the weak and electromagnetic interaction properties of the quarks, the quark contribution to the τ^- decay final states is as many times stronger as the quark has additional (color) degrees of freedom. Allowing for small QCD and phase space corrections, the number of colors turns out to be three. For these reasons, the fractionally charged, colored quark model is at present in much better but not yet perfect shape, and we will adopt its assignments.

Deep inelastic scattering. [Cl 76, Mo 77, Ne 78] When the first spectroscopic indications of a new substructure have been established, the next step usually is to probe the constituent particles using high resolution equipment. The structure of the baryon-, and especially the nucleon-target is examined in deep inelastic scattering experiments, with charged lepton and neutrino beams. Only the outgoing lepton is observed (energy E' , angle Ω'). The advantage of using charged leptons is that one precisely knows the lepton-photon vertex from QED. One can check that up to high values for the momentum transfer $q^2 = -Q^2 < 0$ to the nucleon the relevant process is indeed one photon exchange. This means, that the response of the nucleon can cleanly be extracted from the doubly differential cross-section $\frac{d^2\sigma}{dE' d\Omega'}$. It can be represented, using Lorentz-, gauge- and parity-invariance, by two so-called structure functions W_1 , which can also be related to the longitudinal and transverse virtual photo-absorption cross sections σ_L and σ_T . From the experimental properties of the structure functions, one can verify that deep inelastic lepton nucleon

scattering, which takes place for $Q^2, W^2 \geq 3 \text{ GeV}^2$ (W is the effective mass of the hadronic final state), arises as the sum of incoherent elastic scattering of the leptons from charged, spin 1/2 constituents of negligible mass, originally called partons, which can consistently be interpreted as quarks. Using ν (\equiv energy loss of lepton in labframe), one finds experimentally, that $W_1 = W_1(\nu, Q^2)$ behaves in first approximation as a function $F_1(x)$ for large, variable Q^2 and x fixed, $x = Q^2/2M\nu$, a phenomenon known as scaling [Bj 69, We 75], which proves, that the parton-photon vertex, in fact up to 20 GeV^2 , has no strong Q^2 dependence, no form factor i.e. partons are structureless point particles. One can calculate the elastic quark-lepton scattering, where the quark carries fraction x of the nucleon momentum (transverse momenta are negligible to the lepton-proton C.M. momenta considered, this is the infinite momentum frame approximation where quark fraction x and scaling variable x can be identified). The data then give the distribution functions $f_Q(x)$ for x , the fraction of the total momentum carried by the quarks, for each flavor, in terms of which sum rules and normalization conditions can be checked. It emerges that the isospin and spin (on the basis of polarization experiments) degrees of freedom of the nucleon can be accounted for successfully by the three 'valence' quark distributions.

Glue. The baryon contains more than just (three valence) quarks. In case of quarks at rest inside the proton one would have a very sharp peak in the doubly differential cross-section at $x = 1/3$, signaling the quasi elastic scattering off three constituents with mass \approx momentum roughly a third of the baryon mass \approx momentum. In practice one sees a broad peak in this area, indicating the motion of quarks inside the restrictive nucleon volume. This means, that the quarks are subject to forces, which keep them inside. From the fact that up to high Q^2 one has not been able to produce a fractionally

charged object, one concludes that these forces are of a type different from hadron-hadron strong forces, mediated by massive mesons. One therefore assumes, that the quarks interact through exchange of a special type of bosons, named gluons. At short distances this interaction is observed to be rather weak. The gluons appear to be electrically neutral, because the valence quarks can saturate the nucleon charge and other nucleon quantum properties. Gluons can couple indirectly to the photon by means of internal conversion into a quark-antiquark pair. This higher order process is clearly present in the data. The quark momentum distribution functions $f_Q(x)$ should behave as x^α , $\alpha > 0$ for $x \rightarrow 0$, if the number of particles in the baryon is fixed to three quarks. One observes that $x f_Q(x) \rightarrow \text{constant}$, $x \rightarrow 0$. This means that for small x the $Q\bar{Q}$ pairs contribute according to $\frac{1}{x}$ which can be interpreted as a bremsstrahlung-like behavior of the gluons. The quark appears to be surrounded by a cloud of soft gluons, which sometimes convert into $Q\bar{Q}$ pairs, much like the electron is surrounded by photons. The presence of these neutral gluons is strongly confirmed by the fact that the momentum contribution of the charged constituents (Q and \bar{Q}) only adds up to roughly half the total baryon momentum. The emission and absorption of soft gluons (radiative gluon corrections) supplies the quark with a fine structure, which destroys the naive scaling behavior. One has observed these scaling violations [Ga 77], which are surprisingly small, but has not yet determined the precise behavior. Theoretically one can calculate these scaling violations, perturbatively, provided one makes assumptions concerning the quark-gluon (i.e. strong) interaction dynamics (see below). Just like quarks, also the gluons have not been observed in the laboratories. From this one might conclude that also gluons carry nonzero color charge, and therefore are confined to the inside of the hadron.

Deep inelastic scattering (cont'd). The charged lepton scattering data are confirmed by the neutrino scattering results. In this case one assumes that

the intermediate particle is the so-called weak boson, which couples to the weak hadron current. At present energies one can neglect Q^2 with respect to M_W^2 , the predicted mass of the weak boson W and again extract full information about the nucleon vertex. Since parity is not conserved in weak interactions, the cross sections for transverse left- and righthanded virtual photo-absorption are no longer identical: $\sigma_L^T \neq \sigma_R^T$, which implies the existence of a third structure function: $W_3 \sim \sigma_R^T - \sigma_L^T$. W_3 has a different sign for particles and antiparticles, and this allows one to separate the contribution of the particles from that of the antiparticles. Indeed, for $x > 0.4$ one measures only contributions of valence quarks which for $x < 0.4$ become supplemented, and for $x \rightarrow 0$ dominated by those of the isoscalar sea of $Q\bar{Q}$ pairs. One finds $f_{\bar{Q}}(x) \rightarrow f_Q(x)$ for $x \rightarrow 0$. Another property of the quarks, their fractional charge assignment can, apart from the indirect tests via sumrules, also be examined more directly. One shoots very fast electrons on a nucleon target and measures the charge distribution of the fast pions, that come out in the incident electron direction. The assumption is that these pions contain the quark that is kicked out of the target by the electron. One finds a positive to negative charge ratio of 5 : 1 for a proton target (theoretically 8 : 1) and of 1.5 : 1 for a neutron (2 : 1), which is consistent with GMZ assignments, allowing for sea quark dilution of the ratio [Ma 76, Ma 77].

Electron-positron annihilation. [Fe 77] Closely related to the deep inelastic lepton-nucleon scattering experiments, is the production of hadrons in electron positron collisions. As can be verified by studying processes like $e^+e^- \rightarrow p\bar{p}$, the important mechanism is e^+e^- annihilation into a virtual photon which couples to the same hadronic current as participates in deep inelastic lepton scattering: the electromagnetic quark current. A momentarily free quark-antiquark pair is created, which later on evolves into hadrons. These quarks have a

pointlike coupling to the photon, just like e.g. the muons, and the ratio R for hadron to muon production in e^+e^- should become constant for large enough Q^2 (q^2 is timelike in this process: $q^2 = Q^2$). Below the charm threshold

(≈ 4 GeV) only u, d and s quarks contribute and the prediction is

$$\sigma(e^+e^- \rightarrow Q\bar{Q} \rightarrow \text{hadrons}) / \sigma(e^+e^- \rightarrow \mu^+\mu^-) = \sum_1 e_1^2 = 3(4/9 + 1/9 + 1/9) = 2$$

($1 = u, d, s + \text{colors}$). Above the charm threshold we have $R = 3 \frac{1}{3}$ due to the

charm contribution. Experimentally R is approximately constant but systematically high w.r.t. the theoretical values (30% for SPEAR, 10% for PLUTO data, which both have sizeable systematic errors).

Another signal for the $Q\bar{Q}$ pair creation, which is extensively studied at present, comes from the fact, that for $5 \text{ GeV} \leq \sqrt{Q^2} \leq 10 \text{ GeV}$ hadrons are mainly produced within two opposite pointing cones (back to back jets) of opening angle δ , which becomes smaller for increasing energy [Fr 78, El 78]. The hadron dynamics appear to be such that the momentum components transverse to the cone/jet axis are sharply restricted and that the distribution of the longitudinal momenta depends on the fraction of the total momentum, and only weakly on the C.M. energy $\sqrt{Q^2}$. The jets have an angular distribution w.r.t. the electron direction (angle θ) of the form $(1 + \cos^2 \theta)$ which is characteristic of the production of a pair of spin 1/2 particles. Jets are also observed in hadron-hadron collisions, where they also appear on the average back to back, at large angles, as well as in lepton-hadron scattering. The origin of the former is speculated to be perhaps the elastic scattering of two fast quarks inside the hadrons. The remnants of the hadron decay in the beam direction. In the latter the lepton is supposed to kick out the quark. In the case of e.g. νp scattering the W^+ boson changes a d-quark into a u-quark and measurements of the charge excess in the target (~ 2 u-quarks) and the W^+ direction (\sim u-quark) show the former to be approximately twice as large as the latter. The relation between the hadrons in a jet and the quark that

originates them can be expressed in terms of so-called quark-parton fragmentation functions. In the infinite momentum frame of the quark, which is kicked out by a lepton or created by a photon these functions give the probability that the quark 'decays' into some hadron h , which has a fraction z , $0 \leq z \leq 1$ of the quark momentum. In practice there will be also a weak dependence on Q^2 and the transverse momentum component k_T . The fragmentation functions can be measured in so-called inclusive processes like $\ell + N \rightarrow \ell' + h + \text{anything}$ and $e^+ e^- \rightarrow h + \text{anything}$. Only in neutrino induced reactions they are directly measurable. Comparison shows that these functions behave consistently for the mentioned processes [Pe 78].

Confinement. The persistent negative results of the searches for fractionally charged objects, such as quarks and other nonzero triality configurations have inspired, apart from the integrally charged, liberated quark models, also the opposite notion: color-confinement [Dr 77]. It is the statement, that the dynamics of colored objects is such, that it requires an infinite amount of energy to split a not colored system into two colored fragments. The interaction energy of the fragments increases with their separation. This results, of course, in a highly unstable situation and at some point there will be sufficient energy in the system to make other processes possible, e.g. the creation of $Q\bar{Q}$ pairs (sparks) which will shield the initial interaction: the system breaks up into two smaller color singlet systems, thereby reducing the effective color separation.

A nice illustration of this phenomenon [No 78] can be seen in the charmonium spectrum, ascribed to the charmed quark and antiquark system. It consists of a number of bound states (bindingenergies up to .9 GeV!) below the production threshold for particles with bare charm at about 3.7 GeV and a number of resonances above it, which can be accounted for by a $Q-\bar{Q}$ interaction

energy which is roughly linear in the $Q-\bar{Q}$ separation. Another illustration [Ja 77] of the consequences of confinement is provided by the occurrence of particles in families, sharing the same quantum numbers for flavor, whose total spin J and mass M obey the rule: $J = \alpha' M^2 + \alpha_0$. The intercept α_0 is characteristic of each family, but the slope α' of these linear 'Regge' trajectories is universal for all Q^3 and $Q\bar{Q}$ systems. The trajectory joins the orbital or L excitations of a specific multiquark system. One has $J = J(L)$. Since the data for charm trajectories are meagre we will restrict ourselves to the light flavors u , d and s , where the trajectory already runs straight for $L = 2$ or 3 . Consider a meson consisting of a quark and an antiquark. To acquire higher L values the meson has to rotate faster. Due to the increasing centrifugal barrier the $Q-\bar{Q}$ separation will become larger. When the forces are of the conventional strong type, originating from the exchange of massive hadrons, which has a limited range, the quarks will very soon come apart, after a maximum value for J is reached. No confinement! One finds $J = 1$ or 2 for O.B.E. type models. The Regge trajectory for the delta still continues at $J = 15/2$ without an indication of impending changes. This behavior is realized in e.g. the dual string model [Re 74] where the length ℓ ($\sim Q-\bar{Q}$ separation) of the rotating string is proportional to the mass ($\ell \sim M$). The string ends have approximately the velocity of light, so that the configuration has maximal angular momentum, whereas the relative momentum p will also be proportional to M and $L \sim p\ell \sim M^2$. Increasing L then means, that the rotation frequency ω will go down: $\omega \sim \frac{1}{\ell} \sim \frac{1}{M}$ and that the system will become heavier, instead of flying apart at once. These high mass states are also, though less, unstable through the 'spark' mechanism, indicated above. Emitting mainly mesons, which lower L step by step the massive hadron cascades into stability. The excited system, however, does exist long enough to allow detection. The universality of the slope α' is also an indication of the fact that the quarks

can only carry a small portion of the energy and angular momentum. First, mesons and baryons contain a different number of quarks and secondly, flavor breaking effects in α' would be clearly visible, if quark contributions are important. These examples support the idea, that color acts as a source for the strong interaction between groups of quarks. There is an increasing effort to derive confinement in 3+1 dimensions, including nonperturbative effects or otherwise, but no convincing results have been obtained so far [Ca 77, Th 78, Le 78]. There exist, however, examples in 1+1 dimensions, where confinement occurs and where the mass is proportional to the separation [Ko 74, Man 76]. These models may be of use when the effective number of dimensions of the physical system is reduced by 2.

On the basis of these experimental data and theoretical ideas we can compose the following picture of the baryon. It is an extended object, deriving its flavor and spin properties from three 'valence' quarks. These quarks are surrounded by a cloud of gluons (and $Q\bar{Q}$ pairs), which are electrically neutral. Gluons and quarks have color degrees of freedom, which act as a source for strong interactions. This interaction is very weak for small separations: quarks and gluons enjoy 'asymptotic freedom', and becomes very strong for increasing distance between two colored objects: confinement. This picture is readily transplanted to any color singlet system. One even entertains speculations on systems containing only 'valence gluons' and no quarks at all [Fr 75, Ja 76, Ro 77].

What at this point still is lacking is a framework for the dynamics governing the strong interactions, within which one can settle questions like if quarks are seen to move freely for short times, what keeps them from moving apart? and, what makes colorless states lighter than colored ones?, or more detailed ones like: what makes the Δ heavier than the N ? and,

why don't we see lowlying flavor exotics? and interpret other experimental findings.

The most simple, and at the same time most promising theory of strong interactions is at present the nonabelian gauge field theory in colorspace [Ma 78]: Quantum Chromodynamics, QCD for short. It follows from the assumption, that color is not only globally conserved but also locally, completely analogous to the way in which the very successful QED theory follows from the local conservation of electric charge. The important difference is, that in QED the electric charge is an additive quantity: QED is invariant under the abelian symmetry group $U(1)$, whereas in QCD the color-charge is non-additive: QCD is invariant under the nonabelian group $SU(3,C)$. The quarks belong to the basic triplet of $SU(3,C)$ and the forces are therefore mediated by an octet of massless, spin 1 gauge bosons, called gluons. The gluons also carry color charge and can couple among themselves. This feature gives rise to two peculiar phenomena, which are thought to be two aspects of the same thing [Dr 77]. From QED one is familiar with the fact that the charge e , seen from distances larger than twice the compton wave length of the electron, λ_e , is smaller than the effective charge measured at smaller distances. This is due to the presence of virtual electron-positron pairs originating from the zero-point quantum fluctuations of the electromagnetic field strengths. The bare electron, charge e_0 , is thus surrounded by e^+e^- pairs, from which it attracts the positrons and repels the electrons. The vacuum becomes polarized and the electron charge is shielded. The coupling strength (e) grows when measured at smaller distances. What happens at very short distances is, due to the breakdown of perturbation theory and the experimental resolution, not known. In QCD the bare color charge of a quark is not only surrounded by $Q\bar{Q}$ pairs but also by gluons, which revert the screening of the $Q\bar{Q}$ pairs into a net

antiscreening: the effective colorcharge of the quark decreases at shorter distances and the quarks are asymptotically free: they only have a very 'weak' interaction at short distances. One could say that the colorcharge of the quark is spread into the field around it and the quarks, close together, only see a small remnant. But one can also look upon this situation from another angle: the effective charge grows, when measured at increasing distances. About this limit not very much is known, since one cannot use perturbation theory around the free quark solution here. One hopes, however, that the resulting, strong coupling will realize color confinement. There are some hints, that confinement may indeed come about. One can show that, in the case of two static oppositely colored sources the colorfluxlines tend to become collimated, when the separation increases and eventually will be concentrated in a thin flux tube connecting the two charges. This property can then be translated in an interaction energy $\sim r$, the intersource distance, or in a string type description of the system. The color charges appear to be acting as condensor plates [Ko 74].

At present calculations with QCD [E1 78] are only possible in the asymptotic free region. There, to lowest order in the coupling g , where only the pointlike quarks contribute, the theory gives the exact scaling mentioned above. Including the next orders in g , one obtains radiative corrections of the form $\ln q^2$, which violate the naive scaling law, and which provide a more quantitative and strict test for the theory. These violations are experimentally established and consistent with QCD predictions. Perturbation calculations i.e. calculations involving quarks and gluons, can also be extended to decay or scattering processes in which quarks or gluons appear to be emitted from the hadron, provided one replaces the quark or gluon with a quark or gluon jet in the real world, cf. the $Q\bar{Q}$ jets in e^+e^- annihilation. Especially the thus expected production of gluon jets at higher energies is a firm test for the theory.

One has also made use of the relatively weak coupling of the gluons to the quarks, when these are sufficiently close to each other inside the hadron to investigate the spin dependence of the hadronmass [DeR 75, DeG 75]. Already at the level of one gluon exchange one can account for the observed systematics, in terms of the signs and the order of magnitude of the splitting.

From this we conclude, that we have reasonable grounds to take QCD as a description of the dynamics of quarks and gluons inside the hadron. To study this composite particle, we also need a well defined description of the hoped for confinement properties of the theory, as long as these are not extracted from the theory itself. Considering its present status, it is best to put in a confinement mechanism by hand. One can do this by taking advantage of the fact that one also has to find a relativistically covariant description of an extended system and associate an energy with the extension of the system. While putting a cost on extension, and thereby limiting the size of the system, one at the same time eliminates the long wave lengths avoiding the unsolved infrared- and strong coupling problems. There are three simple measures of such an extension [Jo 76]. They are all generalizations of the classical, relativistically invariant action, describing the motion of a massive point particle, given by

$$W = - m \int dt (1 - \vec{v}^2)^{1/2}$$

where \vec{v} is the velocity and m the mass of the point particle. This action was generalised by Nambu [Na 70], to describe an object with a one dimensional spatial extension. It is the continuum limit of a linear chain of geometrical points, the so-called string

$$W_{st} = - T \int dt \int ds (1 - \vec{v}_\perp^2)^{1/2}$$

where ds is the length of the line element at some point along the string and

\vec{v}_\perp is the transverse velocity at that point. The constant T, which has dimension energy (or mass)/length, is the proper tension of the string. The quantization of this Nambu string yields the excitation spectrum of the dual resonance model [Re 74]. The tension T satisfies $T = 1/2\pi\alpha'$, where α' is the universal slope of the linear Regge trajectory in the dual resonance model. W_{st} depends only on that part of the internal motion which is transverse to the local spatial extension of the string. Classically, only these motions contribute to the dynamics of the system. The longitudinal expansion of the line element does not change the kinetic energy and is interpreted as potential energy.

The generalization to a two dimensional geometrical aggregate of points had, prior to Nambu, already been proposed by Dirac [Di 62], who suggested the following action for the surface (membrane, if open, or bag, if closed)

$$W_S = - \sigma \int dt \int d^2S (1 - \vec{v}_\perp^2)^{1/2} .$$

Here d^2S is the area of the surface element and \vec{v}_\perp is its velocity in the transverse direction. Now, σ is a surface tension of dimension energy/area and again only \vec{v}_\perp contributes to the dynamics of the system. It is by adding W_S to the QCD lagrangian, that the Budapest group generates confinement [Gn 75].

The third and last step in this sequence is to consider the geometrical action associated with a three dimensional set of points, a volume, also called a bag:

$$W_V = - B \int dt \int d^3r .$$

Here B is for dimensional reasons a (vacuum) pressure. Because $\int dt \int d^3r$ is a Lorentz invariant, four dimensional volume element, no transverse velocity factors occur. The volume action has no dynamics of its own. Nevertheless, the addition of W_V to a system, which already has dynamical degrees of freedom,

can have important physical consequences, because it can be interpreted as a generalized potential energy. The differences between the various possibilities is best demonstrated with a 1 + 1 dimensional example. There are two possible actions in this case; one for a masspoint or equivalently a surface point with tension: $W = - m \int dt \left(1 - \left(\frac{dx}{dt} \right)^2 \right)^{1/2}$, and one for a volume: $W = - B \int dt \int dx$. The combined action:

$$W = - m \int dt \left(1 - \left(\frac{dx_1}{dt} \right)^2 \right)^{1/2} - m \int dt \left(1 - \left(\frac{dx_2}{dt} \right)^2 \right)^{1/2} - B \int dt \int dx$$

then describes a system of two massive particles ($m_1 = m_2 = m$), which enclose a one-dimensional volume, or equivalently ($m \leftrightarrow \sigma$) a one-dimensional bag with surface tension, under vacuum pressure. The hamiltonian becomes

$$H = (p_1^2 + m^2)^{1/2} + (p_2^2 + m^2)^{1/2} + B |x_1 - x_2|$$

and we find that the particles are bound together by the long range vacuum pressure potential. We find, that one can take $B > 0$ in both the action, and the hamiltonian: it yields a system of two free particles in both cases.

Taking m to zero in the hamiltonian yields a system of two massless particles, bound by the pressure. However, taking $m = 0$ in the action just leaves the volume term, with which no dynamics can be associated: it describes an empty bag. We find that two completely different systems emerge. The MIT formulation of the bagmodel adds W_V to the QCD action, thereby avoiding the introduction of new dynamical degrees of freedom to the theory. This procedure has the drawback, that one obtains a constrained dynamical system, which severely hampers quantization.

We will study the MIT bagmodel in Chapter 2, in a simple approximation and apply it to the static properties of the light hadrons. In Chapter 3 we will study another approximation, which is better adapted to the study of all-quark states with baryon number $B = 2$ to 6. Finally in Chapter 4 we

will investigate the spectroscopic properties of the $Q^2\bar{Q}^2$ system. Especially multiquark systems like Q^{3B} , $B > 1$, and $Q^2\bar{Q}^2$ could not be treated in the old, naive quark model and were called exotic. It is through the MIT bagmodel that the study of these exotic systems has become feasible.

Quark	Q	B	I	I_z	S	C	T	B
u	2/3	1/3	1/2	1/2	0	0	0	0
d	- 1/3	1/3	1/2	- 1/2	0	0	0	0
s	- 1/3	1/3	0	0	- 1	0	0	0
c	2/3	1/3	0	0	0	1	0	0
t	2/3	1/3	0	0	0	0	1	0
b	- 1/3	1/3	0	0	0	0	0	- 1

Table. Quark flavors and the associated quantum numbers: electric charge (Q), baryon number (B), isospin (I), and its z-component (I_z), strangeness (S), charm (C), truth (T) and beauty (B). At present only the t-flavor has not been found.

CHAPTER 2: THE MIT BAGMODEL

In this chapter we will cast the underlying dynamical assumptions of the MIT bagmodel [Cho 74] in a Lagrangian form and examine some of the simplest consequences [Chp 74, DeG 75].

I. The equations of motion and constraint [Jo 75, Jo 76]

In our description of the hadron, we will take the quark field (denoted by a spin $S = 1/2$ Dirac field $\psi(x)$) and the gluon field (denoted by an $S = 1$ vector field $A^\mu(x)$) as fundamental fields. Since quarks and gluons are supposed to occur only inside the physical hadron, their fields will also be defined only there. In this respect the bag theory differs from conventional (space time) field theories, such as QED where the electron and photon fields are defined everywhere. Space integrations in the bag action only extend across the bag volume. To elucidate this feature and to facilitate forthcoming technical manipulations, we will introduce the auxiliary function $\theta_B(x)$ which has the following properties:

$$\begin{aligned} \theta_B(x) &= 1 && \text{inside the bag} \\ &= 0 && \text{outside the bag} \end{aligned} \tag{1}$$

Function $\theta_B(x)$ only depends on the coordinates of the bag boundary, not on its velocities. θ_B has no dynamics of its own. Introducing θ_B in the Lagrangian, we can extend the integration volume over all space time in any Lorentz frame. Another property of θ_B is the following:

$$\partial_\mu \theta_B(x) = n_\mu \delta_S(s) \tag{2}$$

where n_μ is the unit, spacelike, inward drawn normal to the surface of the bag. In the instantaneous restframe of a point on the surface n_m is the usual unit space normal, while $n_0 = 0$. The surface δ -function $\delta_S(x)$ satisfies:

$$\int d^4x \delta_S(x) f(x) \equiv \int (d^3x)_S f(x) = \int dt \int d^2S (1 - \vec{v}_T^2)^{1/2} f(x)$$

The lefthandside expression is Lorentz covariant. In the righthandside one a noncovariant parametrization of the surface has been chosen, which is compensated by the factor $(1 - v_T^2)^{1/2}$, which depends on the transverse velocity \vec{v}_T of the surface element.

- Quarks -

We will introduce the bag action step by step. Let us start from the action for a free, massive Dirac particle:

$$W = - \int d^4x \left\{ \frac{1}{2} \bar{\psi} \overleftrightarrow{\partial}_\mu \gamma^\mu \psi + m \bar{\psi} \psi \right\} \quad (3)$$

using $a \overleftrightarrow{\partial}_\mu b = a(\partial_\mu b) - (\partial_\mu a)b$ for the derivative operator. For the metric and γ matrix-definition see appendix A. From this action we obtain the Dirac equation:

$$(\gamma^\mu \partial_\mu + m)\psi = 0$$

Instead of $\gamma^\mu \partial_\mu$, equivalently $\gamma \cdot \partial$ and $\not{\partial}$ will be used. The Dirac field here can in principle be defined everywhere in the 3 + 1 dimensional space.

The second step is to generate confinement in a relativistically covariant way. To achieve this a 'vacuum pressure' is included, which is a Lorentz scalar:

$$W = \int d^4x \alpha_0 = - \int d^4x \left[\left\{ \frac{1}{2} \bar{\psi} \overleftrightarrow{\partial} \cdot \gamma \psi + m \bar{\psi} \psi + B \right\} \theta_B + \frac{1}{2} (\bar{\psi} \psi) \delta_S \right] \quad (4)$$

Requiring that the action be stationary against variations in $\bar{\psi}$, we obtain the following Euler-Lagrange (EL) equation:

$$\theta_B (\not{\partial} + m)\psi + \frac{1}{2} \delta_S (\not{\partial} + 1)\psi = 0$$

which implies both the free quark equation of motion

$$(\not{\partial} + m)\psi = 0 \quad \text{inside the bag} \quad (5)$$

and the constraint equation or boundary condition:

$$\not{n} \psi = - \psi \quad \text{on the surface} \quad (6)$$

For the conjugate field we find similarly

$$\bar{\psi} (\not{\partial} - m) = 0 \quad \text{inside the bag, and} \quad (7)$$

$$\bar{\psi} \not{n} = \bar{\psi} \quad \text{on the surface} \quad . \quad (8)$$

Equations 5 to 8 correspond to the situation, in which confinement is realized by a scalar potential [Bo 68]. The quarks are endowed with an effective mass m inside a finite region R of space and with a mass M elsewhere. One takes $M \gg m$. Demanding continuity of the upper and lower components of the quark spinor wave function then gives a set of equations, which reduce to eqs (6) and (8) in the limit $M \rightarrow \infty$, in which the quarks become confined to region R (cf. also [Cho 74]). Combining eqs (5) and (7) we find that the quark current is locally conserved inside the bag: $\partial_{\mu} j^{\mu} = \partial_{\mu} (i \bar{\psi} \gamma^{\mu} \psi) = 0$. Eqs (6) and (8) state that there is no current across the boundary

$$\begin{aligned} n_{\mu} j^{\mu} &= n_{\mu} (i \bar{\psi} \gamma^{\mu} \psi) = i (\bar{\psi} \gamma \cdot n) \psi = i \bar{\psi} \psi \\ &= i \bar{\psi} (\gamma \cdot n \psi) = -i \bar{\psi} \psi = 0 \end{aligned} \quad (9)$$

Stability against small excursions of the surface i.e. against small changes of the volume yields:

$$\frac{1}{2} \bar{\psi} \not{\partial} \cdot \gamma \psi + m \bar{\psi} \psi + B = \frac{1}{2} \partial^{\mu} (n_{\mu} \bar{\psi} \psi) \quad \text{on the surface} \quad (10)$$

To obtain the righthandside, one has to use the δ_S -definition in terms of θ_B : $(\bar{\psi} \psi) \delta_S = n^{\mu} (\bar{\psi} \psi) (\partial_{\mu} \theta_B)$. With the aid of eqs (5) to (8), eq (10) reduces to:

$$n_{\mu} \partial^{\mu} (\bar{\psi} \psi) = 2B \quad \text{on the surface} \quad . \quad (11)$$

We note here, that what would have been an equation of motion for the surface variables becomes an equation of constraint for the constituent fields due to the absence of a surface kinetic energy term. The energy and momentum content of the system can be summarized in the stress tensor

$$T^{\mu\nu} = \theta_B \left\{ \frac{1}{2} \bar{\psi} \gamma^{\mu} \not{\partial}^{\nu} \psi + g^{\mu\nu} \mathcal{L}_0 \right\} = \theta_B \left\{ \frac{1}{2} \bar{\psi} \gamma^{\mu} \not{\partial}^{\nu} \psi - g^{\mu\nu} B \right\} = T_Q^{\mu\nu} - g^{\mu\nu} B \quad (12)$$

which satisfies

$$\partial_{\mu} T^{\mu\nu} = 0 \quad \text{inside the bag, and therefore} \quad (13)$$

$$P^{\nu} = \int dV T^{0\nu} \quad \text{is a conserved, i.e. constant quantity.} \quad (14)$$

We find that all the momentum is carried by the quarks, while the energy:

$$E = \int dV \left\{ \frac{1}{2} \bar{\psi} \gamma^0 \not{\partial} \psi + B \right\} = E_Q + BV \quad (15)$$

contains contributions from both the quark fields and the volume. One can show, that in case the bag is boosted to a velocity \vec{v} in the limit $v \rightarrow 1$, also all the energy will be carried by the quarks. The volume term vanishes due to the Lorentz Fitzgerald contraction. The scalar potential confinement-mechanism only gives a $T_Q^{\mu\nu}$ part and is not Lorentz covariant. For fixed E, the size of the bag is limited by the volume term in eq (15). On the surface eq (13) develops into

$$n_{\mu} T^{\mu\nu} = \frac{1}{2} \partial^{\nu} (\bar{\psi}\psi) - n^{\nu} B = 0 \quad . \quad (16)$$

Because $\bar{\psi}\psi = 0$ on the surface, its derivative is proportional to the normal

$$\frac{1}{2} \partial^{\nu} (\bar{\psi}\psi) = n^{\nu} P_Q = n_{\nu} T_Q^{\mu\nu} \quad . \quad (17)$$

Since, in the instantaneous restframe, this equals the momentum flow normal to the surface, P_Q is the pressure exerted by the quarks on that surface, going with the concept of stress tensor. From eq (11), we conclude that $P_Q = B$ which can be interpreted as the statement, that the quarks pressure, which is directed outwards (quarks are fermions) is balanced by the vacuum pressure, which keeps the volume from becoming too large. The origin of B is unclear. Similar to B, also P_Q is a Lorentz scalar.

Eq (11) is nonlinear in the quark fields and can be interpreted as a definition of the surface coordinates in terms of the quark fields. It is a local equation which preserves causality. The surface variables of the bag are no new dynamical degrees of freedom. This can also be seen from eq (15), where

no reference is made to time derivatives of these variables: they do not contribute to the energy. We furthermore see, that the surface term $W_S = \frac{1}{2} \int d^4x (\bar{\psi}\psi)\delta_S = \frac{1}{2} \int dt \int d^2S \sqrt{1 - v_T^2} (\bar{\psi}\psi)$ does not contribute to the extremized Lagrangian density, by virtue of eq (9). Its presence is however needed to obtain a consistent set of EL equations. In case of omission, we obtain, next to eqs (5) and (7) the boundary conditions

$$\left. \begin{aligned} n \cdot \gamma \psi &= 0 \\ \frac{1}{2} \bar{\psi} \not{\partial} \cdot \gamma \psi + m \bar{\psi} \psi + B &= 0 \end{aligned} \right\} \text{ on the surface} \quad \begin{array}{l} (6a) \\ (11a) \end{array}$$

Combining eq (11a) with eqs (5) and (7) yields: $B = 0$. This implies that confinement can only be maintained by introduction of additional (boson) fields for which the quarks can act as a source. These fields will then completely determine the motion of the boundary. One can verify, that eqs (6a) and (11a) also follow from eq (4), provided one lets $v_T = 1$ in the surface term. The boundary moves with the speed of light. In this case eq (6a) becomes $\psi = 0$ on the surface: the slowly (w.r.t. $v = 1$) moving quark will never reach the surface. The boson fields, dragged along by the quarks, and also confined, will be reflected at the opaque boundary and cause the source-quark to turn around before it gets there. An equivalent result is obtained, when one lets the quarks become very heavy: $m_Q \rightarrow \infty$. This picture is advocated by the Budapest group [HaK 78]. It does not seem to cover some of the simplest cases, such as the spherical bag containing massless quarks, treated in detail below. The boundary condition $\psi = 0$ is much too restrictive for the linear Dirac equation.

- Gluons -

At this level still one quark bags can occur. To eliminate these, we have to take a third step, which is to introduce the gluon fields. This can be done in the standard Yang-Mills-like way by noting, that the quarks have $SU(3,C)$

color quantum numbers, which have been ignored in the above discussion, and replace all ordinary derivatives in eq (4) by gauge covariant ones and adding a kinetic term for the gluon gauge fields in order to make the total Lagrangian locally gauge invariant:

$$\partial_{\mu} \rightarrow (D_{\mu})_{ab} = \partial_{\mu} \delta_{ab} - i g (F_c)_{ab} A_{c\mu} \quad (18)$$

The covariant derivative $(D_{\mu})_{ab}$ acts on a field, which transforms according to an n-dimensional irreducible representation (irrep) of $SU(3,C)$ and is represented by an $(n \times n)$ matrix in color space (a and b are color indices: $a, b = 1, \dots, n$). The identity matrix is denoted by δ_{ab} , and $(F_c)_{ab}$ denotes the n-dimensional representation of one of the eight ($c = 1, \dots, 8$) generators of $SU(3,C)$. The F_c matrices have the following properties:

$$[F_a, F_b] = i f_{abc} F_c \quad \text{Tr } F_a F_b = \frac{1}{2} \delta_{ab} \quad a, b, c = 1, \dots, 8 \quad .$$

Here the f_{abc} are the structure constants of $SU(3,C)$, completely antisymmetric w.r.t. interchange of any pair of indices. (See also appendix B.) In the three-dimensional irrep of the quark, we have $F_a = \frac{\lambda_a}{2}$, where λ_a is one of the eight Gell-Mann matrices. Furthermore, $\{F_a, F_b\} = \frac{1}{3} \delta_{ab} + d_{abc} F_c$ in this case. The constants d_{abc} are completely symmetric under the interchange of indices. In the 3^* irrep of the antiquark, we have the representation: $F_a = -\frac{\lambda_a^*}{2}$.

Finally, acting on the gluon octet irrep the matrix elements of the generator become $(F_a)_{bc} = -i f_{abc}$. The antisymmetric field tensor, corresponding to the gluon vector field A_c^{μ} is given by:

$$G_a^{\mu\nu} = \partial^{\mu} A_a^{\nu} - \partial^{\nu} A_a^{\mu} + g f_{abc} A_b^{\mu} A_c^{\nu}$$

where the third term is a consequence of the nonabelian nature of the color symmetry.

- Quarks and Gluons -

The action for the mixed (i.e. quarks and gluons) bag theory becomes

$$W = - \int d^4x \left\{ \frac{1}{4} G_a^{\mu\nu} G_{\mu\nu}^a + B + \frac{1}{2} \bar{\psi} \overleftrightarrow{D}\gamma\psi + m \bar{\psi}\psi \right\} \theta_B - \frac{1}{2} (\bar{\psi}\psi) \delta_B \quad (19)$$

From this action the following set of equations is obtained:

for the quark fields: $(\gamma \cdot \partial - ig\gamma^\mu F_a^\mu A_a + m)\psi = (\gamma \cdot D + m)\psi = 0$ inside the bag (20)

$$(\gamma \cdot n + 1)\psi = 0 \quad \text{on the surface} \quad (6)$$

and $\bar{\psi}(\overleftarrow{\partial} \cdot \gamma + ig\gamma^\mu F_a^\mu A_a - m) = \bar{\psi}(\gamma \cdot \overleftarrow{D} - m) = 0$ inside the bag (21)

$$\bar{\psi}(\gamma \cdot n - 1) = 0 \quad \text{on the surface} \quad (8)$$

for the gluon fields: $D_\mu G_a^{\mu\nu} = -ig \bar{\psi} \gamma^\nu F_a \psi$ or (22)

$$-\partial_\mu G_a^{\mu\nu} = ig \bar{\psi} \gamma^\nu F_a \psi + g f_{abc} A_{\mu b} G_c^{\mu\nu} \equiv \bar{D} J_a^\nu \quad \text{inside the bag} \quad (23)$$

and $n_\mu G_a^{\mu\nu} = 0$ on the surface (24)

and the nonlinear condition becomes:

$$\partial_\rho (\bar{\psi}\psi) = 2 n_\rho \left[B + \frac{1}{4} G_a^{\mu\nu} G_{\mu\nu}^a \right] \quad \text{on the surface} \quad (25)$$

For the gluon fields one can also introduce the relations $G_a^{oi} = E_a^i$ and

$G_{aij} = \epsilon_{ijk} H_{ak}$ denoting the color-electric and color-magnetic field strengths respectively. An important difference with electrodynamics is that we now have

eight, instead of one, electric and as many magnetic fields, because SU(3,C)

has eight charges. In terms of \vec{E}_a and \vec{H}_a we find:

$$\vec{n} \cdot \vec{E}_a = 0 \quad \text{on the surface} \quad (24a)$$

$$\vec{n} \times \vec{E}_a + \vec{n} \times \vec{H}_a = 0 \quad (24b)$$

These conditions assure, that also the gluon fields will be confined.

On the surface the quark and gluon fields satisfy both a separate and a common boundary condition. The former relates the various components of the field among themselves. In case of a prescribed boundary eqs 6, 8 and 24, also referred to as linear boundary conditions, determine the eigenvalues of the energy-eigenmodes inside the bag. The bag theory offers the possibility of hadrons consisting of just gluons, both gluons and quarks, or just quarks. The common condition, dubbed nonlinear or quadratic boundary condition, defines

the surface as the locus, where the fermion and boson pressure balance the vacuum pressure. Also the boson term: $\frac{1}{4} G_{\mu\nu}^a G_a^{\mu\nu}$ is a Lorentz scalar. We can rewrite eq (25) to

$$(n \cdot \partial) (\bar{\psi} \psi) + \frac{1}{2} \vec{E}^2 = B + \frac{1}{2} \vec{H}^2 \quad (26)$$

which illustrates the inflatory activities of the electric fields, whereas the magnetic fields contribute to the compression.

One again can define a stress tensor density $T^{\mu\nu}$

$$\begin{aligned} T^{\mu\nu}(x) &= \theta_B \left\{ G_a^{\mu\rho} \partial^\nu A_{\rho\sigma} + \frac{1}{2} \bar{\psi} \gamma^\mu \overleftrightarrow{\partial}^\nu \psi + g^{\mu\nu} \mathcal{L} \right\} \\ &= \theta_B \left\{ G_a^{\mu\rho} \partial^\nu A_{\rho\sigma} + \frac{1}{2} \bar{\psi} \gamma^\mu \overleftrightarrow{\partial}^\nu \psi - g^{\mu\nu} \left[B + \frac{1}{4} G_a^{k\lambda} G_{k\lambda}^a \right] \right\} \end{aligned} \quad (27)$$

One verifies that

$$\partial^\mu T_{\mu\nu} = 0 \quad \text{inside the bag} \quad (28a)$$

$$n_\mu T^{\mu\nu} = 0 \quad \text{on the surface} \quad (28b)$$

which assure, that the energy and momentum are conserved quantities.

Similarly

$$\partial_\mu J_a^\mu = 0 \quad \text{inside the bag, by eq (23)} \quad (29a)$$

$$n_\mu J_a^\mu = 0 \quad \text{on the surface, by eqs (6), (8) and (24), (29b)}$$

state that the total color charge is a locally conserved quantity. We find that

$$Q_a = \int_{\text{bag}} J_a^0 = - \int \partial_1 G_a^{10} = - \int d^2S \hat{n}_1 G_a^{10} = - \int d^2S \sqrt{1 - v_T^2} \vec{n} \cdot \vec{E}_a = 0 \quad (30)$$

Hence only colorless bags can occur by virtue of Gauss' law and the boundary condition, that \vec{E}_a be tangential to the surface. No bag with the quantum numbers of a quark can be observed. This result is obtained for any value of the coupling strength g , which is not equal to zero. Eq (30) also forbids colorless bags to fission into two colored parts. Imagine a bag with the shape of a sausage, in which the quarks are distributed over the ends. Suppose one

group of quarks has a total charge $Q_a \neq 0$, the other then has the opposite charge. This means that inside the bag, at some point between these two groups, a color electric field will exist of (average) strength $E_a = Q_a/A$, where A is the local cross section of the bag. The total field energy in a little volume $V = L \cdot A$ then amounts to $U = \frac{1}{2} (Q_a/A)^2 L \cdot A = \frac{1}{2} Q_a^2 \frac{L}{A}$. When one tries to fission the bag, one has to reduce A to zero, for which clearly an infinite amount of energy is required. A colorsinglet bag therefore can only fission into other smaller colorsinglet bags.

II. Spherical cavity approximation 1: Gross features [DeG 75]

The set of equations (6), (8), (20) to (25) is a complicated one, for which no general, explicit solution exists. One has to make several approximations, in order to obtain a more manageable one. A first step is to ignore the coupling between the quarks and the gluons. In this zeroth order approximation the equations of motion become independent of color, and one has to solve the free Dirac equation for a colored spinor field with mass m , and the homogeneous Maxwell equations for a massless vectorfield of color a .

In setting $g = 0$, one assumes that in practice g will be small enough to admit the application of perturbation theory in g^2 . The physical picture behind this assumption is, that the size of the hadron will be kept sufficiently small by the vacuum pressure for the theory to be already in the asymptotically free region. Moreover [Ja 75, JaP 75], the surface, apart from the boundary condition, is expected to have little influence on the inside dynamics.

For this simplified set of equations of motion and boundary conditions no general solutions in three space dimensions exist either. This is mainly due to the presence of the nonlinear constraint equation, which impedes the full quantization of the theory. However, the classical equations admit a class of solutions in which the bag is a sphere (in its restframe) of fixed

radius R . This can be seen as follows. One expects the lowest energy eigenmode, that a quark can occupy, to be the one, in which the quark has the least kinetic energy. The quark will therefore move in the most symmetrical way through the bag. From this motion a pressure results, which is spherically symmetric, a property shared by the poincaré invariant bag pressure B . The surface, where these two pressures balance, will therefore be a sphere, which is classically at rest. Within this static sphere one is able to obtain the eigenmodes of the noninteracting, confined quarks and gluons. The nonlinear boundary condition then fixes the radius of this bag, in terms of the energy of the whole system. This procedure bears some resemblance to the Born-Oppenheimer approach in molecular physics. This adiabatic approximation works for dynamical systems, in which one can single out a slowly moving part, whose motion is instantaneously followed by the swiftly moving remainder of the system.

In molecular physics the nuclei are the slowly moving objects, whereas the much lighter electrons (a mass ratio of about 2000) are usually much faster, but still nonrelativistic. The electron orbits can then, to good accuracy, be calculated in the approximation that the nuclei have fixed positions. This then results in electron energy eigenvalues and eigenfunctions, which depend on the nuclear coordinates. Provided stationary electron solutions can be found for all nucleon configurations, also the motion of these slow ones can be solved. The energy of the electrons, as a function of the nuclear positions, now constitutes the potential in which the nuclei move. Apart from this potential contribution, the Schrödinger equation for the nuclei decouples from that for the electrons, provided the influence of the nuclear kinetic energy operator on the electron motion can be neglected [HaK 78].

In the spherical cavity approximation one calculates the quark and gluon energies, given a fixed radius R , using the equation of motion and the linear boundary condition. However, the procedure is now exact, since, at least in

the MIT formulation, there is no kinetic energy term for the bag surface. Instead of a surface equation of motion, one has the quadratic boundary condition, which determines the motion of the bag surface in terms of the motion of the fields inside. In this static case it determines the radius R of the bag as the one for which the bag-energy is a minimum. This exact classical solution is unsatisfactory from the quantum mechanical standpoint because of the sharply determined R -value. In the rigorous, quantum mechanical treatment the fields, then operators, defining R , will have fluctuations around their energy eigenstates, and then also R will fluctuate: the boundary is fuzzy. Using the Budapest formulation of the bagmodel [Gn 78], which includes surface dynamics and thereby avoids nonlinear boundary conditions one can study the quantum mechanical aspects and show, that, in the BO approximation, the distribution for the radius peaks rather sharply around the classical value, and also that the surface excitations can be sufficiently heavy, depending on the smallness of the surface tension, to allow a study of the particle excitations in case the surface is in its groundstate. The zeropoint oscillations do contribute a little in addition to the classical energy. This calculation may serve as an indication, that fixing the bag radius is a reasonable approximation.

There have been several attempts to develop the quantum mechanics in the presence of boundary conditions, in the context of the MIT bagmodel. A complete solution in one space-one time dimension exists [Cho 74, Sh 75]. In three space and one time dimension no explicit solutions exist. One approach, by Johnson [Jo 76], yields a well defined formulation, but is even in an approximate form still too complicated to be readily applicable. Another attempt, by Rebbi [Re 75], studies small oscillations around the classical solutions. In this approximation he is able to cast the constraint equations in a manageable form. In this treatment the spherical cavity approximation is of central

importance, and several limitations to its validity have been uncovered. Let us now obtain the cavity eigenmodes for the quarks and gluons separately.

1. Valence quarks [Chp 74]

The problem of solving eqs (6), (8), (20), (21) and (25) is now reduced to solving the following equation inside a static sphere of radius R.

$$(\gamma \cdot \partial + m) \psi_\alpha = 0 \quad r < R \quad (5)$$

Using the fact that for a static sphere we have $n^\mu = (0, -\hat{r})$ eq (6) becomes

$$\hat{r} \cdot \vec{\gamma} \psi_\alpha = \psi_\alpha \quad r = R \quad (6b)$$

$$-\frac{\partial}{\partial r} (\sum_\alpha \bar{\psi}_\alpha \psi_\alpha) = 2 B \quad r = R \quad (11b)$$

We have exhibited the internal quantum number dependence by a label α . This dependence includes the flavor quantum numbers. Although flavor symmetry turns out to be broken, we will continue our discussion for the flavor symmetric case, and introduce the flavor breaking at a later stage. All quark flavors are taken to have the same mass. The solutions of eq (5) listed below constitute a complete set of four spinor eigenstates, with the boundary condition that they are regular at $r = 0$. These states can be labeled with the eigenvalues of total angular momentum j and its z-component $j_z = m$. For each combination of j and m the quark can occur in two states, having opposite parity, which are eigenstates of the Dirac operator K , with the eigenvalues $k = + (j + 1/2)$ for the $j = (\ell + 1/2)$ solution, and $k = - (j + 1/2)$ for the $j = (\ell' - 1/2)$ one. This reflects the two possibilities of combining the orbital angular momentum ℓ and the spin s (neither are good quantum numbers in this j-j coupling scheme) to a total spin j . We will use the label η defined by $\eta = k/(j + 1/2)$. Due to eq (6b), which has to be satisfied at $r = R$ for every combination of j and η separately, the momentum of the quarks p will take on discrete values, which will be labeled by n : $p_{n\eta j}$. The general solution to our problem therefore is

a superposition of the above mentioned solutions.

$$\psi_{\alpha}(x, t) = \sum_{n, \eta, j, m} N(p_{n\eta j}) a_{\alpha}(n\eta j m) \psi_{n\eta j m}(x, t) \quad (31)$$

Using the spinor harmonics

$$\phi_{jm}^{+} = C_{m_1}^{\ell} \frac{1/2}{m_2} \frac{\ell + 1/2}{m} Y_{m_1}^{\ell}(\hat{r}) \chi_{m_2}^{1/2}$$

and

$$\phi_{jm}^{-} = - \left(\frac{\vec{\sigma} \cdot \vec{r}}{r} \right) \phi_{jm}^{+} = C_{m_1}^{\ell} \frac{1/2}{m_2} \frac{\ell + 1/2}{m} Y_{m_1}^{\ell}(\hat{r}) \chi_{m_2}^{1/2}$$

where $\chi_m^{1/2}$ is the conventional two component Pauli spinor, the $\vec{\sigma}$'s are the appropriate Pauli (2x2)-spin matrices, and $Y_m^{\ell}(\hat{r})$ is the usual spherical harmonic, we can write down the solutions for j, m and n :

$$\psi_{n+jm}(\vec{x}, t) = \begin{bmatrix} j_{\ell}(p_{n+j} r) \phi_{jm}^{+} \\ \frac{-1}{p_{n+j} + \mu} j_{\ell+1}(p_{n+j} r) \phi_{jm}^{-} \end{bmatrix} e^{-i p_{n+j}^0 t} \quad (32a)$$

$$\psi_{n-jm}(\vec{x}, t) = \begin{bmatrix} j_{\ell+1}(p_{n-j} r) \phi_{jm}^{-} \\ \frac{1}{p_{n-j} + \mu} j_{\ell}(p_{n-j} r) \phi_{jm}^{+} \end{bmatrix} e^{-i p_{n-j}^0 t} \quad (32b)$$

The $p_{n\eta j}^0$ are the energies corresponding to the momenta $p_{n\eta j}$, according to $p_{n\eta j}^0{}^2 - p_{n\eta j}^2 = \mu^2$, with μ for the particle mass. The $j_{\ell}(pr)$ are the usual spherical Bessel functions. With this choice of wavefunction the normalization constants become, suppressing the p and p^0 labeling on the right hand side:

$$\int_{\text{bag}} dV \psi_{n\eta j m}^{+} \psi_{n\eta j m} = N_{n\eta j}^{-2} = N_{n\eta j}^{-2} (p_{n\eta j}) = R^3 j_{\ell}^2(pR) \frac{\{2p^0 R (p^0 R - (\ell + 1)\eta) + \mu R\}}{(p^0 R + \mu R)(p^0 R - \eta \mu R)} .$$

Let us introduce $x_{n\eta j} = p_{n\eta j} R$. Because eqs (32) are up to an overall sign

invariant under the transformation $x \rightarrow -x$, we can take the x 's to be positive.

For our simple system, the spinor harmonics drop from eq (6b), and it reads

$$j_{\ell}(x_{n\eta j}) = \frac{x_{n\eta j}}{\eta p_{n\eta j}^0 R + \mu R} j_{\ell+1}(x_{n\eta j}) \quad (33)$$

For $(j, \eta) = (1/2, \eta)$ this can be reshaped into a simple transcendental equation of the form

$$\text{tg } x = \frac{x}{1 - \eta p_{n\eta j}^0 R - \mu R} \quad (34)$$

which gives us the energies of the eigenmodes. We note that eq (33) allows both positive and negative roots for $\eta p_{n\eta j}^0 R$. This means, that for each combination of positive energy E and parity η , we have another one with negative energy $-E$ and parity $(-\eta)$. This verifies that the theory allows for both fermion- and antifermion-eigenmodes. A few eigenfrequencies $x_{n\eta j}$ have been listed in Table I.

$j \backslash n\eta$	1+	1-	2+	2-
1/2	2.043	3.812	5.396	7.002
3/2	3.204	5.123	6.758	

Table I: Quark eigenfrequencies $x_{n\eta j}$ for $m_Q = 0$.

We define: $p_{n\eta j}^0 = \frac{1}{R} \{x_{n\eta j}^2 + \mu^2 R^2\}^{1/2} = -p_{-n, -\eta, j}^0 = E_{n\eta j} > 0$.

Eq (32) then gives a quark spinor, in case $p_{n\eta j}^0 > 0$, or an antiquark spinor, if $p_{n\eta j}^0 < 0$. From eq (33) we find that the roots x will depend on the mass of the

particle and radius of the bag R through the product μR . Combining eqs (32)

and (34) we can derive a special property of our wavefunctions:

$$\frac{\partial}{\partial r} \left\{ \frac{1}{4\pi} \int d\Omega \bar{\psi}_{n\eta j m} \psi_{n\eta j m} \right\} = \frac{\partial}{\partial r} \left\{ \frac{1}{2j+1} \sum_m \bar{\psi}_{n\eta j m} \psi_{n\eta j m} \right\} = \frac{N_{n\eta j}^{-2}}{2\pi R^3} \frac{\partial}{\partial R} p_{n\eta j}^0 \quad (35)$$

which will prove to be quite useful in handling the quadratic boundary condition.

At this point we have solved the problem of obtaining the normal modes of a massive spin 1/2 particle, confined to a spherical bag of radius R (eqs (5) and (6)). We now proceed by applying canonical quantization to the normal mode amplitudes a and a^* , which are the dynamical variables of the problem. The radius is treated as a parameter. We can write down the hamiltonian in terms of the classical solutions

$$H = \int_{\text{bag}} dV \mathcal{H} = \int_{\text{bag}} dV \left\{ \frac{1}{2} \bar{\psi} \gamma^0 \not{\partial} \psi + B \right\} \quad (36)$$

$$= \sum_{\substack{\alpha, n, \eta, j, m \\ n', \eta', j', m'}} N_{n\eta j} N_{n'\eta' j'} a_{\alpha}^*(n\eta jm) a_{\alpha}(n'\eta' j' m') \frac{1}{2} (p_{n\eta j}^0 + p_{n'\eta' j'}^0) \cdot \int_{\text{bag}} dV \psi_{n\eta jm}^+(\vec{x}, t) \psi_{n'\eta' j' m'}(\vec{x}, t)$$

We observe the following features.

The bag integral vanishes, unless $j = j'$ and $m = m'$ by virtue of the orthogonality of the spinor harmonics. Furthermore: when also $n = -n'$ and $\eta = -\eta'$, $p_{n\eta j}^0 + p_{n'\eta' j'}^0 = 0$. Because of eq (13): $\partial_{\mu} T^{\mu\nu} = 0$, one has $H \Big|_{t=t_1} = H \Big|_{t=t_2}$, which implies, that H is time independent. The temporal dependence of eq (36) is of the form $\exp i(p_{n\eta j}^0 - p_{n'\eta' j'}^0)t$. This only vanishes for $n = n'$, $\eta = \eta'$, and $j = j'$. We therefore have to impose the following condition on the normal mode amplitudes:

$$\sum_{\alpha} a_{\alpha}^*(n, \eta, j, m) a_{\alpha}(n', \eta', j', m') = 0 \quad (37)$$

unless $n = -n'$, $\eta = -\eta'$ or $n = n'$, $\eta = \eta'$, to satisfy eq (13). Eq (36) now becomes in terms of the independent dynamical variables $a_{\alpha}(n\eta jm)$ and the conjugate $a_{\alpha}^*(n\eta jm)$

$$H = \sum_{\alpha, n, \eta, j, m} a_{\alpha}^*(n, \eta, j, m) a_{\alpha}(n, \eta, j, m) p_{n\eta jm}^0 + \frac{4\pi}{3} B R^3$$

We now pass over to the quantum theory by letting the normal mode amplitudes become operators, interpreted according to:

$$\begin{aligned} a_{\alpha}(n, \eta, J, m) &= b_{\alpha}(n, \eta, J, m) && \text{for } n > 0 \\ &= d_{\alpha}^{\dagger}(-n, -\eta, J, m) && \text{for } n < 0 \end{aligned} \quad (38)$$

The action of these operators is such that $b_{\alpha}|0\rangle = d_{\alpha}|0\rangle = 0$ for the no-fermion state $|0\rangle$, which still may contain gluons, and therefore need not be the physical vacuum. At this point

$$H = \frac{4\pi}{3} B R^3 + \sum'_{\alpha n \eta J m} \left\{ (b_{\alpha}^{\dagger}(n, \eta, J, m) b_{\alpha}(n, \eta, J, m) - d_{\alpha}^{\dagger}(n, -\eta, J, m) d_{\alpha}(n, -\eta, J, m)) \right\} E_{n \eta J}^{\alpha}$$

where the prime indicates that $n > 0$ is taken. This quantity is clearly not bounded from below, a problem well known for Dirac particle systems, which is resolved, by introducing anticommutation, instead of commutation relations, for the particle operators

$$\{b_{\alpha}(n, \eta, J, m), b_{\alpha}^{\dagger}(n, \eta, J, m)\} = \{d_{\alpha}(n, -\eta, J, m), d_{\alpha}^{\dagger}(n, -\eta, J, m)\} = 1 \quad (39)$$

with our normalization of the wave functions, and all other combinations zero.

One has

$$H = \sum'_{\alpha, n, \eta, J, m} \{N_{\alpha}(n, \eta, J, m) + N_{\bar{\alpha}}(n, -\eta, J, m)\} E_{n \eta J} + E_{0Q} + \frac{4\pi}{3} B R^3$$

introducing the number operators $N_{\alpha} = b_{\alpha}^{\dagger} b_{\alpha}$ and $N_{\bar{\alpha}} = d_{\alpha}^{\dagger} d_{\alpha}$, which have only eigenvalues $n_{\alpha} = 0$ and 1, by virtue of eq (39), characteristic for fermions.

The expectation value of H in a state $|\alpha\rangle$ is denoted by $\langle \alpha | H | \alpha \rangle = E_Q + E_{0Q} + E_V$, where E_Q stands for the quark kinetic energy term (\sum' term) and E_V for the volume energy: $E_V = \frac{4\pi}{3} B R^3$. The zeropoint energy E_{0Q} is defined by

$$E_{0Q} = - \sum_{n \eta J \alpha} (2J + 1) E_{n \eta J} \quad . \quad (40)$$

Unlike in e.g. QED, where it is an infinite constant one has to include this zeropoint energy term, because it depends, through the energy-eigenvalues, on the geometry of the bag, and therefore changes e.g. in going from a bag with radius R_1 to one with radius R_2 . The fermions contribute negatively to E_0 . We will return to this finite volume effect below. The eigenstates of H are

obtained by letting any combination of creation operators b_{α}^{+} and d_{α}^{+} , in accordance with colorsinglet and statistics conditions, act on $|0\rangle$. Of these states, those are admitted to the physical Hilbertspace, which next to eq (13), also satisfy eq (16)

$$n_{\mu} T^{\mu\nu} = \frac{1}{2} \partial^{\nu} (\bar{\psi}\psi) - n^{\nu} B = 0 \quad \text{at } r = R \quad (16)$$

which is taken to be a condition on the matrix elements. Its effect is to select those states which have a spherically symmetric energy density. Between eigenstates of H one has, using eq (35):

$$2B + \sum'_{\alpha n \eta j m} \left(\frac{\partial}{\partial R} E_{n \eta j} \right) \frac{\phi_{j m}^{+\eta} \phi_{j m}^{\eta}}{2\pi R^2} (W_{\alpha}(n \eta j m) - 1) = 0 \quad (41)$$

where $W_{\alpha}(n \eta j m)$ gives the weight, with which a quark of the specified quantum numbers occurs in the eigenstate: $\sum_{\alpha n \eta j m} W_{\alpha}(n \eta j m) = n$, the number of constituents. Only those states in which no angular dependence remains, can satisfy this condition and are admitted to the spherical cavity eigenstate space. This happens quite naturally for states with $j = 1/2$, which have an angle independent scalar density $\bar{\psi}_{\alpha} \psi_{\alpha}$. Another example is provided by those states for which $W_{\alpha}(n \eta j m) = W_{\alpha}(n \eta j)$, causing the summation to become an averaging over m, for each contribution of n, η , and j separately. For these allowed states one has:

$$2B + \frac{1}{2\pi R^2} \frac{\partial}{\partial R} (E_Q + E_{0Q}) = 0 \quad , \quad (42a)$$

or alternatively

$$\frac{1}{2\pi R^2} \frac{\partial}{\partial R} \left\{ \frac{4\pi}{3} B R^3 + E_{0Q} + \sum'_{n \eta j} n(n \eta j) E_{n \eta j}(\mu R) \right\} = 0 \quad (42b)$$

where n denotes the number of quarks with energy $E_{n \eta j}$. This is nothing, but the statement that $\langle H \rangle$ be stationary with respect to small changes of the, in this case one parameter, volume $\cdot \frac{\delta}{\delta V} \langle H \rangle = 0$ [DeT 78], precisely the type of variations considered in deriving eqs (10) and (25). The energy eigenvalues

$E_{n\eta j} = E_{n\eta j}(\mu R)$ are monotonously decreasing functions of R . In the absence of the terms E_{0Q} and especially E_V this does not yield a stable system. By introducing the vacuum pressure B , the bag theory supplies a balance for the outward fermion pressure. Equilibrium in some eigenstate is reached when $\langle H(R) \rangle$ assumes its minimum value at R_0 , for which $\frac{\partial}{\partial R} \langle H \rangle = 0$. This probably also has the consequence, that the energy of a bag state will not be affected too much by the fuzziness of its surface, caused by the zeropoint oscillations of the fields inside.

An alternative way [Chp 74] is to apply eq (11b): $-\frac{\partial}{\partial R} (\bar{\psi}\psi) \Big|_{R=R} = 2B$ already at the classical level. Chodos et al consider only the $j = 1/2$ solutions, but obtain essentially the same results. Because of its technical advantages, we will calculate the energy of a spherical bag system by minimizing the hamiltonian eigenvalues w.r.t. R . In this way one can also include perturbations in a transparent way [DeG 75].

Concerning the internal symmetry and more specific the color part of the wave function the following can be remarked. There are essentially two ways to construct a colorsinglet wavefunction using quarks. Denote the color part of the quark wavefunction by Q^i , $i \in (1,2,3)$ and represent the antiquark color wavefunction by \bar{Q}^i . The first combination is the all quark colorsinglet:

$$Q^3 = \frac{\epsilon_{ijk}}{\sqrt{6}} Q^i Q^j Q^k, \text{ where } \epsilon_{ijk} \text{ is completely antisymmetric in its indices:}$$

$$\epsilon_{123} = 1. \text{ The second one is the quark-antiquark colorsinglet: } Q\bar{Q} = \frac{\delta_{ij}}{\sqrt{3}} Q^i \bar{Q}^j,$$

where $\delta_{ij} = 1$ for $i = j$ and 0 otherwise. Typically a colorsinglet has the form $Q^m \bar{Q}^n$ where n and m are integers and $n-m$ is an integer multiple of three.

It may be useful to illustrate the above described approach by a simplified application. We will neglect the zeropoint energy and restrict ourselves to massless nonstrange quarks. Consider a colorsinglet n quark state, in which all quarks occupy the $1s_{1/2}$ mode. Its energy is given by

$$E(R) = \frac{4\pi}{3} B R^3 + \frac{n}{R} x_{1+1/2}. \text{ Minimizing } E: \quad \frac{\partial E}{\partial R} = 0 = 4\pi B R^2 - \frac{nx_{1+1/2}}{R^2}, \text{ we}$$

find: $R(n) = \left(\frac{n \times_{1+1/2}}{4\pi B} \right)^{1/4}$, which is a nice function of the particle number operator, as well as $E(n) = \frac{4}{3} (4\pi B)^{1/4} (n \times_{1+1/2})^{3/4}$. Interpreted as such $[H, R] = 0$, consistent with expectations. We can estimate B from equating E for $n = 3$ to the average $N-\Delta$ mass

$$E(n) = E(3) = \frac{4 M(N) + 16 M(\Delta)}{20} = 1.180 \text{ GeV}$$

or $B^{1/4} = .121 \text{ GeV}$. The average mass for a nonstrange meson

$M = E(2) = \left(\frac{2}{3} \right)^{3/4} 1.18 = .87 \text{ GeV}$ is then determined. Experimentally one finds

$M = \frac{M(\pi) + 3 M(\rho)}{4} = .61 \text{ GeV}$. This result may be acceptable for the ρ -meson,

it surely is not for the pion. The thus obtained results are a clear indication,

that the n -dependence of the radius is not what it should be. This can also be

seen from the fact that the theory predicts for a bag with six quarks with the

quantum numbers of the deuteron a mass $E(6) = (2)^{3/4} E(3)$. This corresponds to a binding energy of .3 to .4 GeV, which certainly has not been observed yet.

The only known $N-N$ bound state, the deuteron, has a binding energy of about

2 MeV, indicating that $E \sim n$. That we nevertheless are on a good track can be

seen from considering

$$R(n) = \frac{4}{3} \frac{(n \times_{1+1/2})}{E(n)} = \frac{8.2}{M_N} \approx 1.4 \text{ fm for the nucleon: } n = 3$$

The size of the bag is large w.r.t. the nucleon compton wavelength. The

uncertainties in the nucleon energy, arising from localizing it in a volume of

this size, i.e. the zeropoint motion of the centre of mass can be neglected

in first approximation. We can treat the hadron as an extended object and

refer justly to the energy of an n quark system as mass.

2. Valence gluons [Ja 76, Jac 75]

The second possible type of excitation is the gluonic one. In the limit

of negligible coupling constant, we now have to solve eq (22), (24) and (25)

for each color a separately, in the static spherical cavity approximation

$$\partial_{\mu} G_a^{\mu\nu} = 0 \quad r < R \quad (43)$$

$$\left. \begin{aligned} \hat{r} \cdot \vec{E}_a &= 0 \\ \hat{r} \times \vec{H}_a &= 0 \end{aligned} \right\} \quad r = R \quad (44a)$$

$$\frac{1}{2} \vec{E}_a^2 = B + \frac{1}{2} \vec{H}_a^2 \quad r = R \quad (44b)$$

Since for $g = 0$ also the dual tensor field is divergenceless:

$$\partial^{\nu} \epsilon_{\mu\nu\rho\sigma} G_a^{\rho\sigma} = g f_{abc} \epsilon_{\mu\nu\rho\sigma} \{G_b^{\nu\rho} - g f_{bde} A_d^{\nu} A_e^{\rho}\} A_c^{\sigma} = 0$$

we obtain the 'homogeneous Maxwell' equations:

$$\vec{\nabla} \cdot \vec{E}_a = 0 \quad (46a)$$

$$\vec{\nabla} \times \vec{H}_a = \partial_t \vec{E}_a \quad (46b)$$

$$\vec{\nabla} \cdot \vec{H}_a = 0 \quad (46c)$$

$$\vec{\nabla} \times \vec{E}_a = - \partial_t \vec{H}_a \quad (46d)$$

Both \vec{E}_a and \vec{H}_a are transverse fields. The solutions of eqs (46) can be divided into two types (we suppress the trivial common time dependent factor $e^{-i\omega t}$ and the color label a).

1. Magnetic (m) or transverse electric (TE) multipole modes

These solutions from the vector potential

$$A_{\ell m}^{(m)}(\vec{r}) = i^{\ell} j_{\ell}(kr) \vec{X}_{\ell m}(\theta, \phi) \quad (47)$$

expressed in terms of the vector harmonics $\vec{X}_{\ell m}(\theta, \phi) = \frac{\vec{L}}{\sqrt{\ell(\ell+1)}} Y_m^{\ell}(\theta, \phi)$ where \vec{L} is the angular momentum operator $\vec{L} = -i \vec{r} \times \vec{\nabla}$, and the spherical Bessel functions $j_{\ell}(kr)$, which are regular for $kr \rightarrow 0$. The potential is labeled with the eigenvalues ℓ and m of \vec{L}^2 and L_z , which coincide with the eigenvalues j and μ of the total spin operator \vec{J}^2 and its z component J_z . It has unnatural parity $P = (-)^{\ell+1}$. The associated fields are:

$$\vec{E}_{\ell m}^{(m)}(\vec{r}) = i k j_{\ell}(kr) i^{\ell} \vec{X}_{\ell m}(\hat{r}) \quad (48a)$$

$$\begin{aligned} \vec{H}_{\ell m}^{(m)}(\vec{r}) &= i^{\ell} \vec{\nabla} \{ j_{\ell}(kr) \vec{X}_{\ell m}(\hat{r}) \} \quad , \quad \text{satisfying} \quad (48b) \\ \hat{r} \cdot \vec{H}_{\ell m}^{(m)}(\vec{r}) &= i^{\ell+1} \sqrt{\ell(\ell+1)} j_{\ell}(kr) Y_m^{\ell}(\hat{r}) \\ \hat{r} \cdot \vec{E}_{\ell m}^{(m)}(\vec{r}) &= 0 \end{aligned}$$

2. Electric (e) or transverse magnetic (TM) multipole modes

In this case the vector potential is:

$$\vec{A}_{\ell m}^{(e)}(\vec{r}) = \frac{i^{\ell}}{ik} \vec{\nabla} \times \{ j_{\ell}(kr) \vec{X}_{\ell m}(\hat{r}) \} \quad (49)$$

and again is labeled by the eigenvalues $j = \ell$ and $\mu = m$, but now it has natural parity $P = (-)^{\ell}$. The fields become:

$$\vec{E}_{\ell m}^{(e)}(\vec{r}) = i^{\ell} \vec{\nabla} \times \{ j_{\ell}(kr) \vec{X}_{\ell m}(\hat{r}) \} \quad (50a)$$

$$\vec{H}_{\ell m}^{(e)}(\vec{r}) = -i k j_{\ell}(kr) i^{\ell} \vec{X}_{\ell m}(\hat{r}) \quad , \quad \text{and satisfy} \quad (50b)$$

$$\begin{aligned} \hat{r} \cdot \vec{E}_{\ell m}^{(e)}(\vec{r}) &= i^{\ell+1} \sqrt{\ell(\ell+1)} j_{\ell}(kr) Y_m^{\ell}(\hat{r}) \\ \hat{r} \cdot \vec{H}_{\ell m}^{(e)}(\vec{r}) &= 0 \end{aligned}$$

These two sets of multipole fields together form a complete set of transverse vector solutions to eqs (46), which are regular at the origin. We have:

$$\begin{aligned} \vec{H}_{\ell m}^{(m)} &= i k \vec{A}_{\ell m}^{(e)} = \vec{E}_{\ell m}^{(e)} \quad (51) \\ \vec{H}_{\ell m}^{(e)} &= -i k \vec{A}_{\ell m}^{(m)} = -\vec{E}_{\ell m}^{(m)} \quad , \quad \text{assuming the same } k \text{ eigenvalue.} \end{aligned}$$

To these fields we can apply the boundary conditions of eqs (44). For the magnetic multipole field we find:

$$\begin{aligned} \hat{r} \cdot \vec{E}_{\ell m}^{(m)}(\vec{r}) &= 0 \\ \hat{r} \times \vec{H}_{\ell m}^{(m)}(\vec{r}) &= -\frac{1}{r} \left(r \frac{\partial}{\partial r} + 1 \right) j_{\ell}(kr) i^{\ell} \vec{X}_{\ell m}(\hat{r}) \quad r = R \quad . \end{aligned}$$

Therefore the energy eigenvalues are found to be independent of m from the condition:

$$\left(r \frac{\partial}{\partial r} + 1 \right) j_{\ell}(kr) = 0 = \frac{\partial}{\partial \rho} \{ \rho j_{\ell}(\rho) \} \quad \text{for } \rho = kr = kR \quad . \quad (52a)$$

Equivalently: $(\ell+1) j_{\ell-1}(kR) = \ell j_{\ell+1}(kR)$.

For the electric multipoles one has:

$$\begin{aligned} \hat{r} \cdot \vec{E}_{\ell m}^{(e)}(\vec{r}) &= \frac{i^{\ell+1}}{r} j_{\ell}(kr) \sqrt{\ell(\ell+1)} Y_{\ell m}(\hat{r}) = 0 \\ \hat{r} \times \vec{H}_{\ell m}^{(e)}(\vec{r}) &= -i k j_{\ell}(kr) i^{\ell} \hat{r} \times \vec{X}_{\ell m}(\hat{r}) = 0 \end{aligned} \quad \text{at } r = R$$

This condition again has to be satisfied by the radial part of the wavefunction and the energy roots are given by

$$j_{\ell}(kR) = 0 \tag{52b}$$

This implies that the magnetic field will vanish at the boundary. The classical magnetic field does not exert any pressure on the bag surface, cf. eq (25)!

We also note that Gauss' law is satisfied by each gluon excitation separately. This is a consequence of setting $g = 0$. Going to lowest order in g resolves this problem. The valence gluons then will act as source, and the resulting electric field $\sim g$ no longer vanishes trivially at the boundary, thereby restricting the allowed color irreps to only the singlet.

We list a number of roots in Table II. They are labeled by the radial quantum number n , ℓ and $i \in \{e,m\}$: $x_{ni\ell}$. We denote: $x_{n\ell} = x_{nm\ell}$ and $Y_{n\ell} = x_{ne\ell}$.

a)	n \ \ell	1	2	b)	n \ \ell	1	2
	1	4.493	7.725		1	2.744	6.117
	2	5.763	9.095		2	3.870	7.443
	3	6.988	10.417		2	4.973	8.722

Table II: Gluon eigenfrequencies.

a) Eigenfrequencies $Y_{n\ell}$ of the TM modes with $J = \ell$ and $P = (-)^{\ell}$.

b) Eigenfrequencies $x_{n\ell}$ of the TE modes with $J = \ell$ and $P = (-)^{\ell+1}$.

From the definition of the vector harmonics we conclude that no monopole solution exists for the fields with $\omega \neq 0$. All other positive J values are allowed. The only spherically symmetric static potential satisfying (44a) is a constant one, which can be taken to be zero.

We can write:

$$\vec{A}_\alpha(\vec{r}, t) = \sum_{n\ell m} N(n\ell) \vec{A}_{n\ell m}^i(\vec{r}) e^{-i\omega n\ell t} a_\alpha^i(n\ell m) \quad (53)$$

where we have adhered an extra label n to the potential to make explicit its energy dependence, as well as a label α to denote its color degree of freedom.

The vector potentials satisfy the following orthogonality relations:

$$\int d\Omega \vec{A}_{n\ell m}^{*\star(m)} \cdot \vec{A}_{n'\ell'm'}^{\star(m)} = \delta_{\ell\ell'} \delta_{mm'} j_\ell(kr) j_{\ell'}(k'r) \quad (54a)$$

$$\int d\Omega \vec{A}_{n\ell m}^{*\star(e)} \cdot \vec{A}_{n'\ell'm'}^{\star(e)} = \delta_{\ell\ell'} \delta_{mm'} \left\{ \frac{\ell}{2\ell+1} j_{\ell+1}(kr) j_{\ell+1}(k'r) + \frac{\ell+1}{2\ell+1} j_{\ell-1}(kr) j_{\ell-1}(k'r) \right\} \quad (54b)$$

$$\int d\Omega \vec{A}_{n\ell m}^{*\star(e)} \cdot \vec{A}_{n'\ell'm'}^{\star(m)} = 0 \quad (54c)$$

The factors $N(n\ell)$ are normalization constants chosen to be ($x > 0$):

$$N(n\ell) = \{R^2 x [j_\ell^2(x) - j_{\ell+1}(x) j_{\ell-1}(x)]\}^{-1/2} .$$

We again find a simple relation between the energy and the wavefunction for the electric and magnetic fields at the boundary:

$$\begin{aligned} \frac{1}{4\pi} \int d\Omega (\vec{E}_{n\ell m}^{*\star} \cdot \vec{E}_{n\ell m}^i - \vec{H}_{n\ell m}^{*\star} \cdot \vec{H}_{n\ell m}^i) &= \frac{1}{2\ell+1} \sum_m (\vec{E}_{n\ell m}^{*\star} \cdot \vec{E}_{n\ell m}^i - \vec{H}_{n\ell m}^{*\star} \cdot \vec{H}_{n\ell m}^i) \\ &= \frac{x_{n\ell}}{4\pi R^4} N^{-2}(n\ell) \end{aligned} \quad (55)$$

Taking into account the fact, that by eq (52) we have both positive and negative energy solutions, with the same modulus, and the fact that the vector potential is a real function of \vec{r} and t, we find, that

$$a_\alpha^{(m)*}(n\ell m) = - (-)^m a_\alpha^{(m)}(-n, \ell, -m) \quad n > 0 \quad (56)$$

$$\text{and } a_{\alpha}^{(e)*}(n\ell m) = (-)^m a_{\alpha}^{(e)}(-n, \ell, -m) \quad n > 0 \quad (56)$$

We therefore can take either the $a(n)$'s for all n , or both $a(n)$ and $a^*(n)$, with $n > 0$, as independent dynamical variables. Quantization of the gluonic degrees of freedom again proceeds in a canonical way, starting from the hamiltonian

$$H = \frac{1}{2} \int_{\text{bag}} dV \{ \vec{E}^2 + \vec{H}^2 \} + \frac{4\pi}{3} B R^3 \quad (57)$$

which becomes time independent if we impose

$$\sum_{\alpha} a_{\alpha}^{(i)}(n\ell m) a_{\alpha}^{(i')}(n'\ell m) = 0 \quad \text{unless } n = n' \text{ and } i = i' \quad (58)$$

and reduces to the following simple form, due to our choice of normalization, in terms of the normal mode amplitudes:

$$H = \sum_{n\ell m\alpha} \frac{x_{n\ell}}{2R} a_{\alpha}^{i*}(n\ell m) a_{\alpha}^i(n\ell m) + \frac{4\pi}{3} B R^3 \quad (59)$$

If we now define:

$$\begin{aligned} c_{\alpha}^i(n\ell m) &= a_{\alpha}^i(n\ell m) \\ c_{\alpha}^{i+}(n\ell m) &= a_{\alpha}^{i*}(n\ell m) \end{aligned} \quad n > 0 \quad (60)$$

and then interpret the c 's as operators, satisfying the commutation relations:

$$[c_{\alpha}^i(n\ell m), c_{\alpha}^{i+}(n\ell m)] = 1 \quad (61)$$

and all other combinations are zero, such that $c|0'\rangle = 0$, where $|0'\rangle$ is a no-gluon state, we obtain a hermitian vector gluonfield and the hamilton operator reads

$$H = \sum_{\alpha n\ell m i} \frac{x_{n\ell}}{R} (c_{\alpha}^{i+}(n\ell m) c_{\alpha}^i(n\ell m) + \frac{1}{2}) + \frac{4\pi}{3} B R^3 \quad (62)$$

The gluons contribute positively to the zeropoint energy according to

$$E_{0G} = 4 \sum_{n\ell} (2\ell+1) \frac{x_{n\ell}}{R} \quad (63)$$

From the eigenstates $|i\rangle$ of H we admit only those to the spherical cavity

spectrum, between which we have (eq (28b))

$$\langle 1 | n_{\mu} T^{\mu\nu} | 1 \rangle = 0 \quad \text{on the surface} \quad .$$

Substituting the energy momentum tensor this becomes

$$\langle 1 | \left\{ \frac{1}{2} (\vec{E}^2 - \vec{H}^2) + B \right\} | 1 \rangle = 0 \quad r = R \quad . \quad (64)$$

This implies, that $\langle \vec{E}^2 - \vec{H}^2 \rangle$ should not contain any angle dependency and then, again, now by virtue of eq (55), we find, that the energy of the spherical cavity state $|1\rangle$ is found by minimizing its hamiltonian expectation value w.r.t. R:

$$\frac{\partial}{\partial R} \langle 1 | H | 1 \rangle = 0 \quad .$$

Eq (64) can only be satisfied if the gluons, occupying some energy level, yield a spherically symmetric distribution by themselves. This is a severe restriction on the number of gluon states. It only allows $J = 0$ states.

There are basically three different ways, in which we can construct a gluon colorsinglet. First we have a two-gluon system. If we denote the color part of the gluon wave function by G^a , this singlet is described by $G^2 = \sum_{a,b} \frac{\delta_{ab}}{\sqrt{8}} G^a G^b$, $a, b \in \{1, \dots, 8\}$. Next we have two three-gluon combinations: one with color wave function $G_f^3 = \frac{f_{abc}}{\sqrt{24}} G^a G^b G^c$, which is completely antisymmetric in all color indices, and one with color wave function $G_d^3 = \frac{\sqrt{3}}{40} d_{abc} G^a G^b G^c$, the completely symmetric three color octet singlet. The lightest glueball has a G^2 configuration, $J^P = 0^+$. With the baryon-meson value for B, this state has, again omitting the zeropoint energy, a mass of $M = 1.0$ GeV, for a radius of $R = 1.5$ fm. This value is certainly comparable with what we, in the same approximation, find for the mesons and baryons and seems very promising.

Anticipating the results of section III, we can attempt a more precise estimate and calculate the glueball masses, including the zeropoint energy.

The bag energy for a state containing N noninteracting valence gluons is given by

$$H = \frac{4\pi}{3} B R^3 - \frac{Z_0}{R} + \sum_i n_i \frac{\alpha_i}{R}$$

where n_i counts the number of gluons of type i present, $\sum_i n_i = N$. We will use $B^{1/4} = 0.1455$ GeV and $Z_0 = 1.842$. Taking the bose statistics of the gluons into account, we can construct Table III, where the lightest all-gluon states are listed. Only those with $J = 0$ have a spherically symmetric energy density and satisfy the quadratic boundary condition. There turn out to be quite an amount of lowlying vacuumlike states. The lightest photon-like state only appears at $M = 1.7$ GeV. The lightest type II exotic meson-like state already appears at 1.180 GeV [Ro 77, Ja 76].

Content	color-configurations	J^{PC}	M(GeV)	$R(\text{GeV}^{-1})$
TE ²	G ²	0 ⁺⁺ , 2 ⁺⁺	0.960	5.04
TETE'	G ²	1 ⁻⁺ , 2 ⁻⁺ , 3 ⁻⁺	1.180	5.40
TETM	G ²	0 ⁻⁺ , 1 ⁻⁺ , 2 ⁻⁺	1.290	5.56
TE' ²	G ²	0 ⁺⁺ , 1 ⁺⁺ , 2 ⁺⁺ , 3 ⁺⁺ , 4 ⁺⁺	1.380	5.67
TE'TM	G ²	1 ⁺⁺ , 2 ⁺⁺ , 3 ⁺⁺	1.490	5.83
TM ²	G ²	0 ⁺⁺ , 2 ⁺⁺	1.600	5.97
TE ³	$\left. \begin{array}{l} G_f^3 \\ G_d^3 \end{array} \right\}$	0 ⁺⁺ , 2 ⁺⁺	1.470	5.80
		1 ^{+ -} , 3 ^{+ -}		
TE ² TE'	$\left. \begin{array}{l} G_f^3 \\ G_d^3 \end{array} \right\}$	1 ⁻⁺ , 2 ⁻⁺ , 3 ⁻⁺	1.660	6.04
		0 ⁻⁻ , 1 ⁻⁻ , 2 ⁻⁻ , 2 ⁻⁻ , 3 ⁻⁻ , 4 ⁻⁻		

Notation: TE : $J^{PC} = 1^{+-}$ glue mode with eigenfrequency $x_{11} = 2.744$
TE' : $J^{PC} = 2^{--}$ glue mode with eigenfrequency $x_{21} = 3.870$
TM : $J^{PC} = 1^{--}$ glue mode with eigenfrequency $y_{11} = 4.493$

Table III: Glueball states

We can also consider states containing both valence quarks and gluons. They are obtained by taking the direct product of pure quark and pure gluon states, which have opposite total color charge, in such a way that a color-singlet results. Because the quarks and gluons have different energy eigenvalues, saturation of the quadratic boundary condition can only be accomplished, if the energy density is angle independent for each occupied energy mode separately. The simplest configuration, naively meeting these requirements, is a $J^P = 0^-$ $Q\bar{Q}G$ -state. The quark-antiquark pair is a color octet system, with $J^P = 1^-$ (both fermions in a $1s1/2$ state), and the color octet gluon occupies a $J^P = 1^+$ mode. Its mass is estimated to be 1.3 GeV [Ba 77, HoM 78].

- Excited Bag Configurations -

A large amount of care is needed in studying configurations, containing e.g. a quark (or a gluon) which does not have a spherically symmetric energy distribution by itself. DeGrand and Jaffe [DeG 76] have studied mesons and baryons in which one quark is excited to a $n\ell j = 1p1/2$ state and the remainder is in the $1s1/2$ quark ground state. The resulting spectrum contains $J^P = \frac{1}{2}^-$ and $\frac{3}{2}^-$ baryons and 0^+ and 1^+ mesons. There are no free parameters. They find a mass spectrum, which, as a whole, is too light compared with what is observed. This statement is independent of the improvements, which will be discussed in section III. More specifically, in the baryon sector, they find that the states, in the usual $SU(6,FS) \otimes O(3)$ terminology [Ko 69] (section IV), generally are mixtures of corresponding members of a [70] $L = 1$ and a there-with degenerate [56] $L = 1$. In nonrelativistic potential models e.g. the harmonic oscillator model [Gr 64, Da 76], relying on twobody forces to generate the binding, this [56] $L = 1$ is an artefact of describing the two particle dynamics by a nailed down potential, and represents a translation

mode of the whole system, not a true particle state [Ka 68]. The [56] $L = 1$ multiplet does occur in the bagmodel, since it is a symmetric excitation of all quark relative to the bag, which here plays the role of 'external object'. It is a typical manybody feature of the model, not shared with nonrelativistic systems. Of course, next to these excitations, also translation modes will be present in the bagmodel, and interfere with the true bag states in the clearly not translationally invariant static cavity formulation. The light mass of the $L = 1$ multiplets can be understood as a signal of this phenomenon. Closer consideration of the states corresponding to a $(1s1/2)^2(1p1/2)$ configuration shows that these do not replenish the [56] $L = 1$ and the [70] $L = 1$ multiplets. Note that here we are comparing the content of a special $\bar{j}-j$ coupling scheme with that of a more familiar LS one (section IV). The missing states are precisely those, which can be supplied by a $(1s1/2)^2(1p3/2)$ configuration. This $1p3/2$ mode has an excitation energy which is in between that of the $1s1/2$ and the $1p1/2$ one ($2.0 < 3.2 < 3.8$ for the nonstrange massless quark roots), and is cheaper to occupy than the $1p1/2$ one. However, a quark in a $1p3/2$ mode does not have a spherically symmetric pressure and therefore cannot locally satisfy the nonlinear boundary condition at the bag surface. A proper description of the $L = 1$ baryon spectrum should take also the $1p3/2$ modes into account. However, putting a $(1s1/2)^2(1p3/2)$ system in a static spherical bag, one compels the center of mass to move inside the bag. The state, obtained this way, also contains a translation mode part and is not a true bag excitation. Rebbi [Re 75] has studied the situation in which the bag surface is allowed to perform small oscillations around a spherical equilibrium shape. These oscillations can be described by an effective hamiltonian, the eigenstates of which are the correct excitations. This approach becomes exact if the system contains a mode, say the $1s1/2$ mode,

which is heavily populated. In practice $n = 2$ is taken to be large enough. This approach is sufficient to treat the translational degrees of freedom correctly. The different partial waves are found to decouple. Attention is focussed on the $\ell = 1$ sector. Rebbi then finds, that there is indeed a zero-frequency eigenmode which corresponds to a uniform translation. It is shown to be a [56] $L = 1$ mode, built from $(1s_{1/2})^2(n\ell j)$ configurations, with the $(n\ell j)$ almost, in the approximation in fact completely, exclusively $1p_{1/2}$ and $1p_{3/2}$. Some other, bag-, eigenfrequencies are found to be pushed up slightly. Thus one finds, that through the coupling with nonspherical modes the eigenvalue of the $1p_{1/2}$ mode is changed to a larger one. Application of these approximate results to the baryon spectrum shows, that there is quite some improvement. The [70] $L = 1$ becomes a little heavier, and the [56] $L = 1$, now orthogonal to the translation mode, has become quite a bit heavier, which is much more in accord with experiment, though still some discrepancies remain [DeG 76]. A similar treatment of the baryonic radial excitations yields, that coupling of the modes by allowing the bag-surface to undergo radial fluctuations [DeG 78], effectively lowers the mass for the lightest excitation, indicating that also the $2s_{1/2}$ eigenfrequency can not be reliably estimated in the static cavity approximation. Effectively only the $(1s_{1/2})$ quark modes seem to be treated properly. The situation looks worse for the $Q\bar{Q}$ mesons [DeG 76]. There are never heavily populated eigenmodes in this system and thus even Rebbi's approach fails. However, considerations, similar to the ones given above, can be seen to apply. In $SU(6,FS) \otimes O(3)$ terms, groundstate $Q\bar{Q}$ mesons are members of a [36] $L = 0$ multiplet. Upon receiving one quantum of orbital angular momentum, they become members of a [36] $L = 1$ multiplet. Again one needs to excite particles to both $1p_{1/2}$ and $1p_{3/2}$ modes, in the spherical cavity description, to be able to construct

all the [36] $L = 1$ states. Because of the nonspherical pressure of the particle in the $1p_{3/2}$ mode also here the translation modes will have to be projected out of the meson wavefunction. This will result in a (different) shift for the eigenvalues of the $1p_{1/2}$ and $1p_{3/2}$ modes and again no reliable estimate of the mass is possible. A way to circumvent these problems is given in Chapter 4. Finally, considering the gluon modes, no solution exists which exerts a spherically symmetric pressure by itself. Therefore, one should beware of taking the glueball estimates too seriously.

It appears, that the static cavity approximation is only reliable for those hadrons, in which all quarks are in the lowest, the $1s_{1/2}$ eigenmode, which motivated it in the first place. But even here further restrictions have to be made, if the number of quarks present becomes large ($n > 3$, see Chapter 3). Still, qualitatively, it gives a clear indication of what kind of unusual states can be expected to exist and have low mass.

III. Spherical cavity approximation 2 Further refinements

In section II, we found that the zeroth order treatment of baryons and mesons, consisting of $1s_{1/2}$ quarks, yielded a spectrum with large degeneracies ($\rho - \pi$, $N - \Delta$), quite sizeable bags and a wrong dependence on the number of quarks for the radius R and the energy E . In this section we want to examine whether and what improvements can be realized, by considering the effects on the particle mass, including a.o. one gluon exchange and the zeropoint energy. In this section the fermions are restricted to occupy only the lowest energy eigenmode.

1. Zeropoint energy [DeG 75, Jo 75, BH 76]

From section II 1 we know, that the quarks contribute a term $E_{0Q} = -\frac{1}{2} \sum E$ (eq (40)) and from section II 2, that the gluons contribute a term $E_{0G} = \frac{1}{2} \sum E'$ (eq (63)) to the zeropoint energy. Both terms depend on the geometry of the

bag, through the energy eigenvalues, and therefore will change, when the bag volume changes (Casimir effect). They therefore have to be calculated explicitly. Since E_0 is a divergent quantity, one can introduce a cut off, e.g. $E_0 \rightarrow E_0(\Omega) = \sum E e^{-E/\Omega}$ and then try to isolate the divergent parts as a function of the cut off parameter Ω . The only shape cavity, that, until now, has allowed explicit analytical calculation, for massless particles, is the slab of thickness L . Using bag type boundary conditions, the energy here typically has the form $E = \left\{ \vec{k}_T^2 + \left(\frac{n\pi}{L} \right)^2 \right\}^{1/2}$ for the vector fields and $E = \left\{ \vec{k}_T^2 + \left(\frac{(n+1/2)\pi}{L} \right)^2 \right\}^{1/2}$ for the Dirac field. To evaluate the contribution of the transverse degrees of freedom ($\sim \vec{k}_T$), one introduces a transverse cut off (the twodimensional box, a square with area A), sums the now discrete transverse eigenfrequencies and subsequently lets $A \rightarrow \infty$. One thus obtains the zeropoint energy per unit area. Just like in the three dimensional, field theoretic case without confinement, this part does not contain any reference to the geometry employed in its evaluation. The longitudinal contribution clearly does, because of the finite value of L involved. The resulting zero-point energies are ($\Omega L \gg 1$).

$$E_0 = \Omega^4 \frac{3V}{\pi^2} - \frac{\pi^2}{720} \frac{V}{L^4} \quad \text{for the vector field} \quad (65)$$

$$E_0 = -\Omega^4 \frac{6V}{\pi^2} - \frac{7}{4} \frac{\pi^2}{720} \frac{V}{L^4} \quad \text{for the spinor field,} \quad (66)$$

where $V = AL$.

The only divergent term is in both cases the quartic one, which can be absorbed as a renormalization in the vacuum pressure constant:

$B_{\text{ren}} = B + (8 \cdot 3 - 3 \cdot 6n) \frac{\Omega^4}{\pi^2}$, which we rename B again. This feature suggests, that B is an uncomputable parameter in the theory, which has to be fitted from the data. Here n is the total number of flavors, the gluons come in eight colors and the fermions in three. It can be shown quite general, that such

a term arises, regardless of the shape of the volume considered and the boundary condition imposed [Ba 70]. In conventional field theory one does away with it by introducing a cut off dependent counterterm in the Lagrangian, which cancels the divergence exactly. In the bag theory a finite renormalized term remains. The second term is finite and cut off independent and contributes to the physical hadron mass. From the slab we find:

$$E_V + E_0 = \frac{4\pi}{3} B R^3 - \frac{Z_0}{R} \quad . \quad (67)$$

To estimate the order of magnitude of Z_0 , we set $V = \frac{4\pi}{3} R^3$ and $L = R$ in the expressions for E_0 and find $Z_0 = 0.05742 (8 + \frac{7}{4} \cdot 3 \cdot n) = 1.36$ for $n = 3$. The pressure of scalar fields would, apart from the above described terms also have given a cubic term, generating a surface tension

$$E_0 = \frac{1}{2} \Omega^4 \frac{3V}{\pi} - \frac{\Omega^3 A}{4\pi} - \frac{1}{2} \frac{\pi^2}{720} \frac{V}{L^4} \quad \text{for the scalar field} \quad . \quad (68)$$

The zeropoint energy of the scalar field can be shown to be equal to that of the (TM) vectorfield. In the gluoncase, also the opposite parity TE modes are present and cancel the surface term. A similar phenomenon occurs for the quarkfields. As has been shown by Bender and Hays, these results are also valid in the case of a static spherical cavity. A bag theory without surface tension remains so, as far as the zeropoint energy is concerned. Apart from these nice features, Bender and Hays also showed, that, next to the quartic divergence a quadratic one $\sim R \Omega^2$ and possibly weaker ones occur. These terms are rather sensitive to the nature of the boundary. They have no counterpart in the original theory, they can be taken to renormalize and constitute a severe problem. The method Bender and Hays used to obtain the divergencies, does not make any reference to the eigenvalues of the energy. It only takes the linear boundary condition into account, i.c. that of the static sphere. Therefore, the quadratic divergence may be seen to disappear in the proper

quantum mechanical treatment allowing for more general shapes, variable in time and space although this by no means is certain.

We will parametrize the zeropoint energy as given in eq (67) and include no more geometry dependent terms, introducing just as much free parameters. In principle Z_0 may be a function of the quark masses, $Z_0 = Z_0(\mu R)$ and therefore also be R-dependent. Since Z_0 has not yet been calculated for the static sphere, we will have to fit it and therefore take it to be a constant. This way we will, at the same time, account for other contributions of the same form, such as the correction, due to the motion of the centre of mass of the quarks inside the static sphere, which also yields a similar negative term [Wo 78], as represent the averaged effect of not yet included terms with a different R-dependence. Its validity is therefore limited to the region where it is fitted. $R \approx 1$ fm.

The impact of Z_0 will be larger the smaller the systems are. Since it has the dimension of a kinetic energy it will effectively reduce the corresponding term. For nonstrange mesons this reduction amounts to almost 50 %, for nonstrange baryons it is less, ≈ 30 %. Therefore E_0 will contribute to the separation of the meson from the baryon masses. The BV and Z_0/R terms are sometimes called geometrical.

2. One-gluon exchange [DeG 75]

To lift the spindegeneracies encountered in section II one can allow the color coupling constant g to become nonzero and study the effect of the resulting quark gluon coupling on the particle mass. This will add one more parameter to the theory: g or equivalently $\alpha_c = g^2/4\pi$. We assume that α_c is a constant, that does not depend on e.g. the mass of the particles. We will restrict our attention to hadrons, consisting exclusively of $1s1/2$ quarks. The quarks generate a color current j_a^μ , which acts as a source for the gluon

field A_a^μ . The color interaction term in the hamilton density has the usual form $\mathcal{H}_{int} = - j_\mu^a(x) A_a^\mu(x)$. One can have, to lowest order in α_c , two types of interaction. A quark can exchange a gluon with another quark. This possibility is depicted in diagram 1a. Secondly, a quark can interact with itself. This is shown in graph 1b. Solid lines represent the (anti)quarks, wavy lines the gluons.

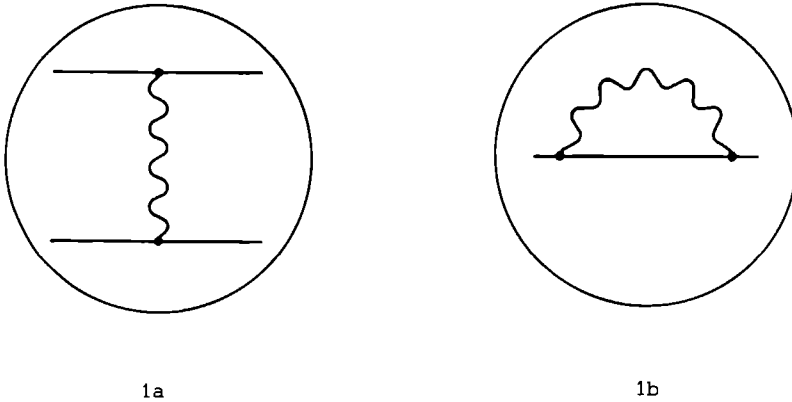


Fig. 1: One gluon exchange graphs

The diagrams are enclosed in a circle to stress the fact that they have to be evaluated for particles confined to the bag. This of course has its effect on the propagators involved. In principle, these can be constructed from the quark and gluon solutions, obtained in section II. To proceed rigorously, one should in the present case evaluate diagrams 1a and 1b, putting the initial and final state quarks in the $1s_{1/2}$ mode. This is readily done for the mutual quark interaction graph 1a. Here the current at the vertex is time independent and one can calculate the color electric and magnetic fields using the static Maxwell equations. The situation is rather more complicated for the selfenergy graph 1b. In QED it is zero for a massless charged fermion. A calculation of

the electromagnetic self energy for a confined massless quark [Ch 74] shows that one obtains a finite value $\delta E = \frac{c \cdot \alpha}{R}$ (α is the fine structure constant) where c for more than 80 % is given by that part of 1b in which the intermediate quark is also in the $1s_{1/2}$ state. It is not known, what happens for massive confined quarks. In QED the contribution of 1b for a free massive charged fermion is infinite and taken to renormalize the massparameter. When the same fermion becomes bound, its selfenergy undergoes a finite (Lamb) shift, depending on the orbit it occupies. For a fermion confined to a sphere the energy eigenvalues will depend on the radius R , and differ from hadron to hadron. Therefore also the selfenergy will vary in magnitude between the hadrons. It is not clear, what changes, when the free photon is replaced by an, in first approximation abelian, confined gluon.

The selfenergy term summed over all quarks i present, and over all intermediate quark states j , looks like $\delta E = \frac{\alpha}{R} \sum_{i,j} g_j (m_i R, m_j R)$ for both chromo-electric and chromo-magnetic contributions, and has the same structure as the quark energy term E_Q . The fact, that its inclusion in the hamiltonian, affects all parameters, instead of just m_u , m_s and Z_0 , indicates that our set of parameters is more strongly correlated than naively is expected. Compare fit C from Table IV with fits A and B.

The color electrostatic piece exactly cancels the corresponding part of diagram 1a, provided the hadron consists of equal mass quarks (e.g. N , Ω , ω) and within 4 MeV when both strange and nonstrange quarks are present (K^* , Σ , Ξ). This is a consequence of the fact that the hadrons are colorsinglet states. One is compelled to take either both, or neither of these two contributions into account, since in both cases the emerging electrostatic fields do not satisfy the linear boundary condition by themselves (see below). One may speculate, that the colorelectrostatic part of the selfenergy which contains

the low Δq part of this interaction, is already represented by the geometrical terms, which provide a natural cut off for the long range phenomena. This raises the question, whether including other parts of 1b may not imply recounting effects already represented. Instead of attempting a, through the uncertainties in the energy eigenvalues, unreliable calculation of the selfenergy, we will include only the color electrostatic term of graph 1b, in our hamiltonian, which is almost equivalent to leaving out the corresponding part of 1a, and omit the color magnetostatic contribution. Although not quite consistent, this latter choice is motivated by the fact that taking the bag to be a sphere, is a better approximation the lighter the quarks are. A massless quark moves with the speed of light, and is not preceded by its gluon field. The pressure on the boundary therefore is provided by the quarks with only a relatively small contribution of the gluons. For a $1s_{1/2}$ mode quark this pressure therefore will be mainly spherical! Small excursions of one quark away from the others, disturb this spherical symmetry and the local pressure balance. They therefore are opposed by the isotropic vacuum pressure, which restores the original shape. Therefore the most favorable geometry for a hadron containing such quarks is a sphere. When the quarks are very heavy, their motion is non-relativistic and the gluon fields around them rearrange themselves to the instantaneous position of the quarks. The latter do not come near the boundary and the vacuum pressure is mainly balanced by that of the gluon fields, which do not have a spherical symmetry [G1 78, HaK 78, Jo 78]. Consider a hadron consisting of a $Q\bar{Q}$ pair, which initially has the shape of a sphere. The quark pressure is not very important now for determining the shape of the bag and the quarks are even stimulated to move away from one another (i.e. to occupy dislocalized orbitals). The bag becomes ellipsoidal, a shape more favored by the glue.

This will tend to concentrate in between the oppositely charged quarks, where it becomes increasingly compressed. At one point a stable configuration is reached in which the gluons balance the vacuum pressure locally and keep the quarks from moving further apart. Such a situation is better described in a non-relativistic potential model. This way one can understand the failure of the attempts to reproduce the spectrum of the charmed mesons, and charmonium using the spherical cavity approximation. The strategy of the MIT group has been to set $m_n = 0$ from the beginning and adjust the other parameters, in order to reproduce the light hadron mass spectrum. This choice has been corroborated by subsequent applications of the model to various areas of high energy physics.

We shall now calculate the one gluon exchange contribution. The interaction energy of the field $A_1^\mu(x)$, generated by quark 1, and the current $J_k^\mu(x)$, generated by quark k, has the form
$$J_{int}^\mu = - \int_{bag} d^3x J_k^\mu(x) A_1^\mu(x)$$
, which for the static quark currents can be rewritten as

$$J_{int}^{st} = \int_{bag} d^3x \{ \vec{E}_1 \cdot \vec{E}_k - \vec{H}_1 \cdot \vec{H}_k \} \quad , \quad (68)$$

where, of course, 1 and k may label the same quark. The field \vec{E}_a and \vec{H}_a have to satisfy the linear boundary conditions:

$$\hat{r} \cdot \vec{E}_a = 0 \quad (44a)$$

for $r = R$, and all colors a .

$$\hat{r} \times \vec{H}_a = 0 \quad (44b)$$

For the color magnetic field we have to solve
$$\vec{\nabla} \times \vec{H}_1^a = J_1^a \quad (69a)$$

$$\vec{\nabla} \cdot \vec{H}_1^a = 0 \quad (69b)$$

$r < R$

for each quark 1, which has a current J_1^a at the vertex, that in terms of spin and color operators reads:

$$\vec{J}_1^a(\vec{r}) = 1g\bar{\psi}_1(\vec{r})\vec{\gamma}_1 F_1^a \psi_1 = \frac{3}{4\pi} (gF_1^a) \vec{r} \times \vec{\sigma}_1 \frac{\mu'_1(m_1, r)}{r^3} \quad (70)$$

Here $\mu'(m_1, r)$ is the derivative of the magnetic moment:
$$\mu'(m_1, r) = \left. \frac{\partial}{\partial Z} \mu(m_1, Z) \right|_{Z=r}$$

(eq (92)). This current is the source for a transverse vectorpotential

$$\vec{A}_1^a(\vec{r}) = gF_a^1 \left(\frac{\vec{r} \times \vec{\sigma}_1}{4\pi} \right) \left\{ \frac{\mu(m_1, r)}{r^3} + \frac{1}{2} \frac{\mu(m_1, R)}{R^3} + \int_r^R dr' \frac{\mu'(m_1, r')}{r'^3} \right\} \quad (71)$$

The corresponding color magnetic field is:

$$\vec{H}_1^a(\vec{r}) = - \left(\frac{gF_a^1}{4\pi} \right) \left\{ [3\vec{r}(\vec{\sigma}_1 \cdot \vec{r}) - \vec{\sigma}_1] \frac{\mu(m_1, r)}{r^3} + \vec{\sigma}_1 \left(\frac{\mu(m_1, R)}{R^3} + 2 \int_r^R dr' \frac{\mu'(m_1, r')}{r'^3} \right) \right\} \quad (72)$$

One has $\vec{r} \times \vec{H}_1^a(\vec{r}) = 0$ at the boundary. The mutual magnetostatic interaction energy associated with this field is

$$\begin{aligned} E_M &= - \sum_{a=1}^8 \sum_{1>J} \int_{\text{bag}} d^3x \vec{H}_1^a(\vec{r}) \cdot \vec{H}_J^a(\vec{r}) \\ &= - \frac{3\alpha_c}{R} \sum_{a, 1>J} \left(\frac{\mu(m_1, R)}{R} F_{1\sigma_1}^{a\vec{\sigma}_1} \right) \left(\frac{\mu(m_J, R)}{R} F_{J\sigma_J}^{a\vec{\sigma}_J} \right) \cdot I_{1J} \end{aligned} \quad (73)$$

This expression has the appearance of an interaction between two effective color magnetic dipole moments, which for a colored quark could be defined as

$$\vec{\mu}_1^a = \mu(m_1, R) g F_{1\sigma_1}^{a\vec{\sigma}_1} \quad (74)$$

in analogy with the electromagnetic case (see section IV 1). The overlap or smearing integral is given by

$$\begin{aligned} I_{1J} &= 1 + 2 z_1 z_J \left\{ - (x_1 \sin^2 x_1)(x_J \sin^2 x_J) - \frac{3}{4} Y_1 Y_J + \right. \\ &\quad \frac{x_1 x_J}{4} [2x_1 S_1(2x_1) + 2x_J S_1(2x_J) - (x_1 + x_J) S_1(2x_1 + 2x_J) - \\ &\quad \left. (x_1 - x_J) S_1(2x_1 - 2x_J) \right] \Big\} \end{aligned} \quad (75)$$

in terms of x_1 , the energy root for the $1s_{1/2}$ mode quark with mass m_1 , and $z_1 = x_1 \sin^2 x_1 - \frac{3}{2} Y_1$, with $Y_1 = x_1 - \sin x_1 \cos x_1$. We denote the sine integral by $S_1(x) = \int_0^x dt \frac{\sin t}{t}$. Thus, $I_{1J} = I(m_1 R, m_J R)$ still depends on the radius R , through the quark masses. One has $I(0,0) = 1.442$ and a slow monotonous limited increase for $mR \rightarrow \infty$, which is too small to compensate for the decreasing behavior of the remaining R dependence. Writing

$$E_M = -\frac{\alpha_c}{R} \sum_{1>J,a} (F_{11}^{a\rightarrow}) (F_{JJ}^{a\rightarrow}) M(m_1 R, m_J R) \quad , \quad (76)$$

one has $M(0,0) > M(0,mR) > M(mR,mR)$ ($0.177 > 0.142 > 0.059$ for $mR = 1.4$).

The chromomagnetic splitting tends to decrease with increasing values of mR .

E_M is spindependent. It is the only term coming from graphs 1a and 1b, which has this property.

For the color electric field the Maxwell equations read

$$\vec{\nabla} \times \vec{E}_1^a = 0 \quad (77a)$$

$$\vec{\nabla} \cdot \vec{E}_1^a = \frac{\rho_1^a}{4\pi} F_1^a \quad r < R \quad (77b)$$

in terms of

$$\rho_1^a = \psi_1^{\dagger}(\vec{r}) \gamma^0 \psi_1(\vec{r}) = \frac{N_{1+1/2}^2}{(ER+mR)} \{ j_0^2(\text{pr})(ER+mR) + j_1^2(\text{pr})(ER-mR) \} \quad (78)$$

One has $\rho(m_1, r) = \int_0^r dr' r'^2 \rho'(r')$ and $\rho(m_1, R) = 1$. This yields:

$$\vec{E}_1^a(\vec{r}) = \frac{\vec{r}}{4\pi r^3} (g F_1^a) \rho(m_1, r) \quad , \quad (79)$$

a chromo-electric field, which does not satisfy the linear boundary condition:

$\hat{r} \cdot \vec{E}_1^a(\vec{r}) = \frac{g F_1^a}{4\pi R^2} \neq 0$ at $r = R$ as a consequence of Gauss' law. We note that this result does not depend on the flavor of the quark, but only on its color. For

a color singlet hadron $|\alpha\rangle$ one has

$$\hat{r} \cdot \vec{E}_1^a |\alpha\rangle = \hat{r} \cdot \int_1^R \vec{E}_1^a |\alpha\rangle = \int_1^R \frac{g F_1^a}{4\pi R^2} |\alpha\rangle = 0 \quad .$$

When we want to calculate the chromo-electric interaction energy we therefore have to take the whole field into account, and cannot suffice with considering only the mutual color electric interaction energy. For a hadron containing only equal mass quarks, the total field energy is proportional to the total color charge and therefore vanishes also locally. If quarks with different masses are present, the interaction energy no longer is zero:

$$E_E = \frac{1}{2} \sum_{a=1}^8 \sum_{l,j} \int_{\text{bag}} dV \vec{E}_l^a(\vec{r}) \cdot \vec{E}_j^a(\vec{r}) = \frac{\alpha}{2R} \sum_{a=1}^8 \sum_{l,j} F_{l,j}^a F_{l,j}^a J_{l,j} \quad (80)$$

We define $J_{l,j} = J(m_l R, m_j R) = R \int_0^R \frac{dr}{r} \rho(m_l r) \rho(m_j r)$. One has $J(0,0) = 0.278$, $J(0,mR) = 0.325$ and $J(mR,mR) = 0.369$ for $mR = 1.4$, indicating a slow increase as a function of mR . E_E can be interpreted as the interaction between two charge densities. It consists of the sum of the positive self interaction and the negative, almost or fully equal mutual interactions, and is never larger than 5 MeV for the below considered hadrons.

The one gluon exchange contributions are included as a perturbation

$$H_G = E_M + E_E \text{ in the hamiltonian } H = H_0 + H_G.$$

Including all these refinements the hamiltonian now contains the following terms:

$$H = E_V + E_0 + E_Q + E_M + E_E \quad , \quad (81)$$

of which the numerically insignificant term E_E will be neglected. The mass of a specific hadron again is given by the minimum, the expectation value of the hamiltonian assumes in that hadron state, treating the bag radius as the variational parameter. To calculate it, we need to know the flavor, spin and color properties of the hadron wavefunction. In this section we will restrict ourselves to $Q\bar{Q}$ meson and Q^3 baryon states. For these hadrons the color and flavor spin parts of the wavefunction can be treated separately.

Giving nonstrange and strange quarks a different mass, the flavor symmetry of H will be broken through the terms E_Q , E_M and E_E . E_0 , by assumption, does not. E_Q is diagonal in the numbers of nonstrange and strange quarks (N_n and N_s , resp.): $E_Q = N_n E_n(R) + N_s E_s(R)$, and dominates the flavor breaking. It causes e.g. the ω and ϕ mesons to be "ideally mixed" combinations of nonstrange and strange quarks respectively. The eigenstates of the unperturbed hamiltonian are the eigenstates of E_Q . This result is reinforced

by the E_M term, which, however, does not have the same simple linear dependence on N_s and N_n . E_E gives a small contribution when both N_n and N_s are unequal to zero.

To determine the color dependence of H_G , we make use of the colorsinglet nature of our states: $Q^a |1\rangle = g \sum_1 F_1^a |1\rangle = 0$. For a $Q\bar{Q}$ colorsinglet one has $(F_Q^a + F_{\bar{Q}}^a) |1, Q\bar{Q}\rangle = 0$, and therefore also

$$\sum_a (F_Q^a + F_{\bar{Q}}^a) (F_Q^a + F_{\bar{Q}}^a) |1, Q\bar{Q}\rangle = \sum_a (F_Q^a)^2 + 2 F_Q^a F_{\bar{Q}}^a + (F_{\bar{Q}}^a)^2 |1, Q\bar{Q}\rangle = 0.$$

The term $\sum_a F_Q^a^2$ acts only on the quark (colortriplet) part of the singlet.

From the representation $F_Q^a = \frac{\lambda^a}{2}$ (appendix B), we find

$$\sum_a F_Q^a^2 |Q\rangle = f^2(\underline{3}) |Q\rangle = \frac{4}{3} |Q\rangle. \text{ We denote the eigenvalues in the irrep } \underline{n}$$

of the quadratic Casimir operator for $SU(3, C)$ $C_2 = \sum_a F_a^2$, which is the generalization of the $SU(2, J)$ operator $C_2 \equiv \sum_1 J_1^2$, with $f^2(\underline{n})$. Similarly

$$f^2(\underline{3}^*) = \frac{4}{3}. \text{ Combining these results we get}$$

$$\sum_a F_Q^a F_{\bar{Q}}^a |1, Q\bar{Q}\rangle = -\frac{4}{3} |1, Q\bar{Q}\rangle \quad (82)$$

One can proceed analogously for the Q^3 baryon colorsinglet:

$$|1, Q^3\rangle = \frac{\epsilon_{1jk}}{\sqrt{6}} Q^1 Q^j Q^k, \text{ which is completely antisymmetric w.r.t. permutation}$$

of the quark color labels. One has $(F_1^a + F_2^a + F_3^a) |1, Q^3\rangle = 0$ (1, 2 and 3 label different quarks), or equivalently $(F_1^a + F_2^a) |1, Q^3\rangle = -F_3^a |1, Q^3\rangle$. Multi-

plying both sides with F_3^a and summing over the color indices we find:

$$\sum_a (F_1^a F_3^a + F_2^a F_3^a) |1, Q^3\rangle = -\frac{4}{3} |1, Q^3\rangle. \text{ Two more such equations can be obtained}$$

through cyclic permutation and one finds

$$\sum_a F_1^a F_j^a |1, Q^3\rangle = -\frac{2}{3} |1, Q^3\rangle \quad (83)$$

for each $1 \neq j$. We see, that the color interaction of the quark and the antiquark in a meson is twice as large as the interaction between two quarks in a baryon, but attractive in both configurations.

The spindegeneracy of H_0 is lifted by the $\vec{\sigma}_i \cdot \vec{\sigma}_j$ dependence of E_M which can be discussed without any reference to color. Again, one can proceed by making use of the quadratic Casimir operators. For a meson with spin j we have $\frac{1}{4} (\vec{\sigma}_Q + \vec{\sigma}_{\bar{Q}})^2 |j\rangle = j(j+1) |j\rangle$. Since the quark and the antiquark both have spin $j = 1/2$, we find

$$\vec{\sigma}_Q \cdot \vec{\sigma}_{\bar{Q}} |j\rangle = \{2j(j+1) - 3\} |j\rangle \quad . \quad (84)$$

Due to the presence of E_M , the pion ($j = 0$) will become lighter by an amount of $\delta E_0 = -4 \frac{\alpha_C}{R} M(m_n R, m_n R)$, whereas the ρ -meson becomes heavier by $\delta E_1 = \frac{4}{3} \frac{\alpha_C}{R} M(m_n R, m_n R)$. In case of the $j = 3/2$ decuplet baryons each pair of quarks has to have a total spin $j = 1$, and consequently

$$\vec{\sigma}_1 \cdot \vec{\sigma}_j |j=3/2\rangle = |j=3/2\rangle \quad (85)$$

for each $1 \neq j$, causing these baryons to become heavier. Taking the bag radius the same for all baryons, we recover to good accuracy the $SU(3,F)$ equal spacing rule. $\Omega^* - \Xi^* = \Xi^* - \Lambda^* = \Lambda^* - \Delta^*$, where the particle names stand for the particle masses. This result will even be improved by the tendency of R to decrease with the increase of N_s (Table IV). A more complicated situation is encountered considering the $j = 1/2$ octet baryons. These particles have a wavefunction, which is completely symmetric w.r.t. simultaneous permutation of the flavor and spin indices, but has a mixed permutation symmetry for flavor and spin separately. This is reflected by the fact that two quarks can in principle be part of time in a spin $j = 0$, and the remainder in a spin $j = 1$ state. Irrespective of the distribution among the quarks, the total spinsplitting is given by

$$(\vec{\sigma}_1 \cdot \vec{\sigma}_2 + \vec{\sigma}_1 \cdot \vec{\sigma}_3 + \vec{\sigma}_2 \cdot \vec{\sigma}_3) |j=1/2\rangle = -3 |j=1/2\rangle \quad . \quad (86)$$

Since the nucleon contains only nonstrange quarks, this is at the same time the correct splitting for this baryon. The Σ -baryon contains two strange

Hadron	Mass (exp)	Bagmass A	Radius A	Bagmass B	Radius B	Bagmass C	Radius C
Nucleon (N)	0.939	0.936	4.97	0.939	5.51	0.939	2.86
Delta (Δ)	1.232	1.233	5.48	1.233	6.21	1.237	3.24
Lambda (Λ)	1.116	1.107	4.92	1.109	5.41	1.093	2.85
Sigma (Σ)	1.193	1.146	4.93	1.151	5.43	1.110	2.85
Sigma (Σ^*)	1.385	1.388	5.43	1.386	6.14	1.384	3.23
X1 (Ξ)	1.318	1.290	4.88	1.292	5.33	1.254	2.84
X1 (Ξ^*)	1.533	1.534	5.39	1.533	6.06	1.530	3.22
Omega (Ω)	1.672	1.673	5.35	1.673	5.99	1.674	3.21
Pion (π)	0.138	0.275	3.29	0.205	2.39	0.236	1.57
Kaon (K)	0.496	0.494	3.18	0.416	2.18	0.410	1.54
Omega (ω)	0.783	0.783	4.71	0.782	5.34	0.778	2.76
Kaon (K^*)	0.892	0.932	4.65	0.929	5.23	0.924	2.75
Phi (ϕ)	1.020	1.067	4.61	1.063	5.13	1.067	2.74
Fit A	$B^{1/4} = 0.1455 (0.03)$	$Z_0 = 1.842 (1.12)$	$m_s = 0.279 (0.07)$	$\alpha_c = 2.198 (0.97)$	$m_n = 0$	(-)	
B	0.1285 (0.12)	1.954 (1.16)	0.345 (0.37)	2.860 (4.79)	0.095 (0.51)		
C	0.2099 (0.25)	1.055 (1.01)	0.255 (0.77)	1.358 (1.93)	0.064 (0.92)		

Table IV: Masses and $B^{1/4}$ in GeV, radii in GeV^{-1} . The number in parentheses denote the percentage change in the parameter necessary to raise the χ^2 of the fit by one unit.

quarks, which have a symmetric flavor wavefunction, and therefore must have exclusively $j = 1$, implying that

$$\vec{\sigma}_{s1} \cdot \vec{\sigma}_{s2} |j=1/2\rangle = |j=1/2\rangle \quad (87a)$$

and consequently: $(\vec{\sigma}_{s1} + \vec{\sigma}_{s2}) \cdot \vec{\sigma}_u |j=1/2\rangle = -4 |j=1/2\rangle$. (87b)

A similar phenomenon occurs for the Λ and Σ baryons. These contain two nonstrange and one strange quark. The Λ has isospin $I = 0$, which implies that the two nonstrange quarks must occupy a $j = 0$ state. It follows that

$$\vec{\sigma}_u \cdot \vec{\sigma}_d |j=1/2\rangle = -3 |j=1/2\rangle \quad (88a)$$

and $(\vec{\sigma}_u + \vec{\sigma}_d) \cdot \vec{\sigma}_s |j=1/2\rangle = 0$. (88b)

The Σ has $I = 1$, implying

$$\vec{\sigma}_u \cdot \vec{\sigma}_d |j=1/2\rangle = |j=1/2\rangle \quad (89a)$$

and $(\vec{\sigma}_u + \vec{\sigma}_d) \cdot \vec{\sigma}_s |j=1/2\rangle = -4 |j=1/2\rangle$ (89b)

for the $I_3 = 0$ state. We find that E_M not only lifts spin degeneracies ($\rho - \pi$, $N - \Delta$), but also the isospin degeneracy for the baryon octet. Furthermore, we see that the entire octet is lowered in mass through E_M . For a (more complete) discussion of the flavor $SU(3,F)$ -tensor structure and -mass formula, see Chapter 3.

We have now all the necessary ingredients, to calculate the masses of the light hadrons. To determine the parameters B , Z_0 , m_n , m_s and α_c one can proceed in various ways. The MIT strategy was to set $m_n = 0$ and adjust the other parameters such that the nucleon, the Δ , Ω and ω masses are reproduced. Since N , Δ and ω contain only nonstrange quarks B , Z_0 and α_c can be determined through analytic calculation. To determine m_s , such that the Ω has the correct mass, one needs the help of a computer (Table IV, fit A). Taking $m_n \neq 0$, analytical calculation no longer is possible and one has to resort to fitting the mass spectrum. To obtain a comparable result one can do a least square

fit in which one gives the N , Δ , Ω and ω a much larger weight (factor 10) than the remaining hadrons. In this case one has to restrict $m_n < 108$ MeV, since for larger values $\frac{\partial H}{\partial R}$ no longer has a minimum for the pion. A typical fit is given in column B. For comparison, also a fit (fit C) is given in which the static current color magnetic self interaction is included. We note that the radii are becoming rather small, while the strengths of the color magnetic splitting become less flavor broken, which we think bad features. In all cases we find, that the N , Δ , Ω and ω masses are reproduced rather accurately, as well as the remaining decuplet masses. The agreement is not so good for the octet baryons, which tend to be rather light. Especially the Λ - Σ splitting, although present, is too small. Also the vector mesons are reproduced reasonably well, the ϕ and K^* being a little bit too heavy. The model does not lift the ρ - ω degeneracy. The masses of the pseudo-scalar mesons π and K are rather sensitive to the precise values of the parameters. They invariably turn out to have much smaller roots for the radius than the other, above mentioned hadrons, which all have about the same size. At one point $\frac{\partial H}{\partial R}$ even ceases to have a solution for the pion radius at all. One expects that the various approximations made above (neglect center of mass motion, constant Z_0 and α_c) will break down when large differences in the radius start to occur. In this respect fit A is preferable to fit B, although the latter reproduces the hadrons around 1 GeV much better than the former. The failure of our approximations here is signalled by the fact that the perturbation term E_M (in fit A) is already of the same order of magnitude as the complete mass: $E_M = -0.415$ versus 0.495 GeV for the kaon and $E_M = -0.465$ versus 0.280 GeV for the pion, which is almost a factor of two larger than the bagmass! These ratios become worse for fit B: $E_M = -2.81$ versus 0.37 GeV for the kaon and $E_M = -1.82$ versus 0.18 GeV for

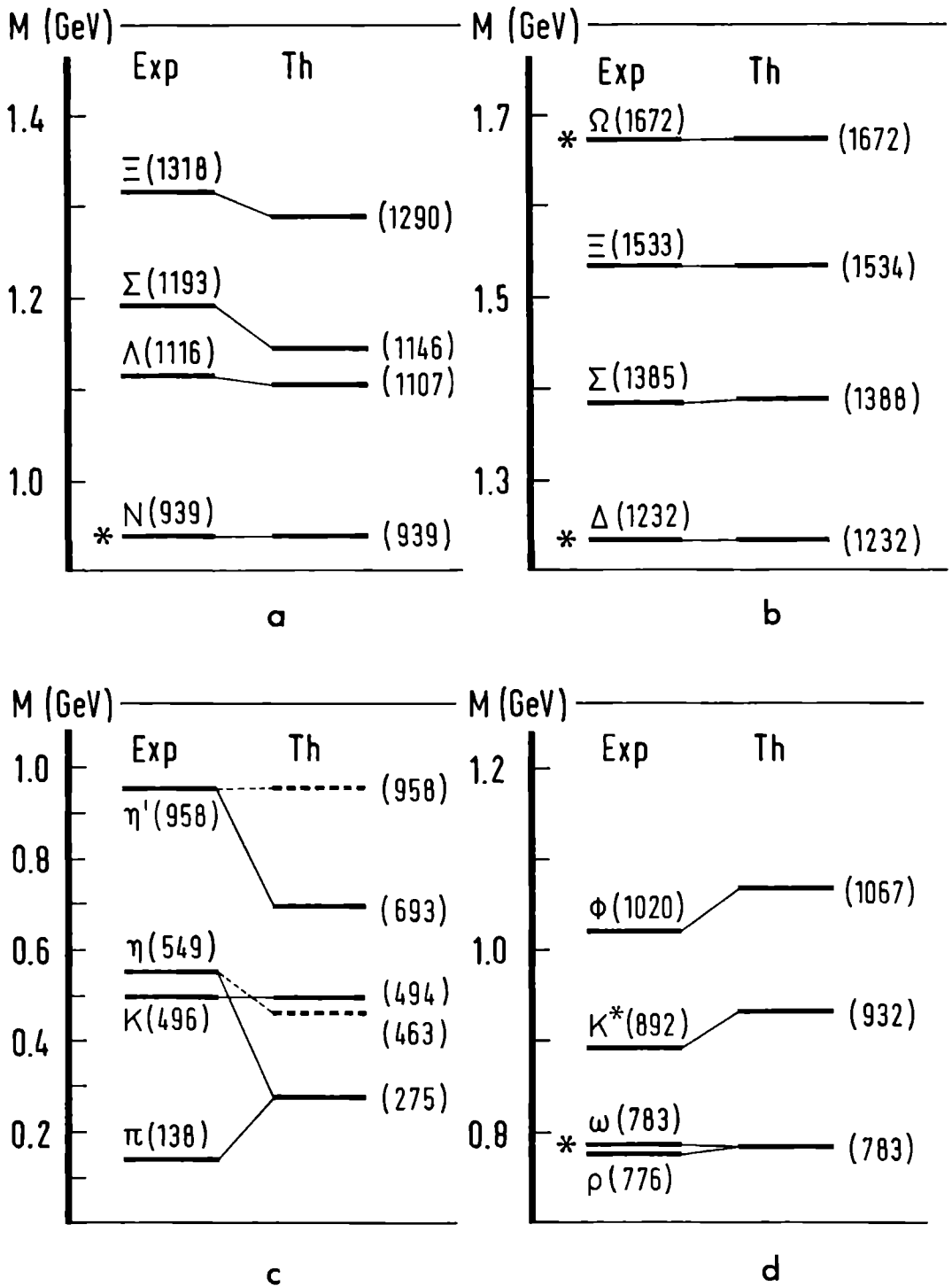


Fig. 2: The mass spectrum, corresponding to fit A, of the baryon $J^P = 1/2^+$ octet (a) and $3/2^+$ decuplet (b), and the 0^- (c) and 1^- (d) meson nonets. States with an * are input. The η and η' have been refitted to account for remixing effects.

the pion. For the other states it is typically 10 to 15 % of the bag mass value. We note, there is something wrong with the strength of E_M , witness the anomalously large values for the strong coupling constant α_c , as compared to more frequently used values $\alpha_c \approx 0.3$. This may be seen as an indication that the spin dependency may already have roughly the right structure, but that still some comparable contributions are being overlooked. Other indications emerge when considering e.g. the η and η' pseudoscalar mesons. The $Y = 0$ $Q\bar{Q}$ meson eigenstates of H consist of either purely nonstrange or strange quarks, implying that the η is degenerate with the pion, as is the ω with the ρ in case of the vector mesons. The η' contains only strange quarks and has (fit A) a mass $m = 0.690$ GeV. This bad agreement points at the neglect of other effects such as the annihilation of a $u\bar{u}$ or $d\bar{d}$ pair into an $s\bar{s}$ pair and vice versa, via a two or more gluon intermediate state. Taking this effect into account results in slightly better values (Fig. 2). The model as formulated above does not take $Q\bar{Q}$ pair creation into account, which makes e.g. Δ and ρ stable w.r.t. strong decay.

On the whole, the spherical cavity approximation proves to be rather satisfactory as a spectroscopic model and can be used as a starting point to investigate more exotic quark configurations, consisting of nonstrange and strange quarks. Especially in the formulation, where the former is chosen massless, one has a quite instructive realization of a confined relativistic quark model. Further properties of this special case will be treated in section IV.

IV. The spherical cavity and SU(6,FJ) [Ko 69, DeG 75, Ba 75, Go 75]

We will conclude the discussion of the spherical cavity approximation by studying some other static properties of the hadron, namely the magnetic moment, the mean square charge radius and the axial vector coupling constant.

These properties have also been studied in the context of the nonrelativistic quark (NRQ) model and a comparison between the two models will be made. Since the above mentioned properties depend on the detailed structure of the space spin flavor part of the wavefunction, they provide a more severe test for this aspect of the hadron description than masses do.

SU(6). The color properties of the quark system under consideration only affect these results indirectly. The hadron must be a colorsinglet. An all (anti)quark configuration has a unique color wavefunction with a well defined permutation symmetry. There is only one possible permutation symmetry for the remainder of the wavefunction which combined with that of the color part yields a completely antisymmetric overall permutation symmetry. For e.g. the Q^3 baryons, it is the completely symmetric one, since the color wavefunction is completely antisymmetric under permutations. For systems containing both quarks and antiquarks these considerations apply to both the fermion and the antifermion subsystem separately. The color wavefunction for the quarks no longer needs to be a colorsinglet one, provided the overall wavefunction is, and the various possibilities may occur within one wave function. The attention will be restricted to quarks occupying the $1s_{1/2}$ ground state mode. Furthermore, we will consider only three flavors: u, d, and s, all of which are associated with small quark mass parameters (see Table IV). In the limit that $m_u = m_d = m_s$ the flavorpart of the wavefunction can be classified using the irreps of flavor SU(3,F), denoted by \underline{n} . The quark transforms as a triplet ($\underline{n} = \underline{3}$) under SU(3,F).

The lowest energy eigenmode in the NRQ model is that of a quark with spin $s = 1/2$, moving nonrelativistically through space with orbital angular momentum $\ell = 0$. In this case ℓ and s are good quantum numbers. We can define a total orbital angular momentum $\vec{L} = \sum_1 \vec{\ell}_1$ and a total intrinsic spin

$\vec{S} = \sum_1 \vec{s}_1$, where the sum runs over all quarks present, which combine to a total angular momentum $\vec{J} = \vec{L} + \vec{S}$, the spin of the hadron. An LS coupling scheme results in which all states are classified according to $O(3)$ for the spatial, and according to $SU(2,S)$ for the spin part of the wavefunction. The space spin classification of systems, in which all quarks occupy $\ell = 0$ orbits, effectively reduces to an $SU(2,S)$ one. The spin wavefunction determines the permutation symmetry, since the spatial part is completely symmetric throughout. The flavor and spin contents of a color singlet hadronic ground state can most economically be summarized in terms of flavor spin irreps. One introduces flavor spin $SU(6,FS)$. A quark transforming as a triplet, $\underline{n} = \underline{3}$, under $SU(3,F)$ and as a doublet, $s = 1/2$, under $SU(2,S)$ transforms as a sextet, $[\underline{6}] = [6]$, under $SU(6,FS)$. Because $SU(6,FS) \supset SU(3,F) \otimes SU(2,S)$ we have the decomposition $[\underline{6}] = [6] = \sum_{\otimes} (\underline{n},s) = (\underline{3},1/2)$. The product e.g. of three quark wavefunctions can be reduced according to

$$[6] \otimes [6] \otimes [6] = [56] \otimes [70] \otimes [70] \otimes [20] \quad .$$

The 56-dimensional irrep is completely symmetric under permutations whereas the 20-dimensional one is completely antisymmetric. The two 70-dimensional irreps have a mixed permutation symmetry. Therefore the [56]-irrep has the correct behavior and from $[56] = (\underline{8},1/2) \otimes (\underline{10},3/2)$ the allowed flavor and spin combinations for the baryonic ground states in this model are found, which is seen to be correct.

In the bagmodel a different classification scheme is encountered. In its ground state, the $1s1/2$ mode, the total angular momentum of the quark is given by $j = 1/2$. This j value is the result of coupling the quark spin $s = 1/2$ to the orbital angular momentum ℓ , which differs between the upper and lower spinor components. The two upper components of the quark four

spinor have $\ell = 0$, the two lower ones $\ell = 1$. The space and spin wavefunctions of the quark are tightly interwoven to yield a good description of the total spin of the relativistically moving quark. A system of such quarks can be classified with the irreps of $SU(2,J)$. The total hadronic angular momentum is found by combining the total spins j of the quarks. This situation is referred to as a j - j coupling scheme. The NRQ- and the bagmodel then have an equivalent classification for the space-spin part of the wavefunction of hadrons containing only groundstate quarks. This implies for the bagmodel that one can also carry through the unification of the flavor and (space-) spin symmetries just as in the NRQ-model. States will now be classified according to the irreps of flavor spin $SU(6,FJ)$:

$$SU(6,FJ) \supset SU(3,F) \otimes SU(2,J) \quad .$$

The NRQ LS- and the bagmodel jj type ground state description are (trivially) related by a unitary basis transformation. Also hadrons, containing excited quarks, are equivalently described in these two ways [DeG 76]. Consider in the NRQ-model a Q^3 baryon in which one quark is excited to an $\ell = 1$ orbit. Next to the completely symmetric one, also a space wavefunction with mixed symmetry can be constructed which can be combined with a 70-dimensional irrep. One obtains the $[70] L = 1$ and $[56] L = 1$ multiplets. As stated in section II, these states are in the bagmodel, described by linear combinations of the configurations $(1s1/2)^2(1p1/2)$ and $(1s1/2)^2(1p3/2)$. In this case one constructs the wavefunctions with the desired total j -value and determines the combinations with definite spin space permutation symmetry for each configuration separately. Space and spin no longer have a separate permutation symmetry due to the compositeness of j , viz. the $(1p3/2)$ mode.

To excite a 20-dimensional irrep one needs three inequivalent excitations. Of course, the fact that a certain space spin flavor combination is allowed on the basis of permutation symmetry arguments, does not imply that it represents a state of the physical spectrum, witness the discussion in section II on the spurious translation modes, the [56] L = 1 states, occurring in the nonrelativistic potential models.

The equivalence of the NRQ- and bagmodel classification of the hadron ground states entails, that those NRQ-model SU(6,FS) results, for which no further assumptions are needed, immediately apply to the bagmodel, e.g. the results for the magnetic moments and charge radii. The axial vector to vector coupling constant ratio, measured in e.g. β -decay processes of the octet baryons needs some additional treatment.

The parameters taken in this discussion are those of the MIT fit (fit A) [DeG 75]. This implies that the SU(6,FJ) symmetry will be broken in two ways. To account for e.g. the $N \Omega^-$ mass difference the strange quark is given a mass $m_s = 0.279$ GeV. The inclusion of spin dependent terms in the hamiltonian lifts the degeneracy of multiplets with identical quark content, but different spin or isospin quantum numbers. This results in different values of the bag radius for which E(R) is minimal.

1. Magnetic moment

The response of the quarks inside the hadron to the electromagnetic field is determined by the properties of the quark current operator $J^\mu = \bar{\psi} \gamma^\mu Q \psi$, where Q is the electromagnetic charge operator. Applying a weak magnetic field $\vec{B} = B\vec{z}$ the resulting energy shift for a state $|\alpha\rangle$ is $\langle\alpha|H_1|\alpha\rangle = -\langle\alpha|\mu_z|\alpha\rangle B$. The magnetic moment operator is given by

$$\vec{\mu} = \frac{1}{2} \int_{\text{bag}} dV \vec{r} \times \vec{j} = \frac{1}{2} \int_{\text{bag}} dV \vec{r} \times \psi^\dagger \vec{\alpha} Q \psi \quad (90)$$

and can therefore be calculated, absolute size and all. Evaluating this expression for the quark groundstate we find:

$$\langle \alpha | \mu_z | \alpha \rangle = \sum_{m', f} \langle \alpha | \sigma_z Q_n(m', f) | \alpha \rangle \mu(m'_f, R) \quad (91)$$

Here $n(m', f)$ gives the number of quarks with flavor f , mass m_f and spin orientation m' , and

$$\begin{aligned} \mu(m, R) &= \int_0^R dr \mu'(m, r) = \left\{ \frac{N^2 x}{ER + mR} \right\} \int_0^R dr r^3 J_0(pr) J_1(pr) \\ &= \frac{1}{2m} \cdot \frac{(mR)}{3} \left\{ \frac{4 ER + 2 mR - 3}{2 ER(ER-1) + mR} \right\} = \frac{g(mR)}{2m} \end{aligned} \quad (92)$$

We see that μ really is the expectation value of the radius, evaluated between a 'big' and a 'small' spinor component. We use $ER = p_{1+1/2}^0(mR) \cdot R$ and $N = N(1+1/2)$ for brevity. For very heavy quarks $\vec{\mu}$ reduces to the non-relativistic quark magnetic moment: $g(mR) \rightarrow 1$ and $\mu \rightarrow \frac{1}{2m}$. For $m = 0$, $ER = x_{1+1/2}$ and one finds:

$$\mu = \frac{R}{12} \left\{ \frac{4x-3}{x(x-1)} \right\} = 0.202 R \quad (93)$$

The function $\frac{\mu(m, R)}{R}$ is a monotonously decreasing function of mR with a maximum value of 0.202 for $mR = 0$. This value is very sensitive to the ratio of the upper and lower spinor component space wavefunctions and any change herein is directly reflected in the size of μ . The proton magnetic moment is given by $\mu = \mu(m_u)$ for degenerate up and down quark masses. From this we can extract a lower bound on the bag radius to fit this value:

$$0.202 R = \frac{2.79}{2M_p} \quad \text{or} \quad R \approx 1.45 \text{ fm.}$$

For $m_u \neq 0$ we need an even larger proton. Therefore, to keep the size of the proton down, we need the up and down quarks to be as light as possible. Apart from the factor $\mu(m, R)$, which is explicitly calculated in this model, we retain the $SU(6, FS)$ ratios through the remaining part of

the matrix elements: $\langle \alpha | \sigma_z Q_n(m', f) | \alpha \rangle$. A consequence of taking $m_u = m_d$, is that the magnetic moment of the neutron is $(-2/3)$ times that of the proton: the exact SU(6,FS) result. In Table V, the ratios of the magnetic moments of the octet baryons to that of the proton are listed: the SU(6,FS), the calculated and the experimental values [PDG 78]. Agreement is good. For the physical proton $R \approx 1.0$ fm and we find $g_p = 1.90$ instead of $g_p = 2.79$. Gluonic vertex corrections tend to decrease this value even more [Ha 77]. This can be interpreted as a hint that in this crude model the wavefunctions may be realistic, whereas the hadron parameters are not quite satisfactory. To conclude we note that the choice of Q to be the electric charge is not exclusive. One can also take it to be $Q^a = g F^a$: the color charge.

Baryon	(μ/μ_p) SU(6)	(μ/μ_p) exp	(μ/μ_p) calc
P (938)	1	1	1
N (940)	- 2/3	- 0.685	- 0.67
Λ (1116)	- 1/3	- 0.217 + 0.012	- 0.26
Σ^+ (1189)	1	1.01 ± 0.09	0.97
Σ^0 (1193)	1/3		0.31
Σ^- (1198)	- 1/3	- 0.53 ± 0.13	- 0.35
Ξ^0 (1314)	- 2/3		- 0.56
Ξ^- (1321)	- 1/3	- 0.66 ± 0.27	- 0.23

Table V: The magnetic moments of the flavor octet baryons, in units μ_p .

Experimentally one has $\mu_p = 2.793 \left(\frac{e}{2M_p} \right)$, calculation gives $\mu_p \approx 1.90 \left(\frac{e}{2M_p} \right)$.

2. Mean square charge radius

For the experimentally more frequently used hadrons an accurate parametrization of the Dirac form factor as a function of the momentum transfer squared, $F_1(q^2)$, $q^2 = t$, is known. When we expand it, for low q^2 , the second term gives a measure for the extension of the hadron:

$$r^2 = -6 \left\{ \frac{dF_1(q^2)/dq^2}{F_1(q^2)} \right\} \Big|_{q^2=0}, \quad (94)$$

called the mean square charge radius. Calculated in the bagmodel it has the form:

$$r_{sc}^2 = \langle \alpha | \int_{\text{bag}} dV |\vec{r}|^2 \psi^\dagger Q \psi | \alpha \rangle = \sum_{m', f} \langle \alpha | n(m', f) Q | \alpha \rangle \bar{r}^2 \quad (95)$$

with

$$\bar{r}^{-2} = \frac{R^2}{6} \frac{2ER\{2x^2(ER-1) + 2mR + 4ER - 3\} - 3mR\{4ER + 2mR - 2x^2 - 3\}}{x^2\{2ER(ER-1) + mR\}} \quad (95a)$$

$$\bar{r}^{-2} \Big|_{m=0} = \frac{R^2}{6} \frac{2x^3 - 2x^2 + 4x - 3}{x^2(x-1)} = 0.531 R^2$$

$$\bar{r}^{-2} \Big|_{m=\infty} = \frac{R^2}{6} \frac{2x^2 - 3}{x^2} = 0.283 R^2$$

The charge radius depends on the quark mass $r_{sc}(m_1) < r_{sc}(m_2)$, for $m_2 > m_1$. Taking $m_u = m_d$ the calculated r_{sc}^2 value for the neutron vanishes. From the fact that in practice it turns out to be positive, one might conclude, that the down quark is heavier than the up quark, in agreement with explaining the P-N mass difference, similar to the P- Ω^- mass difference, i.e. by giving m_u and m_d different values. Because the strange quark does have $m_s \neq m_u = m_d$, r_{sc}^2 is also positive, for the Λ , γ^0 and Ξ^0 , of course violating SU(3,F) symmetric relations.

Comparison of the theory with data gives Table VI. The charge radius for the neutron is obtained indirectly ($F_1^N(0) = 0$), using the proton- and isoscalar Dirac form factors: $2 F_1^S(q^2) = F_1^P(q^2) + F_1^N(q^2)$.

Hadron	P	N		π^+	K^+	K^0
Theory (bag)	0.72	0.0		0.48	0.44	0.14
Exp	0.76 ± 0.02	0.10 ± 0.01		0.695 ± 0.005	...	0.28 ± 0.09
Ref	[Ho 76]	[Ho 76]		[Ge 77]	...	[Dy 76]

Hadron	Λ	Σ^+	Σ^0	Σ^-	Ξ^0	Ξ^-
Theory (bag)	0.16	0.73	0.16	-0.69	0.22	-0.67
Exp
Ref

Table VI: Mean square charge radius r_{sc}^2 . We list the sign of r_{sc}^2 times

$$\sqrt{|r_{sc}^2|}, \text{ in fm.}$$

3. The axial vector coupling constant

A third application of SU(6,FJ) symmetry emerges from the study of the semileptonic decay of baryons. We will restrict our attention to the octet members of the [56] irrep. The relevant hadronic part of the weak interaction current density is given by

$$J_h^\mu(x) = \bar{u}(x) \gamma^\mu (1 + \gamma_5) (d(x) \cos \theta_c + s(x) \sin \theta_c) + h.c. \quad (96)$$

where $u(x)$, $d(x)$ and $s(x)$ denote the quark fields of the specified flavor and θ_c is the Cabibbo angle, giving the correct observed relative strength to the u and s contribution. Let us consider the β -decay of the neutron into the proton, as an illustration. The expectation value of the weak interaction hamiltonian is then given by

$$\langle Pe^- \bar{\nu}_e | H_w | N \rangle = \frac{G \cos \theta_c}{\sqrt{2}} \int dV \langle Pe^- \bar{\nu}_e | \bar{u}(x) \gamma_\mu (1 + \gamma_5) d(x) e^- (x) \gamma^\mu (1 + \gamma_5) \nu(x) | N \rangle \quad (97)$$

where the exchange of a rather heavy weak boson is seen to have resulted

in an effectively local interaction. The small momentum transfer of the leptons to the outgoing baryon has two consequences. The wavefunction of the leptons which are not confined to the bag, is approximately independent of x , as far as the interaction region is concerned. This approximation is reasonable for $|\vec{q}_e + \vec{q}_\nu|c < .2 \text{ GeV}$. The matrix element of H_W then factorizes into a leptonic and a hadronic part, and we can study the latter separately. Secondly, both nucleons can be taken at rest. Furthermore, we shall take the bags to have both the same radius, for which we choose the equal weight value. This latter approximation is exact for the proton-neutron case, since these states have a degenerate bagmodel configuration. The space integration reduces to a bag integration. Consider

$$\langle P | J_h^\mu | N \rangle = \cos \theta_c \int_{\text{bag}} dV \langle P | \bar{u}(x) \gamma^\mu (1 + \gamma_5) d(x) | N \rangle \quad . \quad (98)$$

This matrix element contains a vector- (v) and an axial vector (a) part. The former only contributes for $\mu = 0$, the latter for $\mu = j$, $j \in (1, 2, 3)$. We find:

$$\langle P | J_h^0 | N \rangle = g_V(m_d, m_u) \int_1 \langle P | u_1^\dagger d_1 \cos \theta_c | N \rangle \quad . \quad (99)$$

We define: $\gamma_V = \cos \theta_c \int_1 \langle P | u_1^\dagger d_1 | N \rangle$ for the neutron β -decay to the proton. One has $\gamma_V = \cos \theta_c$. The index 1 denotes that the transition operator, in this case the quark isospin raising operator $I_1^+ = u_1^\dagger d_1$, which replaces, if available, a d with a u quark, acts on the 1th quark in the neutron. This transition conserves strangeness: $\Delta S = 0$. The overlap factor $g_V(m, m')$ depends on the quarkmasses:

$$g_V(m, m') = \frac{2xx'}{x'^2 - x^2} \frac{(m'R - mR)}{\sqrt{2E'R(E'R-1) + m'R}} \frac{1}{\sqrt{2ER(E R-1) + mR}} \quad . \quad (100)$$

Here $x = x_{1+1/2}(mR)$ and $x' = x_{1+1/2}(m'R)$. We have $g_V(m, m) = 1$ and

$g_V(m_s, 0) \approx 0.985$ for the relevant range of R. The vector coupling constant G_V is then related to the weak coupling constant G by:

$$G_V = g_V \gamma_V \frac{G}{\sqrt{2}} \quad . \quad (101)$$

To evaluate the axial vector part we can take $s_z = 1/2$ for both the proton and the neutron, and consequently $j = 3$:

$$\langle P, s_z=1/2 | J_h^3 | N, s_z=1/2 \rangle = g_a(m_d, m_u) \gamma_a \quad . \quad (102)$$

Here

$$\gamma_a = \int_1 \langle P, s_z=1/2 | I_{1z}^+ | N, s_z=1/2 \rangle \cos \theta_c = \frac{5}{3} \cos \theta_c \quad (102a)$$

$$g_a(m, m') = \frac{1}{3} \left(\frac{2(ER - E'R)}{mR - m'R} + 1 \right) g_V(m, m') \quad (103)$$

$$= \frac{1}{3} \left(\frac{2ERER + mR(4ER - 3)}{2ER(ER - 1) + mR} \right) \quad \text{for } m = m'$$

Numerically we have $g_a(0, 0) = 0.653$ and $g_a(m_s, 0) = 0.72 g_V$. The axial vector coupling constant is related to G by:

$$G_a = \gamma_a g_a \frac{G}{\sqrt{2}} \quad . \quad (104)$$

For $m, m' \rightarrow \infty$, we recover the SU(6,FS) result: $G_a = \frac{5}{3} G_V$ for the neutron β -decay. In the bagmodel version ($m_u = m_d = 0$) this value is reduced to $G_a = 0.653 \cdot \frac{5}{3} G_V = 1.09 G_V$, closer to the experimental value of 1.24 ± 0.03 . This reduction is a consequence of the fact that one, contrary to the non-relativistic SU(6,FS) model, now also gets contributions from the lower spinor components, which have opposite spin orientation, and is another argument in favor of light quarks.

The factors γ_a and γ_V contain the SU(6,FJ) symmetric part of the matrix elements [Sw 66]. Considering $B^+ \rightarrow Be^- \bar{\nu}_e$, instead of $N \rightarrow Pe^- \bar{\nu}_e$ we have

$$\gamma_V = \int_1 \langle B | (\cos \theta_c I_1^+ + \sin \theta_c K_1^+) | B^+ \rangle \quad \text{and} \quad (105a)$$

$$\text{and} \quad \gamma_a = \frac{1}{2} \int_1 \langle B | (\cos \theta_c I_1^+ + \sin \theta_c K_1^+) S_{1z} | B^+ \rangle \quad (105b)$$

The V-spin raising operator, which changes an s-quark into a u-quark is denoted by K_1^+ . It raises the strangeness by one unit: $\Delta S = 1$. By using the explicit form of the flavor-spin part of the wavefunction, γ_v and γ_a can be calculated exactly. One subsequently assumes that G_a and G_v still are related to G as defined, substituting the proper mass and radius parameters. One then obtains the calculated values for G_a/G_v as listed in Table VII. Since the wavefunctions are SU(3,F) symmetric one can also express G_a and G_v in terms of the Cabibbo parameters F_a , D_a and θ_c . We have the following relations:

$$G_v = \frac{G}{\sqrt{2}} \langle B | (F_{1\ 1\ 0} \cos \theta_c + F_{1/2\ 1/2\ 1} \sin \theta_c) | B' \rangle \quad (106a)$$

$$G_a = \frac{G}{\sqrt{2}} \langle B | \left\{ F_a (F_{1\ 1\ 0} \cos \theta_c + F_{1/2\ 1/2\ 1} \sin \theta_c) + D_a (D_{1\ 1\ 0} \cos \theta_c + D_{1/2\ 1/2\ 1} \sin \theta_c) \right\} | B' \rangle \quad (106b)$$

The currents are denoted by their SU(3,F) octet transformation properties according to $O_I I_Z Y$. The currents can couple to the two octet baryons in two independent ways, a completely antisymmetric f type and a completely symmetric d type coupling. For $q^2 = 0$ the conserved vector current is assumed to have only f type, the partially conserved axial vector current can have both f- and d-type couplings. This property is reflected in the notation of the matrix elements. Comparison with the specific bagmodel case allows us to explicitly calculate F_a and D_a . We find, that $F_a = f g_a/g_v = \frac{2}{3} g_a/g_v$ and $D_a = d g_a/g_v = g_a/g_v$. This implies, that the F/D ratio, due to the SU(6,FS) symmetry of the bagmodel flavor spin wavefunctions is $F/D = \frac{2}{3}$, the SU(6,FS) result. This ratio is not changed by the breaking of SU(6,FJ) from section III since this only affects the overall factor g_a/g_v . The absolute SU(6,FJ) symmetric values for F_a and D_a are, in the MIT bagmodel, reduced by a factor 0.65 for the $\Delta S = 0$ transition ($d \rightarrow u$) and by a factor of about 0.71 for

Process $B \rightarrow B'$	γ_v	γ_a	g_a/g_v (exp) [PDG 78]	g_a/g_v (calc)
$N \rightarrow P$	1	$f + d$	$- 1.253 \pm 0.007$	1.09
$\Sigma^- \rightarrow \Sigma^0$	$\sqrt{2}$	$\sqrt{2} f$		0.44
$\Sigma^- \rightarrow \Lambda$	0	$\sqrt{\frac{2}{3}} d$	$g_a = 0.24 \pm 0.23$	$g_a = 0.53$
$\Xi^- \rightarrow \Xi^0$	1	$f - d$		- 0.22
$\Lambda \rightarrow P$	$\sqrt{\frac{3}{2}}$	$\frac{1}{\sqrt{6}} (3f+d)$	$- 0.62 \pm 0.05$	0.72
$\Sigma^- \rightarrow N$	1	$f - d$	$\pm (0.385 \pm 0.070)$	- 0.24
$\Sigma^0 \rightarrow P$	$\frac{1}{\sqrt{2}}$	$\frac{1}{\sqrt{2}} (f-d)$		- 0.24
$\Xi^- \rightarrow \Lambda$	$\sqrt{\frac{3}{2}}$	$\frac{1}{\sqrt{6}} (3f-d)$		0.24
$\Xi^- \rightarrow \Sigma^0$	$\sqrt{\frac{1}{2}}$	$\frac{1}{\sqrt{2}} (f+d)$		1.2
$\Xi^0 \rightarrow \Sigma^+$	1	$f + d$		1.2

Table VII: Ratio of the axial vector to vector coupling constant G_a/G_v for the octet baryon

β -decay process $B \rightarrow B' e^- \bar{\nu}_e$ in terms of the Cabibbo parameters θ_c , F_a and D_a ,

$f = g_v^F/g_a$ and $d = g_v^D/g_a$. The columns γ_v and γ_a contain the $SU(3,F)$ symmetric

results. The bagmodel gives $f = \frac{2}{3}$, $d = 1$, consistent with $SU(6,FJ)$.

the $\Delta S = 1$ transition ($s \rightarrow u$), which accounts for the $SU(3,F)$ breaking.

One obtains

$$\Delta S = 0 \qquad F_a = 0.44 \qquad D_a = 0.65$$

$$\Delta S = 1 \qquad F_a = 0.47 \qquad D_a = 0.71$$

and experimentally $F_a = 0.41 \pm 0.02$ $D_a = 0.83 \pm 0.02$.

One finds improvement to the nonrelativistic values, but not absolute agreement. Shifting the mass parameters will not improve things substantially since F_a and D_a change in proportion.

CHAPTER 3: Q^6 DIBARYON STATES

I. Introduction

In the naive quark model [Ko 69] one was able to explain many features of the hadrons. Relations between mass differences within SU(3) multiplets could be derived. However, it was impossible to say anything sensible about the masses of the individual hadrons. In particular any indication about the masses of the exotic mesons ($Q^2\bar{Q}^2$), the exotic baryons ($Q^4\bar{Q}$) and the dibaryons (Q^6) was lacking. One of the reasons was our ignorance about the interactions between the quarks.

This situation has changed in the last few years, with the recognition that quarks have additional degrees of freedom, so-called color. With these color quantum numbers a different kind of interaction can be associated, which is thought to be governed by the equations of Quantum Chromodynamics.

A particular realization of QCD, which incorporates many of its established and expected properties, is the MIT bagmodel [Cho 74, DeG 75]. In chapter 2 we found that this model allows solutions, which are particularly suited for the description of hadronic states. The colored quarks are confined to a definite region of space, which in the simplest case is taken to be a sphere, and allowed to interact weakly with each other through the exchange of colored vector bosons, the gluons [DeR 75, Fr 71]. This way one can rather well reproduce the masses of the colorless S-wave $Q\bar{Q}$ and Q^3 baryons. The model contains in case of 3 flavors only 5, physically interpretable, parameters. Without introducing new parameters one can calculate in this bagmodel also the masses of exotic states like the S-wave $Q^2\bar{Q}^2$ mesons [Jb 77] and the S-wave Q^6 dibaryons [Jc 77]. The discussion of the former is postponed to chapter 4, the latter shall be dealt with here.

The results of the dibaryon calculations were quite interesting. It was shown that one must expect some 6 quark states with relatively low mass. These states must show up as resonances in NN, ΛN and ΣN scattering, and in the

$\Lambda\Lambda$, ΞN , $\Sigma\Lambda$, and $\Sigma\Sigma$ channels. Especially significant are the predictions of a $\Lambda\Lambda$ bound state with a binding energy of about 50 MeV and of possible NN resonances.

Experimental verification of these predictions is quite important, because the existence or non-existence of these states will be quite an important test of the applicability of the present form of the MIT bagmodel to exotic states.

Although these six quark states and in general the colorless N quark states ($N = 3, 6, 9, \dots$) also manifest themselves in scattering processes like pd , $p^3\text{H}$, or Λd , they are different from nuclear states like ^3He , ^4He , or hypernuclear states like $^3_{\Lambda}\text{H}$, because they are *single* hadron states. They are unaccounted for by the spectrum of resonances and bound states arising in standard potential model [Sw 71] or shell model [Ho 73] calculations.

In this chapter we will consider all colorless N quark states, where the quarks are in the $1s_{1/2}$ states of a spherical bag. These hadrons have thus all positive parity. Since all particles should be color singlets and since the color symmetry is unbroken, the old mass formulas [Ok 62, Gu 64, Be 64] obtained from specific assumptions about the breaking of flavor-spin symmetry are not affected. The difficulty in applying these mass formulas was that one had to determine the coefficients for each flavor-spin multiplet separately from the experimentally known masses of the hadrons. The MIT bagmodel offers a way to calculate these coefficients for the colorless N quark states, which will belong for fixed N to only one flavor-spin SU(6) irreducible representation. Because the allowed states must be totally antisymmetric with respect to flavor, spin and color, the color-spin tensor operators occurring in the spherical bag mass operator can be expressed in simple flavor-spin tensor operators. We then can identify the contributions of the different SU(6) breaking tensor operators, the coefficients being known functions of the bag radius.

In order to satisfy one of the boundary conditions in the bagmodel the mass of a particular state is found by minimizing the expectation value of the mass operator with respect to the bag radius R . As this radius does not vary too much between different members of the same $SU(6)$ multiplet, it is possible to choose only one R value for an entire multiplet without introducing significant numerical inaccuracies. This way we obtain for fixed N mass formulas, which suffice to obtain the masses of all the S -wave $N = 6, 9, 12, 15$ and 18 quark states, without introducing any new parameters.

At this point we would like to stress the importance of the prediction of several six quark states in the NN channel, because these predictions could at present be checked experimentally, if their width (about which we cannot say anything sensible) is not too large. We expect Q^6 -states in the 3S_1 channel at $T_{lab} \approx 0.61$ GeV, in the 1S_0 channel at $T_{lab} \approx 0.79$ GeV and two (almost?) degenerate states in the 1D_2 and 3D_3 channels at $T_{lab} \approx 1.04$ GeV.

In the hyperon-nucleon (ΛN and ΣN) channel many 6 quark states are expected. In the experimental data (only available for the lower energies) several enhancements can be seen next to the resonance H , seen [Br 77] at 2127 MeV. The resonance H is certainly not a six-quarks-in-one-bag state, because it can quite naturally be explained in the ordinary potential picture [Sw 62].

In the $Y = 0$ channels ($\Lambda\Lambda$, ΞN , $\Lambda\Sigma$ and $\Sigma\Sigma$) we expect an $I = 0$ 1S_0 bound state about 30 MeV below the $\Lambda\Lambda$ threshold. One predicts bagstates in the $I = 0$ and $I = 1$ 3S_1 channels at $M \approx 2.35$ GeV and $M \approx 2.39$ GeV. The Pauli principle forbids the $I = 0$ state at $M \approx 2.35$ GeV to decay in the $\Lambda\Lambda$ channel, it can only decay in ΞN .

II. Classification of the N quark states

In the MIT bagmodel [Cho 74, DeG 75] we will consider multibaryon states with baryon number B , described by a wave function of $N = 3B$ quarks, all in $1s1/2$ states of the bag. These states have an $SU(2, J)$ classification for the

space-spin part, an $SU(3,F)$ classification for the flavor part (assuming only three flavors), and an $SU(3,C)$ classification for the color part. Because of generalized Fermi statistics the N quark states must be totally antisymmetric. We therefore can place up to 18 colored quarks in these states of the bag. There is a one-to-one correspondence between the irreducible representations (irreps) of $SU(n)$ and those of the symmetric group $S(n)$, the permutation group of n objects. The objects are in this case the n values the $SU(n)$ quark degree of freedom can assume. Because

$$S(18) \supset S(3,F) \otimes S(2,J) \otimes S(3,C)$$

a classification of the states with the help of the group $S(18)$ is quite useful. We will represent the permutation symmetry of the states by means of Young diagrams [L1 50, It 66]. If the states contain N quarks, the corresponding Young diagrams contain N boxes. Because of Fermi statistics the N quark states must belong to the totally antisymmetric irrep of $S(18)$, described by a Young diagram of only 1 column and N rows.

To get some of the important quantum numbers of these states we consider the classification according to the oldfashioned (flavor-spin) $SU(6,FJ)$ and $SU(3,C)$,

$$SU(6,FJ) \supset SU(2,J) \otimes SU(3,F) \quad .$$

The physical states must be $SU(3,C)$ singlets. The corresponding Young diagram for the $SU(3,C)$ part of the state therefore is rectangular and contains 3 rows and $B = N/3$ columns. Because the state must be totally antisymmetric, the permutation symmetry of the $SU(6,FJ)$ part of the state is described by the associate diagram of the diagram describing the permutation symmetry of the color part of the state. This associate diagram thus has 3 columns and B rows. This uniquely determines the $SU(6,FJ)$ irrep $[\mu]$ to which the colorless states belong. They are given in Table I. At this point we should note that in $SU(n)$ the irrep described by the rectangular Young diagram with x columns and y rows

N	=	3	6	9	12	15	18
[μ]	=	[56]	[490]	[980]	[490 [*]]	[56 [*]]	[1]

Table I: The SU(6,FJ) irreps [μ] of the colorless N quark states

is the complex conjugate irrep of the irrep described by the Young diagram with x columns and (n-y) rows. We see this property clearly reflected in Table I. Next we consider the decomposition

$$SU(6,FJ) \supset SU(3,F) \otimes SU(2,J)$$

For the relevant SU(6,FJ) irreps [μ] the decomposition

$$[\mu] = \sum_{\oplus} (\underline{n}, J)$$

in the different SU(3,F) irreps \underline{n} together with their spins J is given in Table II. For the content of SU(3,F) irreps we refer to reference [Sw 63].

B = 1	[56]	=	(<u>8</u> ,1/2) \oplus (<u>10</u> ,3/2)
B = 2	[490]	=	(<u>1</u> ,0) \oplus (<u>8</u> ,1) \oplus (<u>8</u> ,2) \oplus (<u>10</u> ,1) \oplus (<u>10</u> [*] ,1) \oplus (<u>27</u> ,0) \oplus (<u>27</u> ,2) \oplus (<u>10</u> [*] ,3) \oplus (<u>35</u> ,1) \oplus (<u>28</u> ,0)
B = 3	[980]	=	(<u>1</u> ,3/2) \oplus (<u>1</u> ,5/2) \oplus (<u>8</u> ,1/2) \oplus (<u>8</u> ,3/2) \oplus (<u>8</u> ,5/2) \oplus (<u>10</u> ,3/2) \oplus (<u>10</u> [*] ,3/2) \oplus (<u>27</u> ,1/2) \oplus (<u>8</u> ,7/2) \oplus (<u>1</u> ,9/2) \oplus (<u>27</u> ,3/2) \oplus (<u>27</u> ,5/2) \oplus (<u>35</u> ,1/2) \oplus (<u>35</u> [*] ,1/2) \oplus (<u>64</u> ,3/2)
B = 4	[490 [*]]	=	(<u>1</u> ,0) \oplus (<u>8</u> ,1) \oplus (<u>8</u> ,2) \oplus (<u>10</u> ,1) \oplus (<u>10</u> [*] ,1) \oplus (<u>27</u> ,0) \oplus (<u>27</u> ,2) \oplus (<u>10</u> ,3) \oplus (<u>35</u> [*] ,1) \oplus (<u>28</u> [*] ,0)
B = 5	[56 [*]]	=	(<u>8</u> ,1/2) \oplus (<u>10</u> [*] ,3/2)

Table II: The decomposition of SU(6,FJ) irreps in flavor and spin. The states are ordered according to increasing mass. It will turn out that the states (27,2) and (10^{*},3) in [490], (27,1/2), (8,7/2) and (1,9/2) in [980], and (27,2) and (10,3) in [490^{*}] are degenerate as long as there is no mixing (see section VI).

Another useful decomposition [Be 64] is determined by

$$SU(6, FJ) \supset U(1, Y) \otimes SU(4, IJ_n) \otimes SU(2, J_s)$$

where J_n (J_s) is the total spin of the nonstrange (strange) quarks, I is the isospin and Y the hypercharge. The decomposition

$$[\mu] = \sum_{\oplus} (Y, (\nu), J_s)$$

is given in Table III. Here (ν) denotes the $SU(4, IJ_n)$ irreps. They are given by their dimension and if necessary an extra index. This decomposition is necessary, because when we calculate the $SU(6, FJ)$ breaking we shall consider the nonstrange and strange quarks contained in a state separately.

$[56] = (1, (20_s), 0) \oplus (0, (10), 1/2) \oplus (-1, (4), 1) \oplus (-2, (1), 3/2)$
$[490] = (2, (50), 0) \oplus (1, (60), 1/2) \oplus (0, (45), 1) \oplus (0, (20_2), 0)$
$\oplus (-1, (20_s), 3/2) \oplus (-1, (20_1), 1/2) \oplus (-2, (10), 1) \oplus (-2, (6), 0)$
$\oplus (-3, (4), 1/2) \oplus (-4, (1), 0)$
$[980] = (3, (20_s), 0) \oplus (2, (45), 1/2) \oplus (1, (60), 1) \oplus (1, (36), 0)$
$\oplus (0, (64), 1/2) \oplus (0, (50), 3/2) \oplus (-1, (60), 1) \oplus (-1, (36), 0)$
$\oplus (-2, (45), 1/2) \oplus (-3, (20_s), 0)$

Table III: The hypercharge, $SU(4, IJ_n)$, and strange spin content of the $SU(6, FJ)$ irreps. For $[490]^*$ and $[56]^*$ the decompositions are the same as for $[490]$ and $[56]$, except that the Y eigenvalue changes sign and (ν) becomes $(\nu)^*$.

The decomposition of the group $SU(4, IJ_n)$ in isospin $SU(2, I)$ and non-strange spin $SU(2, J_n)$

$$SU(4, IJ_n) \supset SU(2, I) \otimes SU(2, J_n)$$

is the non-strange analog of the flavor-spin decomposition in flavor and spin.

We get

$$(\nu) = \sum_{\oplus} (I, J_n)$$

These decompositions are given in Table IV.

(1)	=	(0,0)
(4)	=	(1/2,1/2)
(6)	=	(1,0) \oplus (0,1)
(10)	=	(1,1) \oplus (0,0)
(20 _S)	=	(3/2,3/2) \oplus (1/2,1/2)
(20 ₁)	=	(3/2,1/2) \oplus (1/2,3/2) \oplus (1/2,1/2)
(20 ₂)	=	(2,0) \oplus (1,1) \oplus (0,2) \oplus (0,0)
(36)	=	(3/2,3/2) \oplus (3/2,1/2) \oplus (1/2,3/2) \oplus (1/2,1/2)
(45)	=	(2,1) \oplus (1,2) \oplus (1,1) \oplus (1,0) \oplus (0,1)
(50)	=	(3,0) \oplus (2,1) \oplus (1,2) \oplus (1,0) \oplus (0,3) \oplus (0,1)
(60)	=	(5/2,1/2) \oplus (3/2,3/2) \oplus (3/2,1/2) \oplus (1/2,5/2) \oplus (1/2,3/2)
		\oplus (1/2,1/2)
(64)	=	(2,1) \oplus (2,0) \oplus (1,2) \oplus 2(1,1) \oplus (1,0) \oplus (0,2) \oplus (0,1)

Table IV: The isospin and non-strange spin content of the SU(4, IJ_n) irreps (ν).

In this specific decomposition the contents of (ν^{*}) are identical
to the contents of (ν).

III. An approximation to the phenomenological bag Hamiltonian [DeG 75]

The MIT bagmodel provides us with a method to calculate the masses of the various N quark states. The bag is taken to be a sphere of radius R and the quarks are placed in 1s1/2 states. Inside this bag the quarks can move freely, except for a weak static interaction between the color charges ($\sim g F_{\alpha}$) and between the color currents ($\sim g F_{\alpha} \sigma_k$). The 8 generators of

SU(3,C) in the irrep $\underline{3}$ we denote by $F_\alpha = \lambda_\alpha^C/2$ with $\alpha = 1$ to 8. They are normalized such that $\text{Tr } \lambda_\alpha^2 = 2$. The three generators of SU(2,J) in the $J = 1/2$ irrep are $\sigma_k/2$ with $k = 1$ to 3 and $\text{Tr } \sigma_k^2 = 2$. The mass operator of an N quark system is given by

$$M = E_B + E_Q + E_M + E_E \quad (1)$$

The energy E_B associated with the bag geometry is

$$E_B = \frac{4\pi}{3} BR^3 - \frac{Z_0}{R} \quad (2)$$

where B is the bag pressure and Z_0 is among other things associated with the zeropoint energy. The rest energy and kinetic energy E_Q of the quarks in the bag is

$$E_Q = \sum_1 N_1 \frac{\alpha_1(R)}{R} = N_n \frac{\alpha_n(R)}{R} + N_s \frac{\alpha_s(R)}{R} \quad (3)$$

We use i and j for the particle indices of the quarks. The indices n and s more specifically refer to the non-strange and strange quarks. N_1 is the number operator for the quarks i . The energy eigenvalue of a quark in a spherical bag is (see Table V)

$$\alpha_i(R)/R = \alpha(m_i R)/R$$

where m_i is the mass of the i^{th} quark. The energy E_M due to the colormagnetic interaction between the quarks is

$$E_M = -\frac{\alpha_c}{R} \sum_{i>j} M_{ij}(R) (F\sigma)_i (F\sigma)_j \quad (4)$$

The energy E_E due to the colorelectric interaction between the quarks is

$$E_E = \frac{\alpha_c}{R} \left\{ \frac{2}{3} \sum_1 E_{11}(R) + \sum_{i>j} E_{ij}(R) F_i \cdot F_j \right\} \quad (5)$$

Here $F_i \cdot F_j = \sum_\alpha (F_\alpha)_i (F_\alpha)_j$ and $\sigma_i \cdot \sigma_j = \sum_k (\sigma_k)_i (\sigma_k)_j$.

The gluon coupling constant g appears in $\alpha_c = g^2/4\pi$. Furthermore:

$M_{ij}(R) = M(m_i R, m_j R)$ and $E_{ij}(R) = E(m_i R, m_j R)$ are functions of the products of R and the quark masses m_i and m_j (see Table V).

B	1	2	3	4	5	6
$\langle (F\sigma)^2 \rangle$	0	3	6	15	24	36
$R_{av} [\text{GeV}^{-1}]$	5.22	6.70	7.57	8.39	9.02	9.60
α_n	2.043	2.043	2.043	2.043	2.043	2.043
α_s	2.9149	3.2113	3.3935	3.5700	3.7085	3.8381
M_{nn}	0.177	0.177	0.177	0.177	0.177	0.177
M_{ss}	0.1127	0.0981	0.0905	0.0839	0.0791	0.0751
M_{ns}	0.1406	0.1310	0.1256	0.1208	0.1173	0.1141
E_{nn}	0.2784	0.2784	0.2784	0.2784	0.2784	0.2784
E_{ss}	0.4091	0.4415	0.4592	0.4748	0.4863	0.4963
E_{ns}	0.3348	0.3466	0.3528	0.3582	0.3620	0.3653
\bar{M}	0.00843	0.01318	0.01625	0.01927	0.02166	0.02388
\bar{E}	0.01799	0.02669	0.03196	0.03694	0.04073	0.04417

Table V: Average radii for multibaryon multiplets and values of functions

$$\alpha_s, M_{ij}, E_{ij}, \bar{M} = M_{nn} + M_{ss} - 2 M_{ns} \text{ and } \bar{E} = E_{nn} + E_{ss} - 2 E_{ns}.$$

The bag radius R is determined according to one of the boundary conditions in the model by minimizing M with respect to R . This should be done for each hadron separately. In order to have a useful mass formula expressed in flavor-spin tensor operators we take an average R_{av} for each entire $SU(6, FJ)$ multiplet. For a particular state we have:

$$M(R) = \frac{4\pi}{3} BR^3 - \frac{Z_0}{R} + \sum_i N_i \frac{\alpha_i(R)}{R} + \frac{f(R)}{R}$$

where $f(R)$ contains the R -dependence of E_M and E_E coming from the functions M_{ij} and E_{ij} . Minimalization gives:

$$R_{\min} = (4\pi B)^{-1/4} \left[\sum_i N_i \left(\alpha_i - R \frac{\partial \alpha_i}{\partial R} \right) - Z_0 + \left(f - R \frac{\partial f}{\partial R} \right) \right]^{1/4} \Big|_{R=R_{\min}}$$

As long as the functions α_i , M_{ij} and E_{ij} are about linear we may approximate:

$$\alpha_i(R) - R \frac{\partial \alpha_i}{\partial R} \approx \alpha_i(0) = \alpha(0)$$

In the bagmodel the non-strange quark mass m_n is chosen to be zero. So we have $\alpha(0) = \alpha(m_n R) = \alpha_n(R) = \alpha_n$. The same we have for $f(R)$. So a reasonable average value for the radius of a whole multiplet is found by minimizing the bag mass for a system of non-strange quarks, taking an average value for the color-magnetic interaction term:

$$R_{av} = (4\pi B)^{-1/4} [N\alpha_n - Z_0 + \alpha_c M_{nn} \langle (F\sigma)^2 \rangle]^{1/4}$$

where $\langle (F\sigma)^2 \rangle$ is an average value of $\sum_{i>j} (F\sigma)_i \cdot (F\sigma)_j$ in an SU(6,FJ) multiplet.

In this case the color-electric part does not contribute. Since we work in the neighborhood of a minimum the R-dependence of $M(R)$ is not too strong. It appears that the values thus found for R_{av} can be parametrized according to:

$$R_{av} = r_0 N^{1/3}$$

where N is the number of quarks, and $r_0 = 0.72 \text{ fm} = 3.63 \text{ GeV}^{-1}$. The masses of the hadrons obtained with R_{av} are only slightly larger than the masses obtained with the radius coming from the minimalization procedure. The differences can easily be estimated and are $\lesssim 20 \text{ MeV}$. Of the five parameters, m_n is fixed to be zero and B , Z_0 , α_c and m_s are made to fit the light hadron mass spectrum, under the condition that we have one radius for the baryons involved. The parameters are: $B^{1/4} = 0.146 \text{ GeV}$, $Z_0 = 1.89$, $\alpha_c = 2.12$, $m_n = 0$ and $m_s = 0.285 \text{ GeV}$. As was already noted above $\alpha_n(R)$, $M_{nn}(R)$ and $E_{nn}(R)$ are independent of R since $m_n = 0$. The values of R_{av} and the values of the functions α_i , M_{ij} , E_{ij} at $R = R_{av}$ are given in Table V.

Using the total quark number operator $N = N_n + N_s$ and the hypercharge operator $Y = (N_n - 2N_s)/3$ we can rewrite (3) as

$$E_Q = N \frac{2\alpha_n + \alpha_s}{3R} - \frac{(\alpha_s - \alpha_n)}{R} Y \quad (7)$$

It also is useful to separate the summations in (4) and (5) into three parts: a summation over all quarks, a summation over only the non-strange quarks and a summation over only the strange quarks. Then we may write:

$$E_M = -\frac{\alpha_c}{R} \left\{ M_{ns} \sum_{1>J} (F\sigma)_1 \cdot (F\sigma)_J \right. \\ \left. + (M_{nn} - M_{ns}) \sum_{n_1>n_2} (F\sigma)_1 \cdot (F\sigma)_2 \right. \\ \left. + (M_{ss} - M_{ns}) \sum_{s_1>s_2} (F\sigma)_1 \cdot (F\sigma)_2 \right\} \quad (8)$$

and

$$E_E = \frac{\alpha_c}{R} \left\{ E_{ns} \left(\frac{2}{3} N + \sum_{1>J} F_1 \cdot F_J \right) \right. \\ \left. + (E_{nn} - E_{ns}) \left(\frac{2}{3} N_n + \sum_{n_1>n_2} F_1 \cdot F_2 \right) \right. \\ \left. + (E_{ss} - E_{ns}) \left(\frac{2}{3} N_s + \sum_{s_1>s_2} F_1 \cdot F_2 \right) \right\} \quad (9)$$

IV. Evaluation of the color-magnetic and color-electric terms

We will make use of the permutation symmetry of the states to replace the sums of the color and color-spin tensor operators in (8) and (9) by more useful sums of flavor, spin and flavor-spin tensor operators. For convenience we introduce the 35 SU(6) generators A_a with $a = 1$ to 35. For the irrep [6] these can be found as the direct product of the generators and the unity operators in the irrep $\underline{3}$ of SU(3) and the irrep $J = 1/2$ of SU(2). These 35 generators, normalized to $\text{Tr } A_a^2 = 1$, are: $\frac{1}{2} (\lambda_\alpha \otimes \mathbf{1})$, $\frac{1}{\sqrt{6}} (\mathbf{1} \otimes \sigma_k)$ and $\frac{1}{2} (\lambda_\alpha \otimes \sigma_k)$ with $\alpha = 1$ to 8 and $k = 1$ to 3. The quadratic Casimir operator C_6 for SU(6) has in the irrep $[\mu]$ the eigenvalue $C_6(\mu)$ and is given by

$$C_6 = \sum_{1,J} A_1 \cdot A_J \quad \text{where } A_1 \cdot A_J = \sum_a (A_a)_1 (A_a)_J \quad .$$

This implies that

$$2 \sum_{1>J} A_1 \cdot A_J = C_6 - N C_6(6) = C_6 - \frac{35}{6} N \quad .$$

We introduce the following permutation operators

$$\begin{aligned} \text{for SU(2):} \quad P_{1j} &= \frac{1}{2} (1 + \sigma_1 \cdot \sigma_j) \\ \text{for SU(3):} \quad P_{1j} &= \frac{1}{2} \left(\frac{2}{3} + \lambda_1 \cdot \lambda_j \right) \\ \text{for SU(6):} \quad P_{1j} &= \frac{1}{2} \left(\frac{1}{3} + 2 A_{1j} \cdot A_j \right) \quad . \end{aligned}$$

The three summation ranges in (8) and (9) we will consider separately.

1. The sum over all quarks

The states can be labeled by quantum numbers belonging to the groups

$$SU(3,F) \otimes SU(6,CJ) \supset SU(3,F) \otimes SU(2,J) \otimes SU(3,C)$$

The wave function is antisymmetric with respect to flavor, spin and color.

$$P_{1j}^F P_{1j}^J P_{1j}^C = -1, \text{ but then also } P_{1j}^{FJ} = -P_{1j}^C \text{ and } P_{1j}^{CJ} = -P_{1j}^F.$$

Equivalently:

$$\sum_{1>j} (1 + 2 A_{1j}^{CJ} \cdot A_j^{CJ}) = - \sum_{1>j} \lambda_1^F \cdot \lambda_j^F \quad (10)$$

Using the explicit expression for A^{CJ} we find:

$$- \sum_{1>j} (\lambda^C \sigma)_1 \cdot (\lambda^C \sigma)_j = \sum_{1>j} \left\{ 2 + \frac{2}{3} \sigma_1 \cdot \sigma_j + \lambda_1^C \cdot \lambda_j^C + 2 \lambda_1^F \cdot \lambda_j^F \right\} \quad (11)$$

The two particle operators on the righthandside can be related to the quadratic

Casimir operators for the whole system:

$$\begin{aligned} \sum_{1>j} \sigma_1 \cdot \sigma_j &= 2 J^2 - \frac{3}{2} N \\ \sum_{1>j} \lambda_1 \cdot \lambda_j &= 2 C_3 - 2 N C_3(3) = 2 C_3 - \frac{8}{3} N \end{aligned} \quad (12)$$

where $C_3 = F^2 = \sum_{1,j} F_1 \cdot F_j = \frac{1}{4} \sum_{1,j} \lambda_1 \cdot \lambda_j$ is the quadratic Casimir operator [Sw 63] in SU(3), which has the value [Sw 66]:

$$C_3(n) = f^2 = \frac{1}{3} (p^2 + pq + q^2) + p + q$$

in the irrep $\underline{n} = D(p,q)$. $C_3(1) = 0$, $C_3(3) = \frac{4}{3}$.

Eq. (10) is also valid, when applied to the flavor-spin and color, and we find

in terms of quadratic Casimir operators:

$$C_6^{(FJ)} + 2 C_3^{(C)} = \frac{1}{2} N (18 - N) \quad (10')$$

where $C_3(C)$ is the quadratic $SU(3,C)$ Casimir operator.

Eq. (11) can be recasted too, using quadratic Casimir operators:

$$-\sum_{1>j} (\lambda^C_\sigma)_1 \cdot (\lambda^C_\sigma)_j = -4 \sum_{1>j} (F\sigma)_1 \cdot (F\sigma)_j = N(N-10) + \frac{4}{3} J^2 + 4C_3(F) + 2C_3(C) \quad (13)$$

2. The sum ranges over all non-strange quarks

The states can be labeled by quantum numbers belonging to the groups

$$U(1,Y) \otimes SU(4,IJ_n) \otimes SU(2,J_s) \otimes SU(3,C)$$

We introduce the 15 $SU(4,IJ_n)$ generators B_b with $b = 1$ to 15. For the irrep

(4) of $SU(4)$ they are normalized such that $\text{Tr } B_b^2 = 1$ and are given by:

$\frac{1}{2} (\tau_k \otimes \mathbb{1})$, $\frac{1}{2} (\mathbb{1} \otimes \sigma_\ell)$ and $\frac{1}{2} (\tau_k \otimes \sigma_\ell)$ with $k, \ell = 1, 2, 3$. Here $\frac{1}{2} \tau_k$ with $k = 1$ to 3, normalized such that $\text{Tr } \tau_k^2 = 2$, are the three $SU(2,I)$ generators

in the $SU(2,I)$ irrep with $I = 1/2$. The quadratic Casimir operator for $SU(4,IJ_n)$

has in the irrep (ν) the eigenvalue $C_4(\nu)$ and is given by

$$C_4 = \sum_{n_1, n_2} B_1 \cdot B_2 \quad .$$

Therefore

$$2 \sum_{n_1 > n_2} B_1 \cdot B_2 = C_4 - N C_4(4) = C_4 - \frac{15}{4} N \quad .$$

For $SU(4)$ one has: $P_{ij} = \frac{1}{2} (\frac{1}{2} + 2 B_i \cdot B_j)$.

The wave function for the N_n non-strange quarks is antisymmetric with respect to non-strange spin and isospin and color, therefore

$$P_{12}^{J_n} P_{12}^I P_{12}^C = -1 \quad \text{and also} \quad P_{12}^{J_n I} = -P_{12}^C$$

This gives:

$$\sum_{n_1 > n_2} \lambda_1^C \cdot \lambda_2^C = - \sum_{n_1 > n_2} (\frac{7}{6} + 2 B_1 \cdot B_2) = - \frac{7}{12} N_n^2 + \frac{13}{3} N_n - C_4 \quad (14)$$

and the relation (using eq. (12)):

$$C_4 + 2 C_3(C, n) = \frac{7}{12} N_n (12 - N_n) \quad (14')$$

Also $P_{12}^{C J_n} P_{12}^I = -1$, from which follows that (compare eq. (13)):

$$\begin{aligned}
 - \sum_{n_1 > n_2} (\lambda^C_{\sigma})_1 \cdot (\lambda^C_{\sigma})_2 &= \frac{4}{3} N_n (N_n - 6) + 4 \vec{I}^2 + \frac{4}{3} \vec{J}_n^2 + 2 C_3(C, n) \\
 &= \frac{3}{4} N_n^2 - N_n - C_4 + \frac{4}{3} \vec{J}_n^2 + 4 \vec{I}^2
 \end{aligned} \tag{15}$$

3. The sum ranges over all strange quarks

The states again can be labeled by the quantum numbers belonging to the groups

$$U(1, Y) \otimes SU(4, IJ_n) \otimes SU(2, J_s) \otimes SU(3, C) \quad .$$

The wave function of the N_s strange quarks is antisymmetric with respect to strange spin and color. Therefore

$$P_{12}^{J_s} P_{12}^C = -1 \quad .$$

This gives:

$$\begin{aligned}
 \lambda_1^C \cdot \lambda_2^C &= -\frac{5}{3} - \sigma_1 \cdot \sigma_2 \\
 - (\lambda^C_{\sigma})_1 \cdot (\lambda^C_{\sigma})_2 &= 3 - \frac{1}{3} \sigma_1 \cdot \sigma_2
 \end{aligned}$$

Therefore we get

$$\sum_{s_1 > s_2} \lambda_1^C \cdot \lambda_2^C = -\frac{5}{6} N_s^2 + \frac{7}{3} N_s - 2 \vec{J}_s^2 \tag{16}$$

or using eq. (12): $2 C_3(C, s) + 2 \vec{J}_s^2 = \frac{5}{6} N_s (6 - N_s)$

and
$$- \sum_{s_1 > s_2} (\lambda^C_{\sigma})_1 \cdot (\lambda^C_{\sigma})_2 = \frac{3}{2} N_s^2 - N_s - \frac{2}{3} \vec{J}_s^2 \tag{17}$$

For a general multiquark system the quadratic $SU(3, C)$ Casimirs $C_3(C, n)$ and $C_3(C, s)$ for the non-strange and strange quarks do not vanish, but the color irreps of the non-strange and strange quarks must be the complex conjugate of each other, so $C_3(C, n) = C_3(C, s)$. Using eqs. (14) and (16), $N_n = \frac{2}{3} N + Y$ and $N_s = \frac{1}{3} N - Y$, we then find:

$$\vec{J}_s^2 - \frac{1}{2} C_4 + \frac{1}{8} Y^2 = \frac{1}{12} N(N - 18) + \frac{2}{3} (N - 9) Y \tag{18}$$

This equation and eqs. (10') and (14') result from the fact that we consider decompositions of totally antisymmetric states. They enable us to calculate the

quadratic Casimir eigenvalues for $su(6, FJ)$ irreps and $SU(4, IJ_n)$ irreps through the related eigenvalues of $C_3(C)$, provided the (sub)system has a unique color-assignment.

V. The mass operator and $SU(6, FJ)$ tensor operators

Because of conservation of spin, isospin and hypercharge the mass operator M must transform as a spin and isospin singlet with $Y = 0$. It therefore can be expressed in irreducible $SU(6, FJ)$ tensor operators $M(\mu, n)$ transforming as the $I = Y = 0$ member of the flavor multiplet \underline{n} with $J = 0$ contained in the flavor-spin multiplet $[\mu]$. Thus

$$M = \sum_{\mu, n} M(\mu, n) \quad .$$

In this version of the bag model these operators $M(\mu, n)$ are quadratic operators constructed from the $SU(6, FJ)$ tensor operators A_a which transform as members of the $SU(6, FJ)$ irrep [35]. The mass operator therefore has parts transforming according to

$$[35] \otimes [35] = [1] \otimes [35]_s \otimes [35]_a \otimes [189] \otimes [405] \otimes [280] \otimes [280]^* \quad ,$$

where s and a mean the symmetric and antisymmetric combinations. From the tensor operators A_a we can make quadratic combinations $\Omega(\mu, n)$ transforming as the $I = Y = 0$ member of the flavor multiplet \underline{n} with $J = 0$ contained in the flavor-spin multiplet $[\mu]$. They are [Be 64]:

$$\begin{aligned} \Omega(1, 1) &= 1 & \Omega(189, 1) &= [C_3 - J^2] - \frac{1}{10} C_6 \\ \Omega(405, 1) &= [C_3 + J^2] - \frac{5}{14} C_6 \\ \Omega(35_a, 8) &= Y & \Omega(35_s, 8) &= J_s^2 - \frac{1}{2} C_4 + \frac{1}{8} Y^2 + \frac{1}{6} C_6 \\ \Omega(189, 8) &= 3[I^2 - \frac{1}{4} Y^2 - J_n^2 + J_s^2] - [C_3 - J^2] - \frac{3}{4} [J_s^2 - \frac{1}{2} C_4 + \frac{1}{8} Y^2 + \frac{1}{6} C_6] \\ \Omega(405, 8) &= 3[I^2 - \frac{1}{4} Y^2 + J_n^2 - J_s^2] - [C_3 + J^2] + \frac{21}{8} [J_s^2 - \frac{1}{2} C_4 + \frac{1}{8} Y^2 + \frac{1}{6} C_6] \\ \Omega(189, 27) &= \frac{4}{3} [I^2 - \frac{1}{4} Y^2 - J_n^2 + J_s^2] - [C_3 - J^2] + \frac{4}{3} [J_s^2 - \frac{1}{2} C_4 + \frac{1}{8} Y^2 + \frac{1}{6} C_6] \\ &\quad - \frac{20}{3} [J_s^2 - \frac{1}{4} Y^2] + \frac{1}{2} C_6 \end{aligned}$$

$$\begin{aligned} \Omega(405,27) &= \frac{4}{3}[\vec{I}^2 - \frac{1}{4}Y^2 + \vec{J}_n^2 - \vec{J}_s^2] - [C_3 + \vec{J}^2] - \frac{4}{3}[\vec{J}_s^2 - \frac{1}{2}C_4 + \frac{1}{8}Y^2 + \frac{1}{6}C_6] \\ &\quad + \frac{20}{3}[\vec{J}_s^2 + \frac{3}{4}Y^2] - \frac{5}{18}C_6 \\ \Omega(280,8) &= \Omega(280^*,8) = 0 \end{aligned}$$

The mass operator for the N quark states in the bagmodel therefore can be rewritten as:

$$M = \sum_{\mu, n} m(\mu, n) \Omega(\mu, n)$$

where $m(\mu, n)$ are constants calculable in the model. Using for convenience the specific operator combinations, occurring in the Ω 's, we can write

$$\begin{aligned} M &= m_0 + m_1[C_3 - \vec{J}^2] + m_2[C_3 + \vec{J}^2] + m_3Y + m_4[\vec{J}_s^2 - \frac{1}{2}C_4 + \frac{1}{8}Y^2] \\ &\quad + m_5[\vec{I}^2 - \frac{1}{4}Y^2] + m_6[\vec{J}_n^2 - \vec{J}_s^2] + m_7\vec{J}_s^2 + m_8Y^2 \quad . \end{aligned}$$

Different from the mass operator containing only the contributions $M(\mu, 1)$ and $M(\mu, 8)$ [Be 64] are the contributions $\sim J_s^2$ and $\sim Y^2$. These tensors come in with the $M(\mu, 27)$.

To see which tensors contribute in a particular $SU(6, FJ)$ irrep, we have to consider the Clebsch-Gordan series

$$\begin{aligned} [56] \otimes [56^*] &= [1] \otimes [35] \otimes [405] \otimes [2695] \\ [490] \otimes [490^*] &= [1] \otimes [35] \otimes [189] \otimes [405] \otimes [2695] \otimes \dots \\ [980] \otimes [980] &= [1] \otimes [35] \otimes [175] \otimes [189] \otimes [405] \otimes \dots \end{aligned}$$

The irrep [35] appears only once in all these products. Therefore the matrix elements of the operators $\Omega(35_a, 8)$ and $\Omega(35_s, 8)$ must be proportional as can be seen in eq. (18). In principle we then are left with a mass operator with 8 nonzero coefficients. However, there is some symmetry left, due to the simple form of the bag hamiltonian. The operators C_3 , \vec{J}^2 , \vec{I}^2 and \vec{J}_n^2 coming only from E_M appear in the bag mass operator in the specific combinations $C_3 + \frac{1}{3}\vec{J}^2$ and $\vec{I}^2 + \frac{1}{3}\vec{J}_n^2$ (see eqs. (13) and (15)). The resulting mass operator then has the following structure:

$$M = a_0 + a_1[C_3 + \frac{1}{3}\vec{J}^2] + a_2Y + a_3[(\vec{I}^2 - \frac{1}{4}Y^2) + \frac{1}{3}(\vec{J}_n^2 - \vec{J}_s^2)] + a_4\vec{J}_s^2 + a_5Y^2 \quad (19)$$

Moreover in the product $[56] \otimes [56]^*$ the irrep $[189]$ does not occur. Therefore the matrix elements of $\Omega(189, n)$ disappear between states belonging to the irreps $[56] \otimes [56]^*$ for $n = \underline{1}, \underline{8}, \underline{27}$. This gives:

$$\begin{aligned} \langle 56 | C_3 - J^2 | 56 \rangle &= \frac{9}{4} \\ \langle 56 | J_n^2 - J_s^2 | 56 \rangle &= \langle 56 | I^2 - \frac{1}{4} Y^2 + Y - \frac{3}{4} | 56 \rangle \\ \langle 56 | J_s^2 | 56 \rangle &= \langle 56 | \frac{1}{4} Y^2 - Y + \frac{3}{4} | 56 \rangle \end{aligned}$$

In the relations for the irrep $[56]^*$ Y has to be replaced by $-Y$. The mass operator for the $B = 1$ and $B = 5$ states therefore can be simplified to

$$M = b_0 + b_1 J^2 + b_2 Y + b_3 [I^2 - \frac{1}{4} Y^2] + b_4 Y^2 \quad (20)$$

Up to the term $\sim Y^2$ coming from the $M(405, 27)$ contribution in this specific case, this is the familiar $SU(6)$ mass operator [Gü 64].

Having performed the summations for the color-magnetic and color-electric interaction terms in section IV we may collect all terms to yield the following mass operator:

$$\begin{aligned} M &= \frac{4\pi}{3} BR^3 - \frac{Z_0}{R} + N \frac{2\alpha_n + \alpha_s}{3R} - \frac{\alpha_s - \alpha_n}{R} Y \\ &+ \frac{\alpha_c}{4R} M_{ns} \{N(N-10) + 4[C_3 + \frac{1}{3} J^2]\} \\ &+ \frac{\alpha_c}{4R} (M_{nn} - M_{ns}) \{\frac{3}{4} N_n^2 - N_n - C_4 + 4[I^2 + \frac{1}{3} J_n^2]\} \\ &+ \frac{\alpha_c}{4R} (M_{ss} - M_{ns}) \{\frac{3}{2} N_s^2 - N_s - \frac{2}{3} J_s^2\} \\ &+ \frac{\alpha_c}{4R} (E_{nn} - E_{ns}) \{\frac{7}{12} N_n(12 - N_n) - C_4\} \\ &+ \frac{\alpha_c}{4R} (E_{ss} - E_{ns}) \{\frac{5}{6} N_s(6 - N_s) - 2 J_s^2\} \end{aligned}$$

M can be rewritten in combinations occurring in (19). The coefficients are:

$$\begin{aligned} a_0 &= \frac{4\pi}{3} BR^3 - \frac{Z_0}{R} + N \frac{2\alpha_n + \alpha_s}{3R} + \frac{\alpha_c}{4R} \{N(N-10) (\frac{2}{3} M_{nn} + \frac{1}{3} M_{ss}) \\ &+ N(18 - N) (\frac{1}{6} \bar{M} + \frac{5}{54} \bar{E})\} \\ a_1 &= \frac{\alpha_c}{R} M_{ns} \end{aligned}$$

$$a_2 = -\frac{\alpha_s - \alpha_n}{R} + \frac{\alpha_c}{4R} \left\{ \left(\frac{5}{3} N - 7\right) (M_{nn} - M_{ss}) + (N - 9) \left(\frac{2}{3} \bar{M} + \frac{5}{9} \bar{E}\right) \right\}$$

$$a_3 = \frac{\alpha_c}{2R} (M_{nn} - M_{ns})$$

$$a_4 = -\frac{\alpha_c}{4R} \left(\frac{2}{3} \bar{M} + 2 \bar{E}\right)$$

$$a_5 = \frac{\alpha_c}{4R} \left(\frac{3}{2} \bar{M} - \frac{5}{6} \bar{E}\right)$$

where $\bar{M} = M_{nn} + M_{ss} - 2 M_{ns}$ and $\bar{E} = E_{nn} + E_{ss} - 2 E_{ns}$. Using the values of the functions α_i , M_{ij} and E_{ij} in Table V, we are able to calculate the coefficients a_0 to a_5 in eq. (19) for $B = 1$ to 6 and b_0 to b_4 in eq. (20) for $B = 1$ and 5 . They are listed in Table VI and VII.

B	a_0	a_1	a_2	a_3	a_4	a_5
1	0.9337	0.0571	-0.1896	0.0148	-0.00422	-0.00024
2	2.2091	0.0414	-0.1613	0.0146	-0.00492	-0.00019
3	3.4789	0.0352	-0.1297	0.0144	-0.00523	-0.00016
4	4.8003	0.0305	-0.0992	0.0142	-0.00548	-0.00012
5	6.1666	0.0276	-0.0680	0.0140	-0.00564	-0.00009
6	7.5766	-	-	-	-	-

Table VI: The coefficients for the general mass formula (see eq. (19)).

B	b_0	b_1	b_2	b_3	b_4
1	1.054	0.0762	-0.1805	0.0197	-0.0013
5	6.221	0.0368	-0.0783	0.0187	-0.0015

Table VII: The coefficients for the mass formula for $B = 1$ and 5 (see eq. (20)).

VI. Numerical analysis and discussion

The bag parameters B , Z_0 , α_c and m_s were determined to give the best overall reproduction of the light ($B = 1$) baryon masses, using one R value for the entire multiplet, as well as reasonable values for the K , K^* , ω , and ϕ meson masses. The model proves to be sensitive to variation in B , whereas the other dependencies do not seem to be very critical. Comparison with the values obtained by the MIT-group [DeG 75] shows that α_c has become a little smaller and Z_0 a little larger. The second parameter shift causes the masses to be somewhat smaller correcting for the fact that, since we do not minimize for each state separately, our masses tend to be slightly above minimum values. The mass spectrum of the $B = 2$ to $B = 6$ baryons does not exhibit significant shifts, when changing from one set of parameters to the other.

In Table VIII the coefficients b_0 to b_4 , following from our parameters, are listed (A), together with the values, which we found by treating these coefficients as independent parameters and determining them directly from the baryon spectrum (B). The resulting masses for both sets of coefficients

	A	B		M_A	M_B	M_{EXP}
b_0	1.054	1.062	N	0.939	0.939	0.939
b_1	0.762	0.717	Λ	1.111	1.116	1.116
b_2	-0.181	-0.192	Σ	1.150	1.186	1.193
b_3	0.020	0.035	Ξ	1.300	1.323	1.318
b_4	-0.0013	-0.0020	Δ	1.227	1.260	1.232
			Σ^*	1.379	1.401	1.385
			Ξ^*	1.529	1.538	1.533
			Ω	1.676	1.672	1.672

Table VIII: Numerical results for $B = 1$ (see text). All values in GeV.

are given together with the experimental values. Comparison gives an indication about the applicability of the mass formula and its MIT bag analog. The calculations were carried out under the assumption that the spherical cavity approximation remains reasonable for higher B-systems.

The computation of coefficient b_4 , occurring in the term $b_4 Y^2$, which for instance breaks the equal spacing in the decuplet, gives the correct sign and order of magnitude as compared with the result in column B of Table VIII. The value of b_3 determining the Σ - Λ splitting, is too small, which seems to be inherent to the bagmodel. The agreement with the experimental spectrum is fairly satisfactory.

For $B = 2, 3, 4$ -states the mass operator is diagonal with respect to J , Y and I . Mixing occurs between different flavor multiplets with the same J , Y and I , when a particular flavor state is a linear combination of some (J_n, J_s) states. Since the contribution of the $SU(3, F)$ quadratic Casimir C_3 in the mass formula is much larger than the contribution of J_n, J_s ($a_1 > a_3, a_4$), the mass operator is almost diagonal in flavor. In Figs. 1, 2, 3 the masses of the multi-baryon states with $B = 2, 3$ and 4 and $S = 0, -1, -2$, have been plotted together with the important thresholds. The states are denoted by their quantum numbers S, I, J , and the flavor multiplet they (mostly) belong to. In Tables IX to XII a complete list of the multi-baryon masses has been given. The states that participate in mixing are supplied by an alphabetic that indicates the uncertainty, induced by this mixing. Apart from these uncertainties, there are of course the ones due to the bagmodel. The almost complete lack of data keeps us from saying anything about the absolute mass scales. This is mainly due to the fact, that the hadron mass rather strongly depends on the volume-term in E_B , which may be too simple a picture to maintain for higher mass states. The relative positions seem to be more reliable, as they depend on the color interaction [DeR 75].

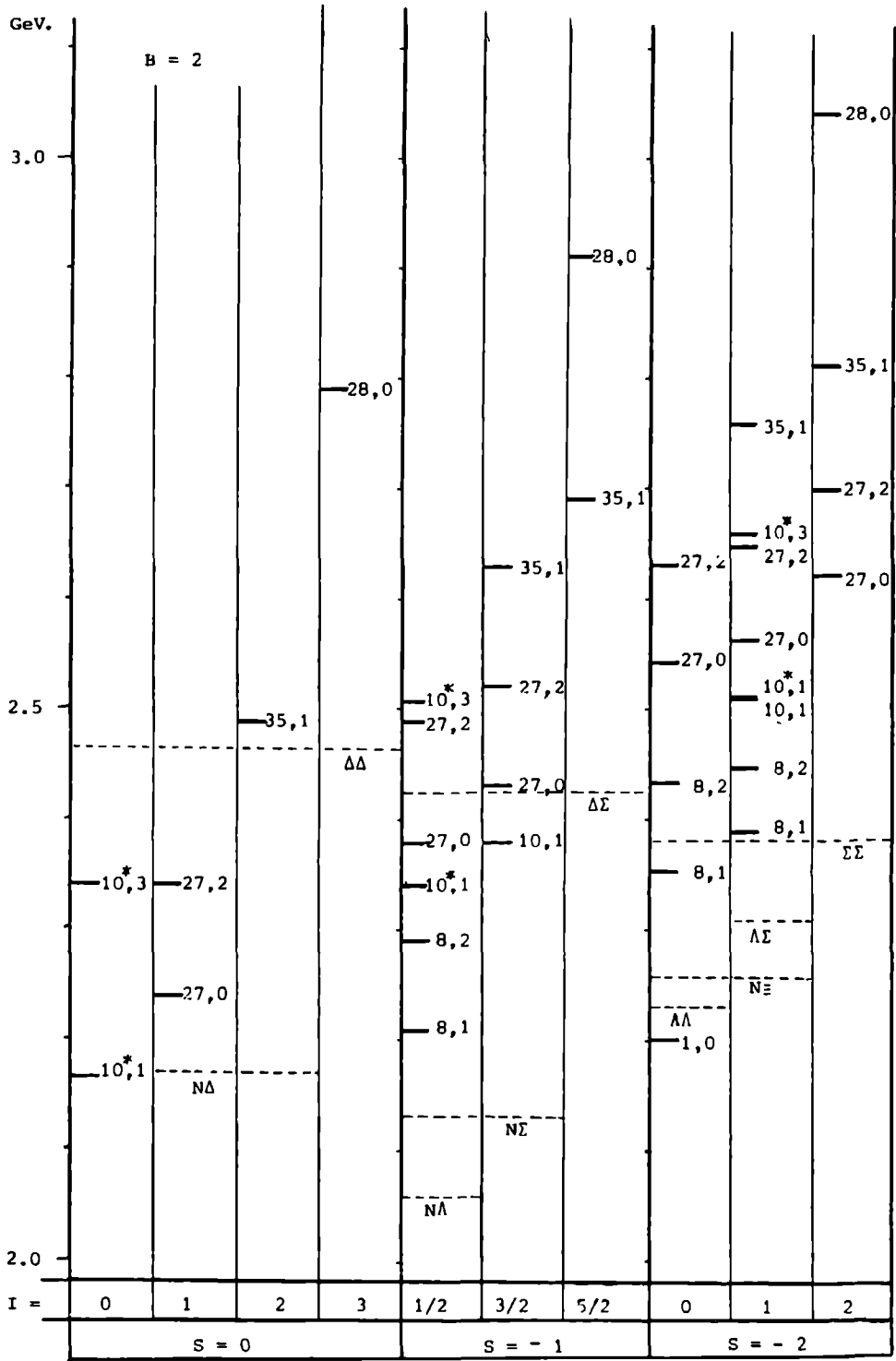


Fig. 1: The masses of the $B = 2$ baryons, for $S = 0, -1$ and -2 (see Fig. 3).

Y	I	J	F	Mass (GeV)	Y	I	J	F	Mass (GeV)
2	3	0	28	2.79					
	2	1	35	2.49			0	27	2.56
	1	2	27	2.34		0	2	27	2.63 b
		0	27	2.24				8	2.43 b
	0	3	10*	2.34			1	8	2.35
		1	10*	2.16			0	27	2.54 a
1	5/2	1	35	2.69				1	2.20 a
		0	28	2.91	-1	3/2	3	10*	2.82
	3/2	2	27	2.52			2	27	2.82
		1	35	2.63 a			1	35	2.94 a
			10	2.38 a				10*	2.69 a
		0	27	2.42			0	28	3.16 a
	1/2	3	10*	2.51				27	2.74 a
		2	27	2.49 a		1/2	2	27	2.78 b
			8	2.29 a				8	2.57 b
		1	10*	2.34 a			1	35	2.89 b
			8	2.21 a				10	2.64 b
		0	27	2.38				8	2.52 b
							0	27	2.71
0	2	2	27	2.70					
		1	35	2.81	-2	1	2	27	2.95
		0	28	3.04 a			1	35	3.06
			27	2.62 a			0	28	3.29 a
	1	3	10*	2.66				27	2.87 a
		2	27	2.65 a		0	1	35	3.04 b
			8	2.45 a				10	2.79 b
		1	35	2.76 b					
			10	2.51 b	-3	1/2	1	35	3.19
			10*	2.51 b			0	28	3.41
		1	8	2.39 b	-4	0	0	28	3.54

Table IX: Masses of the $B = 2$ baryons in GeV. The uncertainties, induced by the mixing, are $a \leq 10$, $10 \leq b \leq 20$, and $20 \leq c \leq 30$, a, b and c in MeV.

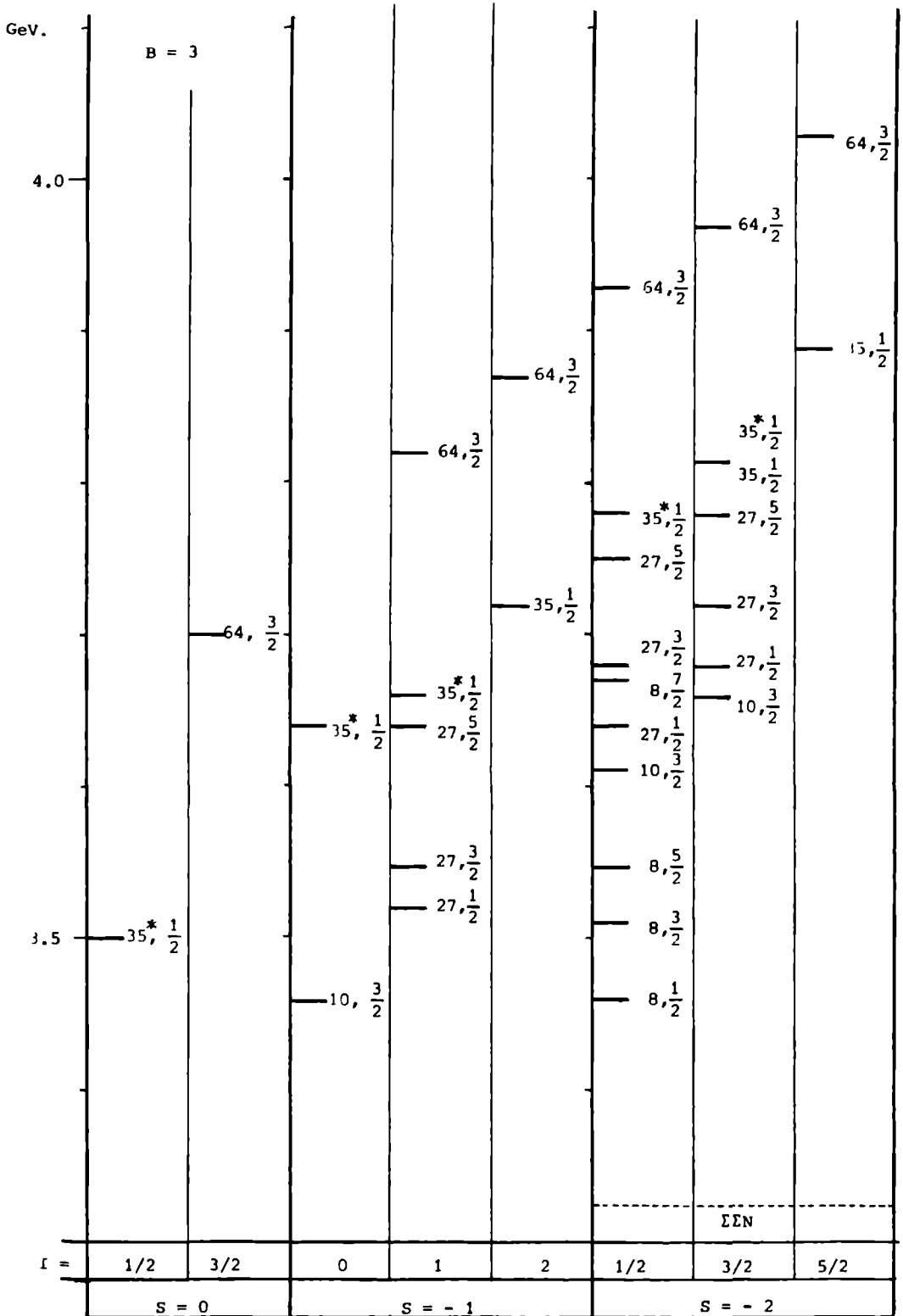


Fig. 2: The masses of the $B = 3$ baryons for $S = 0, -1$ and -2 (see

Fig. 3).

Y	I	J	F	Mass (GeV)	Y	I	J	F	Mass (GeV)
3	3/2	3/2	64	3.70	0	3	3/2	64	4.19
	1/2	1/2	35*	3.50		2	5/2	27	3.92
2	2	3/2	64	3.87			3/2	64	4.12 b
		1/2	35	3.72			27	3.87 b	
	1	5/2	27	3.64		1/2	35	3.98 b	
		3/2	64	3.82 a		35*	3.98 b		
			27	3.57 a		27	3.84 b		
			1/2	35*		3.66 a	1	7/2	8
			27	3.52 a		5/2	27	3.90 b	
			0	3/2		10*	8	3.72 b	
			1/2	35*		3.63	3/2	64	4.07 c
			10*	3.46		27	3.83 c		
1	5/2	3/2	64	4.03	10	3.76 c			
		1/2	35	3.89	10*	3.76 c			
	3/2	5/2	27	3.78	8	3.65 c			
		3/2	64	3.79 b	1/2	35	3.94 a		
			27	3.73 b	35*	3.94 a			
			10	3.66 b	27	3.80 a			
			1/2	35	3.82 a	8	3.62 a		
			35*	3.82 a	0	9/2	1	3.79	
			27	3.68 a	7/2	8	3.79		
			1/2	7/2	8	3.67	5/2	27	3.86 c
			5/2	27	3.75 a	8	3.68 c		
			8	3.57 a	1	3.58 c			
			3/2	64	3.93 b	3/2	64	4.05 c	
			27	3.68 b	27	3.80 c			
			10*	3.61 b	8	3.63 c			
			8	3.51 b	1	3.52 c			
		1/2	35*	3.78 a	1/2	27	3.76 b		
		27	3.64 a	8	3.58 b				
		8	3.46 a						

Table X: Masses of the B = 3 baryons.

Y	I	J	F	Mass (GeV)
-1	5/2	3/2	64	4.29
		1/2	35*	4.15
	3/2	5/2	27	4.04
		3/2	64	4.23 b
			27	3.99 b
			10*	3.92 b
		1/2	35	4.08 a
			35*	4.08 a
			27	3.94 a
	1/2	7/2	8	3.93
			5/2	27
			8	3.83 a
		3/2	64	4.19 b
			27	3.94 b
			10	3.87 b
			8	3.77 b
		1/2	35	4.04 a
			27	3.90 a
			8	3.72 a
	-2	2	3/2	64
1/2			35*	4.24
1		5/2	27	4.16
		3/2	64	4.34 a
		27	4.09 a	
1/2		35	4.18 a	
		27	4.04 a	
0		3/2	10	3.98
	1/2	35	4.15	
-3	3/2	3/2	64	4.48
	1/2	1/2	35	4.28

Table X continued

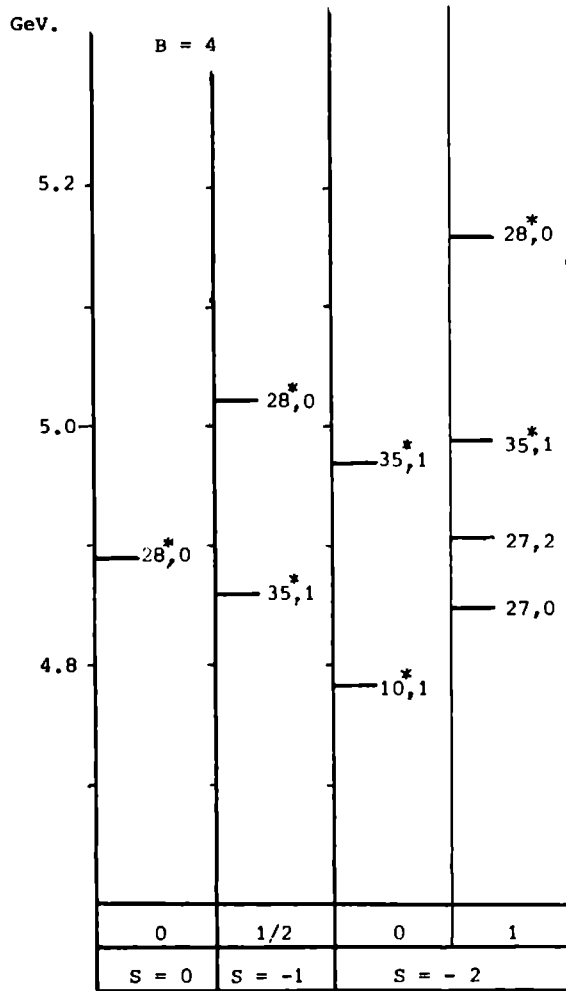


Fig. 3: The masses of the $B = 4$ baryons for $S = 0, -1$ and -2 . The states are characterized by the flavor representation, they dominantly belong to, and their spin. Nearby thresholds are represented by dashed lines, labeled with the name of the corresponding channel.

Y	I	J	F	Mass (GeV)	Y	I	J	F	Mass (GeV)
4	0	0	28*	4.89			1	35*	5.21 b
3	1/2	1	35*	4.86				10*	5.03 b
		0	28*	5.03				10	5.03 b
2	1	2	27	4.91				8	4.94 b
		1	35*	4.99			0	27	5.06
		0	28*	5.16 a		0	2	27	5.11 b
			27	4.85 a				8	4.96 b
	0	1	35*	4.97				1	8
			10*	4.79			0	27	5.04 a
1	3/2	3	10	5.04				1	4.80 a
		2	27	5.04	-1	5/2	1	35	5.40
		1	35*	5.13 a			0	28*	5.57
			10	4.94 a		3/2	2	27	5.26
		0	28*	5.29 a			1	35*	5.34 a
			27	4.98 a				10*	5.15 a
	1/2	2	27	5.00 b			0	27	5.19
			8	4.85 b		1/2	3	10	5.25
		1	35*	5.08 b			2	27	5.23 a
			10*	4.90				8	5.08 a
			8	4.81 b			1	10	5.11 a
		0	27	4.95				8	5.02 a
0	2	2	27	5.18			0	27	5.15
		1	35*	5.26	-2	3	0	28*	5.70
		0	28*	5.43 a		2	1	35*	5.47
			27	5.12 a		1	2	27	5.35
	1	3	10	5.14			0	27	5.27
		2	27	5.13 a		0	3	10	5.35
			8	4.98 a			1	10	5.20

Table XI: Masses of the B = 4 baryons.

Y	I	J	F	Mass (GeV)
1	3/2	3/2	10	1.227
	1/2	1/2	8	0.939
0	1	3/2	10	1.379
		1/2	8	1.150
	0	1/2	8	1.111
-1	1/2	3/2	10	1.529
		1/2	8	1.300
-2	0	3/2	10	1.676

B = 1

Y	I	J	F	Mass (GeV)
2	0	3/2	10*	6.18
1	1/2	3/2	10*	6.29
		1/2	8	6.18
0	1	3/2	10*	6.40
		1/2	8	6.29
	0	1/2	8	6.25
-1	3/2	3/2	10*	6.50
	1/2	1/2	8	6.34

B = 5

Table XII: Masses of the B = 1 and
B = 5 baryons.

Next we will discuss some of the the predictions.

NN system:

We find one resonance at $E_{CM} = 2.16$ GeV ($T_{lab} = 610$ MeV) in the ${}^3S_1 - {}^3D_1$ wave, one in the 1S_0 wave at $E_{CM} = 2.24$ GeV ($T_{lab} = 790$ MeV) and two (almost?) degenerate resonances: one in the 1D_2 and one in the ${}^3D_3 - {}^3G_3$ waves at $E_{CM} = 2.34$ GeV ($T_{lab} = 1040$ MeV). At present we are not able to extract information about the widths from the bagmodel.

The experimental evidence comes mainly from two experiments, the below quoted resonance parameters are assignments emerging from the subsequent analyses. The first source is a transmission experiment, performed at Argonne, using polarized proton targets and beams [Yo 78, Ho 78]. One finds support for a 1D_2 pp resonancelike structure with $M = 2.14 - 2.17$ GeV and $\Gamma = 50 - 100$ MeV, which, however, by its position is suspected of being a ΔN threshold effect (cusp), and possibly a 1S_0 (or 1G_4) resonance at $M = 2.43 - 2.50$ MeV, $\Gamma = 150$ MeV. If these J^P assignments prove to be correct the uncovered level ordering is the inverse of what is expected on the basis of the MIT bagmodel extrapolation, and the thereby made approximations need to be reexamined. In the second experiment [Ka 77, Na 78, Ho 78] the reaction $\gamma d \rightarrow np$ is studied. Here one finds indications for resonant behavior at $M = 2.38$ GeV ($\Gamma \simeq 200$ MeV), for which the assignments $I > 0$ and $J^P = 1^+$ and 3^+ are favored. This effect could be due to the degenerate 1D_2 or 3D_3 states.

Both experiments agree on the existence of an $I = 1$, 3F_3 resonance around 3.26 GeV, $\Gamma \simeq 100$ MeV, which may be interpreted as an $L = 1$ dibaryon state and therefore lies outside the scope of this treatment [Ae 78].

YN system:

In the ΔN channel we predict a.o. an (8, 1^+) resonance at 2.21 GeV, an (8, 2^+) resonance at 2.29 GeV and a (10^{*}, 1^+) resonance at 2.34 GeV. Established

[Br 77, Sh 73, Ka 71, Ta 69] is the Λp resonance at the $\Sigma^+ n$ threshold ($M = 2.13$ GeV). Because this state can very well be explained in potential theory [Sw 62] being the YN equivalent of the deuteron, it certainly is not one of the states mentioned above.

No structures are found in direct Λp scattering experiments [Al 68, HaK 77] nor in pp reactions [Ca 78]. The main positive experimental evidence comes from interactions with deuterium and heavier nuclei as targets. Four mass regions show to be of interest. A region around 2.1 GeV, where a Λn resonance with $M = 2098$ MeV, $\Gamma = 20$ MeV has been proposed [Co 64]. Secondly a region around $M = 2.14$ GeV just above the ΣN threshold where there is weak evidence for another resonance [Br 77, Sh 73, Ka 71, Ta 69]. This could be the above mentioned $(\underline{8}, 1^+)$ resonance. Another region around 2.24 GeV, where a resonance is found by Shahbazian [Sh 73] at 2.25 GeV, $\Gamma = 20$ MeV. The Berkeley data also show a peak at 2.24 GeV [Ka 71], which however, has not been confirmed later, by the same group [HaK 77]. Furthermore, an enhancement at 2.22 GeV, $\Gamma = 20$ MeV has been reported by Buran [Bu 66]. This structure probably is the $(\underline{8}, 2^+)$ resonance. A fourth region is around 2.34 GeV where the Berkeley [Ka 71], Dubna [Sh 73] and Princeton Penn accelerator [Pi 64] data show peaks (statistically not significant). We would like to assign this effect to the $(\underline{10}^*, 1^+)$ state. Of course additional information about J^P is needed to decide these questions.

YY and ΞN system:

The most remarkable prediction is that of a bound $(\underline{1}, 0^+)$ state at 2.20 GeV. Furthermore there are the $I = 0$ states at $M = 2.35$ GeV $(\underline{8}, 1^+)$ and at 2.43 GeV $(\underline{8}, 2^+)$ and the $I = 1$ states at 2.39 GeV $(\underline{8}, 1^+)$ and 2.45 GeV $(\underline{8}, 2^+)$.

For $\Lambda\Lambda$ this means a bound state about 30 MeV below threshold in the 1S_0 wave. The $(\underline{8}, 1^+)$ resonance should appear in the $^3S_1 - ^3D_1$ waves of ΞN and possible $\Sigma\Sigma$. Due to the Pauli principle the isoscalar $J^P = 1^+$ state can not decay in the $\Lambda\Lambda$ channel.

A possible candidate for the $(\underline{8}, 2^+)$ $I = 0$ state is the $\Lambda\Lambda$ resonance at 2.37 GeV, $\Gamma = 50$ MeV, reported by Shahbazian [Sh 73] and Beillière [Be 72]. None of these structures have been confirmed by later, more sensitive experiments [Wi 75].

If the above arguments are correct, we see that our lowest states are consistently 40 - 60 MeV high. This would mean that the $\Lambda\Lambda$ bound state may even be 90 MeV below threshold at 2.14 - 2.16 GeV.

Next to the standard resonance interpretation, an alternative is proposed by DeTar [DeT 78]. He observes, that the lowest $Y = 2$ dibaryon state has the quantum numbers of the deuteron, but a much higher mass. It is a color singlet six-quark bag, which part of the time consists of two threequark color singlets (a proton and a neutron) and therefore is unstable. To study the expected fission process he distributes the quarks evenly over 'left' and 'right' orbitals, which to good approximation are mixtures of the static spherical cavity $1s_{1/2}$ (S) and $1p_{3/2}$ (P) modes of the form:

$$q_{Lm} = q_{Sm} - \sqrt{\mu} q_{Pm} , \text{ and the plus sign for the right orbital.}$$

By letting μ go from 0 to 1 the two groups of three quarks become completely separated. In the course of this variation the shape of the bag changes from sphere through peanut to two spheres. Calculating the semiclassical energy of the deformed system, he finds that it is minimal at a partial 'two nucleon' separation, for some finite value of μ between 0 and 1. This result suggests that we may interpret the deuteron like state at 2.16 GeV as manifestation of the repulsive, finite height, core in the two nucleon interaction. Between this very short range and the free two nucleon limit (1 fm) is an intermediate

region of attraction between the two nucleons due to the fact that (with decreasing separation) the fusion of the two bags into a single larger one initially lowers the quark energy eigen values, because of the larger space available. Further refinements and extension to all available channels allow DeTar to extract the various two nucleon potential terms (central, tensor, etc.). His results are in, mainly qualitative, agreement with some of the existing potentials, but the model is still too crude to expect quantitative agreement. We think this example illustrative of the fact, that the different nature of the instability of systems containing color singlet subsystems as compared to unstable systems, which decay through e.g. $Q\bar{Q}$ pair creation (Δ, ϕ, ρ), may require a different interpretation for the parameters characterizing these systems. The interpretation, that the singlet baryon pair component is at the root of the problem, is also supported by independent analyses of another hadron system with an exotic quark content, the $Q^2\bar{Q}^2$ system [Ja 78]. This configuration displays the first kind of instability at one (low) level of excitation, whereas its behavior shows the standard resonance properties at another higher one. In the latter case the hadron is successfully described as two (quark) concentrations of opposite color, separated by an angular momentum barrier. No singlet components are present and decay is supposed to proceed via $Q\bar{Q}$ pair creation. The $Q^2\bar{Q}^2$ system is the subject of chapter 4.

CHAPTER 4: THE $Q^2\bar{Q}^2$ SYSTEM

Next to the $Q\bar{Q}$ mesons and Q^3 baryons the most simple all quark color-singlet states have a $Q^2\bar{Q}^2$ (dimeson or baryonium) configuration. The study of these mesons, which quantitatively has become feasible only rather recently [Ja 76], is interesting because of several reasons. First of all, it is the smallest system, in which the color degrees of freedom are not frozen out completely, and as such may provide a way for verifying the validity of the concept of color, and add support to the theory of strong interactions based on it: QCD.

Until now, every new degree of freedom but one has manifested itself spectroscopically through the increase of the number of physical states. A nice example of this is the discovery of the flavor degree of freedom: charm, which has opened up an entirely new field of spectroscopy. One has been able to produce charm in both its hidden (in hadrons containing equal amounts of charmed quarks and antiquarks and therefore without net charm) and overt form [Fe 77]. One has identified a threshold, above which strong decay into charmed particles is possible. Similarly, the existence of the color degree of freedom may be demonstrated by the discovery of colored particles (quarks?), making themselves known by characteristic decay patterns. However, no such thing as a color threshold has been found, within the present range of energies. This is formulated in the color confinement hypothesis which states that only color singlet hadrons are physical. This implies, that overt color will only be demonstrable at a subhadronic level, e.g. through the scaling violations predicted by QCD. However, the hidden form can be detected through e.g. multi-quark systems like $Q^2\bar{Q}^2$ [ChH 77, Jc 78].

There is only one way in which a $Q\bar{Q}$ meson can exist as a color singlet. Because the quarks transform as a color triplet (3) and the antiquarks as a

color antitriplet (3^*), the $Q\bar{Q}$ system can in principle occur in a color singlet (1) or color octet (8) configuration. $3 \otimes 3^* = 1 \oplus 8$, of which the octet has to be excluded here. Considering for the moment only S-wave hadrons, in which the quarks all occupy their lowest energy eigenmode, and only three quarkflavors: u, d and s, one finds two flavor multiplets: a $J^P = 0^-$ and a $J^P = 1^-$ nonet.

Also the Q^3 baryon has no color freedom left. The Q^2 (diquark) configuration has either a symmetric, color sextet (6) or an antisymmetric, color antitriplet (3^*) wave function: $3 \otimes 3 = 3^* \oplus 6$. Only the 3^* state can combine with the remaining quark to form a color singlet. One has: $6 \otimes 3 = 8 \oplus 10$, i.e. no singlet for the other state. Again one finds two flavor multiplets, the $J^P = 1/2^+$ octet and the $J^P = 3/2^+$ decuplet.

The $Q^2\bar{Q}^2$ meson consists of a diquark-antidiquark combination. The \bar{Q}^2 occurs in $3^* \otimes 3^* = 3 \oplus 6^*$. Now there are two ways to obtain a color singlet. First, there is the $3^* - 3$ singlet. Secondly, also the sextets can be matched into a singlet: $6 \otimes 6^* = 27 \oplus 8 \oplus 1$. For each flavor multiplet expected from the direct product of two $Q\bar{Q}$ color singlets ($1 \otimes 1 = 1$), one obtains an additional one which is unambiguously confirming the extra color freedom: since $8 \otimes 8 = 1 \oplus 8_1 \oplus 8_2 \oplus \dots$, also with $Q\bar{Q}$ color octets a singlet can be constructed. We find, that already at the level of $Q^2\bar{Q}^2$ S-wave hadrons the number of predicted states is beginning to explode. A large amount of heavily mixed, generally rather broad hadrons emerges. This illustrates a little the nature of complications associated with the extra color freedom. To study systems with still more color freedom therefore is not attractive, since it also entails an of necessity larger number of quarks, accompanied by an even larger number of flavor spin multiplets, cf. $Q^3\bar{Q}^3$. The next simplest system probably is the $Q^4\bar{Q}$ baryonic one [Fu 78].

Secondly, several of the $Q^2\bar{Q}^2$ states possess remarkable features, which may allow detection in a large background. In the mass region of the S-wave $Q^2\bar{Q}^2$ states ($M \approx 1$ to 2 GeV) also many orbitally and radially excited $Q\bar{Q}$ mesons are expected. These are the states known from the nonrelativistic quark (NRQ) model, which classification scheme provided until lately the sole candidates for the hadron states, reported by the experimentalists. Besides $Q^2\bar{Q}^2$ systems, QCD also predicts the existence of hadrons, containing only glue (glueballs) [Ro 77] and both glue and quarks (e.g. $Q\bar{Q}G$) [HoM 78]. One does not expect such configurations to be prominent, because the gluon content must be converted into colored $Q\bar{Q}$ pairs in order to allow decay into ordinary $Q\bar{Q}$ mesons. Even the configurations with exotic J^{PC} quantum numbers (0^{--} and 0^{+-} , 1^{-+} , 2^{+-} , etc.) do not seem to be easily detectable, both through their weak coupling, and through the experimentally rather inaccessible decay and production channels. Some of the dimesons, on the other hand, contain a large fraction of color singlet meson pairs and decay by simply falling apart into S-wave meson-meson channels. Since several of these are even lighter than the corresponding $Q\bar{Q}$ excitations, they may be quite prominent. Also because of the excess flavor combinations of the four quark system over the two quark system, some dimesons have exotic (i.e. not available for ordinary NRQ-model mesons) flavor quantum numbers, which yield clear and uncontested decay patterns. Further distinct signals are expected to come from orbitally excited $Q^2\bar{Q}^2$ systems. Here one has to make several additional assumptions concerning the color dynamics. In the emerging model the hadron is thought, for sufficient large orbital angular momentum ℓ ($\ell \geq 3$), to consist of two quark clusters of opposite color charge, which are spatially separated by an angular momentum barrier. In our case a possible cluster is a diquark in a pure color antitriplet or sextet or a $Q\bar{Q}$ pair in a color octet configuration. The color-triplet type

of these hadrons is supposed to couple strongly to baryon-antibaryon- and only weakly to meson-meson-channels [Ro 68]. It presumably has a usual hadronic width ($\Gamma \sim 100$ MeV). The second and third variety are expected to couple weakly to both these channels, preferring to cascade via meson emission to lighter hadrons with the same color configuration [ChH 77]. They therefore must be much more narrow, despite their high mass. Identification of such states will mean an important support for the concept of color.

In section I we will set the notation and discuss the S-wave $Q^2\bar{Q}^2$ states. In section II we focus our attention on orbitally excited $Q\bar{Q}$ mesons, and try to read off some dynamical properties. In section III the observations of the previous section will be brought to bear upon the orbitally excited $Q^2\bar{Q}^2$ system. In section IV a comparison with the available data is attempted.

Section I. S-wave $Q^2\bar{Q}^2$ states [Jc 77]

We will calculate the masses of the unexcited or S-wave $Q^2\bar{Q}^2$ mesons and obtain the corresponding wavefunctions, using the spherical cavity approximation to the MIT bagmodel. To this end, only quarks, that occupy the lowest energy eigenstate, will be considered. We will also make the restriction, that only those quark flavors are taken into account, that correspond to the smallest quark mass parameters: u, d and s.

1. Basisstates

To study two quarks and two antiquarks in one bag it is most convenient, in view of the FD statistics, to take those basis states in which the total (anti) quark permutationsymmetry is evident: the $Q^2-\bar{Q}^2$ basis. The $Q^2\bar{Q}^2$ states are then given by the direct product of the Q^2 and \bar{Q}^2 basis states. The quark wavefunction consists of three parts:

1. Flavor

The quark transforms as a triplet ($\underline{n} = \underline{3}$) under the flavor group SU(3,F).

The states with the correct SU(3,F) transformation behavior are denoted by

ϕ_{ν}^{μ} , where the labels stand for dimensionality (μ) and quantum numbers (ν):

$(\mu; \nu) = (\underline{n}; i, i_z, y)$, indicating the total and z-component of isospin and hypercharge eigenvalues. We will use the shorthand notation

$$u = (\underline{3}; 1/2, 1/2, 1/3)$$

$$d = (\underline{3}; 1/2, -1/2, 1/3)$$

$$s = (\underline{3}; 0, 0, -2/3) \quad .$$

The antiquark transforms as an antitriplet ($\underline{n} = \underline{3}^*$, where the asterisk is used to distinguish it from the three-dimensional quark irrep). The triplet and antitriplet are related according to:

$$\phi_{-\nu}^{(3^*)} = (\phi_{\nu}^3)^* \eta, \text{ with}$$

$$(-\nu) = (i_1, -i_z, -y). \text{ The phasefactor is taken to be real: } \eta = (-)^{Q(\nu) + 1/3},$$

with $eQ(\nu) = (i_z + y/2)e$, the quark charge. The factor 1/3 can be generalized to

$$1/3 \rightarrow 1/3 \cdot [(\text{number of quarks} - \text{number of antiquarks}) \text{ modulo } 3].$$

One finds the shorthand

$$\bar{u} = - (\underline{3}^*; 1/2, -1/2, -1/3)$$

$$\bar{d} = (\underline{3}^*; 1/2, 1/2, -1/3)$$

$$\bar{s} = (\underline{3}^*; 0, 0, 2/3) \quad .$$

This convention coincides with de Swart's [Sw 63] for states with integer

baryon number. Note that $I_+ d = u$, but $I_+ \bar{u} = -\bar{d}$ for the isospin raising

operator I_+ . The $Q\bar{Q}$ octet then has the following flavor wave functions

$$\begin{aligned} K^+ &= u\bar{s} & ; & & K^0 &= d\bar{s} & ; & & \pi^+ &= u\bar{d} & ; & & \pi^0 &= -\frac{u\bar{u} + d\bar{d}}{\sqrt{2}} \\ K^- &= -s\bar{u} & ; & & \bar{K}^0 &= s\bar{d} & ; & & \pi^- &= -d\bar{u} & ; & & \eta_8 &= -\frac{1}{\sqrt{6}}(u\bar{u} + d\bar{d} - 2s\bar{s}) \end{aligned}$$

and $\eta_1 = -\frac{1}{\sqrt{3}}(u\bar{u} + d\bar{d} + s\bar{s})$ is the singlet wavefunction.

One can define the special combinations $\eta_0 = \frac{1}{\sqrt{2}}(u\bar{u} + d\bar{d})$ and $\eta_s = s\bar{s}$.

When we are referring only to the flavor aspect, the pseudoscalar meson symbols will be used without any assumptions for the spin.

2. Color

The quark is classified according to the three dimensional defining irreducible representation (irrep) $c = 3$ of color $SU(3,C)$. The conventions for flavor are also taken for color. For shorthand one may now use (r,b,y) instead of (u,d,s) .

3. Relativistic spin

The bagmodel gives a relativistic covariant description of the quark dynamics. The space and spin properties are represented by means of a Dirac spinor, which is characterized by the total spin j ($\vec{j} = \vec{l} + \vec{s}$), its z-component m , its parity and the radial quantum number n . The lowest energy quark eigenmode has $n = 1$, $j = 1/2$ and positive parity and is referred to as the $1s1/2$ mode, a name also used for the corresponding antiquark groundstate. This quark therefore transforms according to the $j = 1/2$ irrep of the relativistic spingroup $SU(2,J)$. We adopt the Condon and Shortley phase conventions.

With the quark wavefunctions, we can construct the diquark states. We have listed the diquark-irreps with the permutation symmetry, for color, spin and flavor separately in Table I. The anti-diquark always belongs to the conjugate representation.

Symmetry	color (c)	flavor (<u>n</u>)	spin (j)
Antisymmetric (-)	3^*	<u>3^*</u>	0
Symmetric (+)	6	<u>6</u>	1

Table I: Permutation symmetry of the diquark configurations.

With the help of this table we can pick out the (anti) diquark product wavefunctions, which meet the FD statistics requirements. We denote the allowed combinations by (c, \underline{n}, j) and list them in column 1 (2) of Table II.

Diquark	⊗	Anti-diquark	⊃	Dimeson	$(c_{Q^2\bar{Q}^2} = 1)$
$(c_{Q^2}, \underline{n}_{Q^2}, j_{Q^2})$		$(c_{\bar{Q}^2}, \underline{n}_{\bar{Q}^2}, j_{\bar{Q}^2})$		$\underline{n}_{Q^2\bar{Q}^2}$	$J_{Q^2\bar{Q}^2}$ label
$(3^*, \underline{3}^*, 0)$		$(3, \underline{3}, 0)$		$\underline{8} \oplus \underline{1}$	0 ϕ_1
		$(3, \underline{6}^*, 1)$		$\underline{10}^* \oplus \underline{8}$	1 ϕ_2
$(3^*, \underline{6}, 1)$		$(3, \underline{3}, 0)$		$\underline{10} \oplus \underline{8}$	1 ϕ_3
		$(3, \underline{6}^*, 1)$		$\underline{27} \oplus \underline{8} \oplus \underline{1}$	0 ϕ_4
					1 ϕ_5
					2 ϕ_6
$(6, \underline{6}, 0)$		$(6^*, \underline{6}^*, 0)$		$\underline{27} \oplus \underline{8} \oplus \underline{1}$	0 ϕ_7
		$(6^*, \underline{3}, 1)$		$\underline{10} \oplus \underline{8}$	1 ϕ_8
$(6, \underline{3}^*, 1)$		$(6^*, \underline{6}^*, 0)$		$\underline{10}^* \oplus \underline{8}$	1 ϕ_9
		$(6^*, \underline{3}, 1)$		$\underline{8} \oplus \underline{1}$	0 ϕ_{10}
					1 ϕ_{11}
					2 ϕ_{12}

Table II: Flavor and spin content of the $Q^2\bar{Q}^2$ color singlet states

The $Q^2\bar{Q}^2$ representations are obtained by taking the direct product of the Q^2 and \bar{Q}^2 irreps in each sector. We are only interested in the color singlets contained in this product. Other color configurations are not included in Table II. We use the convention of listing the diquark properties each time before the anti-diquark ones. The isospin (i) and hypercharge (y) content of the occurring flavor multiplets is given in Table III. Next to the representations with non exotic flavor quantum numbers $\underline{8}$ and $\underline{1}$, we also encounter

\underline{n}	$\sum_{\oplus} (i, y)$
<u>1</u>	(0, 0)
<u>3</u>	(1/2, 1/3) \oplus (0, -2/3)
<u>3*</u>	(0, 2/3) \oplus (1/2, -1/3)
<u>6</u>	(1, 2/3) \oplus (1/2, -1/3) \oplus (0, -4/3)
<u>6*</u>	(0, 4/3) \oplus (1/2, 1/3) \oplus (1, -2/3)
<u>8</u>	(1/2, 1) \oplus (1 + 0, 0) \oplus (1/2, -1)
<u>10</u>	(3/2, 1) \oplus (1, 0) \oplus (1/2, -1) \oplus (0, -2)
<u>10*</u>	(0, 2) \oplus (1/2, 1) \oplus (1, 0) \oplus (3/2, -1)
<u>27</u>	(1, 2) \oplus (3/2 + 1/2, 1) \oplus (2 + 1 + 0, 0) \oplus (3/2 + 1/2, -1) \oplus (1, -2)

Table III: Reduction of flavor multiplets \underline{n} in terms of isospin (i) and

$$\text{hypercharge (y): } \underline{n} = \sum_{\oplus} (i, y).$$

exotic ones, from the point of view of the non relativistic quarkmodel in the irreps 10, 10* and 27. The $Q^2\bar{Q}^2$ states with singlet or octet flavor-q-numbers will be called crypto-exotics (C states), the others are true exotic (E) states. We will return to flavor matters after treatment of the bag hamiltonian and concentrate on the color and spin properties of the wavefunction first.

The $Q^2\bar{Q}^2$ basis is very useful for taking stock of the allowed states. To find out, which $Q^2\bar{Q}^2$ states couple to a particular meson-meson channel, one has to decompose them in terms of $Q\bar{Q}-Q\bar{Q}$ basis states. The $Q\bar{Q}$ system can occur in, color or flavor, octet or singlet configurations with spin $J = 0$ or 1. In this basis the quark permutation symmetry no longer is obvious, but as a consequence, only definite linear combinations can occur. These are found by a recoupling of the $Q^2\bar{Q}^2$ wavefunctions. One writes down explicitly

the wavefunction of a suitable $Q^2-\bar{Q}^2$ representative in terms of the quark degrees of freedom and determines the overlap with $Q\bar{Q}-Q\bar{Q}$ wavefunctions, with the same quantum numbers, also written in terms of quarks. This can be done for color and spin separately. The results are listed in Table IV. Because the color and flavor part of the wavefunction both have SU(3) as a symmetry group, we have gathered all occurring SU(3) combinations in one table.

J = 0	(1,1;0)	(0,0;0)	J = 2	(1,1;2)
(1,1;0)	$-\frac{1}{4}$	$\frac{3}{4}$	(1,1;2)	1
(0,0;0)	$\frac{3}{4}$	$\frac{1}{4}$		
J = 1	(1,1;1)	(1,0;1)	(0,1;1)	
(1,1;1)	0	$\frac{1}{2}$	$\frac{1}{2}$	
(1,0;1)	$\frac{1}{2}$	$\frac{1}{4}$	$-\frac{1}{4}$	
(0,1;1)	$\frac{1}{2}$	$-\frac{1}{4}$	$\frac{1}{4}$	

Table IVa: Recoupling matrices for spin J: $(J_{Q^2}, J_{\bar{Q}^2}; J) \leftrightarrow (J_{Q\bar{Q}}, J'_{Q\bar{Q}}; J)$

<u>n</u> = <u>1</u>	(<u>1,1;1</u>)	(<u>8,8;1</u>)		
(<u>3*</u> , <u>3</u> ; <u>1</u>)	$-\frac{1}{3}$	$-\frac{2}{3}$		
(<u>6</u> , <u>6*</u> ; <u>1</u>)	$\frac{2}{3}$	$-\frac{1}{3}$		
<u>n</u> = <u>8</u>	(<u>8,8;8_d</u>)	(<u>8,8;8_f</u>)	(<u>1,8;8</u>)	(<u>8,1;8</u>)
(<u>3*</u> , <u>3</u> ; <u>8</u>)	$\frac{5}{6}$	0	$-\frac{1}{12}$	$-\frac{1}{12}$
(<u>6</u> , <u>6*</u> ; <u>8</u>)	$\frac{1}{6}$	0	$\frac{5}{12}$	$\frac{5}{12}$
(<u>3*</u> , <u>6*</u> ; <u>8</u>)	0	$\frac{1}{2}$	$\frac{1}{4}$	$-\frac{1}{4}$
(<u>6</u> , <u>3</u> ; <u>8</u>)	0	$\frac{1}{2}$	$-\frac{1}{4}$	$\frac{1}{4}$
<u>n</u> = <u>10</u>	(<u>8,8;10</u>)	<u>n</u> = <u>10*</u>	(<u>8,8;10*</u>)	<u>n</u> = <u>27</u>
(<u>6</u> , <u>3</u> ; <u>10</u>)	1	(<u>3</u> , <u>6</u> ; <u>10*</u>)	1	(<u>6</u> , <u>6*</u> ; <u>27</u>)
				1

Table IVb. Recoupling matrices for SU(3): $(\underline{n}_{Q^2}, \underline{n}_{\bar{Q}^2}; \underline{n}) \leftrightarrow (\underline{n}_{Q\bar{Q}}, \underline{n}'_{Q\bar{Q}}; \underline{n})$

A $\sqrt{\quad}$ is to be understood over every coefficient, e.g. for $\frac{3}{4}$ read $\sqrt{\frac{3}{4}}$.

2. The hamiltonian (see Chapter 2, II and III)

To estimate the masses of the $Q^2\bar{Q}^2$ meson states, we make use of the MIT bagmodel. In this relativistic quark model there is no essential difference in the description of the $Q\bar{Q}$, Q^3 , $Q^2\bar{Q}^2$ or other multiquark states. The masses of the particles are the eigenvalues M of the spherical bag hamiltonian [DeG 75] (cf. Chapter 2, eq. (81)):

$$H = E_V + E_G + E_M + E_E$$

$$E_V = \frac{4\pi}{3} B R^3 - \frac{Z_0}{R} \quad : \text{ the energy associated with the bag geometry.}$$

$$E_Q = \sum_i n_i \frac{\alpha(m_i R)}{R} \quad : \text{ the rest + kinetic energy of the } n_i \text{ quarks and anti-quarks with mass } m_i.$$

$$E_M = \frac{\alpha_c}{R} \sum_{i>j} M(m_i R, m_j R) (F\sigma)_i (F\sigma)_j \quad : \text{ the mutual color magnetostatic interaction energy of the (anti)quarks.}$$

$$E_E = \frac{\alpha_c}{R} \sum_i E(m_i R, m_i R) F_i^2 + \sum_{i>j} E(m_i R, m_j R) F_i F_j \quad : \text{ the total color electrostatic interaction energy of the (anti)quarks.}$$

In case of only weak residual interactions between the quarks, one would expect the average masses of the multiquark states to be roughly proportional to the number of quarks: $Q\bar{Q} \sim 2M \sim 700 \text{ MeV}$, $Q^3 \sim 3M \sim 1050 \text{ MeV}$, in case of just nonstrange quarks. One finds: $Q^2\bar{Q}^2 \sim 4M \sim 1400 \text{ MeV}$. This suggests that the lightest four quark states will lie amid of the heavier two and three quark ones. It may then constitute a good first order approximation to take the parameters obtained by fitting the $Q\bar{Q}$ and Q^3 mass spectrum. One has

$$\begin{aligned} B^{1/4} &= 0.146 \text{ GeV} & \text{or} & & B &= 56.8 \text{ MeV fm}^{-3} \\ Z_0 &= 1.84 & \text{or} & & Z_0 &= 368 \text{ MeV fm} \\ m_n &= 0 \text{ GeV} & m_s &= 0.279 \text{ GeV} & \alpha_c &= 2.20 \end{aligned}$$

Of these B , which is thought to be a property of the vacuum, and $m_n (= 0)$

are expected to be real constants. The parameters m_s and α_c may, on the basis of asymptotic freedom arguments, have a weak dependence on the total mass. The behavior of Z_0 is rather uncertain. One should not expect the estimates to be very accurate (+ 50 MeV or so). However, taking these parameters will be justified for most $Q^2 \bar{Q}^2$ states by the mass eigenvalues.

The bagradius R is determined by the condition, that $M = M(R)$ be minimal: $\frac{\partial M}{\partial R} = 0$. In this mass operator $\alpha(m_1 R)$, $M(m_1 R, m_j R)$ and $E(m_1 R, m_j R)$ are functions of the products of the mass m_1 of the quark and the bagradius R . One has $\alpha(0) = 2.043$ and $M(0,0) = 0.177$. For systems in which all quarks and antiquarks have the same mass $E_E = 0$. It is positive and negligible otherwise, due to our choice of $m_s - m_n$. For simplicity we therefore shall omit E_E from our calculations. Finally we have: F_1 , which is one of the eight generators of $SU(3,C)$ and takes the form (see appendix B):

$$F_1^a = \frac{\lambda_1^a}{2} \quad \text{in the irrep } 3, \text{ in case } 1 \text{ is a quark label } (a = 1, \dots, 8) \text{ and}$$

$$= -\frac{\lambda_1^{a*}}{2} \quad \text{in the irrep } 3^*, \text{ in case } 1 \text{ is an antiquark label, } (\text{Tr } \lambda^2) = 2,$$

and σ_1 , which is one of the three generators of $SU(2,J)$. Acting on the quarks they are represented by the Pauli spin matrices: $\text{Tr } \sigma^2 = 2$.

We can divide the study of the eigenstates of H in two parts:

1) Vanishing quark gluon coupling: $\alpha_c = 0$ (flavor basis states)

The hamiltonian now consists of the terms E_V and E_Q . For a particular multiquarksystem (here the $Q^2 \bar{Q}^2$ one) its eigenvalues only depend on the number of strange quarks n_s . This is a direct consequence of giving the strange and nonstrange quarks different mass parameters. This situation, called ideal mixing, is familiar from the $J^P = 1^-$ vector mesons, where it can be observed in a rather pure form. The $I = 0$ states of the octet and singlet: η_8 and η_1 in our flavor notation, are mixed to such extent that the

resulting physical states appear to contain almost exclusively nonstrange, η_0 , or strange, η_8 , quarks. One refers to this heavily mixed octet and singlet multiplet as a nonet. Also in case of the dimesons it is not proper anymore to refer to SU(3,F) irrep dimensions. Rather

$$\begin{array}{ll} \underline{3^*} \otimes \underline{3} = \underline{9} & \underline{6} \otimes \underline{3} = \underline{18} \\ \underline{3^*} \otimes \underline{6^*} = \underline{18^*} & \underline{6} \otimes \underline{6^*} = \underline{36} \end{array}$$

The ideally mixed states will be taken as basis states for the flavor part of the wavefunction. Following Jaffe [Jb 77] we adopt the following nomenclature for $Q^2\bar{Q}^2$ states with nonet quantum numbers will be denoted by a capital C, the other states by a capital E. When a crypto-exotic state contains one or two $s\bar{s}$ pairs the C will be furnished with a superscript s or ss respectively. It carries as a subscript the name of the (pseudoscalar) meson with the identical quantum numbers. The $I = 0 = Y$ states only have a superscript, which may now also be a zero, indicating an exclusively nonstrange quark content. The true exotics are labeled by the flavor of the meson-meson channel they recouple to. Again pseudoscalar meson names will be used.

The $Q^2\bar{Q}^2$ flavor basis states, in terms of quarks, their names, their decomposition into proper SU(3,F) multiplets and their recoupling into $Q\bar{Q}-Q\bar{Q}$ flavor basis states are given in Table V. The phases of the quark wavefunctions are chosen such that the coefficients, occurring in the proper flavor multiplet decomposition, are precisely the isoscalar factors, arising in the SU(3,F) Clebsch Gordan series $Q^2 \otimes \bar{Q}^2 = \sum_{\oplus} Q^2\bar{Q}^2$. These extra phases arise from our using short hand. All states have positive parity $P = +$. Combining the results of Tables V, II and IVa, we can now also determine the C and G parity properties of our states. This is done by simply looking at the expressions for the dimeson representatives in the meson-meson ($Q\bar{Q}-Q\bar{Q}$) basis.

(I, Y)	Name	Quark wavefunction	Isoscalar factors			Recoupling to meson-meson basis
(1, 2)	$E_{\bar{K}K}$	$u\bar{s}\bar{s}$	0	0	1	$\bar{K}K$
(3/2, 1)	$E_{\pi K}$	$uu(\bar{d}\bar{s})$	0	0	1	(πK)
(1/2, 1)	C_K	$-\sqrt{\frac{2}{3}}uu(\bar{u}\bar{s}) - \sqrt{\frac{1}{3}}(ud)(\bar{d}\bar{s})$	0	$\sqrt{\frac{3}{5}}$	$\sqrt{\frac{2}{5}}$	$-\sqrt{\frac{3}{4}}(\eta_0 K) - \sqrt{\frac{1}{4}}[\pi K]$
(1/2, 1)	C_K^S	$(us)\bar{s}\bar{s}$	0	$-\sqrt{\frac{2}{5}}$	$\sqrt{\frac{3}{5}}$	$(\eta_S K)$
(2, 0)	$E_{\pi\pi}$	$u\bar{u}\bar{d}\bar{d}$	0	0	1	$\pi\pi$
(1, 0)	C_π	$-\sqrt{\frac{1}{2}}uu(\bar{u}\bar{d}) - \sqrt{\frac{1}{2}}(ud)\bar{d}\bar{d}$	0	$\sqrt{\frac{4}{5}}$	$\sqrt{\frac{1}{5}}$	$-(\eta_0\pi)$
(1, 0)	C_π^S	$(us)(\bar{d}\bar{s})$	0	$-\sqrt{\frac{1}{5}}$	$\sqrt{\frac{4}{5}}$	$\sqrt{\frac{1}{2}}(\eta_S\pi) + \sqrt{\frac{1}{2}}(K\bar{K})$
(0, 0)	C^0	$\sqrt{\frac{1}{3}}uu\bar{u}\bar{u} + \sqrt{\frac{1}{3}}(ud)(\bar{u}\bar{d}) + \sqrt{\frac{1}{3}}d\bar{d}\bar{d}\bar{d}$	$\sqrt{\frac{1}{2}}$	$\sqrt{\frac{2}{5}}$	$\sqrt{\frac{1}{10}}$	$\sqrt{\frac{3}{4}}\eta_0\eta_0 - \sqrt{\frac{1}{4}}\pi\pi$
(0, 0)	C^S	$-\sqrt{\frac{1}{2}}(us)(\bar{u}\bar{s}) - \sqrt{\frac{1}{2}}(ds)(\bar{d}\bar{s})$	$-\sqrt{\frac{1}{3}}$	$\sqrt{\frac{1}{15}}$	$\sqrt{\frac{3}{5}}$	$-\sqrt{\frac{1}{2}}(\eta_0\eta_S) + \sqrt{\frac{1}{2}}[K\bar{K}]$
(0, 0)	C^{SS}	$ss\bar{s}\bar{s}$	$\sqrt{\frac{1}{6}}$	$-\sqrt{\frac{8}{15}}$	$\sqrt{\frac{3}{10}}$	$\eta_S\eta_S$
(3/2, -1)	$E_{\pi\bar{K}}$	$(us)\bar{d}\bar{d}$	0	0	1	$(\pi\bar{K})$
(1/2, -1)	$C_{\bar{K}}$	$-\sqrt{\frac{2}{3}}(ds)\bar{d}\bar{d} - \sqrt{\frac{1}{3}}(us)(\bar{u}\bar{d})$	0	$\sqrt{\frac{3}{5}}$	$\sqrt{\frac{2}{5}}$	$-\sqrt{\frac{3}{4}}(\eta_0\bar{K}) + \sqrt{\frac{1}{4}}[\pi\bar{K}]$
(1/2, -1)	$C_{\bar{K}}^S$	$(us)\bar{s}\bar{s}$	0	$-\sqrt{\frac{2}{5}}$	$\sqrt{\frac{3}{5}}$	$(\eta_S\bar{K})$
(1, -2)	$E_{\bar{K}\bar{K}}$	$ss\bar{d}\bar{d}$	0	0	1	$\bar{K}\bar{K}$

Table V: Flavor basis states a) $\underline{6} \otimes \underline{6}^* = \underline{36} = \underline{1} \oplus \underline{8} \oplus \underline{27}$

(I, Y)	Name	Quark wavefunction	Isoscalar factors		Recoupling to meson-meson basis
(3/2, 1)	$E_{\pi K}$	$uu[\bar{d}\bar{s}]$	0	1	$[\pi K]$
(1/2, 1)	C_K	$\sqrt{\frac{2}{3}} uu[\bar{u}\bar{s}] + \sqrt{\frac{1}{3}} (ud)[\bar{d}\bar{s}]$	1	0	$\sqrt{\frac{3}{4}} [\eta_0 K] + \sqrt{\frac{1}{4}} (\pi K)$
(1, 0)	C_π	$uu[\bar{u}\bar{d}]$	$\sqrt{\frac{2}{3}}$	$\sqrt{\frac{1}{3}}$	$\sqrt{\frac{1}{2}} [\eta_0 \pi] + \sqrt{\frac{1}{2}} \pi\pi$
(1, 0)	C_π^S	$(us)[\bar{d}\bar{s}]$	$-\sqrt{\frac{1}{3}}$	$\sqrt{\frac{2}{3}}$	$-\sqrt{\frac{1}{2}} [\eta_s \pi] - \sqrt{\frac{1}{2}} [K\bar{K}]$
(0, 0)	C^S	$\sqrt{\frac{1}{2}} (us)[\bar{u}\bar{s}] + \sqrt{\frac{1}{2}} (ds)[\bar{d}\bar{s}]$	1	0	$\sqrt{\frac{1}{2}} [\eta_0 \eta_s] + \sqrt{\frac{1}{2}} (K\bar{K})$
(1/2, -1)	$C_{\bar{K}}$	$(us)[\bar{u}\bar{d}]$	$\sqrt{\frac{1}{3}}$	$\sqrt{\frac{2}{3}}$	$\sqrt{\frac{1}{4}} [\eta_0 \bar{K}] + \sqrt{\frac{3}{4}} (\pi K)$
(1/2, -1)	$C_{\bar{K}}^S$	$ss[\bar{d}\bar{s}]$	$-\sqrt{\frac{2}{3}}$	$\sqrt{\frac{1}{3}}$	$-[\eta_s \bar{K}]$
(0, -2)	$E_{\bar{K}\bar{K}}$	$ss[\bar{u}\bar{d}]$	0	1	$\bar{K}\bar{K}$

Table V: Flavor basis states b) $\underline{6} \otimes \underline{3} = \underline{18} = \underline{8} \oplus \underline{10}$

(3/2, -1)	$E_{\pi\bar{K}}$	$[ds]\bar{u}\bar{u}$	0	1	$[\pi\bar{K}]$
(1/2, -1)	$C_{\bar{K}}$	$\sqrt{\frac{2}{3}} [us]\bar{u}\bar{u} + \sqrt{\frac{1}{3}} [ds](\bar{u}\bar{d})$	1	0	$-\sqrt{\frac{3}{4}} [\eta_0 \bar{K}] + \sqrt{\frac{1}{4}} (\pi\bar{K})$
(1, 0)	C_π	$-[ud]\bar{u}\bar{u}$	$-\sqrt{\frac{2}{3}}$	$\sqrt{\frac{1}{3}}$	$\sqrt{\frac{1}{2}} [\eta_0 \pi] + \sqrt{\frac{1}{2}} \pi\pi$
(1, 0)	C_π^S	$-[ds](\bar{u}\bar{s})$	$\sqrt{\frac{1}{3}}$	$\sqrt{\frac{2}{3}}$	$-\sqrt{\frac{1}{2}} [\eta_s \pi] + \sqrt{\frac{1}{2}} [K\bar{K}]$
(0, 0)	C^S	$-\sqrt{\frac{1}{2}} [us](\bar{u}\bar{s}) - \sqrt{\frac{1}{2}} [ds](\bar{d}\bar{s})$	1	0	$-\sqrt{\frac{1}{2}} [\eta_0 \eta_s] + \sqrt{\frac{1}{2}} (K\bar{K})$
(1/2, 1)	C_K	$[ud](\bar{u}\bar{s})$	$-\sqrt{\frac{1}{3}}$	$\sqrt{\frac{2}{3}}$	$\sqrt{\frac{1}{4}} [\eta_0 K] - \sqrt{\frac{3}{4}} (\pi K)$
(1/2, 1)	C_K^S	$[ds]\bar{s}\bar{s}$	$\sqrt{\frac{2}{3}}$	$\sqrt{\frac{1}{3}}$	$-[\eta_s K]$
(0, 2)	E_{KK}	$-[ud]\bar{s}\bar{s}$	0	1	$-KK$

Table V: Flavor basis states c) $\underline{3}^* \otimes \underline{6}^* = \underline{18}^* = \underline{8} \oplus \underline{10}^*$

(I, Y)	Name	Quark wavefunction	Isoscalar factors		Recoupling to meson-meson basis
(1/2, 1)	C_K	$- [ud][\bar{d}\bar{s}]$	0	1	$\sqrt{\frac{1}{4}} (\eta_0 K) - \sqrt{\frac{3}{4}} [\pi K]$
(1, 0)	C_π^S	$[us][\bar{d}\bar{s}]$	0	1	$\sqrt{\frac{1}{2}} (\eta_S \pi) - \sqrt{\frac{1}{2}} (K\bar{K})$
(0, 0)	C^0	$- [ud][\bar{u}\bar{d}]$	$\sqrt{\frac{1}{3}}$	$\sqrt{\frac{2}{3}}$	$-\sqrt{\frac{1}{4}} \eta_0 \eta_0 - \sqrt{\frac{3}{4}} \pi\pi$
(0, 0)	C^S	$\sqrt{\frac{1}{2}} [us][\bar{u}\bar{s}] + \sqrt{\frac{1}{2}} [ds][\bar{d}\bar{s}]$	$-\sqrt{\frac{2}{3}}$	$\sqrt{\frac{1}{3}}$	$\sqrt{\frac{1}{2}} (\eta_0 \eta_S) + \sqrt{\frac{1}{2}} [K\bar{K}]$
(1/2, -1)	$C_{\bar{K}}$	$[us][\bar{u}\bar{d}]$	0	1	$\sqrt{\frac{1}{4}} (\eta_0 \bar{K}) + \sqrt{\frac{3}{4}} [\pi \bar{K}]$

Table V: Flavor basis states d) $\underline{3}^* \otimes \underline{3} = \underline{9} = \underline{1} \oplus \underline{8}$

Table V: Flavor basis states for $Q^2-\bar{Q}^2$ systems. The quark wave function represents the member with $(I, I_z) = (i, 1)$ in tables a, b and d, and with $(1, -1)$ in table c. The isoscalar factors give the weights for its decomposition into the proper $SU(3, F)$ states with the same quantum numbers.

In the last column MM' denotes the linear combination of M and M' charge states with the correct total isospin I : $MM' = C_m^I M^I M'^I + C_{m'}^I M^I M'^I$. $(AB) = \sqrt{\frac{1}{2}} \{AB + BA\}$, $[AB] = \sqrt{\frac{1}{2}} \{AB - BA\}$.

The mesons are in an S-wave with respect to one another. For the 36 and 9 $Y = 0$ states one obtains the usual $C = (-)^S$ and $G = (-)^{S+I}$ formulas. One can also combine the $Y = 0$ members of the 18 and 18* to obtain G parity eigenstates. One obtains the linear combinations $\{C_M(18) \pm C_M(18^*)\}/\sqrt{2}$. The (+) states have the abovementioned parities, the other ones get an additional (-) sign.

Similar to the pseudoscalar and vector nonet cases, also here deviations from ideal mixing are expected. Vector mesons appear to be almost ideal, the pseudoscalar ones not quite. This is qualitatively [Ap 75] understood by attributing this remixing to conversion of one isoscalar color singlet state (say η_0) into another one (η_s) via a multigluon intermediate state. Pseudoscalar quantum numbers require at least two gluons, which allows this process at order α_c^2 , vectormesons need three gluons and for these states the mixing is of order α_c^3 . Apparently, the pseudoscalar remixing is less depressed: the octet-singlet mixing angle is far from the ideal value. This has been attributed, using asymptotic freedom arguments, to the fact that, the $J^P = 0^-$ isoscalars being lighter than their $J^P = 1^-$ brothers, the energy dependent coupling constant satisfies $\alpha_c(m_p) > \alpha_c(m_v)$. Therefore, $\alpha_c^2(m_p) \gg \alpha_c^3(m_v)$ may be possible. Our value $\alpha_c = 2.2$ is an average for states in the 1 GeV mass region. In the dimeson system, $Q\bar{Q}$ isoscalar subsystems with $J^{PC} = 1^{--}$ occur in color octet configurations, and remixing arises already at the $O(\alpha_c)$ level. The lightest dimeson system ($M = .64$ GeV) has an octet configuration about 40 % of the time (see eq (3)). Although α_c is expected to be smaller than in the pseudoscalar case (higher masses) considerable effects may be present.

11) Nonvanishing quark-gluon coupling: $\alpha_c \neq 0$

We now let the quark-gluon coupling constant become nonzero. Gluons are flavorless. Their action will therefore not affect the flavorpart of wave-

function, but mix the color and spin parts. For systems like $Q^2\bar{Q}^2$, which still have very simple color and spin wavefunctions, it is convenient to retain the two particle interaction character of the colormagnetic term E_M of H. This method avoids the introduction of color-spin $SU(6,C) \supset SU(3,C) \otimes SU(2,J)$, which allows more general conclusions about $Q^m\bar{Q}^n$ S-wave systems, but is not readily extendible to excited $Q^2\bar{Q}^2$ systems. We then have three types of two particle operators: $O(Q,Q')$, $O(\bar{Q},\bar{Q}')$ and $O(Q,\bar{Q}')$: the operators acting on two quarks, two antiquarks, and a quark and an antiquark respectively. We let the prime (') distinguish between different (anti)quarks. Due to the permutation symmetry of the quark and the antiquark wavefunctions, there is only one antiquark-quark interaction: $O(Q_1,\bar{Q}_j) = O(Q,\bar{Q}) \forall 1,j$.

$$\begin{aligned} \text{We have: } F_1 \cdot F_j &= \sum_a F_1^a F_j^a = \frac{1}{2} \{ (F_1 + F_j)^2 - F_1^2 - F_j^2 \} = \frac{1}{2} F_{1j}^2 - \frac{4}{3} \\ \vec{\sigma}_1 \cdot \vec{\sigma}_j &= (2 S_{1j}^2 - 3) \\ (\vec{F\sigma})_1 \cdot (\vec{F\sigma})_j &= \left(\frac{1}{2} F_{1j}^2 - \frac{4}{3} \right) (2 S_{1j}^2 - 3) \end{aligned}$$

Here F_{1j}^2 is the quadratic Casimir operator for $SU(3,C)$ for the two particle subsystem formed by the fermions i and j , which may be 1, 3, 6 or 8 dimensional, and S_{1j} is the total spin of this subsystem (0 or 1), where i and j may be both quark and antiquark labels, provided $i \neq j$.

We introduce the following notation ($Q \neq Q'$):

$$\begin{aligned} - (\vec{F\sigma})_Q (\vec{F\sigma})_{\bar{Q}} &= A \\ - (\vec{F\sigma})_Q (\vec{F\sigma})_{Q'} &= B \\ - (\vec{F\sigma})_{\bar{Q}} (\vec{F\sigma})_{\bar{Q}'} &= C \end{aligned}$$

From the definitions we can see that B and C will be diagonal in the diquark-antidiquark basis. Furthermore, they will be identical, when the diquark and the antidiquark have conjugate color and spin configurations. This happens in combinations which have flavor $\underline{n} = \underline{36}$ or $\underline{9}$. From Table IV it follows that

A cannot always be purely diagonal, since $Q^2\bar{Q}^2$ basis states recouple to linear combinations of $Q\bar{Q}-Q\bar{Q}$ basis states. In cases, where more than one possibility exists to construct a $Q^2\bar{Q}^2$ state with the same spin (J) and flavor (μ, ν) quantum numbers, off diagonal matrix elements will emerge. A can be calculated using the recoupling coefficients from Table III. In the $Q\bar{Q}-Q\bar{Q}$ basis A, B nor C, except for the trivial one dimensional cases, will be diagonal, as a consequence of the imposed FD statistics. We have listed the thus obtained matrices in Table VI.

One can rewrite the interaction part of the hamiltonian:

$$E_M = \frac{\alpha}{R} C [A\{M(Q, \bar{Q}) + M(Q', \bar{Q}) + M(Q', \bar{Q}')\} + B M(Q, Q') + C M(\bar{Q}, \bar{Q}')] \quad (1)$$

denoting $M(Q, \bar{Q}') = M(m_{QR}, m_{\bar{Q}'R})$. For systems in which all quarks have the same mass m, E_M becomes simply

$$E_M = \frac{\alpha}{R} C M(mR, mR) \{4A + B + C\} \quad (2)$$

In the first instance, this makes only sense for $m = m_{\underline{n}} = 0$, for all flavor-multiplets, and $m = m_{\underline{s}}$ for $\underline{n} = \underline{36}$ (see also below). With our choice of flavor basis, only E_M , which acts in the color and spin space, has nondiagonal matrix elements left. It will determine the precise color-spin mixtures to go with the flavor part of the wavefunction. The eigenstates found this way are the eigenstates of the full hamiltonian. The splitting between the states is then given by the eigenvalues $E_{M1} = \frac{\alpha}{R} C M(mR, mR) \Delta_1$. Similar to the $\rho-\omega, \pi-\eta$ cases, E_M again does not lift the isospin degeneracies of systems containing identical quark flavors. This is a consequence of the fact that both quarks and antiquarks are present. Their combination to the total quantum numbers of the system is not restricted by any statistics requirement, in contradistinction to the baryon case. We have listed the eigenvalues Δ_1 of the matrix $\{4A + B + C\}$ and the corresponding color spin eigenfunctions in Table VI. For systems

A	B	C	basis	\underline{n}^J	eigenvectors	Δ	M(GeV)	$\Delta M(\text{GeV})$
$\begin{bmatrix} 0 & -\sqrt{\frac{3}{2}} \\ -\sqrt{\frac{3}{2}} & -\frac{5}{3} \end{bmatrix}$	$\begin{bmatrix} -2 & 0 \\ 0 & -\frac{1}{3} \end{bmatrix}$	$\begin{bmatrix} -2 & 0 \\ 0 & -\frac{1}{3} \end{bmatrix}$	ϕ_1	$\underline{9}^0$	$\begin{bmatrix} .582 \\ .813 \end{bmatrix}$	-10.84	0.64	.24
			ϕ_{10}	$\underline{9}^0$	$\begin{bmatrix} .813 \\ -.582 \end{bmatrix}$	-0.49	1.43	.17
$\begin{bmatrix} 0 & \sqrt{\frac{1}{2}} \\ \sqrt{\frac{1}{2}} & 0 \end{bmatrix}$	$\begin{bmatrix} -2 & 0 \\ 0 & -\frac{1}{3} \end{bmatrix}$	$\begin{bmatrix} -2 & 0 \\ 0 & -\frac{1}{3} \end{bmatrix}$	ϕ_2	$\underline{18}^{*1}$	$\begin{bmatrix} \sqrt{\frac{2}{3}} \\ -\sqrt{\frac{1}{3}} \end{bmatrix}$	$-\frac{10}{3}$	1.23	.19
			ϕ_9	$\underline{18}^{*1}$	$\begin{bmatrix} \sqrt{\frac{1}{3}} \\ \sqrt{\frac{2}{3}} \end{bmatrix}$	$\frac{8}{3}$	1.63	.15
$\begin{bmatrix} 0 & \sqrt{\frac{1}{2}} \\ \sqrt{\frac{1}{2}} & 0 \end{bmatrix}$	$\begin{bmatrix} -2 & 0 \\ 0 & -\frac{1}{3} \end{bmatrix}$	$\begin{bmatrix} -2 & 0 \\ 0 & -\frac{1}{3} \end{bmatrix}$	ϕ_3	$\underline{18}^1$	$\begin{bmatrix} \sqrt{\frac{2}{3}} \\ -\sqrt{\frac{1}{3}} \end{bmatrix}$	$-\frac{10}{3}$	1.23	.19
			ϕ_8	$\underline{18}^1$	$\begin{bmatrix} \sqrt{\frac{1}{3}} \\ \sqrt{\frac{2}{3}} \end{bmatrix}$	$\frac{8}{3}$	1.63	.17
$\begin{bmatrix} \sqrt{\frac{1}{2}} & 0 \\ -\frac{2}{3} & -\sqrt{\frac{3}{2}} \end{bmatrix}$	$\begin{bmatrix} 0 & 1 \\ \frac{2}{3} & 0 \end{bmatrix}$	$\begin{bmatrix} 0 & -\frac{1}{3} \\ \frac{2}{3} & 0 \end{bmatrix}$	ϕ_4	$\underline{36}^0$	$\begin{bmatrix} .813 \\ -.582 \end{bmatrix}$	-4.84	1.12	.20
$\begin{bmatrix} -\sqrt{\frac{3}{2}} & 0 \\ 0 & 1 \end{bmatrix}$	$\begin{bmatrix} 0 & 1 \\ 0 & 1 \end{bmatrix}$	$\begin{bmatrix} 0 & 1 \\ 0 & 1 \end{bmatrix}$	ϕ_7	$\underline{36}^0$	$\begin{bmatrix} -.582 \\ .813 \end{bmatrix}$	5.51	1.82	.13
$-\frac{1}{3}$	$\frac{2}{3}$	$\frac{2}{3}$	ϕ_5	$\underline{36}^1$	1	0	1.46	.17
$\frac{1}{3}$	$\frac{2}{3}$	$\frac{2}{3}$	ϕ_6	$\underline{36}^2$	1	$\frac{8}{3}$	1.63	.15
$-\frac{5}{6}$	$-\frac{1}{3}$	$-\frac{1}{3}$	ϕ_{11}	$\underline{9}^1$	1	-4	1.18	.20
$\frac{5}{6}$	$-\frac{1}{3}$	$-\frac{1}{3}$	ϕ_{12}	$\underline{9}^2$	1	$\frac{8}{3}$	1.63	.15

Table VI. Matrix representations of the two particle operators $A = (\vec{F}\vec{\sigma})_Q(\vec{F}\vec{\sigma})_{\bar{Q}}$, $B = (\vec{F}\vec{\sigma})_Q(\vec{F}\vec{\sigma})_{\bar{Q}}$, and $C = (\vec{F}\vec{\sigma})_{\bar{Q}}(\vec{F}\vec{\sigma})_Q$.

The basis states are corresponding members of the representations, denoted by the labels ϕ_k , defined in Table II, together with the associated flavor \underline{n} and spin J , notation \underline{n}^J . The eigenvectors of the matrix $\{4A + B + C\}$ are listed in column 6 and 7, the eigenvalue in column 8; the top one corresponds to the eigenvector in column 6, the bottom one to column 7, if occurring in pairs. The 8th column lists the eigenvalue of the total hamiltonian, in GeV, corresponding to the Δ in the preceding column, for a $Q\bar{Q}$ system consisting exclusively of nonstrange quarks. ΔM gives the increase in mass when a nonstrange quark is replaced by a strange one.

containing both nonstrange and strange quarks the eigenvectors will depend on n_s , but the variations are very small. This is mainly due to the fact that $M(0, m_s R)$ and $M(m_s R, m_s R)$ are practically linear in $m_s R$ in the relevant range of R , and the fact that the influence, which the presence of an extra s (instead of n) quark or $s\bar{s}$ (instead of $n\bar{n}$) pair exerts on the splitting, is distributed evenly among the two particle operators. This can be simulated to good approximation by representing eq (1) by eq (2), provided M is replaced by a suitable average \bar{M} , or m by an appropriate \bar{m} . The largest deviations are encountered in systems with a quark content of the form $nn\bar{s}\bar{s}$. Even here the deviation from the $m_Q = 0$ - eigenvectors in the final result will be only 2 or 3 tenths of a percent for the dominant modes, in the final, recoupled result. We find that the ordering of the levels is the same for all values of n_s . The deviations are of the order of 10 MeV, whereas the spacings are 50 MeV or more.

Examining the resulting mass spectrum we find, that the lightest, most strongly bound dimeson multiplet is a nonexotic $J^{PC} = 0^{++}$ nonet! This is consistent with the general rule for finding the lightest $Q^m \bar{Q}^n$ multiplet [Jc 77], which can be read off from the expression for E_M in terms of $SU(6, CJ)$ invariants. It consists out of taking two steps. The first is to put the quarks and anti-quarks separately in the most antisymmetric, i.e. smallest, flavor representation, here the $\underline{3}^*$ and $\underline{3}$. This step implies small total flavor irreps. The second step is to accomodate the Q^2 and \bar{Q}^2 in the smallest $SU(6, CJ)$ $Q^2 \bar{Q}^2$ irrep. This is the one in which all allowed color and spin orientations occur with equal weight. This favors small total spin values, here $J = 0$.

To obtain the wavefunctions, in the meson-meson basis, one proceeds by diagonalizing E_M for a specific member of the multiplet, which yields a linear combination of the color and spin wavefunctions: e.g. $\psi = .813 \phi_7 - .582 \phi_4$ for $C^0(1.82)$. With the help of Tables IV and V these then are recoupled to

the meson-meson basis. We find e.g.

$$C^0(1.82) = \sqrt{\frac{3}{4}} \{0.743 \omega \cdot \omega + 0.041 \eta_0 \eta_0 - 0.169 \underline{\omega} \cdot \underline{\omega} - 0.646 \underline{\eta_0} \cdot \underline{\eta_0}\} \\ - \frac{1}{2} \{0.743 \rho \cdot \rho + 0.041 \pi \cdot \pi - 0.169 \underline{\rho} \cdot \underline{\rho} - 0.646 \underline{\pi} \cdot \underline{\pi}\} \quad (3)$$

Here the particle symbols stand for the corresponding particles and contain the flavor and spin information. The color octet states are underlined to distinguish them from the singlets: $\underline{\pi}$ is a $J^P = 0^-$ isotriplet color octet meson, built from nonstrange quarks.

Considering the wavefunction of C^0 one finds, that the four quark state, whose radius (and mass) was determined by the balance of the quark pressure and the vacuum pressure, turns out to be in a two color singlet meson state for about 55 % of the time. These mesons form (smaller) bags of their own, and there is no boundary condition which keeps them inside the larger bag, nor is there any reason, why they should contribute to the quark pressure in the big bag. This latter phenomenon generates large uncertainties for the radius- and mass-value of the bag state, on top of the calculational ones. The former implies, that C^0 is unstable, in an approximation in which states like the ρ meson and the Δ baryon still are stable. Its largest component is a free two meson system. Such properties make a conventional (resonance) interpretation for states far above the threshold somewhat dubious.

A similar situation in the Q^6 system: the deuteronlike state at 2.16 GeV consists for 80 % out of colored and for 20 % out of colorless baryon pairs, the latter of which are NN (11 %) or $\Lambda\Lambda$ (9 %), led DeTar [DeT 78] to calculate the energy of a deformed bag and deduce the form of the NN potential from it. The 2.16 GeV deuteron state shows up as a soft repulsive core. For the Q^2-Q^2 system a different approach has been taken by Jaffe and Low [Ja 78]. They studied the phaseshift in a (multichannel) meson-meson scattering process. It turns out that only a resonant phase shift is

obtained, when the $Q^2_{\bar{Q}^2}$ bag state is below or at the dominant decay (see below) threshold. When just above it a broad non resonant enhancement in the cross section will be seen. Finally a bag state far above its dominant threshold gives rise to a slowly falling negative phase shift. This last case is consistent with DeTars soft core interpretation.

The connection with the decay channels can be made by assuming, that the color spin recoupling coefficients give the decay amplitudes, up to a universal coupling constant g_0 . The dimesons are able to dissociate into two mesons, which are in a relative S-wave, without any effort or inhibition. Any other decay mode, because it will need additional (gluon) interactions, is expected to be suppressed and is consequently neglected.

In terms of vector (V) and pseudoscalar (P) mesons the wavefunction of a member of the lowest 0^{++} flavor nonet reads:

$$\psi \sim - 0.041 V \cdot V + 0.743 P \cdot P + 0.646 \underline{V \cdot V} - 0.169 \underline{P \cdot P} \quad .$$

These light states only couple to the S-wave pseudoscalar colorsinglet meson-meson channels. Their decay then is governed by a reduced coupling constant: $\bar{g}_0 = 0.743 g_0$, and the relative strengths can be read off from Table Vd. In Table VII we list the nonet members, their mass and dominant decay modes, as well as a tentative assignment.

Name	(I,Y)	Mass (GeV)	Flavor content	Decay	Assignment
C^0	(0,0)	0.64	$-\sqrt{\frac{1}{4}} \eta_0 \eta_0 - \sqrt{\frac{3}{4}} \pi\pi$	$\pi\pi$	ϵ (650)
C_K	(1/2,1)	0.89	$\sqrt{\frac{1}{4}} (\eta_0 K) - \sqrt{\frac{3}{4}} [\pi K]$	πK	κ (850)
$C_{\bar{K}}$	(1/2,-1)	0.89	$\sqrt{\frac{1}{4}} (\eta_0 \bar{K}) + \sqrt{\frac{3}{4}} [\pi \bar{K}]$	$\pi \bar{K}$	$\bar{\kappa}$ (850)
C_{π}^S	(1,0)	1.12	$\sqrt{\frac{1}{2}} (\eta_s \pi) - \sqrt{\frac{1}{2}} (K\bar{K})$	$\eta\pi, K\bar{K}$	δ (980)
C^S	(0,0)	1.12	$\sqrt{\frac{1}{2}} (\eta_0 \eta_s) + \sqrt{\frac{1}{2}} [K\bar{K}]$	$K\bar{K}$	S^* (980)

Table VII: Properties of the $J^{PC} = 0^{++}$, $n = 9$ dimesons.

In comparison with a $Q\bar{Q}$ nonet, say the $J^{PC} = 1^{--}$ nonet, the identification of $SU(3,F)$ states with the particles is inverted. In the $Q\bar{Q}$ nonet the ρ and ω contain no and the ϕ two strange quarks, approximately, and the K^* one. Consequently: $m(\rho) \simeq m(\omega) < m(K^*) < m(\phi)$. In the $Q^2\bar{Q}^2$ nonet the ρ - (C_π^S) and ω - (C^S) like states are heavier than the K^* - (C_K) like states, since they contain an $s\bar{s}$ pair. C_K only contains one strange quark, and is, in turn, heavier than the ϕ -like (C^0) state, which contains none. One has $M(C_\pi^S) \simeq M(C^S) > M(C_K) > M(C^0)$! This is a very peculiar consequence of the ideal mixing. The predictions seem to be confirmed by experiment. Both S-wave $\pi\pi$ and πK ($\pi\bar{K}$) phase shifts are non resonant, yet slowly varying and nonzero in the correct mass region, suggestive of the presence of particles with a mass of about 650 and 850 MeV respectively. $S^*(980)$ lies at the $K\bar{K}$ threshold, and manifests itself as a narrow peak in this channel. The observation of also a $\pi\pi$ decay signal indicates an ϵ -admixture to the S^* . The branching ratios into $K\bar{K}$ and $\pi\pi$, which are not known at present may provide a clue w.r.t. the strength of the deviation from ideal mixing for the isoscalars. The $\delta(980)$ is seen to decay in $K\bar{K}$ and $\eta\pi$, but is suppressed in the latter channel because of the limited η content of the η_S .

There are strong indications for another complete 0^{++} nonet, around 1300 MeV, which may provide the candidates for an orbitally excited $Q\bar{Q}$ system, which indeed is expected in that area (see Table VIII).

The next $Q^2\bar{Q}^2$ multiplet to be expected is the $J^{PC} = 0^{++}$, $n = 36$ multiplet. Its lightest members are predicted at 1.120 GeV, among which an exotic $I = 2$ $\pi\pi$ state. The exotic $I = 3/2$ $K\pi$ state is expected at 1.320 GeV. Also for these states phase shift indications seem to exist at a slightly lower mass. From the above stated considerations it may be clear that $Q^2\bar{Q}^2$ spectroscopy has entered a hope-inspiring stadium, and that the effort to

create new approaches to this subject these last few years, is beginning to bear fruits. We will see, that more support for these states can be drawn from the study of orbital excitations for these systems, to which we shall now proceed.

Section II. Mesons and angular momentum [Jp 76]

Next to the spherical bag, which appears to be a good approximation for a system of light (or even massless) quarks in their lowest energy eigenstate, also the stringlike bag has yielded several interesting results. It is a description for hadrons, which have a high orbital excitation, and whose orbital angular momentum is such, that it is the largest one compatible with their mass, i.e. for hadrons which lie high on the leading Regge trajectories.

Following Johnson and Thorn [Jp 76], one tries to give the bag such a shape that, classically and nonrelativistically, it has the largest moment of inertia for rotating around a well chosen axis. For this purpose the following configuration seems to be the most suitable one to start with. One takes the bag to be a static cylinder of length l and places a set of quarks (and antiquarks) at each end. Their number need not be the same. The quarks at one end combine their color charges to a total charge $Q^a = \sum_1 Q_1^a = g \sum_1 F_1^a$, which transforms according to the $SU(3, C)$ irrep c . The total system must be in a color singlet state, therefore the quarks at the other end will form the opposite charge. The simplest set possible consists of a single quark, a color triplet. An obvious match then is the single antiquark set, and one has a model for an excited or $Q-\bar{Q}$ meson. Another common antitriplet is formed by a diquark. This yields a model for the excited or $Q-Q^2$ baryon. One color charge acts as a source (obviously $c \neq 1$) for a chromo-electric field E^a , which is taken to be homogeneous over the whole cylinder, and the other as sink. The flux lines of this field run parallel to the cylinder axis, in

order to satisfy the linear bag boundary condition: $n_\mu G_a^{\mu\nu} = 0$, which for the static case (subscript 0) reduces to $\vec{n} \cdot \vec{E}_0^a = 0$. Here \vec{n} is the ordinary space normal of the cylinder surface. When the surface moves, it develops a fourth component $n^0 \neq 0$.

It is assumed, that the influence of the quarks is only felt at the ends of the elongated bag. Their function is to generate and end the flux-lines, and smooth out any discontinuity which may arise in this tube approximation at the top and the basis of the cylinder. This implies, that the vacuum pressure at the sides of the cylinder will be balanced exclusively by the gluon field. One has (eq 2 (25)) $B = -\frac{1}{4} G_a^{\mu\nu} G_{\mu\nu}^a$, which reduces to $B = \frac{1}{2} \int_a \vec{E}_0^a{}^2$. Using Gauss' law we find $E_0^a A_0 = Q^a$ or $E_0^a = Q^a/A_0$, where A_0 is the cross section of the cylinder, which has its normal parallel to the cylinder axis. The size of A_0 is a function of the color charge and the bag parameters according to: $A_0 = \{2\pi\alpha_c f_c^2/B\}^{1/2}$, where f_c^2 is the eigenvalue of the operator $\int_a F_a^2$ in the irrep c : $f_c^2 = \langle c | \int_a F_a^2 | c \rangle$. Its scale derives from the bagpressure B . One has $(f_3^2 = \frac{4}{3}) R_0 = \sqrt{A_0/\pi} = 1.59 \text{ fm}$ (cf. the proton has a radius of 1 fm in this model).

The pressure at the top and bottom plane will be balanced by quarks and glue together. This will determine the remaining parameter ℓ . The situation described above is clearly unstable for light quarks. Nothing opposes the color electric field, which will pull the two sets of quarks towards each other. The cylinder collapses: $M = M(\ell)$ will only be minimal for $\ell = 0$. Stability will be realized by letting the cylinder rotate. One chooses an axis through the center of mass, perpendicular to the symmetry axis, with respect to which the inertial moment is maximal. To obtain the largest possible angular momentum for fixed bag length ℓ , we let the tube rotate with a uniform frequency ω , such that the endpoints move at the speed of

light. Since we did not put any restriction on the distribution of the quarks over the ends of the bag to obtain a color charge Q^a , this implies that the quark energy has to be negligible w.r.t. that of the glue. The centre of mass should (in first approximation) be equidistant to both ends.

To an observer, somewhere on the rotation axis, at rest w.r.t. its centre of mass, the bag now no longer looks like a cylinder (Fig. 1). Consider a point inside the bag or on its surface. It has a distance x from the rotation axis, and therefore moves with a speed $\beta = \omega x$. When $x = \frac{\ell}{2}$, the point is at one of the bags' ends, $\beta = 1$ and we find $\omega = \frac{2}{\ell}$. In order to determine the important properties of the rotating bag one starts from the observation, that the points on the rotation axis are at rest. In their rest frame, the cross section of the bag is a circle with radius R_0 , rotating with frequency ω . The electric field going through the bag, has a constant strength \vec{E}_0^a , perpendicular to this surface. There is no magnetic field. For every x there is a set of

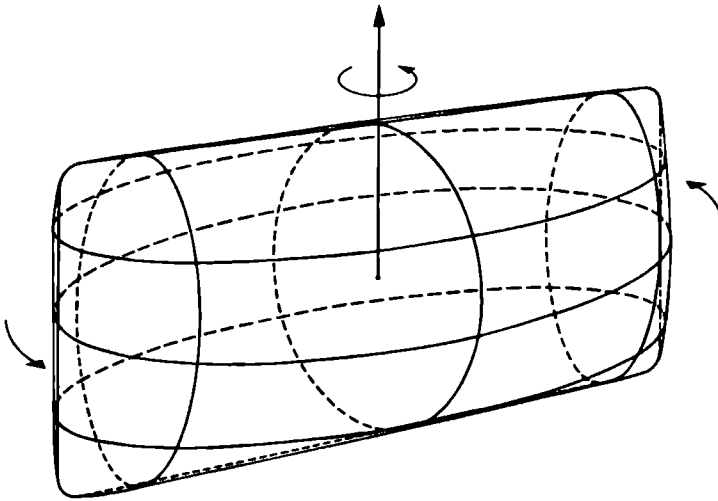


Fig. 1: Tubularbag with length ℓ , rotating with frequency $\omega = \frac{2}{\ell}$, around an axis through the bag's centre of mass, perpendicular to the symmetry axis, as seen by an observer at rest w.r.t. the rotation axis.

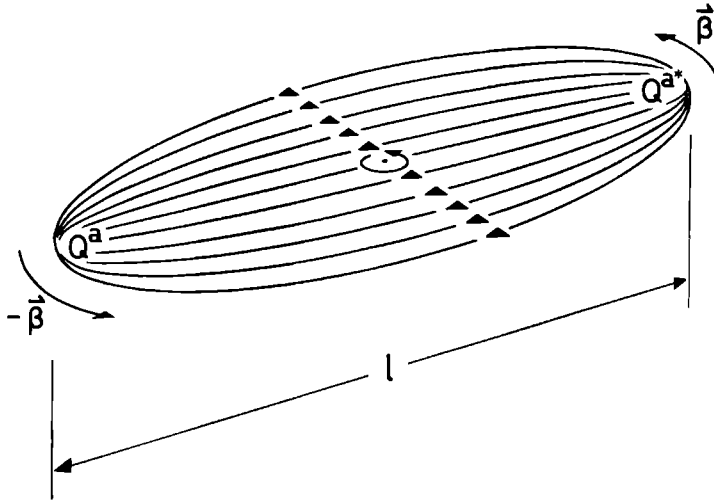


Fig. 2: Cross section of the rotating bag of Fig. 1, taken perpendicular to the rotation axis.

points which have identical properties in their instantaneous rest (ir) frame. Boosting these so-called central points back to their original velocity $\vec{\beta}$ they constitute the mayor axis of an ellips, which has its minor axis, length $2R_0 \sqrt{1 - \beta^2}$, parallel to $\vec{\beta}$ (Fig. 2). The area of the cross section now has become $A = A_0 \sqrt{1 - \beta^2}$. The transformed electric field strength is $\vec{E}^a(\vec{\beta}) = \gamma \vec{E}_0^a$ and remains perpendicular to the surface A. One has $E^a A = Q^a$. An additional effect of the boost is the presence of a magnetic field $\vec{H}^a = \vec{\beta} \times \vec{E}^a$, $H^a = \beta E^a$. We will use these expressions for \vec{H}^a , \vec{E}^a and A in our calculations. Other choices are also possible and, of course, related by boosts and rotations. The fields \vec{E}^a and \vec{H}^a , obtained by special Lorentz transformations from \vec{E}_0^a naturally satisfy the bagboundary conditions, which are Lorentz invariant statements and thus also determine the shape of the rotating bag. Note that the top and bottom surfaces of the bag have shrunk into lines, reducing the role of the quarks still further.

We have now determined the necessary quantities to be able to calculate the mass and angular momentum of the rotating bag. There are three contributions to the mass

$$M = E_G + E_Q + E_V \quad (4)$$

and two to the orbital angular momentum, which can simply be added for the leading trajectory

$$L = L_G + L_Q \quad . \quad (5)$$

The labels G, Q and V refer to glue, quarks and volume respectively. In case of the rotating bag $\frac{\partial}{\partial L} M(L) = 0$, expressing the balance of the field pressure against that of the vacuum, at the bag's ends, will have a root for non-vanishing L , provided we keep its angular momentum L fixed. This root is equal to the one we get, when we maximize L for fixed M .

We will now calculate each contribution separately. Instead of the distance to the rotation axis x it is in this approximation more convenient to use the speed β as coordinate: $x = \frac{L}{2} \beta$. The volume energy is:

$$E_V = B \int dV = 2B \int_0^{L/2} dx A(x) = B L \int_0^1 d\beta A_0 \sqrt{1 - \beta^2} = \frac{\pi}{4} B A_0 L \\ \equiv \frac{\pi}{4} B V' \quad .$$

It is reduced by a factor $\frac{\pi}{4}$ w.r.t. the cylinder volume, due to Lorentz contraction. The energy stored in the fields is

$$E_G = \frac{1}{2} \int dV \int_a (\vec{E}_a^2 + \vec{H}_a^2) = B A_0 L \int_0^1 d\beta \frac{1 + \beta^2}{\sqrt{1 - \beta^2}} = \frac{3\pi}{4} B A_0 L = 3 B V' \quad .$$

Two thirds of this contribution come from the color-electric field. It follows that formally: $\int dV B = \frac{1}{2} \int_a \int dV (\vec{E}_a^2 - \vec{H}_a^2)$. The energy of the quarks is represented by (cf. also [Jo 79]):

$$E_Q = 2p$$

where the p indicates that the momentum and energy of a set of quarks at the

end of the bag are approximately equal. The contributions are taken the same, for both ends, in view of the position of the centre of mass. E_Q does not depend on l . The relevant dimensional parameter is R_0 , representing the size of the volume to which the quarks are confined. We include it, to verify, that its contribution is indeed negligible w.r.t. the other terms. Summing up:

$$H = 2p + \pi B l A_0 \quad .$$

The angular momentum carried by the fields is:

$$\vec{L}_G = \int dV \int_a \vec{r} \times (\vec{E}_a \times \vec{H}_a) \quad .$$

Using the centre values for \vec{E}_a and \vec{H}_a we find

$$L_G = B A_0 l^2 \int_0^1 d\beta \frac{\beta^2}{\sqrt{1-\beta^2}} = \frac{\pi}{4} B l^2 A_0 \quad .$$

The orbital momentum of the quarks is:

$$L_Q = p l$$

The total orbital angular momentum then is given by:

$$L = p l + \frac{\pi}{4} B l^2 A_0 \quad .$$

We can solve: $p = \frac{L}{l} - \frac{\pi}{4} B l A_0$

and eliminate it from the bag mass expression. The bag length l can now be determined as a function of L , which is kept fixed:

$$\left. \frac{\partial}{\partial l} M(l) \right|_L = \frac{\partial}{\partial l} \left(\frac{2L}{l} + \frac{\pi}{2} B A_0 l \right) = -\frac{2L}{l^2} + \frac{\pi}{2} B A_0 = 0 \quad .$$

Thus $l = l(L)$ and:

$$M = \pi B l A_0 = 4 B l \quad (7)$$

$$L = \pi B l^2 A_0 / 4 \quad . \quad (8)$$

The final result is an asymptotically linear trajectory in the L - M^2 plane

$$L = \alpha' (c) M^2 \quad , \quad (9)$$

with $\alpha'(c) = (2\pi \alpha_c f_c^2 B)^{-1/2}$. (10)

Taking $c = 3$, we obtain $\alpha'(3) = 0.88 \text{ GeV}^{-2}$. Experimentally one finds that $\alpha' \approx 0.9 \text{ GeV}^{-2}$ for $Q-Q^2$ baryons and $\alpha' \approx 0.8 \text{ GeV}^{-2}$ for $Q-\bar{Q}$ mesons. Eqs (9) and (10) are a result of treating the bag as a fat string. From this treatment follows another result shared with the string. In the dual string model (see chapter 1, pg 19) the slope of the trajectory is related to the proper tension T of the string by

$$T = (2 \pi \alpha')^{-1} . \quad (11)$$

The tension T is defined in the instantaneous restframe of some central point as the amount of energy required to stretch the string by a unit length. For the bag this becomes $T = \frac{1}{2} \int_a^a \vec{E}_0^2 A_0 + B A_0 = 2 B A_0$, consistent with eq (11). Of course $T/A_0 = 2 B$ is not the average energy density of the rotating bag. This density is: $U = M/V' = 4 B$ (eq (7)), in agreement with the general result for bags containing only massless constituents [Cho 74]. The apparent discrepancy is accounted for by the rotation energy.

After substitution of \bar{l} , we find that $p = 0$, which means that the quark contribution to both mass and angular momentum can be neglected, and guarantees the continuity of the glue determined boundary over the bag ends. All sufficiently high-excited bags have the same form. Omitting p from the beginning we find that L and M are homogeneous in \bar{l} and again satisfy eq (9). The bag is all 'sides'. There is no end surface, where pressures have to be balanced. Its shape is fixed and only the overall scale is still free, to be determined by L or M .

One can try to specify somewhat better which value of L is already asymptotic. The relevant condition, to be expressed in terms of L is:

$$M \gg p \approx \frac{\bar{\gamma}d}{R_0} \quad \text{or} \quad \{4L \cdot 2\pi \alpha_c f_c^2\}^{1/2} \gg \bar{\gamma}d \quad \text{or} \quad L \gg 1$$

where we have used a boosted value (Lorentz factor $\bar{\gamma}$) of the static sphere (radius R_0) result (see chapter 2, Table I): $E_Q = \frac{d}{R_0}$ for p. This result is not very conclusive. Because larger color charges (larger f_c^2) also require a larger number of quarks (larger d) the color charge does not appear to be very helpful in bringing asymptotia closer. The $Q\bar{Q}$ meson data suggest that the trajectories may already run straight from $L = 3$ for $c = 3$ trajectories. This implies, that eq (9) gives a good estimate of the bag mass differences for $L \geq 3$.

The premature onset of asymptotic behavior is also encountered in another situation by Giles [Gl 78]. Solving the problem of two opposite static electric charges confined to an MIT bag in two space dimensions, he obtained both the shape and the electrostatic potential for arbitrary charge separation l . For large l the bag has a cigar shape and the potential is linear in l . The second property, however, which dominates the mass spectrum, is present well before the first.

To be able to use eq (9) to obtain the bagmass, its position in the L - M^2 plane needs to be fixed. The stringlike bag-picture does not provide any clues for calculating trajectory intercepts. It is an asymptotic description for fast-spinning particles. One can try to extrapolate the trajectory by assuming that it is linear for all L . The derivation of eq (9) is insensitive to the replacement $L \rightarrow L' = L - L_0$, where L_0 is a (negative) constant. We can write:

$$L = \alpha' M^2 + L_0 \quad \bar{D} \quad \alpha' (M^2 - M_0^2) \quad \text{or} \quad M^2 = M_0^2 + L/\alpha' \quad (12)$$

Here L_0 (M_0^2) is the intersection of the trajectory with the $M^2 = 0$ ($L = 0$) -axis in the L - M^2 plane. In general M_0 is not the mass of a physical S-wave hadron. These masses should be calculated using the spherical cavity approximation and involve quark spin effects, which have been omitted from

the discussion so far. For example, vector (triplet) - and pseudoscalar (singlet) - $Q\bar{Q}$ -mesons are treated as similar systems, since for high L the two quark sets (apart from the color charge) are expected to be completely ignorant of each others properties, due to the large angular momentum barrier in between them. Asymptotically the ρ and π trajectory become degenerate. For low L there is no such degeneracy. This is especially clear for $L = 0$, where, in the bagmodel interpretation, color magnetic interactions split the singlet ($J = 0$) from the triplet ($J = 1$) states (\sim spin-spin interaction). For $L = 1$, if we correct for the spin orbit and tensor type splitting, other aspects of the same interaction, it is already much less important, whereas for $L = 2$ it appears to be almost absent.

This observation suggests the following prescription for calculating M_0 for $Q\bar{Q}$ mesons: it is the mass of a spherical bag, in which no color magnetic interactions are taking place between the quark and antiquark. From this recipe, it is clear that M_0 is a kind of average of physical state masses and L_0 should be negative. M_0 still depends on the number of strange quarks. For $Q\bar{Q}$ mesons we expect three asymptotic trajectories in the $L-M^2$ plane: one for $n\bar{n}$, one for $n\bar{s}$ and $s\bar{n}$, and one for $s\bar{s}$ states. The resulting 'central' masses, using a tentative slope of $\alpha'(3) = 0.83 \text{ GeV}^{-2}$, and those mesons, which may be considered for classification as orbitally excited $Q\bar{Q}$ states are listed in Table VIII. This table includes all PDG 78 mesons, containing u , d and s quarks, except the $J^{PC} = 0^{++}$ mesons discussed in section I, and the S , T and U $N\bar{N}$ resonances. The observation, that all listed states (with possible exception of the $\rho'(1600)$) can be classified as leading trajectory states, seems to provide us ample justification to restrict our attention to this particular configuration.

L	J ^{PC}	I = 1 (n \bar{n})	I = 0 (n \bar{n})	I = 0 (s \bar{s})	I = 1/2 (n \bar{s} /s \bar{n})
0	0 ⁻⁺	π ; 138	η ; 549	η' ; 958	κ ; 496
	1 ⁻⁻	ρ ; 776 \pm 3	ω ; 783	ϕ ; 1020	κ^* ; 892
	M _C (0)	670	670	990	840
1	1 ⁺⁻	B; 1231 \pm 10			Q _A ; \sim 1340
	0 ⁺⁺	δ' ; \sim 1270	S*; \sim 1300	ϵ ; \sim 1300	κ ; 1400 \sim 1450
	1 ⁺⁺	A ₁ ; \sim 1100	D; 1276 \pm 3	E; 1431 \pm 3	Q _B ; \sim 1355
	2 ⁺⁺	A ₂ ; 1312 \pm 5	f; 1271 \pm 5	f'; 1516 \pm 10	κ^{**} ; 1434 \pm 5
	M _C (1)	1285	1285	1475	1380
2	2 ⁻⁺	A ₃ ; \sim 1640			L; 1765 \pm 10?
	1 ⁻⁻	ρ' ; \sim 1600?			
	2 ⁻⁻				
	3 ⁻⁻	g; 1688 \pm 20	ω ; 1668 \pm 10		κ^{**} ; 1784 \pm 10
M _C (2)	1685	1685	1840	1765	
3	3 ⁺⁻				
	2 ⁺⁺				
	3 ⁺⁺				
	4 ⁺⁺	1982 \pm 9?	h; 2040 \pm 20		
M _C (3)	2010	2010	2140	2080	

Table VIII: $Q\bar{Q}$ meson states. The particles are denoted as a function of their quantum numbers L, J, P, C and I. The particle names are separated from their masses (in MeV) by a semi-colon. The mass is followed by an error, when known, and by a question mark, when some of its quantum numbers are uncertain. When preceded by a tilde, the mass, and possibly also some q-numbers are not (well) established. M_C(L) is the linearized trajectory mass.

The states with $L = 2$ and 3 already are quite close to the trajectory, which seems to indicate the vanishing of LS, tensor and singlet-triplet splitting. Unfortunately, for these L values only the peripherally produced $J = (L + 1)$ states are well known. For $L = 1$ both spin effects are present and one can try to estimate their strength. The spin orbit and tensor splittings together are several tens of MeV large. This crude estimate requires some optimism about the classification of not too well established states. E.g. the $A_1(1100)$ seems to be a case on its own, which until now can hardly be forced into any regular spin orbit scheme and is left out of consideration. Also the isoscalars appear to be rather sensitive to the inclusion of LS and tensor forces: $M(D) > M(F)$ [MaR 78]! One then finds that the residual color magnetic singlet-triplet splitting is reduced to about 20 % of the $L = 0$ strength. For $L = 2$ a good guess seems to be 5 %. We will add these small residual interactions as perturbations to the mass obtained from eq (12), notwithstanding its obvious L dependence, by way of a more accurate procedure. This approach appears to work reasonably well.

The actual trajectories thus prove to be bent for low L , when plotted in the $L-M^2$ plane, but very rapidly converge to a highly degenerate straight line. There is a smooth connection between $L = 0$ and high L . To translate this picture to the $J-M^2$ plane, one replaces \vec{L} by $\vec{L}' = \vec{J} - \vec{S}$. Only the two $J = L$ trajectories will remain degenerate for sufficiently high mass. The $J = L \pm 1$ trajectories become parallel to these. Also in the $J-M^2$ plane the trajectories will exhibit curvature.

Section III: $Q\bar{Q}^{2-2}$ mesons and orbital excitations

In the last decade many resonances, with widths varying from 3 to 280 MeV, have been observed to couple to the baryon-antibaryon system [Mon 78].

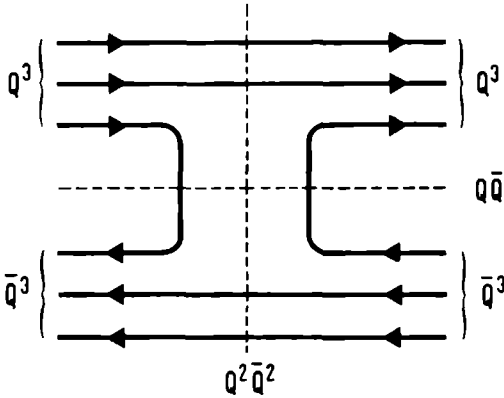


Fig. 3: Quarkline diagram for antibaryon-baryon elastic scattering via meson exchange, or a $Q^2 \bar{Q}^2$ intermediate state.

Among these are several, now well established states, which have been detected first in elastic nucleon-antinucleon scattering. This process, which to lowest order, proceeds through one meson ($Q\bar{Q}$) exchange, is depicted in the Harari-Rosner [Ha 69] (quark-line) diagram of Fig. 3. From this diagram it may be clear that meson exchange is closely related ("dual") to the formation of a resonant $Q^2 \bar{Q}^2$ intermediate state. It was on the basis of this duality in $B\bar{B}$ scattering [Ro 68] that $Q^2 \bar{Q}^2$ states and their properties were first predicted. Conform to expectation [Ro 70] many resonances were discovered (first) in the $B\bar{B}$ channels. Surprisingly, several of these also appear to couple almost exclusively to them. This phenomenon has started the interest in orbitally excited $Q^2 \bar{Q}^2$ systems of which the present model allows a systematic examination. The $L = 0$ states have been treated in section I. The orbital excitations will be studied here. We will first enumerate the possible trajectory configurations and proceed with a classification of the corresponding states and an estimate of their mass spectrum.

The $Q\bar{Q}$ system, considered in the previous section, is a minimal one as far as color and quark spin are concerned. Asymptotically only one leading

trajectory survives in the $L-M^2$ plane. The $Q^2\bar{Q}^2$ system shows more variation, even if we restrict our attention to leading trajectory configurations. Of course, severely deformed bags, with three or four lobes, each of which has at least one quark in it, are thinkable. Such starlike formations are, however, not likely to maximize the orbital angular momentum and thus will be buried under the higher spin states. Large $l - Q^2\bar{Q}^2$ spectroscopy, just as its $Q\bar{Q}$ -companion, is expected to be dominated by stringlike bags. We assume, that quarks in the same cluster move in s-waves relative to each other, whereas the clusters themselves move in a relative l -wave. This notation will from now on be used for the interquark orbital momentum in ordinary $Q\bar{Q}$ mesons too.

- Trajectory configurations -

The number of independent ways, in which the quarks can be distributed over two colored clusters, increases from one to four, when another $Q\bar{Q}$ -pair is added. Again, one has the single quark cluster, this time in combination with a three quark one. The corresponding so-called $3-3^*$ -trajectory is assumed to have an asymptotic slope $\alpha'(3) = 0.83 \text{ GeV}^{-2}$ (eq (10)) and states on it, in view of their inclination to multi-meson decay, will be called three-mesonia. Next, a cluster may contain a Q^2 or a $Q\bar{Q}$ pair. The Q^2 set can couple to either a $c = 3^*$ or a $c = 6$ color charge. The former yields a $3^* - 3$ or 3-baryonium trajectory [Jb 78] with the usual slope $\alpha'(3)$, the latter a $6 - 6^*$ or 6-baryonium one [ChH 77] with an anomalous slope of $\alpha'(6) = 0.53 \text{ GeV}^{-2}$ ($f_6^2 = 10/3$). The name baryonium was proposed by Chew [Che 76] for meson states which couple dominantly to baryon-antibaryon channels. Although this ordinarily only applies to the color 3 variety, it is often, and also here, used in a more generalized sense to refer to orbitally excited $Q^2\bar{Q}^2$ states with (anti)diquark clusters. The quark-anti-

quark cluster can occur in a $c = 1$ or a $c = 8$ irrep. The neutral singlet is not interesting from the point of view of orbital excitations. The 8-8-trajectory has an anomalous slope too, $\alpha'(8) = 0.56 \text{ GeV}^{-2}$ ($f_8^2 = 3$). These systems will be called 8-mesonia.

1. Asymptotia (Large orbital angular momentum region)

For sufficiently large ℓ (i.e. $\ell \geq 3$) the above mentioned clusters form the natural building blocks in terms of which the $Q^2\bar{Q}^2$ orbital excitations will be classified. These clusters, sitting at the ends of the fast rotating stringlike bag, can not change color or spin, because the large angular momentum barrier virtually forbids the exchange of quarks and gluons between them. Color flip moreover is impeded by the wide energy gaps, which will arise as a result of the different slopes. The cluster basis states are obtained by reducing the direct product of the color, spin and flavor wavefunctions of the (anti) quarks contributing, and diagonalize their total color charge and spin. We list the total quantum numbers of the relevant irreps in Tables IX and XIc. The two and three quark clusters each have their own particular complications and will be treated more or less separately. The basis states for the whole system are given by the reduction of the direct product of two 2-, or a 3- and a 1-quark cluster basis irreps. Only those color singlets are allowed, which satisfy the generalized Pauli-principle.

- Classification -

When both (anti)quarks are placed in the same cluster, their color spin flavor wavefunction has to be totally antisymmetric. This allows only specific combinations, which is most clearly reflected in the resulting flavor irreps (see Table Xa and Xb). There are less restrictions on the

color spin flavor part of the wavefunctions, when one of the (anti)quarks is lodged in a different cluster. Their space wavefunctions are clearly distinguishable now and have no overlap. The clusters will couple to flavor-quark spin combinations, which were excluded for the $L = 0$ mesons (see Table XIc). Since there is no energy associated with the coupling to overall quark spin and flavor representations, all levels, with the same quark content (n_s), will be degenerate. Finally, one can have an aggregate of two color octet clusters. The quark and antiquark are close together, in an s-wave with respect to each other. This assumption excludes the existence of simple relations between operations such as quark permutations, exchanging the quarks between the bag ends, and space reflections, which exist for some excited Q^3 baryons. The combination behaves as a colored boson. The spectrum of allowed states is now restricted by the BE statistics, which has to be satisfied by this two colored meson system. When the mesons have the same isospin, hypercharge and spin quantum numbers, one has to distinguish odd and even L (see Table Xc).

- Colormagnetic splittings -

The presence of more than one quark in a cluster has yet another consequence. Unlike the quark and antiquark in the $Q\bar{Q}$ meson, quarks in the same cluster will unhamperedly continue to exchange gluons. It is useful to split the colormagnetic interaction term into two parts:

$$E_M = \frac{\alpha_c}{R} \sum_{1>2} M(m_{1R}, m_{2R}) (\vec{F}\vec{\sigma})_1 \cdot (\vec{F}\vec{\sigma})_2 \quad (13)$$

$$E_M = E_{MR} + E_{MP}$$

The residual part E_{MR} is the interaction between quarks in different clusters, familiar from the $Q\bar{Q}$ mesons, and has the form:

$$E_{MR} = \sum_{1,2} m(1_1, 2_2) (\vec{F}\vec{\sigma})_{1_1} \cdot (\vec{F}\vec{\sigma})_{2_2} \quad (14)$$

Content	c	s	<u>n</u>	Δ	Name
Q^2	3*	0	<u>3*</u>	- 2	χ_1
	6	1	<u>3*</u>	- 1/3	χ_2
	3*	1	<u>6</u>	2/3	χ_3
	6	0	<u>6</u>	1	χ_4
$Q\bar{Q}$	8	1	<u>9</u>	- 1/6	χ_5
	8	0	<u>9</u>	1/2	χ_6

Table IX: Basic irreps for two particle clusters, as a function of the quark content $Q^{n-m}\bar{Q}^m$, color c , spin s and flavor \underline{n} . Also the eigenvalues Δ of the two particle operator $O = - (\vec{F}\vec{\sigma})_1 \cdot (\vec{F}\vec{\sigma})_2$ are given (1 (2): first (second) particle).

The subscript $n \in \{1,2\}$ of the summation label indicates its restriction to cluster n . One has $m(i,j) \rightarrow 0$, for $\ell \rightarrow \infty$, rather fast, as suggested by the $Q\bar{Q}$ -trajectory data. E_{MR} is therefore not expected to contribute for large ℓ .

The persistent part of the colormagnetic interaction E_{MP} is composed of two contributions, one for each cluster: $n \in \{1,2\}$.

$$E_{MP}^n = \sum_{i_n > j_n} \tilde{M}(i_n, j_n) (\vec{F}\vec{\sigma})_{i_n} \cdot (\vec{F}\vec{\sigma})_{j_n} \tag{15}$$

The summation is restricted to the quarks in the n -th cluster. It is trivial for the two particle clusters. The cluster basis states $|a\rangle$ are eigen states of E_{MP} : $-(\vec{F}\vec{\sigma})_1 \cdot (\vec{F}\vec{\sigma})_2 |a\rangle = \Delta |a\rangle$. The eigenvalues Δ are also listed on Table IX.

- 3-Mesonium states -

A little more effort is needed for the three quark cluster. For each permutation symmetry of the flavor wavefunction of the diquark, one has two

Trajectory	Representation	s	<u>n</u>	C_n	ℓ	Δ
a) 3*-3	(1,1)	0	<u>9</u>	$(-)^{\ell}$	e & o	- 4
	(1,3)	1	<u>18*</u>	$\eta(-)^{\ell+1}$	e & o	- 4/3
	(3,1)	1	<u>18</u>			
	(3,3)	0,1,2	<u>36</u>	$(-)^{\ell+s}$	e & o	4/3
b) 6-6*	(2,2)	0,1,2	<u>9</u>	$(-)^{\ell+s}$	e & o	- 2/3
	(2,4)	1	<u>18*</u>	$\eta(-)^{\ell+1}$	e & o	2/3
	(4,2)	1	<u>18</u>			
	(4,4)	0	<u>36</u>	$(-)^{\ell}$	e & o	2
c) 8-8	(5,5)	0,2	<u>9</u> \oplus <u>36</u>	+	e	} - 1/3
		1	<u>18</u> \oplus <u>18*</u>	- η	e	
		0,2	<u>18</u> \oplus <u>18*</u>	- η	o	
		1	<u>9</u> \oplus <u>36</u>	+	o	
	(5,6)	1	<u>9</u> \oplus <u>36</u>	$(-)^{\ell+1}$	e & o	} 1/3
	(6,5)		<u>18</u> \oplus <u>18*</u>	$\eta(-)^{\ell+1}$	e & o	
	(6,6)	0	<u>9</u> \oplus <u>36</u>	+	e	} 1
			<u>18</u> \oplus <u>18*</u>	- η	o	

Table X: Properties of the color singlet two quark cluster product states.

(i,j) denotes $\chi_i \otimes \chi_j^*$, where the χ_i are defined in Table IX. One has $P = (-)^{\ell}$ under space inversion. ℓ is the orbital angular momentum, which can be even (e) or odd (o). The isotopic parity (G) of the hypercharge $Y = 0$ members of the flavor multiplets is given by $G = (-)^I C_n$, where C_n is the charge parity of the neutral member, and I its isotopic spin. The restriction on ℓ for the color octet states applies only to clusters, which have identical I and Y values. Other combinations occur for all ℓ values and an extra (-) sign should be added to the C_n listed above, when appropriate. Δ gives the size of the colormagnetic splitting.

ways of constructing a $(c,s) = (3,1/2)$ color spin wavefunction. For example, the diquark $c-s$ -irreps $(6,1)$ and $(3^*,0)$ are both symmetric under simultaneous color spin permutation and both can combine with the $(3^*,1/2)$ irrep of the antiquark to yield an overall $(3,1/2)$ irrep. As basic irreps we take those that also diagonalize E_{MP} . Calculation of the appropriate two particle operators proceeds along the lines, specified in section I for the $L = 0$ mesons. Taking all quark masses the same, we have to diagonalize the matrix $\{M\} = \{2A + B\}$. The recoupling matrices for color and spin, the composition of the basis irreps, and the necessary two particle operators are listed in Table XI. We have restricted ourselves to list only $Q^2\bar{Q}\bar{Q}$ configurations. One, of course, has also the conjugate system $Q\bar{Q}Q^2$, which yields a degenerate mass spectrum. The physical states are those linear combinations, which diagonalize G-parity, when they have $Y = 0$. Considering the recoupling matrices and $\{M\}$, it is not surprising, that the eigenvalues turn out to be precisely half as large as those listed in Table VI for the $J = 0$ and $J = 2$ $L = 0$ meson irreps. Although these clusters yield the largest negative eigenvalue for Δ , it also may be clear from the color recoupling $Q^2\bar{Q} \rightarrow (Q\bar{Q})Q$, that orbitally excited states with this cluster buildup will be just, if not even more so, elusive as their $L = 0$ brothers, because of the large color singlet content. They have a predilection for falling apart into MM^* channels (M^* is the orbital $Q\bar{Q}$ excitation with angular momentum $\ell' \approx \ell$ and decays into two or more meson states), which means final states with three or more mesons. Because there always appears to be sufficient phase space available for at least one of the larger decay components of the wavefunction, these states are expected to be broad and non resonant and therefore hard to detect. We will from now on concentrate mainly on the trajectories with diquark clusters.

a)	(<u>8</u> , <u>3</u> ; <u>3</u>)	(<u>1</u> , <u>3</u> ; <u>3</u>)	b)	(<u>1</u> , <u>1/2</u> ; <u>1/2</u>)	(<u>0</u> , <u>1/2</u> ; <u>1/2</u>)
(<u>6</u> , <u>3*</u> ; <u>3</u>)	$-\sqrt{\frac{1}{3}}$	$\sqrt{\frac{2}{3}}$	(<u>1</u> , <u>1/2</u> ; <u>1/2</u>)	$-\sqrt{\frac{1}{4}}$	$\sqrt{\frac{3}{4}}$
(<u>3*</u> , <u>3*</u> ; <u>3</u>)	$\sqrt{\frac{2}{3}}$	$\sqrt{\frac{1}{3}}$	(<u>0</u> , <u>1/2</u> ; <u>1/2</u>)	$\sqrt{\frac{3}{4}}$	$\sqrt{\frac{1}{4}}$

a) Recoupling matrices for SU(3): $(\underline{n}_{Q2}, \underline{n}_{\bar{Q}}; \underline{n}_{Q2\bar{Q}}) \leftrightarrow (\underline{n}_{Q\bar{Q}}, \underline{n}_Q; \underline{n}_{Q2\bar{Q}})$.

b) Recoupling matrices for SU(2): $(\underline{j}_{Q2}, \underline{j}_{\bar{Q}}; \underline{j}_{Q2\bar{Q}}) \leftrightarrow (\underline{j}_{Q\bar{Q}}, \underline{j}_Q; \underline{j}_{Q2\bar{Q}})$.

C_{Q2}	j_{Q2}	$j_{Q2\bar{Q}}$	$J_{Q2\bar{Q}}$	\underline{n}_{Q2}	$\underline{n}_{Q2\bar{Q}}$	$\underline{n}_{Q2\bar{Q}^2}$	Name
3*	0	1/2	0,1	3*	3 ⊕ 6*	9 ⊕ 18*	φ ₁
6	1	1/2	0,1				φ ₂
		3/2	1,2				φ ₃
6	0	1/2	0,1	6	3 ⊕ 15	18 ⊕ 36	φ ₄
3*	1	1/2	0,1				φ ₅
		3/2	1,2				φ ₆

c) Quantum numbers of the color singlet three ⊗ one quark cluster product representations.

A	B	Basis	Eigenvector	Δ
$\begin{bmatrix} 0 & -\sqrt{\frac{2}{3}} \\ -\sqrt{\frac{2}{3}} & -\frac{5}{3} \end{bmatrix}$	$\begin{bmatrix} -2 & 0 \\ 0 & -\frac{1}{3} \end{bmatrix}$	φ ₁	$\begin{bmatrix} .582 \\ .813 \end{bmatrix}$	- 5.42
		φ ₂	$\begin{bmatrix} .813 \\ -.582 \end{bmatrix}$	- 0.25
$\frac{1}{3}$	$\frac{2}{3}$	φ ₃	1	$\frac{4}{3}$
$\begin{bmatrix} 0 & -\sqrt{\frac{2}{3}} \\ -\sqrt{\frac{2}{3}} & -\frac{2}{3} \end{bmatrix}$	$\begin{bmatrix} 1 & 0 \\ 0 & \frac{2}{3} \end{bmatrix}$	φ ₄	$\begin{bmatrix} .813 \\ .582 \end{bmatrix}$	- 2.42
		φ ₅	$\begin{bmatrix} -.582 \\ .813 \end{bmatrix}$	2.75
$\frac{5}{6}$	$-\frac{1}{3}$	φ ₆	1	$\frac{4}{3}$

d) Matrix representations of the two particle operators A and B. The eigenvectors and eigen values Δ of the matrix M = 2A + B (see Table VI).

Table XI.

To arrive at the masses of asymptotic $Q^2\bar{Q}^2$ -trajectory states we still have to fix the intercepts M_0 , the strength of E_{MP} and the way it has to be included.

- Intercept -

Building on the success of the M_0 prescription for $Q\bar{Q}$ trajectories, we will take $M_0(Q^2\bar{Q}^2)$ to be the mass of a spherical bag in which the quark-gluon coupling has been turned off. Because of the fair amount of color singlet $Q\bar{Q}$ -subsystems, there probably is a non spherical bag shape, which provides a lower minimum for the bag mass. The actual intercept then may be somewhat smaller. Compare for instance also $M_0(Q^2\bar{Q}^2) = 1.46$ GeV for nonstrange quarks, with $2M_0(Q\bar{Q}) = 1.35$ GeV, a difference, which is mainly due to the (to Q^3 and $Q\bar{Q}$ ground states) fitted, geometry dependent parameter Z_0 . M_0 (by assumption) will *not* depend on the color of the trajectory passing through it. This is only natural, because most $\ell = 0$ meson states, from which the orbital excitations originate, contain equal (up to factors 2 or 3) amounts of color three and six or eight and one clusters, depending on the basis one uses. M_0 does depend on the number of strange quarks n_s , and this time as much as five different trajectories (for $n = 36$) may emerge.

- Color magnetic interaction strength -

The effective volume for a colored quark cluster, for some large value of ℓ , will differ from that of the same cluster at $\ell = 0$. First, there is the reduction of the number of quarks and the Dirac-pressure going with it. Secondly, the net color charge of the cluster generates a color electric field, which adds a color dependent pressure. Because the confinement volume of the quarks will not go on growing or shrinking indefinitely, a new stable configuration is expected asymptotically, which is independent of ℓ . We approximate this volume by a sphere of radius R_a . This enables us to give the color magnetic

interaction strength the R-dependence of the $\ell = 0$ bag functions, and incorporate the flavor-breaking parameter-free. Because only one length scale in the stringlike bag is independent of ℓ : R_0 , the size of the cluster volume will be proportional to it. One has (see section II):

$$R_0(c) \sim (f_c^2)^{1/4} \tag{16}$$

and finds

$$R_a(3) : R_a(8) : R_a(6) = 1 : (9/4)^{1/4} : (5/2)^{1/4} = 1 : 1.22 : 1.26$$

The effective volume is larger, when the color charge is, and the quarks consequently are, on the average, farther apart: the color magnetic splitting is smaller. It remains to determine one of the $R_a(c)$. We will take $c = 3$, the weakest charge, which will influence the cluster volume the least.

Interpreting the mass of the intercept $M_0 = (16/3) \pi B R_1^3$ (massless quarks) as the sum of the masses of two clusters, we find $R_a(3) = (1/2)^{1/3} \cdot R_1$. For color singlet N-quark bags one has $R = r_0 N^{1/3}$, a relation, satisfied by R_1 , and consequently by $R_a(3)$. The error we make in taking the radius of a color singlet two quark bag for the cluster, i.e. in neglecting the color electric energy, we compensate to a large extent by continuing to include the volume energy, which for large ℓ has already been accounted for in the trajectory slope. The inflation of the cluster volume with growing color charge in an asymptotic phenomenon, which is not encountered for small ℓ . We assume these relations to be valid for $\ell \geq 3$. For $\ell = 2$ and 1 we take them, for definiteness, to be color independent: $R(\ell) = R(2) = R_1 \cdot (1/2)^{1/3}$ and $R(1) = R_1 \cdot (3/4)^{1/3}$ as transition values. We denote the persistent color magnetic interaction strength, calculated for $R = R_a(c)$ by \tilde{M} . Furthermore, R is taken to be independent of flavor.

Extrapolating eq (10) back to $\ell = 0$, one could have taken the intercepts to be also color dependent, proportional to $R_a^3(c)$. From $M_0(3) = 1.46$ GeV one

deduces: $M_0(8) = 2.68 \text{ GeV}$ and $M_0(6) = 2.90 \text{ GeV}$. This implies, under the assumption that the trajectory is a continuous function of ℓ , that contrary to the $3^* - 3$ one, the $6 - 6^*$ and $8 - 8$ trajectories will be highly bent for small ℓ values. A similar curvature arises for a classical relativistic string with massive ends, there the low ℓ states lie farther away from the linearized trajectory as they are more massive [Jo 79]. The stringlike bag, however, contains the same (almost) massless quarks for all three trajectories, and we expect these therefore to be linear, up to color magnetic splittings, for all ℓ .

- Large ℓ mass formula -

Just as for the $Q-\bar{Q}$ trajectories, we will treat the color magnetic energy

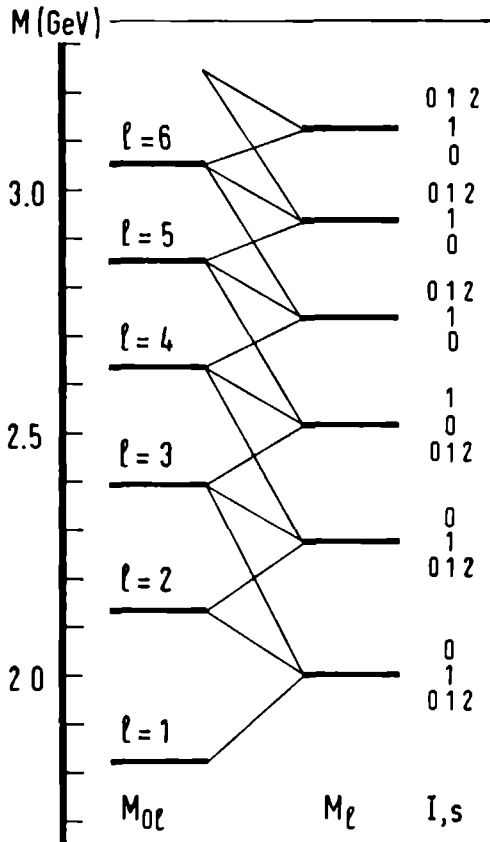


Fig. 4: Stylized mass spectrum for the $3^* - 3$ trajectory states around $\ell = 4$.

contributions as perturbation w.r.t. $M_{0\ell} = \sqrt{M_0^2 + \ell/\alpha'(c)}$. From Table IX it follows that this simply amounts to adding the color magnetic interaction energies for both clusters, evaluated at R_a , to $M_{0\ell}$:

$$M_\ell = M_{0\ell} + \tilde{M}_{MP}^1 \Delta_1 + \tilde{M}_{MP}^2 \Delta_2 \tag{17}$$

This prescription renders the trajectory linear in the M^2 - ℓ plane up to small corrections of order $\sqrt{\ell}$. Studying Table X, we see that eq (17) predicts equal mass splittings ΔM for states, with the same value of n_s , c and ℓ . When moreover, $|M_{0\ell\pm 1} - M_{0\ell}| \simeq \Delta M$ a highly degenerate spectrum results. For the $3^* - 3$ trajectory this happens around $\ell = 4$. Such a situation has, for massless quarks, been plotted in Fig. 4 for our values of $\tilde{M} = 85$, $\alpha'(3) = 0.83 \text{ GeV}^{-2}$ and $M_0(3) = 1.46 \text{ GeV}$. This type of degeneracy also occurs for the sextet and octet trajectories, but at a larger value of ℓ . It is accidental and will happen again, when $2|M_{0\ell\pm 1} - M_{0\ell}| \simeq \Delta M$. It is encouraging to know, that this clustering is also observed experimentally. The numerical values for the intercepts and asymptotic color magnetic strengths have been given in Table XII.

n_s	0	1	2	3	4
$M_0(n_s)$	1.458	1.634	1.802	1.965	2.121
c	3	8	6		
$\tilde{M}(n,n)$	85	69	67		
$\tilde{M}(n,s)$	70	57	56		
$\tilde{M}(s,s)$	58	47	46		

Table XII: Intercepts M_0 (in GeV) of the linearized trajectories as a function of n_s . The color magnetic interaction strength \tilde{M} (in MeV) between nonstrange (n) and/or strange (s) quarks as a function of the color c .

2. Small orbital angular momentum ($0 < \ell < 3$)

For $\ell = 1$ and 2 the quark clusters will not be as widely separated from each other as they presumably are for $\ell \geq 3$ and the particles in the different clusters will be able to interact with one another. We will try and show that this will hardly affect the composition of the clusters. The migration of quarks between the bag ends - by means of tunneling - is argued to be relatively unimportant, although the angular momentum barrier is only moderately high. Consequently the clusters are again the natural basic units for the description of the system. The dominant interaction, in our rather crude approximation, is found to be that between the static multipole moments of the clusters. This situation is very similar to that encountered in the $Q-\bar{Q}$ system with little orbital excitation.

- The $Q-\bar{Q}$ system with small ℓ -

Consider the $\ell = 1$ $Q-\bar{Q}$ states. Next to the color electric monopole interaction the color magnetic dipole one $\sim (\vec{F}_Q) \cdot (\vec{F}_{\bar{Q}})$ appears to be most important. These dipole forces are seen to loose their strength with increasing ℓ or bag length $l = l(\ell)$. One does not expect to have an inverse cube law in the effective cluster separation for the interaction energy, as in the electromagnetic case, because of the confinement of the color fields to the bag. Its strength for $\ell = 1$ (2) was estimated to be 20 (5) % of that for $\ell = 0$ (section II, page 147). There may be also a color electric dipole contribution $\sim F_Q \cdot F_{\bar{Q}}$ because the quark distribution in the rotating bag will not be spherical any longer (cf. Fig. 1). This interaction has the same color dependence as the mutual part of the monopole term and cannot be isolated from it for the $Q\bar{Q}$ mesons. There will be no tunneling in the $Q\bar{Q}$ system. Each quark will stick to its own end of the bag. When these particles would be able to come close together, the color electric field, which supports the dominant

part of the angular momentum $\vec{\ell}$, would disappear, thereby violating an important conservation law. In this situation the quarks can only interact by means of the multipole moments of their color charge distribution, described above.

Consider next the $Q^2\bar{Q}^2$ states with $\ell = 1$. This time there is no conservation law which forbids one of the particles to tunnel from bag end 1 to bag end 2, provided at least one colored particle stays behind in end 1. This phenomenon in principle allows mixing between $Q^2\bar{Q}-\bar{Q}$ or $Q-Q\bar{Q}^2$ and $Q^2-\bar{Q}^2$ or $Q\bar{Q}-Q\bar{Q}$ configurations. We will now demonstrate, that the probability for this to take place is rather small.

- The $Q^2-\bar{Q}$ basis states and tunneling -

The argument rests on what is observed in an $\ell = 1$ (or 2) $Q^2-\bar{Q}$ baryon system. To avoid inessential complications we will take the Δ -like configuration as example. We denote the situation, that quarks 1 and 2 reside in bag end 1, and that quark 3 sits in bag end 2, by $|\phi\rangle = |Q, Q' - Q''\rangle = |1, 2-3\rangle$. When particle 2 tunnels to the other end, this situation is changed to $|\phi'\rangle = |1-2, 3\rangle$. The final state again is a $Q^2-\bar{Q}$ baryon with $\ell = 1$ (or 2). The nonzero energy associated with this process is given by the matrix element of the tunneling hamiltonian H_T between these states, denoted by $m_{\phi, \phi} = \langle \phi' | H_T | \phi \rangle$. This operator conserves the overall quantum numbers of the system. It has $J = I = Y = 0$ and $c = 1$. It annihilates a quark in one bag end and recreates it in the other end of the same bag. Because the initial baryon is transformed to a similar one, H_T can be expressed in terms of symmetry operators of the baryon system: in this case the permutation operator of quark 1 and 3 (P_{13}) and the space inversion operator P . We find: $H_T = m(\ell) \cdot P_{13} \cdot P$, and

$$m_{\phi, \phi} = \langle \phi' | H_T | \phi \rangle = \langle 1-2, 3 | m(\ell) \cdot P_{13} \cdot P | 1, 2-3 \rangle = m(\ell) \quad . \quad (18)$$

For Q^3 baryon systems, the color wave function is unique [Mu 79]. This implies that the permutation symmetries of the space and flavor spin parts of the wavefunction are complementary. The tunneling hamiltonian primarily affects the spatial configuration of the system. In as much as it has a different effect on systems with different space or equivalently flavor spin properties, its contribution to the hamiltonian can be expressed in terms of flavor spin projection operators. One has:

$$H_T = (-)^{\ell+1} m(\ell) \cdot (2 P_{56} - P_{70}) \quad . \quad (19)$$

P_N is the projection operator on the N-dimensional flavor spin irrep. In the quark-diquark (cluster) basis this operator has off diagonal matrix elements. A fit to the baryon mass spectrum yields $m(1) = 100$ MeV, $m(2) = 45$ MeV. The effect of tunneling is not large enough to ensure a pure permutation symmetry for the flavor spin part of the wavefunctions. One finds, where possible, mixtures of both the 56 and 70 dimensional flavor spin irreps. Compared to $\ell = 1$, most $\ell = 2$ states are appreciably purer in the asymptotic cluster basis, which then provides the more economic description.

- The $Q^2 \bar{Q}^2$ basis states and tunneling -

When we apply the simple baryonic tunneling model to the $Q^2 \bar{Q}^2$ excitations, we find that some of the consequences are different. This is caused by the fact, that we now have an even number of - partly distinguishable - fermions: two quarks and two antiquarks. Take as a starting point an $\ell = 1$ three-baryonium state. The quarks (labels 1,2) sit in bag end 1, the antiquarks ($\bar{3}, \bar{4}$) in bag end 2, a situation denoted by $|\phi\rangle = |Q, Q' - \bar{Q}, \bar{Q}'\rangle = |1, 2-\bar{3}, \bar{4}\rangle$. When antiquark $\bar{3}$ tunnels through the angular momentum barrier, the $Q^2 - \bar{Q}^2$ configuration goes over in a $Q^2 \bar{Q} - \bar{Q}$ one. Since this is an altogether different system, there

exist no symmetric operators, which can convert this $Q^2\bar{Q}-\bar{Q}$ final state back to a $Q^2-\bar{Q}^2$ initial one. The tunneling hamiltonian H_T then can not be expressed in terms of symmetry operators either.

Since the color and angular momentum conditions have not changed w.r.t. the baryon example, the tunneling hamiltonian is expected to have about the same strength in both cases. The action of H_T on the three-baryonium initial state is approximated by: $H_T|1,2-\bar{3},\bar{4}\rangle = m(\ell)|\phi'\rangle$, where $|\phi'\rangle = |1,2,\bar{3}-\bar{4}\rangle$ denotes the three-baryonium state in which particles 1, 2 and $\bar{4}$ have the same wavefunctions as they had in the state $|\phi\rangle$, and $\bar{3}$ has a three-baryonium antiquark wavefunction, but now also concentrated in bag end 1. The dissimilarity of the transformed baryonium state $|1,2,\bar{3}-\bar{4}\rangle$ and the physical mesonium final state $|\chi\rangle$ manifests itself in a reduced overlap: $\langle\chi|\phi'\rangle < 1$. One finds

$$m'_{\chi\phi} = \langle\chi|H_T|\phi\rangle = m(\ell) \langle\chi|\phi'\rangle < m(\ell) \quad . \quad (20)$$

This reduction of the matrix element, due to the space part, may even be quite severe. The centre of mass in the baryonium state lies approximately in between the two bag ends. For $\ell = 1$ the quark energy dominates the field energy and the centre of mass of a three-mesonium state lies much closer to the $Q^2\bar{Q}$ end than to the \bar{Q} one. This type of state has a rather asymmetric space distribution, quite different from the symmetric baryonium one. Moreover, the initial and final state very often have different energies, and the transition may only be possible thanks to the wideness of the mesonium final state.

Although all three-baryonium color spin and flavor configurations are present in the three-mesonium spectrum, also here further suppression of tunneling activities may arise. In a $Q^2\bar{Q}$ cluster the diquark wavefunction for a given flavor state often is a mixture of $c = 3^*$ and 6 configurations, which distributes the transition probability over two non degenerate final states (cf.

Table Xa and XIc). This effect is to some extent of course already accounted for in the space part of the matrix element. Clearly, tunneling transitions from three-mesonium to baryonium states are even more suppressed. For about half these states it is even completely forbidden.

Comparing with the baryon results we expect $m'(\ell) = \langle \chi | H_T | \phi \rangle$ to be of the order of 10 MeV for $\ell = 1$ and negligible for $\ell = 2$, where the angular momentum barrier is higher. For the three-baryonium states, the clusters therefore may yield an even more surveyable picture than for the baryons. Already for $\ell = 1$ the quarks will submerge in the, from the point of view of tunneling rather stable, clusters, which will be the active, subhadronic constituents.

The generalization to 6-baryonia and 8-mesonium, for which tunneling also involves a color flip, does not add any qualitative changes. Since these states are usually heavier (especially for $\ell = 2$) the arguments are expected to hold even better. For many $Q\bar{Q}-Q\bar{Q}$ states transition to a $Q^2\bar{Q}-\bar{Q}$ or conjugate configuration is even completely forbidden. Mixing between 3 and 6-baryonium or baryonium and 8-mesonium states via tunneling involves this process at two stages and thus can be neglected. This kind of mixing will be even more suppressed, because the 3-mesonium intermediate states are highly unstable and a multi-meson decay is much more probable than a tunneling transition. Since the communication with 3-mesonium states will connect any other $Q^2\bar{Q}^2$ state to the multi-meson decay channels, establishment of the branching ratios of such states into these decay modes will provide more quantitative information (upper limits) about the importance of tunneling. The fact that for some state these modes are not observed (yet) is interpreted as support for the above described picture.

- The residual interaction -

The clusters, being quite cleanly separated, will interact via their static color multipole moments. The residual colormagnetic interaction in the 3-baryonia is quite similar to that of the mesons. The main difference is, that for $\ell = 1$ the quark contribution to the mass is twice as large, implying that the clusters will be closer together. We will simulate this effect by taking the strength of the residual part to be 20 (5) % of the $\ell = 1$ (2), i.e. enhanced (see section III 1, page 157), persistent part. These numbers were only crude estimates, and the changes brought about by this prescription still are within the estimated uncertainties. For this reason we will apply the same value also for the sextet and octet strengths, since these clusters have a separation, which is in between that of the $Q\bar{Q}$ and 3-baryonium ones.

For $\ell = 1$ and 2 the residual part will be included in the mass at the same point as the persistent one. Its inclusion will, because it contains operators, which are not diagonal in the asymptotic basis states, mix states on different color trajectories. For example, in the $J = 0$ baryonium sector, color spin flip transitions between $(C,S) = (3^*,0)$ and $(6,1)$ clusters are allowed and mixing analogous to, only much less strong than, that in the same sector for $\ell = 0$, occurs. Because the color triplet and sextet states lie on different trajectories and have a reduced strength, the total effect is at the percent level.

More important is the mixing among the color octet and singlet states, for the $Q\bar{Q}-Q\bar{Q}$ trajectory. This color spin flip interaction couples the rather stable octet configuration to highly unstable dimeson molecule states and permits the first to decay into the two meson channels.

The interaction of the color electric dipoles on the orbitally excited $Q^2\bar{Q}^2$ states is only noticeable for the 8-mesonia. It causes color flip

transitions, which again enlarge the color singlet component, adding to the instability of these states. In favorable cases, an $\ell = 1$ strength of 40 MeV will induce an increase of the color singlet content of 10 %. This number decreases for heavier systems, for $\ell = 2$ it is only 2 %. We have no example from which we can obtain a scale for the strength of this interaction. Compared to the color magnetic interaction 40 MeV is to be considered a large value.

To conclude this prescription to calculate the $Q^2\bar{Q}^2$ masses, we note that in this cluster approximation the $\ell = 1$ and 2 color octet masses are calculated without any Fermi-Dirac statistics restrictions on the quark wavefunctions. This tends to enlarge the splitting somewhat. Another consequence is that now no longer the mutual interaction of a $Q\bar{Q}$ pair in one bag end equals that of a quark and antiquark located in different bag ends ($A(Q\bar{Q}) \neq A(Q\bar{Q}')!$).

The present approach is not sophisticated enough to comprise spin orbit and tensor type interactions, which can not be treated separately [MaR 78]. Although the corresponding mass contributions will not be large (a few tens of MeV) the combination of the two is sufficiently powerful to destroy simple level ordering schemes, e.g. larger spin has not always a higher mass. We will present these levels therefore as degenerate.

This mass description leads to a spectrum of which the $Y = 0$ members are listed in Table XIII for $c = 3$ (a), $c = 8$ (b) and $c = 6$ (c). We have included only the $\ell = 1$ and 2 multiplets. A calculational uncertainty of at least 50 MeV should be kept in mind. Higher multiplet masses can easily be calculated using Tables X and XII.

	Mass (GeV)	n_s	I	s	J, C_n
$\ell^P = 1^-$	1.50	0	0	0	1-
	1.72	0	1	1	$0\pm, 1\pm, 2\pm$
	1.83	2	0,1	0	1-
	1.86	0	0,1,2	0	1-
	1.90	0	0,1,2	1	$0+, 1+, 2+$
	1.94	0	0,1,2	2	$1-, 2-, 3-$
	2.02	2	0,1	1	$0\pm, 1\pm, 2\pm$
	2.14	2	0,1	0	1-
	2.17	2	0,1	1	$0+, 1+, 2+$
	2.21	2	0,1	2	$1-, 2-, 3-$
	2.42	4	0	0	1-
	2.44	4	0	1	$0+, 1+, 2+$
	2.47	4	0	2	$1-, 2-, 3-$
	$\ell^P = 2^+$	1.76	0	0	0
2.01		0	1	1	$1\pm, 2\pm, 3\pm$
2.07		2	0,1	0	2+
2.23		0	0,1,2	0	2+
2.23		0	0,1,2	1	$1-, 2-, 3-$
2.24		0	0,1,2	2	$0+, 1+, 2+, 3+, 4+$
2.28		2	0,1	1	$1\pm, 2\pm, 3\pm$
2.46		2	0,1	0	2+
2.47		2	0,1	1	$1-, 2-, 3-$
2.48		2	0,1	2	$0+, 1+, 2+, 3+, 4+$
2.70		4	0	0	2+
2.70		4	0	1	$1-, 2-, 3-$
2.71		4	0	2	$0+, 1+, 2+, 3+, 4+$

Table XIIIa: Masses, quantum numbers (I, ℓ, S, J, P, C_n) and strange quark content

(n_s) of the $Y = 0$ color 3-baryonia. One has $G = C_n (-)^I$.

	Mass (GeV)	n_s	I	s	J, C_n
$\ell^P = 1^-$	1.94	0	1	0	1^\pm
	1.96	0	0,0,1,2	1	$0^+, 1^+, 2^+$
	1.98	0	1	1	$0^\pm, 1^\pm, 2^\pm$
	1.99	0	1	2	$1^\pm, 2^\pm, 3^\pm$
	2.00	0	0,0,1,2	1	$0^+, 1^+, 2^+$
	2.01	0	1	0	1^\pm
	2.16	2	0,1	0	1^\pm
	2.18	2	0,0,1,1	1	$0^+, 1^+, 2^+$
	2.24	2	0,0,1,1	1	$0^+, 1^+, 2^+$
	2.25	2	0,1	2	$1^\pm, 2^\pm, 3^\pm$
	2.27	2	0,1	1	$0^\pm, 1^\pm, 2^\pm$
	2.29	2	0,1	0	1^\pm
	2.45	4	0	1	$0^+, 1^+, 2^+$
	2.55	4	0	1	$0^+, 1^+, 2^+$
$\ell^P = 2^+$	2.38	0	0,0,1,2	0	2^+
	2.38	0	1	1	$1^\pm, 2^\pm, 3^\pm$
	2.39	0	0,0,1,2	2	$0^+, 1^+, 2^+, 3^+, 4^+$
	2.40	0	0,0,1,2	1	$1^-, 2^-, 3^-$
	2.40	0	1	1	$1^\pm, 2^\pm, 3^\pm$
	2.42	0	0,0,1,2	0	2^+
	2.58	2	0,0,1,1	0	2^+
	2.58	2	0,1	1	$1^\pm, 2^\pm, 3^\pm$
	2.60	2	0,0,1,1	2	$0^+, 1^+, 2^+, 3^+, 4^+$
	2.61	2	0,1	1	$1^\pm, 2^\pm, 3^\pm$
	2.64	2	0,0,1,1	1	$1^-, 2^-, 3^-$
	2.66	2	0,0,1,1	0	2^+
	2.80	4	0	0	2^+
	2.83	4	0	2	$0^+, 1^+, 2^+, 3^+, 4^+$
	2.87	4	0	1	$1^-, 2^-, 3^-$
	2.91	4	0	0	2^+

Table XIIIb: Same as Table XIIIa for color 8-mesonia.

	Mass (GeV)	n_S	I	s	J, C_n
$\ell^P = 1^-$	1.87	0	0	0	1-
	1.91	0	0	1	0+, 1+, 2+
	2.01	0	0	2	1-, 2-, 3-
	2.06	0	1	1	0±, 1±, 2±
	2.15	2	0, 1	0	1-
	2.17	0	0, 1, 2	0	1-
	2.18	2	0, 1	1	0+, 1+, 2+
	2.27	2	0, 1	2	1-, 2-, 3-
	2.31	2	0, 1	1	0±, 1±, 2±
	2.40	2	0, 1	0	1-
	2.64	4	0	0	1-
$\ell^P = 2^+$	2.35	0	0	0	2+
	2.36	0	0	1	1-, 2-, 3-
	2.39	0	0	2	0+, 1+, 2+, 3+, 4+
	2.49	0	1	1	1±, 2±, 3±
	2.58	2	0, 1	0	2+
	2.59	2	0, 1	1	1-, 2-, 3-
	2.60	0	0, 1, 2	0	2+
	2.62	2	0, 1	2	0+, 1+, 2+, 3+, 4+
	2.70	2	0, 1	1	1±, 2±, 3±
	2.79	2	0, 1	0	2+
	3.00	4	0	0	2+

Table XIIIc: Same as Table XIIIa, for color 6-baryonia.

Section IV: Results and discussion

Several general comments can be made at once. With exception of one isoscalar $J^{PC} = 2^{++}$ state at 1.76 GeV, all states below 2.0 GeV are expected to be $\ell^P = 1^-$ states. Below 2.2 GeV the highest spin value is $J = 3$. This means that in this region (see e.g. Table VIII) nonstrange mesons with a higher spin value are likely to be orbital $Q\bar{Q}$ excitations. The first $J = 5$ (6) system is expected around 2.5 (2.75) GeV. The heaviest $J = 1$ ($J^{PC} = 1^{--}$) state has a mass of 2.93 GeV, still below the charmonium region. The heaviest $J = 2$ ($J^{PC} = 2^{++}$) state lies at 3.25 GeV. The lowest exotic states lie at 1.72 GeV. They have $J^{PC} = 0^{--}$ and 1^{-+} . Another type of exotic state occurs at 1.86 GeV. It has $I = 2$.

- Formation -

The $Q^2\bar{Q}^2$ meson states, on the basis of diagrams as depicted in Fig. 3, are expected to occur as resonances in elastic $B\bar{B}$ scattering [Ro 68, Ro 74]. They consequently are looked for in antinucleon formation experiments [Ei 76]. This method is quite suitable for the detection of high mass ($> 2 M_N$), narrow meson states. A disadvantage is that the resolution of broad states is quite cumbersome. Moreover, the experiments, using on-shell nucleon (i.e. hydrogen) targets, are difficult for very low beam momenta. Improvement is attained by using "off-shell" targets (i.e. nucleons, bound in e.g. deuterium). Only non exotic I, J^{PC} states can be excited directly this way. Information on the quantum numbers of such states can be obtained by looking at final states like $\pi^+ \pi^-$, $\pi^0 \pi^0$, $\pi^0 \eta$ or $K^+ K^-$ which, although their branching ratios ($\ll 1$ % of the total cross section to be compared with 7 to 8 % for the elastic T and U bumps) are small, have a very simple amplitude structure. Also mesons with mass $M < 2 M_N$ can be studied through $N\bar{N}$ annihilation processes and show up in the multimeson invariant mass plots (e.g. D(1281) and $F_1(1540)$).

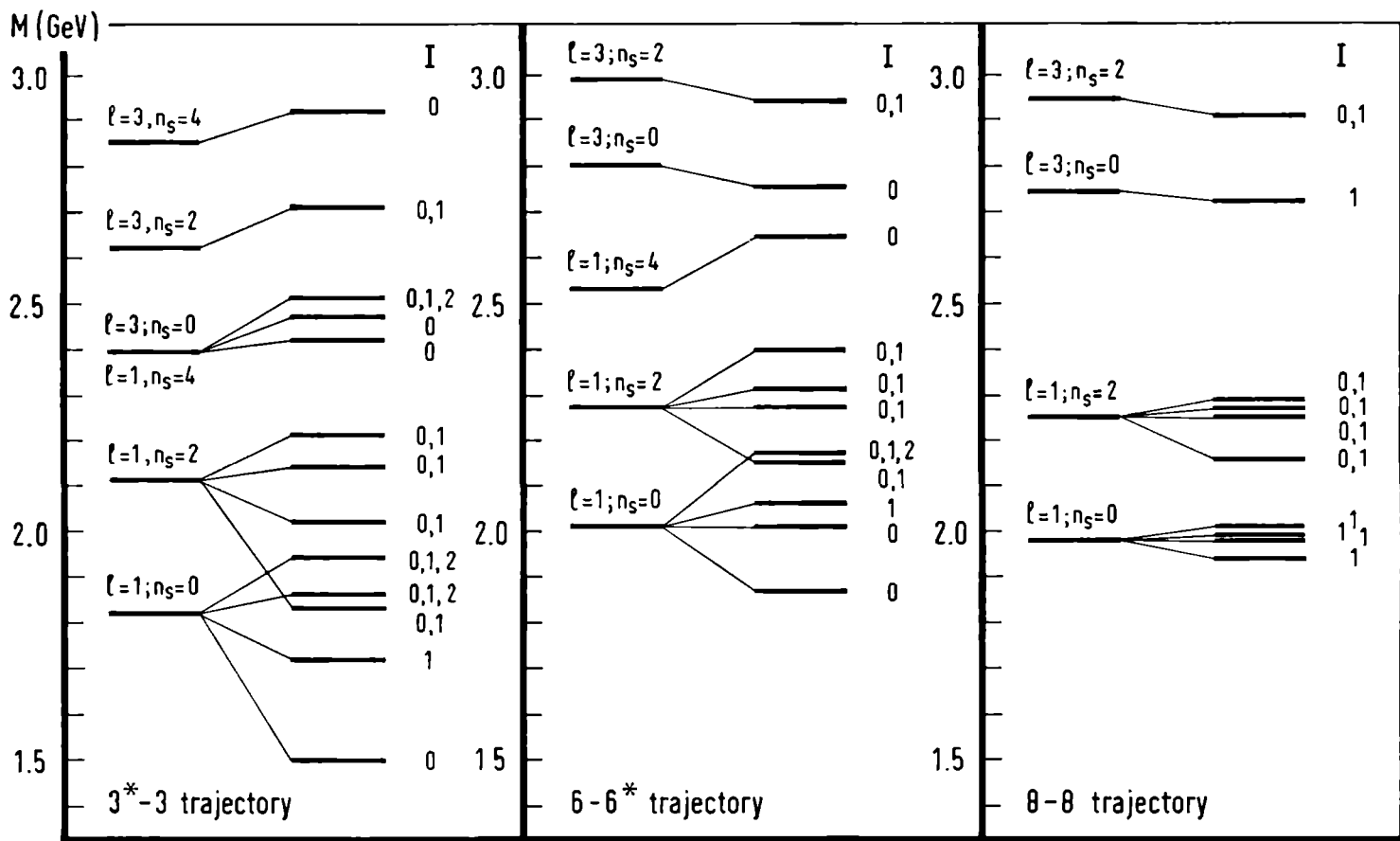


Fig. 5: Leading trajectory states with photonlike quantum numbers: $J^{PC} = 1^{--}$ and $Y = 0$, as a function of the orbital angular momentum l and the number of strange quarks n_s .

An important variant of this method for on-shell meson formation is electron positron annihilation. This electromagnetic process allows exclusively $J^{PC} = 1^{--}$ states. Present searches scan the region between 1 and 3 GeV in which also the photon-like $Q^2 Q^2$ states are supposed to lie. We have plotted these photon-like states separately in Fig. 5.

- Production -

A distinct kind of experimental method is to produce heavy mesons "off-shell" by letting a boson or lepton beam fall on a nucleon target. One has a variety of options for the final state. One can trigger on a $B\bar{B}$ pair, coming out in the forward direction e.g.: $\pi^- p \rightarrow (p\bar{p})_F n$. Drawing the Harari-Rosner diagram for this process one finds it is already possible via meson exchange. Resonances may be extracted by making a partial wave analysis of the process $\pi^- \pi^+ \rightarrow p\bar{p}$. Just as in the antiproton formation process broad resonances emerge (Table XIVa). One can select a baryon exchange production mechanism by triggering on a single forward proton: $\pi^- p \rightarrow p_F + X$ (Fig. 6) and analyse the invariant mass plot of the final states containing $B\bar{B}$ pairs e.g. $X = (p\bar{p}\pi^-)$. This way narrow resonances have been detected (Table XIVb). Also

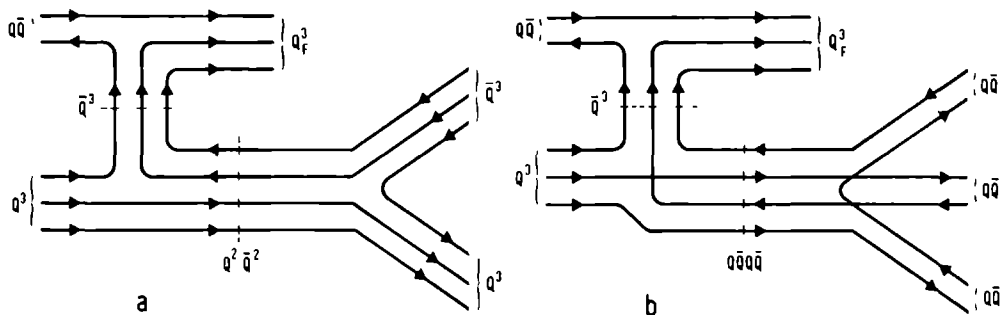


Fig. 6 Harari-Rosner diagrams for the production of a 3-baryonium (a) or 8-mesonium (b) state. The production of a 6-baryonium state proceeds as in diagram (a), only this time a multimeson final state is more probable.

Mass (GeV)	Width (MeV)	Source	Quantum numbers
1.92	190	Ev 78; $\pi^- \bar{p} \rightarrow (\pi \bar{p})_F n$, PWA	$J^{PC} = 1^{--}, I^G = 1^+$
1.94	55	De 76; $\bar{p} \bar{p} \rightarrow \rho^0 \omega^0, \bar{p} \bar{p}, \bar{n} \bar{n}$ Mon 78; $\bar{p} n \rightarrow \pi^- \pi^- \pi^+$	$I^G = 1^-, J = 1$ or 2 $J^P = 2^+, I^G = 1^-$
1.95	240	Ev 78; $\pi^- \bar{p} \rightarrow (\pi \bar{p})_F n$, PWA	$J^{PC} = 1^{--}, I^G = 1^+$
2.01	100	De 76; $\bar{p} \bar{p} \rightarrow 5\pi, \bar{n} \bar{n}$ De 76; $\bar{p} \bar{p} \rightarrow K^0 K^+ \pi^-$	$J \leq 2, G = -$
2.02	160	Ev 78; $\pi^- \bar{p} \rightarrow (\pi \bar{p})_F n$, PWA	$J^{PC} = 2^{++}, I^G = 0^+$
2.15	200	Car 77, DeM 76; $\bar{p} \bar{p} \rightarrow \pi^+ \pi^-, K^+ K^-$	$J^{PC} I^G = 3^{--}, 0^-$ & 1^+
2.185	130	Ab 70, Co 77; σ_T, σ_{EL} in $\bar{p} \bar{p}$	$I = 1$
2.31	210	Car 76, 77, DeM 76; $\bar{p} \bar{p} \rightarrow \pi^+ \pi^-,$ $\pi^0 \pi^0, K^+ K^-$	$J^{PC} I^G = 4^{++}, 0^+$
2.350	190	Ab 70, Co 77; σ_T, σ_{EL} in $\bar{p} \bar{p}$	$I = 1$
2.385	80	Ab 70, Co 77; σ_T, σ_{EL} in $\bar{p} \bar{p}$	$I = 0$
2.48	280	Car 77, DeM 76; $\bar{p} \bar{p} \rightarrow \pi^+ \pi^-, K^+ K^-$	$J^{PC} I^G = 5^{--}, 0^-$ & 1^+

Table XIV: Possible candidates for baryonium and mesonium states (a) broad states. The two entries between parentheses are an alternative to the $M = 1.95$ -entry.

in photo- and electro (or virtual photo-) production experiments, viz. $\gamma p \rightarrow p + X$ and $e p \rightarrow e p + X$ respectively, this method of analysis may be applied. These kinds of experiments, in the energy region of interest, have begun only recently and from this source only preliminary results are available [Oz 78, Ri 78]. One can also trigger on more complicated forward systems. A reaction like $K^+ p \rightarrow (\bar{\Lambda} p \pi^+)_F n$, which requires the exchange of an exotic $Q^2 Q^2$ meson, has uncovered a narrow exotic forward final state.

Mass (GeV)	Width (MeV)	Source	Quantum numbers
1.395	≤ 34	Pa 78; γ from atomic $\bar{p}p$	
1.470	10	Bem 77; e^+e^- , $\bar{p}p$ annihilation	$J^{PC} = 1^{--}$
1.646	≤ 21	Pa 78; γ from atomic $\bar{p}p$	
1.684	≤ 19	Pa 78; γ from atomic $\bar{p}p$	
1.795	< 8	Gr 71; $\bar{p}d$ annihilation at rest	
1.820	~ 25	Bem 77; e^+e^- , pp annihilation	$J^{PC} = 1^{--}$
1.875	< 10	Gr 73; $\bar{p}d$ annihilation at rest	$I^G = 1^+$
1.897	25	Ka 76; $\bar{p}d$ annihilation at rest	Complex, $I = 1$
1.936	3	Ca 74, Ch 76, Br 77; $\sigma_T, \sigma_A, \sigma_{EL}$ in $\bar{p}p$ Cu 78, Sa 78; σ_{CE} in $\bar{p}p$	$I = 0 ?$
1.954	≤ 10	Wp 78; $\pi^+p \rightarrow \pi^+p$ ($\bar{p}p$) _F	
1.975	< 2	Su 76, Ca 75; $\bar{n}p \rightarrow N$ pions, dip in σ_A	$I^G = 1^-$
1.986	~ 8	Su 76; $\bar{n}p \rightarrow (K\bar{K}\pi) \pi$	$I = 1$
2.020	24 ± 12	Be 77; $\pi^-p \rightarrow p_F(\bar{p}p\pi^-)$ Oz 78; $ep \rightarrow ep$ ($p\bar{p}$)	$I = 0 ?$
2.130	30	Bem 77; e^+e^- annihilation	$J^{PC} = 1^{--}$
2.204	$16 \begin{smallmatrix} + 20 \\ - 12 \end{smallmatrix}$	Be 77; $\pi^+p \rightarrow p_F \bar{p}p\pi^+$	$I = 0 ?$
2.207		Gr 78; $\bar{p}p \rightarrow \pi_F^+ (\pi^- K^+ K^-)$	$I = 1$
2.461	< 10	Ar 78; $K^+p \rightarrow (\bar{\Lambda}p\pi^+)_F n$	$S = +1, Q = 2$
2.85	< 40	Br 76; $\bar{p}n \rightarrow \pi^- X^0$	$I = 0 ?$
3.43	< 45	Ba 76; $\pi^-p \rightarrow (\Lambda\bar{\Lambda})_F n$	

Table XIV: Possible candidates for baryonium and mesonium states (b) narrow states.

It is from these sources that the evidence for l -excited $Q^2\bar{Q}^2$ states may be drawn. We will mainly restrict our considerations to the strong interaction aspects. Some of the more pronounced signals in the above cited processes have been listed in Table XIV. This table is not complete. Many more candidates have been proposed. Of some of these the existence has been contested by later experiments. Other still await confirmation or rejection. The available data also suggest many additional structures, corresponding to effects which have not yet been properly investigated. Especially in the $J^{PC} = 1^{--}$ sector many states below 2 GeV have been reported. Some of these are wide, having multipion decay modes, while others are rather narrow (e.g. $M = 1.47, 1.82$ and 2.13 GeV) and have been seen to decay into kaons, which may favor an interpretation as radial recurrences of the ρ and ω , and ϕ respectively. Table XIVb contains a doubly charged, strange meson with a mass of 2.461 GeV which may be the first unambiguously exotic state observed. Its establishment will be the strongest evidence in favor of hadrons containing more than two or three quarks.

1. Broad states

Table XIVA contains several states whose quantum numbers have been determined completely by making use of their $\pi\pi$ and $K\bar{K}$ decay modes [Car 77]. It was found, that these resonances couple dominantly to the $N\bar{N} J = L - 1$ amplitude and rather accurately satisfy the peripherality relation $L = kR$ [Da 64], with L the angular momentum, k the center of mass momentum and $R = (m_\pi)^{-1} = 1.4$ fm the range of the forces in the $N\bar{N}$ channel. Also the $J^P = 1^-$ state at 1.95 GeV from the Ev 78 partial wave analysis of the process $\pi^-\pi^+ \rightarrow p\bar{p}$ lies rather close to this curve. When this state turns out to prefer the $J = L - 1$ wave too, one is inclined to expect another one - with $J^P = 2^+$ - near 2.05 GeV. The Ev 78 analysis requires considerable model

dependent input. It also allows a (better) fit for resonances at $M = 1.92$ and 2.02 GeV with $J^P = 1^-$ and 2^+ respectively. A $J^P = 2^+ Q^2 \bar{Q}^2$ state is expected at $M = 2.01$ GeV, but it has $I = 1$ and couples to $K\bar{K}$, not to $\pi\pi$. The $I = 0$ $\pi\pi$ state then probably has a $Q\bar{Q}$ origin. No $0^+ Q^2 \bar{Q}^2$ (or leading $Q\bar{Q}$) resonance near 1.90 GeV is expected in the 3P_0 $N\bar{N}$ wave.

One observes, that the broad resonances, discovered otherwise also tend to lie near the peripherality curve $L = kR$. This suggests that one can get a first indication of the relative prominence of the orbital $Q^2 \bar{Q}^2$ excitations by comparing the proximity of the masses in Table XIII of states with the correct $N\bar{N}$ quantum numbers to those, on the peripherality curve. Because the range R of the $N\bar{N}$ interaction is rather long ($m_\pi < M_N$), one finds that for $J \leq 10$ the peripheral $N\bar{N}$ states are light in comparison with $Q^2 \bar{Q}^2$ states with the same spin. This implies, that only those $Q^2 \bar{Q}^2$ states will be close to it that are comparatively light or, when heavy, align a high quark spin with ℓ to obtain the highest possible J .

One finds, that for $J \geq 3$ and $M \geq 2.25$ GeV (or $\ell > 1$) the 6-baryonium and 8-mesonium states as well as all states with $n_s \geq 2$ are too heavy and decouple, and that one can identify the following prominent 3-baryonium trajectories in the $N\bar{N}$ channels:

1. $N\bar{N}$ triplet, $J = L - 1$: the $s = I = 0$, $J = \ell$ trajectory lies practically on top of the curve $L = kR$. The $s = I = 1$, $J = \ell$ trajectory is close to it. The $s = 1$, $I = 0$ and 1 , $J = \ell - 2$ trajectory virtually decouples.
2. $N\bar{N}$ triplet, $J = L$: only the $s = I = 1$, $J = \ell + 1$ trajectory lies pretty close.
3. $N\bar{N}$ triplet, $J = L + 1$: here the $s = I = 0$, $J = \ell$ and the $s = 2$, $I = 0$ and 1 , $J = \ell + 2$ states are the most peripheral ones. They are almost degenerate.

4. $\bar{N}N$ singlet, $J = L$: this channel will be dominated by the $s = I = 1$,
 $J = \ell + 1$ trajectory.

We find that the $\bar{N}N$ channel with the most peripheral states has $J = L - 1$ and will show both through an $I = 0$ and an $I = 1$ trajectory. In our model this isospin doublet is not degenerate, the $I = 0$ states being lighter and more prominent. The splitting between the $I = 0$ and 1 states will be a measure for the color magnetic splitting which is predicted to be about 200 MeV for $\ell \geq 3$. Because the $J = 3, 4$ and 5 states on the peripherality curve, when considered by themselves, appear to lie on a trajectory with a steeper (in the $J-M^2$ plane) slope, they can not belong to a single $Q^2\bar{Q}^2$ trajectory like e.g. that with $I = 0$ and 1, $J = \ell$ and $s = 0$ or 2 [CH 77]. One would like to see a better resolution of the $I = 0$ and 1 components (if present) of the reported states. The $J = L + 1$ channel is dominated by an $I = 0$ and an $I = 0$ and 1 trajectory. The $J = L$ channels favor $I = 1 = s$.

When the intercept of the trajectories is shifted by 50 MeV, these observations will still be valid. Only when it is taken to lie more than 100 MeV lower, the $I = 0$ states in the $\bar{N}N$ triplet $J = L - 1$ and the $I = 1$ states in the $\bar{N}N$ singlet channel may become too light to be peripheral. The at present lower lying trajectories: the $I = 1 = s$ and $I = 0$ and 1, $J = \ell$, $s = 0$ and 2, and $I = 0$ and 1, $J = \ell + 1$ and $s = 1$, respectively will become more important.

For states with $J \leq 3$ and $1.88 \leq M \leq 2.25$ GeV the situation is slightly different. Only one state around 2.05 GeV exists with $n_s = 0$ and $J^{PC} = 2^{++}$. It is a 3-baryonium state with $I = 1$. Another 2^{++} state nearby has $n_s = 2$ and $I = 0$ and 1. Because of the strange quark content this state is not expected to be very broad. Candidates for the peripheral state near 1.95 GeV should be recruited from the $\ell^P = 1^-$ multiplets. Here $n_s = 0$ 3-baryonium and

8-mesonium states are available. As we shall argue below we do not expect the mesonium state to have a strong coupling to the D-wave $B\bar{B}$ system. From the 3-baryonium configurations (at 1.94 GeV) both $I = 0$ and 1 are expected. The mixing of this $N\bar{N} \ ^3D_1$ with the $\ ^3S_1$ wave may explain its large width so close to the $N\bar{N}$ threshold. Since we have no reason to think, that the $\ell = 1$ and 2 masses are more accurate than those for $\ell \geq 3$, also in this mass region uncertainties of 50 MeV should be reckoned with.

None of the states with $J \geq 3$ is close to the $\pi\pi$ -peripherality curve $J = L = kR_\pi$, $R_\pi \leq 0.5$ fm, which favors heavy low spin state production. Only $J = 2$, around 2.0 GeV, and possibly $J = 1$ states, around 1.9 GeV, in the $N\bar{N}$ $J = L \pm 1$ channels may be more pronounced and consequently easier detectable in the $\pi^+ \pi^- \rightarrow p\bar{p}$ type processes.

One could also attempt a classification of the states in Table XIVA in terms of orbital $Q\bar{Q}$ excitations. Comparing the masses for states with the same quantum numbers one finds that the observed value lies each time in between the $L = J - 1$ and the $L = J + 1$ candidate, about 200 MeV away from both (see Table VIII). Furthermore $Q\bar{Q}$ resonances can by means of $Q\bar{Q}$ pair creation easily decay into two (or more) meson final states, whereas decay into $B\bar{B}$ requires an additional $Q\bar{Q}$ pair and is expected to be more suppressed, and certainly not as dominant as observed for $J \geq 3$. We think the comparison here unfavorable for the $Q\bar{Q}$ excitations. However, just above the $N\bar{N}$ threshold, they (i.e. members of the $\ell = 3$ multiplet: $J^{PC} = 2^{++}, 3^{++}, 4^{++}, 3^{+-}$) may certainly manifest themselves. In this region indications exist for broad positive parity states with sizable, if not dominant multimeson decay modes $M = 1.94$ and, somewhat higher $M = 2.02$ GeV.

- Narrow states: $M = 2.020$ and 2.204 GeV -

A surprising feature of the states which have been found to couple to $N\bar{N}$ initial or final states is that next to the broad (peripheral) states also - sometimes very - narrow ones are found (collected in Table XIVb), not only below the $N\bar{N}$ threshold, but also quite far above it. A striking example is formed by the states at $M = 2.020$ and 2.204 GeV. They were first detected [Be 77] in the process $\pi^+ p \rightarrow B_F^{++} M^0$, where the forward baryon B_F is a $\Delta^{++}(1232)$, decaying into $p\pi^+$, and $M^0 \rightarrow p\bar{p}$ (cf. Fig. 6a). The assumption of a simple isospin structure yields a large branching ratio for M^0 into $N\bar{N}$, but no significant $\pi\pi$ or $K\bar{K}$ decay rates have been found. One has searched for, but not (yet) found, charged partners (M^-). The 2.02 GeV state has also been produced by a virtual photon: $\gamma_{\nu} p \rightarrow p(\bar{p}p)$ [Oz 78], but has not been seen in formation experiments. At a mass of 2.207 GeV a narrow state has been observed [Gr 78] in the process $p\bar{p} \rightarrow \pi_F^+ (K^+ K^- \pi^-)$, suggesting an isovector character.

When the signals at 2.207 and 2.204 GeV are due to a single state, one may assume that, because of the large $p\bar{p}$ branching ratio, the two narrow states - interpreted as $Q^2\bar{Q}^2$ states - both have a nonstrange quark content. The $K\bar{K}$ pair then results from a decay via an $s\bar{s}$ pair creation and requires, since the creation of an $n\bar{n}$ pair usually is a little easier, the presence of a $\pi^+\pi^-\pi^-$ decay mode. When the states at 2.207 and 2.204 GeV are different, one of them probably has $n_s = 0$ and is not seen in formation experiments, whereas the other state may have $n_s = 2$. In any case, since no J^{PC} assignment is known, the number of theoretical candidates exceeds the number of experimental ones by far (see Table XIIIa, b and c). We note that the model predicts the state near 2.2 GeV to have a composite isospin structure, whereas the peak at 2.02 GeV may also be due to a single isospin level. We will use the above described data in conjunction with a model for

the formation and decay in an attempt to reduce the number of candidates.

2. The QPC or 3P_0 model

A particularly simple model which may be extended to describe the coupling of $Q^2\bar{Q}^2$ states to the $B\bar{B}$ system, has been proposed ten years ago by Micu [Mu 69] to account for the decay rates of meson resonances to two meson final states. It is called the Q(uark) P(air) C(reation) or 3P_0 model. One imagines a process of the type $Q \xrightarrow{*} \bar{Q} \rightarrow Q(\bar{Q}Q)\bar{Q} \rightarrow (Q\bar{Q}) + (Q\bar{Q})$. A $Q\bar{Q}$ color singlet pair is created with vacuum quantum numbers $I^G J^{PC} = 0^+ 0^{++}$, which corresponds to a ${}^{2S+1}L_J = {}^3P_0$ configuration. It is assumed, that the original (anti)quarks do not change their spin, color or flavor state during the creation process, but recombine only later with the new quarks to form color singlet final state mesons. The model turns out to give a rather adequate description of the decay rates of meson resonances. It also appears to describe the decay of baryonic resonances to meson baryon final states well [Co 71, Mu 79].

Recently Jaffe [Jb 78] applied the QPC model to try and select the 3-baryonium states, which are most prominent in the $B\bar{B}$, and in particular in the $N\bar{N}$, channels. The decay of a $Q^2\bar{Q}^2$ to a $B\bar{B}$ state again proceeds via the creation of a color singlet $Q\bar{Q}$ pair in a 3P_0 state. One has: $Q\bar{Q} \xrightarrow{*} \bar{Q}Q \rightarrow QQ(Q\bar{Q})\bar{Q}\bar{Q} \rightarrow Q^3 + \bar{Q}^3$. The original (anti)diquarks behave as spectators and are recovered in the final state (anti)baryon in their original quantum state. The $B\bar{B}$ pair content of the final state follows from a recoupling of the quark and diquark wavefunction to a baryonic one. Of course, the same model can be used to describe the formation of a 3-baryonium state by considering the annihilation of a $Q\bar{Q}$ pair in a $B\bar{B}$ initial state.

In this approximation the transition matrix element (see Fig. 7) is

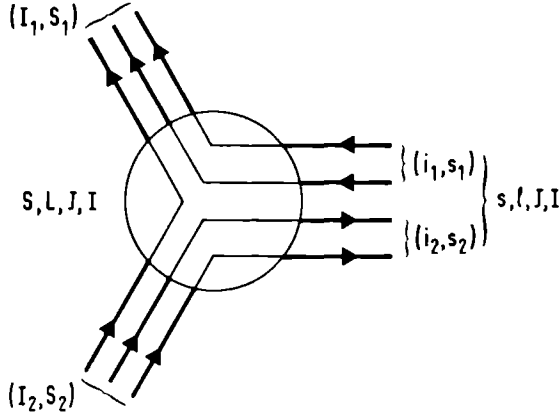


Fig. 7: The vertex for the decay of a $Q^2\bar{Q}^2$ resonance to a baryon-antibaryon final state.

given by:

$$\begin{aligned} \langle f|H|i\rangle &= \langle B, I_1, S_1; \bar{B}, I_2, S_2; I, S, L, J | H(^3P_0) | Q^2, i_1, s_1; \bar{Q}^2, i_2, s_2; I, S, \ell, J \rangle \\ &= C(k, \ell, L) \cdot g_{in} \cdot g_s \cdot g_J \cdot g_c \end{aligned} \quad (21)$$

The recoupling of (iso)spins is given by the factors g :

$$g_s = \begin{bmatrix} s_1 & \frac{1}{2} & S_1 \\ s_2 & \frac{1}{2} & S_2 \\ s & 1 & S \end{bmatrix} \quad g_J = \begin{bmatrix} s & 1 & S \\ \ell & 1 & L \\ J & 0 & J \end{bmatrix} \quad g_{in} = \begin{bmatrix} i_1 & \frac{1}{2} & I_1 \\ i_2 & \frac{1}{2} & I_2 \\ I & 0 & I \end{bmatrix} \quad (22)$$

The recoupling coefficients are related to a 9j symbol [Br 71] by:

$$\begin{bmatrix} S_1 & T_1 & U_1 \\ S_2 & T_2 & U_2 \\ S_3 & T_3 & U_3 \end{bmatrix} = ((2S_3+1)(2T_3+1)(2U_1+1)(2U_2+1))^{1/2} \left\{ \begin{matrix} S_1 & T_1 & U_1 \\ S_2 & T_2 & U_2 \\ S_3 & T_3 & U_3 \end{matrix} \right\} \quad (23)$$

From eq. (22) it immediately follows that one has $|s-1| \leq S \leq |s+1|$ and that

$L = |\ell \pm 1|$, because of parity conservation.

- $C(k, \ell, L)$ -

The coefficient $C(k, \ell, L)$ represents the space part of the matrix element. It contains the unknown dynamics of the decay and accounts for the transition of one elongated bag into two spherical ones. $C(k, \ell, L)$ depends on the angular momentum L of the $B\bar{B}$ final state and the angular momentum ℓ of the resonant state. It furthermore depends on the CM momentum k of the two particle state. In principle, also a dependence on the symmetry of the space wavefunction is possible. For example, in the Q^2 - \bar{Q} orbital excitation spectrum, for the lower values of the orbital momentum ℓ (1,2) between the quark and the diquark evidence for two flavor spin multiplets is found: a 56- and 70-plet. For this all quark system the flavor spin symmetry reflects the spatial one, and it is found [Mu 79], that $C(k, \ell, L, 56) \neq C(k, \ell, L, 70)$. However, with our restriction to s-wave diquarks this freedom is not present in the Q^2 - \bar{Q}^2 orbital excitation spectrum. In this model only processes with the same ℓ and L values can be compared. As a simple approximation one may take the k dependence to be a phase space factor. We will also use C to absorb common factors, such as the coupling constants.

- g_{1n} -

The initial state of a formation experiment consists of an $N\bar{N}$ pair. We therefore consider only one iso singlet configuration: that containing nonstrange quarks. Taking also creation of $s\bar{s}$ pairs into account we have to replace $g_{1n} \rightarrow g_{1n} + c' g_{1s}$, where $g_{1s} = \delta_{1_1 I_1} \delta_{1_2 I_2}$ and c' represents possible dynamical differences of $s\bar{s}$ with $n\bar{n}$ pair creation. In the $SU(3, F)$ -symmetric case one has $c' = 1/\sqrt{2}$. The flavor normalization factor $\sqrt{2/3}$ then can be absorbed in $C(k, \ell, L)$.

- Colorless baryons in the final state -

Since the baryons in the initial and elastic final states all have

ground state configurations, the quark must be created in a relative s-wave with respect to the diquark, at least part of the time. The baryons emerging after recombination are expressed in terms of diquark-quark basis states and still need to be expressed in terms of the Q^3 basis states of the initial or final state baryons. This requires another coupling. For our purposes it is enough to know that the nucleonic diquark spends half its time in an $l = 1, s = 1$ and the other half in an $l = 0, s = 0$ configuration. Next to nucleons also Δ 's will be created. We will find, that also $N\bar{N}\pi$ and $N\bar{N}\pi\pi$ final states are present. The diquark in a final state Δ is always in an $l = 1, s = 1$ state. A nucleon in the final state thus gets an extra factor of $\sqrt{1/2}$. A considerable part of the time the $Q\bar{Q}$ pair will be created near one of the bag ends and then also excited baryons will be formed. This is another source for mesons in addition to a $B\bar{B}$ pair in the final state.

- To flip or not to flip -

The statement, that the color configuration of the original quarks does not change, is a trivial one for the $Q\bar{Q}$ and the Q^3 decays: the quark and diquark can only occur in a color triplet configuration. The same statement involves an extra assumption for the $Q^2\bar{Q}^2$ states [Jc 78]. It is possible that, when the elongated $Q^2\bar{Q}^2$ bag splits into two spherical baryonic ones under the influence of a $Q\bar{Q}$ pair creation, the diquarks exchange (color octet) gluons, which flip the color from 3^* to 6 or vice versa. Such a flip by itself is forbidden, because of the Pauli Principle, and thus must be accompanied by e.g. a spin flip or a spatial (de)excitation of the diquark. One expects the interactions, needed to realize these flips, to be similar to the color magnetic dipole - dipole ones, and thus to fall off rapidly with the intercluster distance. Their influence then perhaps will only be noticeable for small l (is 1 or 2).

One assumes as a rule of thumb, that only 3-baryonium states will couple strongly to the $B\bar{B}$ system. This assumption seems reasonable in case of a peripheral formation process. The baryon behaves as a diquark quark system, of which the quark annihilates the corresponding antiquark in the antibaryon, and an orbitally excited 3-baryonium intermediate state is formed. The spectator diquarks are kept apart by the angular momentum barrier and do not come close enough to flip color (and spin). No 6-baryonium will easily be formed in, or decay to a $B\bar{B}$ channel. Their width is thus expected to be appreciably smaller than that of their color 3 nephews. Of course, also 8-mesonium states will not couple to $B\bar{B}$ decay channels.

- Colored baryons in the final state -

When a diquark and quark couple to a Q^3 baryon, next to the color singlet flavor spin multiplet [56] also a color octet [70] may be formed. The 3-baryonium state thus may also couple to (virtual) $Q^3-\bar{Q}^3$ 8-8 trajectory states. Estimating the mass of such bag states one finds ($n_s = 0$) an intercept of $M = 2.125$ GeV and the following central masses $M(L)$: $M(1) = 2.48$, $M(2) = 2.80$, and $M(3) = 3.08$. The persistent color magnetic splitting has a strength of 75 MeV. The most lowlying configuration consists of a $B\bar{B}$ pair, with both $l = s = \frac{1}{2}$: $\Delta = -1$ and $E_M = -75$ MeV. Assuming that for $L = 1$ one has $E_M = -200$ MeV, the lightest $L = 1$ $Q^3-\bar{Q}^3$ still lies above the heaviest $l = 2$ $Q^2-\bar{Q}^2$ ($n_s = 0$, $c = 3$) state! Only the $L = 0$ may lie amid of the $l = 1$ $Q^2-\bar{Q}^2$ states.

The 8 - 8 $Q^3-\bar{Q}^3$ trajectories are not expected to have a large influence on the $N\bar{N}$ final states. For example, a 3-baryonium state with $l = 1$ may couple to $L = 0$ and $L = 2$ $Q^3-\bar{Q}^3$ states. The latter is much too heavy: $2.7 < M < 3.3$ GeV. The former simply falls apart, analogous to the $l = 0$

$Q^2-\bar{Q}^2$ bag state, in three mesons in relative s-waves. No (anti)baryons will be seen in this case. The $L = 1$ $Q^3-\bar{Q}^3$ states are expected at masses $2.3 < M < 3.0$ GeV. They may decay by means of emission of a meson (pion) to an $L = 0$ bag, yielding multimeson final states. Decay may also proceed through color singlet admixtures, arising from color magnetic and electric dipole interactions just as for the $\ell = 1$ 8-mesonium states. Such admixtures are not possible for all members of the 70-plet, because the limited overlap of the flavor quantum numbers with the 56-plet. Nevertheless, there may be color singlet $B\bar{B}$ decay modes, which are sufficiently strong to blur the branching ratios for decay into $B\bar{B}$ channels, which are calculated using exclusively the direct produced color singlet baryons [K1 78].

- g_c -

In view of these decay modes, the $L = 1$ states are not expected to have an exceedingly large width, and due to their high mass are not easily formed as intermediate state in an $\ell = 1$ $Q^2-\bar{Q}^2$ decay. For $L = 2$ and larger the coupling is ever weaker. This situation is therefore quite similar to that for $Q-\bar{Q}$ and $Q^2-\bar{Q}^2$ resonance decays, where the color singlet MM and BM final states to good accuracy are also entirely due to direct decay. To first order only 3-baryonia will produce $B\bar{B}$ final states. One has $g_c (Q^2\bar{Q}^2 \rightarrow B_1\bar{B}_1) = 1/3$. This factor is usually absorbed in the unknown function $C(k, \ell, L)$. Comparing it with the recoupling coefficient to color 8-baryon final states $g_c (Q^2\bar{Q}^2 \rightarrow B_8\bar{B}_8) = \sqrt{8/9}$, one is inclined to expect a considerable branching ratio to three or more meson final states for $\ell = 1$ baryonium states. For the color sextet variety it probably is a main decay mode.

- The 3P_0 model and peripherality -

The couplings of the 3-baryonia to $N\bar{N}$ (as well to $N\bar{\Delta}$, $\Lambda\bar{N}$ and $\Delta\bar{\Delta}$) have

	I	s	S	$N\bar{N}$	$\frac{\Delta\bar{N} + N\bar{\Delta}}{\sqrt{2}}$	$\frac{\Delta\bar{N} - N\bar{\Delta}}{\sqrt{2}}$	$\Delta\bar{\Delta}$
(1,1)	0	0	1	$\frac{1}{2}$	-	-	-
$\{(1,3)+(3,1)\}/\sqrt{2}$	1	1	0	$-\sqrt{\frac{1}{6}}$	-	-	-
			1	-	-	$\frac{1}{3\sqrt{2}}$	-
			2	-	$\frac{1}{\sqrt{6}}$	-	-
$\{(1,3)-(3,1)\}/\sqrt{2}$			1	$\frac{1}{3}$	$-\frac{1}{3\sqrt{2}}$	-	-
			2	-	-	$-\frac{1}{\sqrt{6}}$	-
(3,3)	0	0	1	$-\frac{1}{18}$	-	-	$\frac{2\sqrt{5}}{9}$
		1	0	$\frac{\sqrt{2}}{6}$	-	-	$-\frac{\sqrt{2}}{3}$
			2	-	-	-	$\frac{2}{3}$
		2	1	$\frac{\sqrt{5}}{9}$	-	-	$-\frac{2}{9}$
			3	-	-	-	$\sqrt{\frac{2}{3}}$
	1	0	1	$\frac{-\sqrt{2}}{18\sqrt{3}}$	$\frac{-\sqrt{8}}{9\sqrt{3}}$	-	$\frac{5\sqrt{2}}{9\sqrt{3}}$
		1	0	$\frac{1}{3\sqrt{3}}$	-	-	$-\frac{\sqrt{5}}{3\sqrt{3}}$
			1	-	-	$\frac{1}{3\sqrt{2}}$	-
			2	-	$\frac{-1}{3\sqrt{6}}$	-	$\frac{\sqrt{10}}{3\sqrt{3}}$
		2	1	$\frac{\sqrt{10}}{9\sqrt{3}}$	$\frac{-\sqrt{5}}{9\sqrt{6}}$	-	$-\frac{\sqrt{10}}{9\sqrt{3}}$
			2	-	-	$\frac{1}{3\sqrt{2}}$	-
			3	-	-	-	$\frac{\sqrt{5}}{3}$
	2	0	1	-	$\frac{-\sqrt{8}}{9}$	-	$\frac{\sqrt{10}}{9}$
		1	0	-	-	-	$-\frac{1}{3}$
			1	-	-	$\sqrt{\frac{1}{6}}$	-
		2	-	$\frac{-1}{3\sqrt{2}}$	-	$\sqrt{\frac{2}{3}}$	
2	2	1	-	$\frac{-\sqrt{5}}{9\sqrt{2}}$	-	$-\frac{\sqrt{2}}{9}$	
		2	-	-	$\sqrt{\frac{1}{6}}$	-	
		3	-	-	-	$\sqrt{\frac{1}{3}}$	

Table XV: Isospin-spin couplings of $Q^2\bar{Q}^2$ to $B\bar{B}$ states after creation of a $Q\bar{Q}$ pair with $I = 0 = n_s$ and $S = 1$. The coefficients given correspond to $g_1 \cdot g_s \cdot (\frac{1}{\sqrt{2}})^N$, where N is the number of nucleons in the $B\bar{B}$ state. The linear combinations correspond to C-parity eigenstates (see Tables IX and X for diquark definition).

s	S	L	J	g_J^2	s	S	L	J	g_J^2
0	1	$\ell-1$	ℓ	$\frac{2\ell-1}{3(2\ell+1)}$	2	1	$\ell-1$	$\ell-2$	$\frac{1}{5}^*$
		$\ell+1$	ℓ	$\frac{2\ell+1}{3(2\ell+1)}$				$\ell-1$	$\frac{\ell+1}{10\ell}^*$
1	0	$\ell-1$	$\ell-1$	$\frac{1}{9}$				ℓ	$\frac{(2\ell+3)(\ell+1)}{30\ell(2\ell+1)}$
		$\ell+1$	$\ell+1$	$\frac{1}{9}$			$\ell+1$	ℓ	$\frac{(2\ell-1)}{30(\ell+1)(2\ell+1)}$
1	1	$\ell-1$	$\ell-1$	$\frac{\ell-1}{6\ell}$				$\ell+1$	$\frac{\ell}{10(\ell+1)}$
			ℓ	$\frac{(\ell+1)(2\ell-1)}{6\ell(2\ell+1)}$				$\ell+2$	$\frac{1}{5}$
		$\ell+1$	ℓ	$\frac{(2\ell+1)}{6(\ell+1)(2\ell+1)}$					
			$\ell+1$	$\frac{\ell+2}{6(\ell+1)}$					

Table XVI: The angular momentum recoupling factor g_J^2 for coupling $Q^2\bar{Q}^2$ states to $N\bar{N}$. The couplings with an asterisk are zero for $\ell = 1$.

been given by Jaffe [Jb 78]. They are listed in Tables XV and XVI. Combining these two tables we see, that the strongest coupling is that of the $I = 0$ $N\bar{N}$ triplet to those $s = 0$ $Q^2\bar{Q}^2$ states which contain isoscalar diquarks. For large ℓ the two degenerate $s = I = 1$ and the $s = 2, J = \ell \pm 2$ with $I = 0$ and 1 states couple considerably weaker to the $N\bar{N}$ $S = 0$ and 1, and $S = 1$ channels respectively, but have a more favorable phase space. The $I = 0$ and 1 states with $s = 0$ and 2 and $J = \ell$ virtually decouple. These statements have only meaning when a comparison is made between states with the same values of ℓ and L , and about the same k . Combining the results with those obtained from peripherality, we find that precisely those states are preferred, which couple moderately to strongly, and which have $\vec{s} // \vec{\ell}$.

The hierarchy of couplings is a little different for $\ell = 1$ and 2. For these small ℓ values the relative strengths still change quite a bit in going from one ℓ to the next. We have listed explicitly in Table XVII the couplings of the $n_s = 0$ 3-baryonium candidates for the narrow $M = 1.90, 1.94, 2.02$ and

	M	representation	s	I ^G	J ^{PC}	S	L	g
$\ell^P = 1^-$	1.90	(3,3)	1	0 ⁺ (1 ⁻)	0 ⁻⁺	0	0	.0786
				0 ⁺ (1 ⁻)	2 ⁻⁺		2	.0786
	1.94	(3,3)	2	0 ⁻ (1 ⁺)	1 ⁻⁻	1	0	.0828
							2	.0185
				0 ⁻ (1 ⁺)	2 ⁻⁻	1	2	.0556
				0 ⁻ (1 ⁺)	3 ⁻⁻	1	2	.1111
$\ell^P = 2^+$	2.01	$\{(1,3)+(3,1)\}/\sqrt{2}$	1	1 ⁺	1 ⁺⁻	0	1	.1361
					3 ⁺⁻		3	.1361
	2.23	(3,3)	0	0 ⁺ (1 ⁻)	1 ⁺⁺	1	1	.0962
					2 ⁺⁺		1	.1291
							3	-.1315
					3 ⁺⁺		3	-.1571
	2.23	(3,3)	1	0 ⁻ (1 ⁺)	1 ⁺⁻	0	1	.0786
					3 ⁺⁻		3	.0786
	2.24	(3,3)	2	0 ⁺ (1 ⁻)	0 ⁺⁺	1	1	.1111
					1 ⁺⁺		1	.0962
					2 ⁺⁺		1	.0657
							3	.0287
3 ⁺⁺						3	.0642	
4 ⁺⁺						3	.1111	

Table XVII: Couplings of selected $n_s = 0$ $Q^2 \bar{Q}^2$ states to $N\bar{N}$. In case of isodoublets only the coupling of the I = 0 member has been given. One has $g(I = 0) = g(I = 1) \cdot \sqrt{3/2}$.

2.20 GeV states. We find that for the $M = 1.90$ and 1.94 GeV states assignments can be made, which have some attractive features. For the heavier states, the situation really does not look very nice. In both cases too many aspects rely on the benevolence of the observer. We will sketch these assignments and use the opportunity to discuss some interesting related features.

3. Narrow states

When we assume the calculated mass values to be accurate, the obvious 3-baryonium candidate for the lower state is the $n_g = 0, I = 1$ level at 2.01 GeV. This exclusive isospin assignment is in experimental difficulty as long as no charged partners of the $M^0(2020)$ are found. For a state with a simple isospin structure the branching ratio to $N\bar{N}$ is larger than 30 %, implying $\Gamma_{N\bar{N}} \geq 4$ MeV (see Table XIV). The $\ell^P = 2^+ Q^2 - \bar{Q}^2$ level also couples to $N\bar{N}$: the $N\bar{N} P$ and F-waves and lies at the $N\bar{N}\pi$ threshold. Until now no structure has been observed to go with the narrow resonances in the $\pi\pi$ or $K\bar{K}$ final states. No member coupling to $N\bar{N}$ can decay into $\pi\pi$ and only the $J^{PC} = 2^{++}$ one can decay into $K\bar{K}$. This $J^{PC} = 2^{++}$ state however, may be peripherally produced in the $N\bar{N}$ F-wave. It thus may be broad, but does, just like the broad $M = 1.95$ GeV and possibly the 2.020 GeV state, not give rise to a bump in the elastic or total cross section. It can not be identified with the latter broad state, which has $I = 0$. The $K\bar{K}$ decay signal of such a broad state may also have a smeared out structure and thus at present still escape observation.

Comparing the couplings for fixed L one finds that these are almost equally large. At order g^4 (i.e. in the elastic cross section) they only differ by factors 2 or 3. The $J = 2$ state couples to both the $N\bar{N} P$ and F-waves and probably is broader than its colleagues anyway. Up to peripherality effects its partial width for decay into the $N\bar{N}$ F-wave system will be similar to that of the $J = 3$ states. Its partial width to P-waves will be about the same as that for the $J = 1$ states.

In view of the closeness to the $\bar{N}\bar{N}\pi$ threshold, this final state is rather improbable. Multimeson final states are accessible though. The $\ell = 2$ states can emit a meson (probably a pion) and cascade to an $\ell = 0$ $Q^2\bar{Q}^2$ bag state, which then falls apart into two mesons, which in turn may decay into two or more mesons themselves (the massive dimeson states usually have a large two vector particle component, see section I). Here the broad state, decaying to 5π and $\bar{n}\bar{n}$, becomes interesting. The small $\bar{N}\bar{N}$ branching ratio of this state does not favor a peripheral interpretation. Creation of an $\bar{s}\bar{s}$ pair near one of the bag ends may yield the $K\bar{K}\pi$ signals. An alternative source for this final state is provided by the $n_s = 2$, $\ell^P = 1^-$ state at $M = 2.02$ GeV, for which however, the formation in $\bar{p}p$ and $\bar{p}d$ is rather problematic. No firm conclusion can be drawn.

An $n_s = 0$ candidate for the $M^0(2204)$ state is provided by the $\ell^P = 2^+$ levels at 2.23 and 2.24 GeV, with both $I = 0$ and 1. Another bad feature of this assignment becomes clear. All members, which couple to $\bar{N}\bar{N}$, can decay to $M^0(2020) + \pi$, e.g. in an $L = 1$ wave, for which only negative evidence has been found.

Also in this region a $K\bar{K}\pi$ signal has been observed in a formation experiment (at 2.20 GeV). The above mentioned levels display a large variety of coupling strengths and none of their members can be produced peripherally. When some of these states, for some reason, are broad in $\bar{N}\bar{N}$, presumably enough narrow ones will remain. Again, not much can be said about the other partial widths.

We find that this assignment of the $M^0(2020)$ and $M^0(2204)$ states to 3-baryonium levels gives rise to quite some problems, but at present it is still possible that one of them or both have this quark and color configuration. This may require another mass spectrum. At this point it still is very attractive though to consider some alternatives.

- Narrow states: $M^0(2020)$ and $M^0(2204)$: 6-baryonium candidates -

The fact, that the narrow $M = 2.020$ and 2.204 GeV states have not been seen in formation experiments, could be due to a combination of weak coupling and experimental resolution rather than true absence (cf. M(1950)). After all, they seem to have, under certain reasonable assumptions, a large branching ratio to $N\bar{N}$. It could also imply that these states are essentially different from the (broad) $N\bar{N}$ resonances, which in the previous subsection have been identified with 3-baryonium states.

- Coupling to $N\bar{N}$ via pair creation -

This observation can be interpreted in favor of 6-baryonium states [ChH 77]. In the idealized context of the 3P_0 model, which seems to be a reasonable description for peripheral states with $\ell > 2$, the $c = 6$ diquark recombines with the $c = 3$ quark to form a $c = 8$ or 10 triquark. No color singlets are formed and - for $\ell > 2$ - no coupling to $N\bar{N}$ initial or final states is possible. For sufficiently large ℓ the baryonium states will only couple to the lighter $c = 8$ $Q^3-\bar{Q}^3$ configurations. These can shake off their angular momentum by emission of mesons (pions) and cascade to a final state containing many mesons and possibly an $N\bar{N}$ pair. In a more probable alternative, the $c = 8$ flux is sealed off by (valence) gluons:

$$Q^3 \text{---} \bar{Q}^3 \rightarrow Q^3(GG)\bar{Q}^3 \rightarrow (Q^3G) + (\bar{Q}^3G). \text{ Subsequently } (Q^3G) \rightarrow (Q^3Q\bar{Q}) \rightarrow Q^3 + Q\bar{Q}.$$

Again no pure $N\bar{N}$ final state will emerge. Using the result of Chapter 2 we find $M(Q^3G) \approx 1.4$ GeV, which requires $\ell \geq 2$ for the $Q^3-\bar{Q}^3$ to occur.

An important alternative is the recombination of the $c = 6$ diquark with the $c = 3^*$ antiquark. Such a mechanism is suppressed as a 3-baryonium decay mode, since it yields a $Q^2\bar{Q}$ cluster with either a $c = 3$ color charge: the color electric flux has to be reversed, or a $c = 6$ one, requiring more energy in the color fields. For $c = 3^*$, recombination with a quark yields a.o. a color singlet configuration and a lot of energy is released by sealing off the

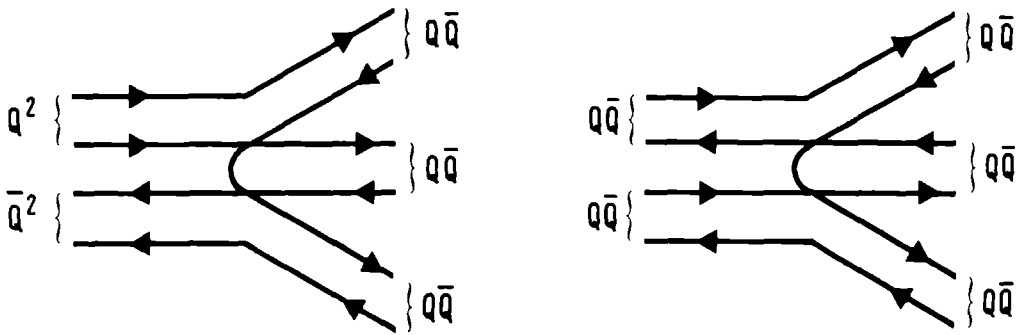


Fig 8: Three meson decay mode of baryonium (a) and 8-mesonium (b) states.

color flux. The $c = 6$ diquark and the antiquark together may form a $c = 3$ color charge. Here, the flux is not sealed off completely, but is reduced quite a bit. The newly formed clusters are highly unstable and a rapid decay into 3-meson final states ensues (see fig. 8).

Because the transition $(Q^2)_{c=6} \rightarrow (Q^2\bar{Q})_{c=3}$ is much more favorable than the $(Q^2)_{c=6} \rightarrow (Q^3)_{c=8}$ one, the former is expected to dominate. Since the energy released in a $c = 6$ to $c = 3$ transition is not as much as that in a $c = 1$ from $c = 3^*$ one, the three meson decay mode may yield a partial width which is smaller than the partial width for decay to $N\bar{N}$ of a comparable 3-baryonium state. It similarly is larger than the 3-meson decay width of the same 3-baryonium state. It presumably is at most several tens of MeV. Another alternative for 6-baryonium states is the cascade decay, which will not yield very wide states either. Far above the $N\bar{N}$ threshold a small width may be a signal for the presence of a 6-baryonium state. For $\ell > 2$ no pure $N\bar{N}$ final states will be produced.

- Coupling to $N\bar{N}$ via shortrange interactions -

For $\ell = 1$ and 2 (see page 183) some 6-baryonium states (ϕ_6) will have

small triplet (ϕ_3) admixtures, which are generated by the residual color magnetic interaction. The mixing pattern is similar to that for the $\ell = 0$ states found in Table VI. For a state $\phi = \alpha\phi_6 + \beta\phi_3$, $|\alpha|^2 + |\beta|^2 = 1$, the average amount of mixing is given by $\beta = \beta(\ell, s)$:

(ℓ, s)	(1,0)	(1,1)	(2,0)	(2,1)
β	0.25	0.13	0.05	0.03

and all other β 's zero.

Via this interaction a partial width for decay to the $N\bar{N}$ channels can be obtained of $\Gamma_{N\bar{N}}(6) \leq 0.06 \Gamma_{N\bar{N}}(3) \leq 10$ MeV for $\ell = 1$ and much smaller for $\ell = 2$. Although 10 MeV is not large, the decay to $N\bar{N}$ still may be a mayor decay mode. This may be another signal for spotting 6-baryonium states. The color magnetic interaction between the clusters thus is important only for $\ell = 1$.

The strength of the interaction between the color electric dipole moments of the quarks in the deformed bag ends is hard to estimate, since in the best known systems ($Q\bar{Q}$ and $Q^2\bar{Q}$) only $c = 3$ configurations occur. In view of its dipole character it probably also will only be noticeable in the small ℓ region, where moreover the deformations are not yet large.

Neither color magnetic nor color electric dipole interactions will change an s-wave $(c, s) = (6, 1)$ diquark into an s-wave $(3^*, 1)$ one. This implies that the $s = 1$ and 2 6-baryonium states which are dominantly composed of such diquarks will not be reached in elastic processes. They may occur as decay product after the formation of a 6-baryonium state, with one or two excited (p-wave) clusters, which decay via emission of a pion or other meson (space-flavor flip!). From these considerations it follows that some 6-baryonium states will be formed only scantily, whereas others (e.g. those with $\ell \geq 3$) will not be formed at all.

- Production -

The above mentioned arguments do not imply that most 6-baryonia will never be seen. One can arrange the experimental conditions in such a way that a diquark and an antidiquark are brought so close together that the dipole forces, in spite of the high angular momentum barrier, are able to change the color state. Examples of these so-called production processes have been given at the beginning of this section. In Fig. 6 (page 172) two situations are depicted in which an energetic $Q\bar{Q}$ meson beam falls on a baryon target. By triggering on a suitable fast forward baryon the short ranged anti-baryon exchange mechanism is selected. This mechanism requires the creation of a diquark-antidiquark (" 1S_0 model") of which the antidiquark recombines with the diquark of the target baryon to form a backward baryonium or mesonium system and the diquark submerges with the quark of the meson in a forward baryon. The higher the spin of the forward baryon is, the higher that of the backward system may be. One can also produce forward $Q^2\bar{Q}^2$ resonances. The simplest exchange is a $Q\bar{Q}$ one which results in a forward $Q\bar{Q}$ system, in which a $Q\bar{Q}$ pair creation can lead to a baryonium or mesonium state. This way also the $s = 2$ and the missing $s = 1$ states will be produced. When one triggers on a final state $p\bar{p}$ pair only 3-baryonia and possibly $\ell = 1$ 6-baryonia [Ev 78] will be seen. The other $Q^2\bar{Q}^2$ states require $Q\bar{Q}$ annihilation followed by the creation of a $Q^2\bar{Q}^2$ pair to generate this trigger, which - on mass shell - does not stimulate their prominence. The next simplest exchange is a $Q^2\bar{Q}^2$ one!

- Candidates -

Consulting Table XIIIc the $n_s = 0$, $I = 0$ $M = 2.01$ GeV state seems to be a good candidate for $M^0(2020)$, and the $n_s = 2$, $I = 0$ and 1 and $M = 2.18$ state may be the $M^0(2204)$. The lower state is not in trouble when $M^0(2020)$

turns out to have $I = 0$ - on the contrary - and does not form a part of the final state in the pioncascade decay of $M^0(2204)$. Both states, because of their diquark composition, will probably suffer the drawback of a weak coupling to $p\bar{p}$.

- Narrow states: $M = 1.897$ and 1.936 GeV -

Since both states are prominent peaks in formation experiments, we will take them to be 3-baryonia. Table XIIIa contains only two $\ell = 1$, $n_s = 0$ levels above the $N\bar{N}$ threshold: one at $M = 1.90$ and one at 1.94 GeV. We have listed also these states and their couplings to $N\bar{N}$ in Table XVII. Again taking the calculated masses at face value, we identify the bump at 1.897 GeV with the level at 1.90 GeV and the S(1936) state with the one at 1.94 GeV. In view of its proximity to the $N\bar{N}$ threshold the former presumably is a pseudoscalar isodoublet of which the $I = 1$ member has been found. An additional $I = 0$ state is required. Of course $J^P = 2^-$ is not excluded.

The level at 1.94 GeV contains a $J^P = 1^-$ state, which couples to the $I = 1$ $\pi\pi$ system and thus provides a natural candidate for the peripheral $N\bar{N} \ ^3D_1$ state. The S(1936) then has $J = 2$ or 3 . Taking into account, that this state has only been seen in elastic and total cross sections and that no $\pi\pi$ decays have been reported, $J = 2$ is favored. This assignment has a quite surprising consequence: denoting $g = g(J)$ we have $g(1) : g(2) : g(3) = 1 : 3 : 6$ for the D-wave couplings, which is largely due to the angular momentum recoupling (Table XVI). These large ratios however, only play a role in the formation of the states (order g^2). In principle all three states may be formed peripherally, coupling to the $J = L - 1$, L and $L + 1$ wave respectively. Until now only a $J = 1$ state has been reported ($M = 1.95$ GeV). When this turns out to be the final situation, the effective couplings to $N\bar{N}$ D-waves may be comparable at this level. Once the $J = 1$ state has been formed in a D-wave, it will very

easily fall apart into the 3S_1 $N\bar{N}$ channel. The $J = 2$ and 3 states will be strongly hampered in their $N\bar{N}$ decay by the centrifugal barrier. Moreover, the recoupling coefficients for the $J = 1$ S-wave and $J = 2$ and 3 D-wave decays have become comparable: $g(1) : g(2) : g(3) = 3 : 2 : 4$. Consequently, the $J = 1$ state may acquire a considerable width in the elastic $N\bar{N}$ channels, while the $J = 2$ and 3 states not necessarily need to become broad. The photonlike state furthermore has the additional feature, that it also may possess a sizable multimeson decay width via its coupling to $L = 0$ colored $Q^3\bar{Q}^3$ states. Combining these remarks we expect the $J = 1$ state to be much broader than its $J = 2$ and 3 partners. This assignment has another attractive feature. It predicts the presence of degenerate $I = 0$ and 1 multiplets. This property may explain, why the charge exchange process: $p\bar{p} \rightarrow n\bar{n}$ is not seen, whereas the elastic process $p\bar{p} \rightarrow p\bar{p}$ is quite clearly visible [K1 78]. Both $p\bar{p}$ and $n\bar{n}$ are mixtures of isospin eigen states: $p\bar{p} \sim ((1,0) + (0,0))$ and $n\bar{n} \sim ((1,0) - (0,0))$ in the notation (I, I_z) . The coupling of $N\bar{N}$ to the $I = 0$ $Q^2\bar{Q}^2$ state is stronger than that to the $I = 1$ one: $g(I=1) : g(I=0) = \sqrt{2} : \sqrt{3}$. Assuming charge independence one finds constructive interference in the elastic process, whereas the charge exchange process displays destructive interference. This results in the ratio $\sigma_{el} : \sigma_{ce} = 25 : 1$ for the cross sections. Of course the coupling to $N\bar{N}$ is not the only possibility. The coupling to mesons will not be the same for the two isospin multiplets (G-parity) and the ratio may not be as large. Still the effect may be considerable. In case only one isomultiplet is present one has $\sigma_{el} : \sigma_{ce} = 1 : 1$, in disagreement with observation. One expects that for the 1.90 GeV state, which is also regarded as a complex structure, $\sigma_{el} \gg \sigma_{ce}$ is valid too. An alternative explanation [E1 76] of the smallness of the σ_{ce}/σ_{el} ratio requires only one narrow resonance, which interferes strongly with the background, a feature neglected in the above presented

explanation. Since this phenomenon recurs at the T and U masses, and since S, T and U all appear to have a composite isospin structure, we think the first explanation more appealing. One should add though that in the T and U region the $I = 0$ and 1 levels are not degenerate, which will reduce the effect, as observed.

- Narrow states below the $N\bar{N}$ threshold -

Including also 6-baryonium states, we find, in the present version of the $Q^2\bar{Q}^2$ mass spectrum, one $\ell^P = 2^+$ and five $\ell^P = 1^-$ levels below the $N\bar{N}$ threshold. The main decay mode of these states presumably is the three meson one, depicted in Fig. 8, yielding multimeson final states. The levels at $M = 1.76$ and 1.83 GeV - the first has $\ell = 2$, the second $n_s = 2$ - probably are more narrow than the other ones, because of the heavier mesons, occurring in their dominant final states. One does not expect any of these states to have widths as large as 100 MeV.

All $\ell^P = 1^-$ levels contain a photonlike member: $J^{PC} = 1^{--}$ (see also Fig. 5), which suggests that their position can be checked in e^+e^- annihilation. Since it is not to be expected that the creation of the heavier diquark-antidiquark pair will be as probable as that of a quark-antiquark pair, their coupling to the photon will be less strong, and a better resolution than the present one may be needed to detect them [To 78]. Still among the many broad e^+e^- resonances also several narrow ones have been reported (Table XIV). In this region the $Q^2\bar{Q}^2$ states lie amid of the orbitally and radially excited $Q\bar{Q}$ systems, from which they have to be distinguished. At present this is not quite feasible due to the scarcity of the theoretical and experimental data on the decay modes. The presence of photonlike $\ell = 0$ $Q^3\bar{Q}^3$ states here presumably does not cause much trouble, since their coupling to e^+e^- is expected to be still weaker than that of the baryonium states.

Important information on the baryonium states below the $N\bar{N}$ threshold may be obtained from the γ ray spectrum of atomic $p\bar{p}$ systems. When the emitted photon results from the annihilation of a $Q\bar{Q}$ pair one may find baryonium final states. In this process also the other J^{PC} members of the $M = 1.72$ and 1.76 GeV levels can be reached. In view of the large variety of quantum numbers decay to these levels may be quite attractive and the two higher γ ray states may be assigned to them. In this case our mass values are about 100 MeV off. The γ ray may also result from the coalescence of two three quark bags into a single $\ell = 0$ $Q^3\bar{Q}^3$ one. Although these states usually simply fall apart to a 3-meson final state, some of the high spin or low mass states may have a sufficiently restrictive final state, to render them narrow, and this possibility then seriously must be taken into account.

We note that the spectrum of narrow e^+e^- resonances does not coincide with the atomic $p\bar{p}$ γ ray one. This might indicate that none of the e^+e^- resonances found until now (as a result of a weak coupling?) are baryonium ones, when we take the γ ray states assignment serious, and vice versa. This situation thus also requires additional research.

- Narrow states: The $S = +1$, $Q = 2$ state at $M = 2.461$ GeV [Ar 78, Ro 70] -

The most unambiguous candidate for $Q^2\bar{Q}^2$ states is the narrow resonance found in the process $K^+_p \rightarrow (\bar{\Lambda}p\pi^+)_F n$ at 2.461 GeV. It shows up as a peak in both the $\bar{\Lambda}\Delta^{++}$ (1232) and $p\bar{L}^+$ (1385) invariant mass plots. From the Harari-Rosner diagram follows that this exotic final state ($\sim uu\bar{d}\bar{s}$) also requires the exchange of an exotic state ($\sim uu\bar{u}\bar{d}$). One finds with the same method [Ja 79] that this forward system can also be produced using a K_L beam, but then instead of a neutron a Δ^- (from the K_0) or a Ξ^- (from the \bar{K}_0) is produced backwardly. A K^- beam may produce the $Q = 1$ isomultiplet member, accompanied by a backward Ξ^- . In our model such a state might be ascribed to an $\ell = 3$ 3-baryonium $\underline{n} = \underline{18}$ level.

- Conclusion -

This treatment of the orbitally excited $Q^2\bar{Q}^2$ system is by no means exhaustive. We have only discussed the nature of a few prominent states and did not touch upon the status of the remaining ones. At present a detailed assignment of all reported states is not yet a feasible undertaking. The theoretical candidates still outnumber the reported ones by far, although the number of the latter is steadily increasing and even a state with an unambiguous $Q^2\bar{Q}^2$ content seems to have been found. Quite a lot of reported states still require confirmations.

Of the orbitally excited $Q^2\bar{Q}^2$ states the baryonium states have been discussed in some detail. The 8-mesonium states have, as a consequence of our attention for states coupling to the $N\bar{N}$ system, only been mentioned casually, in the discussion of production and decay mechanisms. Next to all-quark clusters interesting configurations, containing also valence gluons, which screen the quark charge, may exist. An example is the $c = 3^*$ Q^2G cluster, built from a $c = 6$ diquark and a $c = 8$ gluon. Two of such clusters can combine to a $3^* - 3$ trajectory which has a larger intercept than, but for sufficiently large l is more prominent than the corresponding $6 - 6^*$ trajectory. Consequently, it may at some point turn out to be more favorable to screen a large color charge ($c \geq 6$) and trajectories with an anomalously steep slope may not be seen any longer [Ho 79].

We have devoted much attention to the study of states with small orbital angular momentum, because the number of experimental candidates in this region is relatively large and more exotic configurations probably do not play an important role here. No firm conclusions could be drawn about our prescription for the calculation of the masses of these states. Since a great many aspects of the couplings to decay channels remain unexploited, severe criteria to elect or reject candidates, are absent.

In such a situation it is nevertheless quite useful to have a reference frame in which one can qualitatively discuss the reported candidates. Although no definite predictions can be made, one may be able to select prominent specimina, which may be relatively easily looked for.

Appendix A: Conventions for metric and γ -matrices

Metric tensor: $g^{\mu\nu}$; $\mu, \nu \in \{0,1,2,3\}$

$$-g^{00} = g^{kk} = 1 \quad k \in \{1,2,3\}$$

$$g^{\mu\nu} = 0, \quad \text{when } \mu \neq \nu.$$

γ -matrices: $\{\gamma_\mu, \gamma_\nu\} = 2 g_{\mu\nu}$.

In terms of the 2×2 matrices:

$$\begin{aligned} \emptyset &= \begin{pmatrix} 0 & 0 \\ 0 & 0 \end{pmatrix}; \quad \mathbf{1} = \begin{pmatrix} 1 & 0 \\ 0 & 1 \end{pmatrix}; \quad \sigma_1 = \begin{pmatrix} 0 & 1 \\ 1 & 0 \end{pmatrix}; \quad \sigma_2 = \begin{pmatrix} 0 & -i \\ i & 0 \end{pmatrix}; \\ \sigma_3 &= \begin{pmatrix} 1 & 0 \\ 0 & -1 \end{pmatrix} \end{aligned}$$

we have:

Standard representation:

Weyl representation:

$$\gamma_0 = i\rho_3 = \begin{pmatrix} i\mathbf{1} & \emptyset \\ \emptyset & -i\mathbf{1} \end{pmatrix}$$

$$\gamma_0 = i\rho_1 = \begin{pmatrix} \emptyset & i\mathbf{1} \\ i\mathbf{1} & \emptyset \end{pmatrix}$$

$$\gamma_k = \rho_2 \sigma_k = \begin{pmatrix} \emptyset & -i\sigma_k \\ i\sigma_k & \emptyset \end{pmatrix}$$

$$\gamma_k = -\rho_2 \sigma_k = \begin{pmatrix} \emptyset & i\sigma_k \\ -i\sigma_k & \emptyset \end{pmatrix}$$

$$\gamma_4 = \rho_3 = \begin{pmatrix} \mathbf{1} & \emptyset \\ \emptyset & -\mathbf{1} \end{pmatrix}$$

$$\gamma_4 = \rho_1 = \begin{pmatrix} \emptyset & \mathbf{1} \\ \mathbf{1} & \emptyset \end{pmatrix}$$

$$\gamma_5 = -\rho_1 = \begin{pmatrix} \emptyset & -\mathbf{1} \\ -\mathbf{1} & \emptyset \end{pmatrix}$$

$$\gamma_5 = -\rho_3 = \begin{pmatrix} -\mathbf{1} & \emptyset \\ \emptyset & \mathbf{1} \end{pmatrix}$$

Relations: $\gamma_\mu^+ = \gamma_0 \gamma_\mu \gamma_0 = -\gamma_4 \gamma_\mu \gamma_4$

using $\gamma_4 = -i \gamma_0$

$$\gamma_5 = i \gamma_0 \gamma_1 \gamma_2 \gamma_3 = \gamma_1 \gamma_2 \gamma_3 \gamma_4$$

Massive Free Fermion Lagrangian:

$$\mathcal{L}_F = -\bar{\psi} (\gamma \cdot \partial + m) \psi$$

with $\bar{\psi} = \psi^+ \gamma_4$; $\gamma \cdot \partial = \partial^\mu \gamma_\mu = i p^\mu \gamma_\mu$

Appendix B. Representations and properties of the SU(3) generators

The eight generators F_a satisfy:

$$[F_a, F_b] = F_a F_b - F_b F_a = i f_{abc} F_c \quad a, b, c \in \{1, \dots, 8\} \quad (i)$$

The $(n \times n)$ -matrix representations are normalized to

$$\text{Tr } F_a F_b = \sum_{i,j=1}^n (F_a)_{ij} (F_b)_{ji} = \frac{1}{2} \delta_{ab} \quad , \quad (ii)$$

where $\delta_{ab} = 1$, when $a = b$, and zero otherwise.

The SU(3) structure constants f_{abc} are completely antisymmetric under permutation of any two indices. Denoting $(abc) = f_{abc}$ one has:

$$\begin{aligned} (123) &= 1 & (458) &= (678) = \sqrt{3}/2 \\ (147) &= - (156) = (246) = (257) = (345) = - (367) = 1/2 \quad . \end{aligned}$$

A (3×3) matrix representation satisfying (i) and (ii) is given by $F_a = \left(\frac{\lambda_a}{2}\right)$ in terms of the Gell-Mann matrices λ_a . For completeness we also introduce λ_0 :

$$\begin{aligned} \lambda_0 &= \sqrt{\frac{2}{3}} \begin{pmatrix} 1 & 0 & 0 \\ 0 & 1 & 0 \\ 0 & 0 & 1 \end{pmatrix} & \lambda_1 &= \begin{pmatrix} 0 & 1 & 0 \\ 1 & 0 & 0 \\ 0 & 0 & 0 \end{pmatrix} & \lambda_2 &= \begin{pmatrix} 0 & -1 & 0 \\ 1 & 0 & 0 \\ 0 & 0 & 0 \end{pmatrix} \\ \lambda_3 &= \begin{pmatrix} 1 & 0 & 0 \\ 0 & -1 & 0 \\ 0 & 0 & 0 \end{pmatrix} & \lambda_4 &= \begin{pmatrix} 0 & 0 & 1 \\ 0 & 0 & 0 \\ 1 & 0 & 0 \end{pmatrix} & \lambda_5 &= \begin{pmatrix} 0 & 0 & -1 \\ 0 & 0 & 0 \\ 1 & 0 & 0 \end{pmatrix} \\ \lambda_6 &= \begin{pmatrix} 0 & 0 & 0 \\ 0 & 0 & 1 \\ 0 & 1 & 0 \end{pmatrix} & \lambda_7 &= \begin{pmatrix} 0 & 0 & 0 \\ 0 & 0 & -1 \\ 0 & 1 & 0 \end{pmatrix} & \lambda_8 &= \frac{1}{\sqrt{3}} \begin{pmatrix} 1 & 0 & 0 \\ 0 & 1 & 0 \\ 0 & 0 & -2 \end{pmatrix} \end{aligned}$$

This 3-dimensional representation further defines the constants d_{abc} , which are completely symmetric under permutation of any two indices by:

$$\{\lambda_a, \lambda_b\} = \lambda_a \lambda_b + \lambda_b \lambda_a = \sqrt{\frac{8}{3}} \delta_{ab} \lambda_0 + 2 d_{abc} \lambda_c \quad .$$

Denoting $(abc) = d_{abc}$:

$$\begin{aligned} (118) &= (228) = (338) = - (888) = \frac{1}{\sqrt{3}} & (448) &= (558) = (668) = (778) = - \frac{1}{2\sqrt{3}} \\ (146) &= (157) = - (247) = (256) = (344) = (355) = - (366) = - (377) = 1/2 \quad . \end{aligned}$$

The constants satisfy $\sum_{a,b,c} (d_{abc})^2 = \frac{40}{3}$ and $\sum_{a,b,c} (f_{abc})^2 = 24$.

An 8×8 matrix representation is given by $(F_a)_{bc} = -i f_{abc}$

References

- Li 50 D. Littlewood, Theory of group characters and matrix representations;
Oxford University Press, New York (1950).
- Da 61 O.I. Dahl et al., Phys.Rev.Lett. 6, 142 (1961);
D. Cline, R. Laumann and J. Mapp, Phys.Rev.Lett. 20, 1452 (1968);
G. Alexander et al., Phys.Rev.Lett. 22, 483 (1969);
P.L. Jain, Phys.Rev. 187, 1816 (1969);
K. Bunnell et al., Phys.Rev. D 2, 98 (1970);
W.H. Simms et al., Phys.Rev. D 3, 1162 (1971);
D. Eastwood et al., Phys.Rev. D 3, 2603 (1971).
- Gl 61 S.L. Glashow, Nucl.Phys. 22, 579 (1961).
- Di 62 P.A.M. Dirac, Proc.Roy.Soc. 268 A, 57 (1962).
- Ok 62 S. Okubo, Prog.Theor.Phys. (Kyoto), 27, 949 (1962).
- Sw 62 J.J. de Swart and C.K. Iddings, Phys.Rev. 128, 2810 (1962);
G. Fast, J.C. Helder and J.J. de Swart, Phys.Rev.Lett. 22, 1453 (1969);
M.M. Nagels, T.A. Rijken and J.J. de Swart, Baryon-baryon scattering
in a one-boson-exchange-potential approach III, THEF-NYM-78.4.
- Sw 63 J.J. de Swart, Rev.Mod.Phys. 35, 916 (1963).
- Be 64 M.A.B. Béq and V. Singh, Phys.Rev.Lett. 13, 418 (1964);
T.K. Kuo and T. Yao, Phys.Rev.Lett. 13, 415 (1964).
- Bj 64 J.D. Bjorken and S.L. Glashow, Phys.Lett. 11, 255 (1964).
- Co 64 H.O. Cohn and K.H. Bhatt, Phys.Rev.Lett. 13, 668 (1964).

- Da 64 A. Dar et al., Phys.Rev.Lett. 12, 82 (1964).
- Ge 64 M. Gell-Mann, Phys.Lett. 8, 214 (1964).
- Gr 64 O.W. Greenberg, Phys.Rev.Lett. 13, 598 (1964).
- Gü 64 F. Gürsey and L. Radicati, Phys.Rev.Lett. 13, 173 (1964),
A. Pais, Phys.Rev.Lett. 13, 175 (1964);
B. Sakita, Phys.Rev. B 136, 1756 (1964).
- Pi 64 P.A. Piroué, Phys.Lett. 11, 164 (1964).
- Zw 64 G. Zweig, CERN preprints TH 401, 412 (1964) (unpublished).
- Ha 65 M. Han and Y. Nambu, Phys.Rev. B 139, 1006 (1965).
- Bu 66 T. Buran et al., Phys.Lett. 20, 318 (1966).
- Na 66 Y. Nambu, Preludes in Theoretical Physics (A. de-Shalit, H. Feshbach
and L. van Hove, eds.); North-Holland, Amsterdam (1966), p. 133.
- It 66 C. Itzykson and M. Nauenberg, Rev.Mod.Phys. 38, 95 (1966).
- Sw 66 J.J. de Swart, Proc. of the 1966 CERN School of Physics, Noordwijk-
aan-zee, CERN-report 66-29, Vol. II.
- Gr 67 O.W. Greenberg and M. Resnikoff, Phys.Rev. 163, 1844 (1967);
D.R. Divgi and O.W. Greenberg, Phys.Rev. 175, 2025 (1968).
- We 67 S. Weinberg, Phys.Rev.Lett. 19, 1264 (1967).
- Al 68 G. Alexander et al., Phys.Rev. 173, 1452 (1968).
- Bo 68 P.N. Bogoliubov, Ann.Inst.Poincaré VIII, 163 (1968).
- Ka 68 G. Karl and E. Obryk, Nucl.Phys. B 8, 609 (1968).
- Ro 68 J.L. Rosner, Phys.Rev.Lett. 21, 950 (1968), 1422 (E).

- Sa 68 A. Salam, Elementary Particle Theory: Relativistic Groups and Analyticity (Nobel Symposium No. 8) (N. Svartholm, ed.) Almqvist and Wiksell, Stockholm (1968), p. 367.
- Bj 69 J.D. Bjorken and E.A. Paschos, Phys.Rev. 185, 1975 (1969); R.P. Feynman, Phys.Rev.Lett. 23, 1415 (1969) and in: High Energy Collisions; Gordon & Breach, New York (1969), p. 237.
- Ha 69 H. Harari, Phys.Rev.Lett. 22, 562 (1969); J.L. Rosner, Phys.Rev.Lett. 22, 689 (1969).
- Ko 69 J.J.J. Kokkedee, The quark model; Benjamin, New York (1969).
- Mi 69 L. Micu, Nucl.Phys. B 10, 521 (1969).
- Ta 69 T.H. Tan, Phys.Rev.Lett. 23, 395 (1969).
- Ab 70 R.J. Abrams et al., Phys.Rev. D 1, 1917 (1970); J. Alspector et al., Phys.Rev.Lett. 30, 1511 (1973), see also [PDG 78] and references therein.
- Ba 70 R. Balian and C. Bloch, Ann.Phys. (NY) 60, 401 (1970); 64, 271 (1971).
- Gl 70 S.L. Glashow, J. Iliopoulos and L. Maiani, Phys.Rev. D 2, 1285 (1970).
- Na 70 Y. Nambu, Lectures for the Copenhagen Summer Symposium (1970) (unpublished).
- Ro 70 J.L. Rosner, Phys.Lett. 33B, 493 (1970).
- Br 71 D.M. Brink and G.R. Satchler, Angular momentum; Clarendon Press, Oxford (Second edition, 1971). See also: H. Appel, in: Landolt-Börnstein: Kernphysik und Kerntechnik, Band 3 (H. Schopper, ed.); Springer-Verlag, Berlin, New York (1968).
- Co 71 E.W. Colglazier and J. Rosner, Nucl.Phys. B 27, 349 (1971).

- De 71 S. Devons et al., Phys.Rev.Lett. 27, 1614 (1971);
C.R. Sun et al., [ST 76], p. 71.
- Fr 71 H. Fritzsche and M. Gell-Mann, Proc. of the International Conference
on Duality and Symmetry in Hadron Physics; Weizmann Science Press,
Jeruzalem (1971).
- Gr 71 L. Gray et al., Phys.Rev.Lett. 26, 1491 (1971).
- Ka 71 J.A. Kadijk, Nucl.Phys. B 27, 13 (1971).
- Sw 71 J.J. de Swart et al., Springer Tracts of Physics 60, 138 (1971).
- Be 72 P. Beillière et al., Phys.Lett. 39B, 671 (1972).
- Fr 72 H. Fritzsche and M. Gell-Mann, Proc. of the VI International Conference
on High Energy Physics, Chicago (1972), vol. 2, p. 135;
also: H. Fritzsche, M. Gell-Mann and H. Leutwyler, Phys.Lett. 47B,
365 (1973) and S. Weinberg, Phys.Rev.Lett. 31, 494 (1973).
- Ba 73 W. Bardeen, H. Fritzsche, M. Gell-Mann, in: Scale and conformal
symmetry in hadron physics (R. Gatto, ed.), J. Wiley and Sons,
New York (1973), p. 139.
- Gr 73 L. Gray et al., Phys.Rev.Lett. 30, 1091 (1973).
- Ho 73 R. Horgan and R.H. Dalitz, Nucl.Phys. B 66, 35 (1973); B 71, 546 (1974) (E).
- Sh 73 B.A. Shahbazian and A.A. Timonina, Nucl.Phys. B 53, 19 (1973);
B.A. Shahbazian et al., in: Proc. of the XVIII International Conference
on High Energy Physics (1976), vol. I, C 35.
- Aub 74 J.J. Aubert et al., Phys.Rev.Lett. 33, 1404 (1974).
- Aug 74 J.E. Augustin et al., Phys.Rev.Lett. 33, 1406 (1974).

- Bl 74 E.D. Bloom, Proc. of the 6th International Symposium on Electron and Photon Interactions at High Energies, Bonn (1973), p. 227.
- Ca 74 A.S. Carroll et al., Phys.Rev.Lett. 32, 247 (1974).
- Cho 74 A. Chodos, R.L. Jaffe, K. Johnson, C.B. Thorn and V.F. Weisskopf, Phys.Rev. D 9, 3471 (1974).
- Chp 74 A. Chodos et al., Phys.Rev. D 10, 2599 (1974).
- Chr 74 A. Chodos and C.B. Thorn, Phys.Lett. 53B, 359 (1974); Nucl.Phys. B 109, 21 (1976).
- Gi 74 F.J. Gilman, Resonances, A quark view of hadron spectroscopy and transitions, see also ref [SIP 77], p. 307.
- Ha 74 F.J. Hasert et al., Gargamelle Collaboration, Nucl.Phys. B 73, 1 (1974).
- Ko 74 J. Kogut and L. Susskind, Phys.Rev. D 9, 3501 (1974);
K. Wilson, Phys.Rev. D 10, 2445 (1974).
- Me 74 H.J. Melosh, Phys.Rev. D 9, 1095 (1974).
- Po 74 H.D. Politzer, Phys.Rep. 14 C, 129 (1974): Asymptotic freedom: an approach to strong interactions.
- Re 74 C. Rebbi, Dual theory (M. Jacob, ed.); North-Holland, Amsterdam (1974), p. 221.
- Ro 74 J.L. Rosner, Phys.Rep. 11 C, 191 (1974): The classification and decay of resonant particles.
- Ap 75 T. Appelquist and H.D. Politzer, Phys.Rev.Lett. 34, 43 (1975);
A. DeRújula and S.L. Glashow, Phys.Rev.Lett. 34, 46 (1975).
- Ba 75 T. Barnes, Nucl.Phys. B 96, 353 (1975).
- Ca 75 D.E. Caro et al., Proc. of the 4th International Symposium on Anti-nucleon-Nucleon Interactions, Syracuse (T.E. Kalogeropoulos and K.C. Wali, eds.); Syracuse University, New York (1975) III, p. 13.

- DeG 75 T.A. DeGrand, R.L. Jaffe, K. Johnson and K. Kiskis, *Phys.Rev. D* 12, 2060 (1975).
- DeR 75 A. DeRújula, H. Georgi and S.L. Glashow, *Phys.Rev. D* 12, 147 (1975).
- Fr 75 P.G.O. Freund and Y. Nambu, *Phys.Rev.Lett.* 34, 1645 (1975);
J.F. Willemsen, *Phys.Rev. D* 13, 1327 (1976).
- Gn 75 P. Gnädig, P. Hasenfratz, J. Kuti and A.S. Szalay, *Proc. of the Neutrino 1975 IUPAP Conference, Vol. 2 (1975)*, p. 251; *Phys.Lett.* 64B, 62 (1976).
- Go 75 E. Golowich, *Phys.Rev. D* 12, 2108 (1975).
- He 75 A.J.G. Hey, *Current and constituent quarks, theory and practice*, in: *Quarks and hadron structure (G. Morpugo, ed.)*, Plenum Press, New York and London (1977), p. 93.
- Ja 75 R.L. Jaffe, *Phys.Rev. D* 11, 1953 (1975).
- Jac 75 J.D. Jackson, *Classical electrodynamics, second edition*; John Wiley & Sons Inc., New York (1975).
- JaP 75 R.L. Jaffe and A. Patrascioiu, *Phys.Rev. D* 12, 1314 (1975).
- Jo 75 K. Johnson, *Acta Phys.Polonica B* 6, 865 (1975).
- Pe 75 M.C. Perl et al., *Phys.Rev.Lett.* 35, 1489 (1975).
- Re 75 C. Rebbi, *Phys.Rev. D* 12, 2407 (1975); *Phys.Rev. D* 14, 2362 (1976).
- Sh 75 D. Shalloway, *Phys.Rev. D* 11, 3545 (1975); *D* 14, 1172 (1976) (E);
D. Shalloway, *Phys.Rev. D* 14, 1032 (1976).
- We 75 G.B. West, *Phys.Rep.* 18 C, 263 (1975): Electron scattering from atoms, nuclei and nucleons.
- Wi 75 G. Wilquet et al., *Phys.Lett.* 17B, 97 (1975).
- BH 76 C. Bender and P. Hays, *Phys.Rev. D* 14, 2622 (1976).
- Bl 76 J. Blietschau et al., *Nucl.Phys. B* 114, 189 (1976).

- Br 76 H. Braun et al., Phys.Lett. 60B, 481 (1976).
- Ch 76 V. Chaloupka et al., Phys.Lett. 61B, 487 (1976).
- Che 76 G.F. Chew, [ST 76], p. 515.
- Cl 76 F.E. Close, see ref. [SSU 76], p. 1.
- Da 76 R. Dalitz, see ref. [SSU 76], p. 151.
- DeG 76 T.A. DeGrand and R.L. Jaffe, Ann.Phys. (NY) 100, 425 (1976);
T.A. DeGrand, Ann.Phys. (NY) 101, 496 (1976).
- De 76 Ch. Defoix et al., [ST 76], p. 169, 175.
- DeM 76 C. DeMarzo et al., [ST 76], p. 139.
- Dy 76 F. Dydack et al., Nucl.Phys. B 102, 253 (1976).
- Ei 76 E. Eisenhandler, [ST 76], p. 91.
- Ho 76 G. Höhler et al., Nucl.Phys. B 114, 505 (1976).
- Hom 76 D. Hom et al., Phys.Rev.Lett. 36, 1236 (1976).
- Ja 76 R.L. Jaffe and K. Johnson, Phys.Lett. 60B, 201 (1976).
- Jo 76 K. Johnson, see ref. [SSU 76], p. 245.
- Jp 76 K. Johnson and C.B. Thorn, Phys.Rev. D 13, 1934 (1976).
- Ka 76 T.E. Kalogeropoulos and G.S. Tzanakos, [ST 76], p. 29.
- Ma 76 J.F. Martin et al., Phys.Lett. 65B, 483 (1976).
- Man 76 S. Mandelstam, Phys.Rep. 23 C, 245 (1976): II. Vortices and quark
confinement in non-Abelian gauge theories.
- Pa 76 J.C. Pati, see ref. [SSU 76], p. 89.
- SSU 76 Proc. of the Seventeenth Scottish Universities Summer School in
Physics, St. Andrews (1976) (I.M. Barbour and A.T. Davies, eds.)
- ST 76 Proc. of the 3rd European Symposium on Antinucleon-Nucleon Interactions,
Stockholm (G. Eksping and S. Nilsson, eds.); Pergamon Press, Oxford
and New York (1976).
- Su 76 A. Subramanian, [ST 76], p. 51.

- Ba 77 T. Barnes, Trieste preprint IC/77/103 (1977).
- Bac 77 C. Bacci et al., Phys.Lett. 68B, 393 (1977);
B. Esposito et al., Phys.Lett. 68 B, 389 (1977);
G. Barbiellini et al., Phys.Lett. 68B, 397 (1977);
G. Cosme et al., Phys.Lett. 67B, 231 (1977).
- Be 77 P. Benkheiri et al., Phys.Lett. 68B, 483 (1977);
P. Benkheiri et al., Phys.Lett. 81B, 380 (1979);
see also J. Six, [MO 78] I, p. 301.
- Bem 77 C. Bemporad, Talk at the 1977 International Symposium on Lepton and
Photon Interactions at High Energies, Hamburg (1977).
- Br 77 O. Braun et al., Nucl.Phys. B 124, 45 (1977).
- Brü 77 W. Brückner et al., Phys.Lett. 67B, 222 (1977).
- Ca 77 C. Callan, R. Dashen and D. Gross, Phys.Lett. 66B, 375 (1977);
Phys.Rev. D 17, 2717 (1978); Princeton University Reports June 1978.
- Car 77 A.A. Carter et al., Phys.Lett. 67B, 117 (1977), see also [ST 76],
p. 117; A.A. Carter, Phys.Lett. 67B, 122 (1977);
A.A. Carter, Nucl.Phys. B 141, 467 (1978).
- Ch 77 M. Chanowitz, Color and experiments, Proc. of the 12th Rencontre de
Moriond (Tran Thanh Van, ed.) (1977), p. 25.
- ChH 77 Chan H.-M. and H. Høgaasen, Phys.Lett. 72B, 121 (1977); Phys.Lett.
72B, 400 (1978); Nucl.Phys. B 136, 401 (1978), [MO 78] I, p. 237.
- Co 77 M. Coupland et al., Phys.Lett. 71B, 460 (1977).
- Dr 77 S.D. Drell, see ref. [SIP 77], p. 81.
- Fe 77 G.J. Feldman and M.L. Perl, Phys.Rep. 33 C, 286 (1977): Recent results
in electron-positron annihilation above 2 GeV.
- Ga 77 E. Gabathuler, Experimental review of deep inelastic scattering with
e and μ beams, Proc. of the 1977 European Conference on Particle
Physics (Jenik and Montvay, eds.), Budapest, vol. II (1977), p. 863.

- Ge 77 P.M. Gensini, SLAC-PUB-1952 (1977).
- Gi 77 F.J. Gilman, Hadron spectroscopy, see ref. [SIP 77], p. 121.
- Gr 77 O.W. Greenberg and C.A. Nelson, Phys.Rep. 32 C, 69 (1977): Color models of hadrons.
- Ha 77 F. Halprin et al., Phys.Lett. 66B, 177 (1977).
- HaK 77 J. Hauptman, J. Kadijk and G. Trilling, Nucl.Phys. B 125, 29 (1977).
- He 77 S. Herb et al., Phys.Rev.Lett. 39, 252 (1977).
- Hem 77 R.J. Hemingway, New results from old spectroscopy, see ref. [SIP 77], p. 401.
- Ja 77 R.L. Jaffe and K. Johnson, Comments Nucl.Part.Phys. 7, 107 (1977).
- Jb 77 R.L. Jaffe, Phys.Rev.Lett. 38, 195 (1977).
- Jc 77 R.L. Jaffe, Phys.Rev. D 15, 267 and 281 (1977).
- Ka 77 T. Kamae et al., Phys.Rev.Lett. 38, 468 (1977).
- La 77 T.A. Lasinski, Progress in K* spectroscopy, see ref. [SIP 77], p. 371.
- Ma 77 J.F. Martin and L. Osborne, Phys.Rev.Lett. 38, 1193 (1977).
- Mo 77 K.C. Moffeit, Quarks and particle production, see ref. [SIP 77], p. 181.
- Ro 77 D. Robson, Nucl.Phys. B 130, 328 (1977)
- SIP 77 Proc. of the Summer Institute on Particle Physics, Stanford (M.C. Zipf, ed.) (1977).
- Ae 78 A.T. Aerts, P.J. Mulders and J.J. de Swart, in: H. Zingl, a.o. (eds.): Lecture Notes in Physics 82: Proc. of the 8. International Conference, Graz (1978), p. 78.
- P.J. Mulders, A.T. Aerts and J.J. de Swart, Phys.Rev.Lett. 40, 1543 (1978).
- Ar 78 T.A. Armstrong et al., Paper no. 608 [TO 78], and [HI 78], p. 110.

- Ba 78 O.N. Baloskin et al., Paper no. 1049 [TO 78].
- Ca 78 A.S. Carroll et al., Phys.Rev.Lett. 41, 777 (1978).
- Ch 78 Chan H.-M. et al., Phys.Lett. 76B, 634 (1978).
- Cu 78 D. Cutts et al., Phys.Rev. D 17, 16 (1978).
- DeG 78 T. DeGrand and C. Rebbi, Phys.Rev. D 17, 2358 (1978).
- DeT 78 C. DeTar, Phys.Rev. D 17, 302, 323 (1978), D 19, 1028 (1979) (E),
University of Utah preprint UU Hep 78/1.
- El 78 J. Ellis, Applications of QCD, SLAC-PUB-2121 (May 1978).
- Ev 78 C. Evangelista et al., Paper no. 521 [TO 78].
- Fr 78 H. Fritzsch, Invited talk at the Stockholm Symposium on Physics at
High Energies, CERN publication TH-2583 CERN.
- Fu 78 M. Fukugita et al., Phys.Lett. 74B, 261 (1978).
- G1 78 R.C. Giles, Phys.Rev. D 18, 513 (1978).
- Gn 78 P. Gnädig, Z. Kunszt, P. Hasenfratz and J. Kuti, Central Research
Institute for Physics, Budapest preprint KFKI-1978-1.
- Gr 78 D.R. Green et al., Paper no. 810 [TO 78].
- Ha 78 H. Harari, Phys.Rep. 42 C, 235 (1978): Quarks and leptons.
- HaK 78 P. Hasenfratz and J. Kuti, Phys.Rep. 40 C, 2 (1978): The quark bag
model.
- HI 78 Proc. of the Meeting on Exotic Resonances (I. Endo et al., eds),
Hiroshima University preprint HUPD-7813 (Oct. 1978).
- Ho 78 N. Hoshizaki, see ref. [HI 78], 29 and references therein.
- HoM 78 D. Horn and J. Mandula, Phys.Rev. D 17, 898 (1978).
- Ja 78 R.L. Jaffe and F.E. Low, MIT preprint: The connection between quark-
model eigenstates and low energy scattering, MIT-CTP 747 (1978).
- Jb 78 R.L. Jaffe, Phys.Rev. D 17, 1444 (1978).
- Jc 78 R.L. Jaffe, [MO 78] I, p. 257.

- Jo 78 K. Johnson, MIT-CTP 725 (1978).
- Jp 78 K. Johnson, Phys.Lett. 78B, 259 (1978).
- Kl 78 J.C. Kluyver, University of Amsterdam preprint (December 1978), and
Private Communication.
- Le 78 T.D. Lee, Columbia University, report CU-TP-127 (1978).
- Ma 78 W. Marciano and H. Pagels, Phys.Rep. 36 C, 139 (1978): Quantum
chromodynamics.
- MaR 78 B.R. Martin and L.J. Reinders, University College London preprint
(May 1978).
- MO 78 Proc. of the 13th Rencontre de Moriond, Les Arcs, Savoie (J. Tran
Thanh Van, ed.); Université Paris Sud, 91405 Orsay, France (1978).
- Mon 78 L. Montanet, [MO 78] I, p. 285 and references therein.
- Na 78 K. Nakamura, see ref. [HI 78], 17 and references therein.
- Ne 78 W.L.G.A.M. van Neerven, Parton models, lecture notes (April 1978)
and references therein.
- No 78 V.A. Novikov et al., Phys.Rep. 41 C, 1 (1978): Charmonium and gluons.
- Oz 78 S. Ozaki, Rapporteur talk on hadron spectroscopy, experimental,
Brookhaven preprint BNL-25057.
- Pa 78 P. Pavlopoulos et al., Phys.Lett. 72B, 415 (1978).
- PDG 78 Particle Data Group, Review of particle properties, Phys.Lett. 75B,
1 (1978).
- Pe 78 M.L. Perl, [MO 78] II, p. 515 and SIAC-PUB-2132 (June 1978) and
references therein.
- Ri 78 F. Richard, [MO 78] II, p. 169.
- Sa 78 S. Sakamoto et al., Paper no. 1058 [TO 78].
- Th 78 C. Thorn, MIT-CTP 722 (1978), published in Phys.Rev. D 19, 639 (1979).
- To 78 D. Tow et al, Orsay preprint IPNO/TH 78-16 (1978).

- TO 78 Proc. of the XIXth International Conference on High Energy Physics,
Tokyo, Japan (1978).
- Wo 78 C.N. Wong and K.F. Liu, Phys.Rev.Lett. 41, 82 (1978).
- Wp 78 M. Wong et al., Paper no. 220 [TO 78].
- Yo 78 A. Yokosawa, see ref. [HI 78], 1 and references therein.
-
- Be 79 H.J. Besch et al., Phys.Lett. 81B, 79 (1979).
- Ho 79 G. 't Hooft, private communication (1979).
- Ja 79 R.L. Jaffe, private communication (1979).
- Jo 79 K. Johnson and C. Nohl, Phys.Rev. D 19, 291 (1979).
- Mu 79 P.J. Mulders, A.T. Aerts and J.J. de Swart, Multiquark states: Q^3
baryon resonances, Phys.Rev. D 19 (1979).
- Na 79 M.M. Nagels et al., Compilation of coupling constants and low energy
parameters, Nucl.Phys. B 147, 189 (1979).

SAMENVATTING

Het proefschrift bestaat uit vier delen:

Hoofdstuk 1. Hierin wordt getracht het beeld te schetsen van hadronen, zoals dat momenteel in de hoge energie fysika in brede kringen bestaat. Tevens wordt geprobeerd een overzicht van de experimentele feiten te geven, waarop dit beeld gebaseerd is. Hadronen zijn deeltjes, die onderhevig zijn aan sterke wisselwerkingen (kernkrachten). Zij worden gewoonlijk verondersteld te zijn opgebouwd uit quarks: deeltjes met 'spin' $j = 1/2$ en een 'color' (kleur) lading. De krachten tussen deze kleurladingen, die overgebracht worden door zelf ook weer kleur dragende gluonen, zorgen ervoor, dat in het hadron alleen zeer bepaalde - kleurloze - quark combinaties kunnen voorkomen. De meest eenvoudige hadronen zijn baryonen (3 quarks: Q^3) of mesonen (quark-antiquark: $Q\bar{Q}$) toestanden. Naast kleur en spin hebben de quarks ook 'flavor' (smaak), een kwaliteit die tezamen met de quarkspin veel van de hadron eigenschappen bepaalt. Tot nu toe is het bestaan van vijf smaken aangetoond, waarvan we in dit proefschrift alleen die drie gebruiken, die het langst bekend zijn.

Hoofdstuk 2. Een specifiek hadron model - het MIT bagmodel - wordt geformuleerd. Het verenigt de meeste in hoofdstuk 1 opgesomde eigenschappen in zich. Er wordt in detail ingegaan op een speciale klasse expliciete oplossingen, behorende bij de statische bolvormige 'bag'. Behalve quark oplossingen laat deze benadering ook gluon oplossingen toe. Dit betekent dat naast hadronen, bestaande uit quarks, ook - nog steeds kleurloze - hadronen kunnen voorkomen, die bestaan uit quarks en gluonen, of alleen maar gluonen. Voor een systeem dat alleen quarks bevat, wordt een uitdrukking voor de energie afgeleid, die uitgebreid wordt met enige fenomenologische termen. Het massa spectrum van de lichte hadronen wordt met deze massaformule gereproduceerd, waarna uitspraken

gedaan kunnen worden over enkele andere, statische eigenschappen van deze deeltjes.

Hoofdstuk 3. De groepentheoretische structuur van de massaformule, afgeleid in hoofdstuk 2, wordt geanalyseerd en een gegeneraliseerde flavor-spin SU(6) massaformule wordt gegeven, waarvan de coëfficiënten functies zijn die m.b.v. het MIT bagmodel kunnen worden berekend. Met deze massaformule wordt het massaspektrum van het dibaryon (zes-quark: Q^6) systeem voorspeld en mogelijke kandidaten besproken.

Hoofdstuk 4. De statische bolvormige 'bag' benadering wordt ook toegepast op meson ($Q^2\bar{Q}^2$) toestanden. Uitgaande van de kleur-krachten kan een voorschrift gegeven worden voor het berekenen van de massa's van (zeer) snel draaiende (en dan sigaarvormige) 'bags'. Hiermee wordt het massa spektrum van snel draaiende $Q^2\bar{Q}^2$ (de zgn. baryonium en mesonium) toestanden bepaald. De aldus verkregen spektra worden vervolgens geanalyseerd en vergeleken met het experimenteel gevonden spektrum.

CURRICULUM VITAE

van Adrianus Theodorus Maria Aerts:

Ik ben op 23 juni 1952 geboren te Etten-Leur (Noord-Brabant) en bezocht de volgende onderwijs instellingen:

van september 1958 tot juli 1964 : Lagere Jongensschool "Gerardus Majella" te Etten-Leur;

van september 1964 tot juli 1970 : "Onze Lieve Vrouwe Lyceum" te Breda.
Het eindexamen Gymnasium B behaalde ik op 10 juni 1970;

van september 1970 tot oktober 1975: Fakulteit der Wiskunde en Natuurwetenschappen van de Katholieke Universiteit Nijmegen. Het doktoraal examen natuurkunde werd met lof afgelegd op 9 oktober 1975. Als specialisatie koos ik Theoretische Hoge Energie Fysika.

Sinds november 1975 ben ik als wetenschappelijk medewerker verbonden aan het Instituut voor Theoretische Fysika te Nijmegen, in dienst van de Stichting voor Fundamenteel Onderzoek der Materie. Naast het onderzoek, onder supervisie van Prof.dr.ir. J.J. de Swart, dat tot deze dissertatie heeft geleid, heb ik, in het kader van mijn onderwijstaak, geassisteerd bij verschillende werkkolleges.

STELLINGEN

I

De argumenten, die in het quark-schillenmodel gebruikt worden voor identifikatie van translatiemodes, kunnen niet zonder meer worden toegepast op een gemengd systeem als de snel roterende bag.

G. Karl and E. Obryk, Nucl.Phys. B 8 (1968) 609

K. Johnson and C.B. Thorn, Phys.Rev. D 13 (1976) 1934

II

Met de door Chan en Høgaasen besproken mechanismen voor produktie van bepaalde nauwe resonanties worden de voornaamste, door deze auteurs voorgestelde kandidaten voor zulke toestanden, de M(2020) en de M(2204), niet geproduceerd.

Chan Hong-Mo and H. Høgaasen, Nucl.Phys. B 136 (1978) 401

P. Benkheiri et al., Phys.Lett. 68B (1977) 483

III

De identifikatie van de $\Lambda(1405)$ en de $\Sigma(1480)$ resonanties met de ontaarde $L = 0$ $Q^4_{\bar{Q}}$ Λ - en Σ -toestanden (bagmassa $M = 1.46$ GeV) is, gezien de invloed van de vervalkanalen op de positie van de corresponderende S-matrixpolen, te verkiezen boven die met de $L = 1$ $Q^2_{\bar{Q}}$ toestanden (bagmassa respectievelijk $M = 1.59$ en 1.66 GeV).

P.J. Mulders, A.T. Aerts and J.J. de Swart, Phys.Rev. D 19 (1979)

IV

Het gebruik van de optimale-polynoom-ontwikkeling voor de verstrooiingsamplitude maakt het in principe mogelijk de trends van de hogere partiële golven betrouwbaar uit het gedrag van de lagere te voorspellen. Echter, uit de toepassingen op nucleon-nucleon verstrooiing blijkt ondubbelzinnig, dat in het algemeen de resultaten van deze methode in de praktijk sterk afhangen van de keuze van de te ontwikkelen amplitudes.

M.J. Moravcsik, in: Proceedings of the KEK Summerschool (M. Kawagushi and K. Takahashi, eds.) National Laboratory for High Energy Physics (KEK), Ibaraki, Japan (1972), page 179-191,

T. Rijken, P. Signell and T. Burt, in: Nucleon-Nucleon Interaction (D.F. Measley et al., eds.); American Institute of Physics, Vancouver (1978), page 130

V

De effectieve-een-boson-uitwisselings-potentiaal voor de sterke wisselwerkingen tussen twee nucleonen en de analoog berekende effectieve-een-foton-uitwisselingspotentiaal V_C , die de elektromagnetische correcties hierop beschrijft, kunnen zodra ze op meer dan alleen de Born term gebaseerd zijn, alleen dan zinvol bij elkaar opgeteld worden als V_C in de Feynman-ijking berekend wordt.

G.J.M. Austen and J.J. de Swart, preprint THEF-NYM-79.7

VI

De geringe aandacht, die in stripverhalen aan vrouwenvraagstukken wordt besteed, kan erop wijzen, dat deze problematiek te weinig vermakelijks of actueels heeft voor het strips-lezende publiek.

VII

De verbreidheid van het konsumptieve gedrag, dat gebaseerd is op de stelregel "veel is lekker", biedt een te rijke voedingsbodem voor verdere groei van de specialistisch-klinische hulpverlening.

A.T. Aerts

mei 1979

